Analysis of RNA stability in forensic specimens

By

Nicola Ann McCallum

Centre for Forensic Science

Department of Pure and Applied Chemistry

University of Strathclyde

A thesis presented in fulfilment of the requirements for the degree of **Doctor of Philosophy**

2015

Centre for Forensic Science

Department of Pure and Applied Chemistry

University of Strathclyde

Analysis of RNA stability in forensic specimens

PhD Thesis

Nicola Ann McCallum

2015

Signed: Date:

Abstract

Ribonucleic acid (RNA) analysis presents a unique, novel opportunity to answer a wide range of questions in forensic science. The dynamicity of the transcriptome has led to it being suggested as a novel source of diagnostic information in forensic pathology. However, RNA is exceptionally labile. This research has characterised the post-mortem degradation behaviour of tissue RNA in an animal model, the laboratory mouse; with the aim of identifying a post-mortem interval during which gene expression analysis provides informative and reliable results. It was extremely encouraging that over the three day post-mortem interval examined, the yield of RNA from skeletal muscle, kidney, liver and heart tissue did not fall to such a level that it became unanalysable. Interestingly, individual RNAs were found to exhibit unique decay behaviour during the post-mortem interval; some significantly more stable than others. In the tissues of mice decomposed at room temperature, RNAs remained stable for at least the first 12 hours post-mortem; after which the observed differential decay skewed their expression profiles. This poses an interpretational obstacle for gene expression data where an extended time lag exists between death and sampling, and highlights the requirement for future work to consider novel data normalisation strategies. Overall, it is suggested that using RNA degradation as an indicator of post-mortem interval is fraught with difficulties: such as its dependence on the environmental conditions (specifically ambient temperature), differential RNA decay behaviour between tissue types and storage media, and inherently strong variability between replicates.

Acknowledgements

Firstly, I would like to thank my supervisors Dr. Nigel Watson, Dr. Lynn Dennany and Dr. Marielle Vennemann for their encouragement, support and guidance throughout the course of my PhD studies.

I would like to thank the Carnegie Trust for the Universities of Scotland, the RSE Scotland Foundation and Strathclyde's Centre for Forensic Science for their financial support, allowing me to fulfil the ambition of studying for a PhD. Without their assistance, this project would simply not have been possible.

I give thanks also to the MSc students Shyrlee Lino and Deirdre Marley for their contributions towards my research, and hope that I was able to impart at least some knowledge in return. In addition, the support and guidance of the staff at the Biological Procedures Unit was invaluable during all stages of experimentation involving live animals.

Mention must go to the FFBs, in particular Gina, Tina, Laura and my partner in crime Felicity. With them I have laughed my way through the last three years. I will sincerely miss our escapades and adventures, and will never look at a plum the same way again.

Finally, the biggest thanks go to my family and friends for their endless support and patience. Special thanks go to my Mum, Lesley, for all those piece boxes and late night pick-ups and to Chris, for listening to my endless gripes and moans and always knowing the right table tennis fact to cheer me up.

Publications and presentations

Journal articles:

Haas, C., Hanson, E., Banemann, R., Bento, A.M., Berti, A., Carracedo, A., Courts, C., De Cock, G., Drobnic, K., Fleming, R., Franchi, C., Gomes, L., Hadzic, G., Harbison, S.A., Hjort, B., Hollard, C., Hoff-Olsen, P., Keyser, C., Kondili, A., Maroňas, O., McCallum, N. *et al*. (2015). RNA/DNA co-analysis from human skin and contact traces – Results of a sixth collaborative EDNAP exercise. *Forensic Science International: Genetics* (Article in Press).

Haas, C., Hanson, E., Anjos, M.J., Ballantyne, K.N., Banemann, R., Bhoelai, B., Borges, E., Carvalho, M., Courts, C., De Cock, G., Drobnic, K., Dötsch, M, Fleming, R., Franchi, C., Gomes, I., Hadzic, G., Harbison, S.A., Harteveld, J., Hjort, B., Hollard, C., Hoff-Olsen, P., Hüls, C., Keyser, C., Maroňas, O., McCallum, N., *et al*. (2014). RNA/DNA co-analysis from human menstrual blood and vaginal secretion stains: Results of a fourth and fifth collaborative EDNAP exercise. *Forensic Science International: Genetics* 8(1), 203-212

Alrowaithi, M., McCallum, N. and Watson, N. (2013). A method for determining the age of a bloodstain. *Forensic Science International* 234(1), e30-e31

Haas, C., Hanson, E., Anjos, M.J., Banemann, R., Berti, A., Borges, E., Carracedo, A., Carvalho, M., Courts, C., De Cock, G., Dötsch, M., Flynn, S., Gomes, I., Hollard, C., Hjort, B., Hoff-Olsen, P., Hribiková, K., Lindenbergh, A., Ludes, B., Maroňas, O., McCallum, N., *et al.* (2013). RNA/DNA co-analysis from human saliva and semen stains – results of a third collaborative EDNAP exercise. *Forensic Science International: Genetics* 7(2), 230-239.

Phillips, K., McCallum, N. and Welch, L. (2012). A comparison of methods for forensic DNA extraction: Chelex-100® and the QIAGEN DNA Investigator Kit (manual and automated). *Forensic Science International: Genetics* 6(2), 282-285.

Poster presentations:

Death investigation using RNA profiling. Strathclyde University Research Day, Glasgow, Scotland (June 2014).

Evaluation of RNA stability in post-mortem tissues: Towards gene expression profiling for the investigation of death. RNA-UK National Conference, Windermere, England (January 2014).

Evaluation of RNA stability in post-mortem tissues: Towards gene expression profiling for the investigation of death. Doctoral Summer School in Forensic Science and Criminology, Arolla, Switzerland (August 2012).

Oral presentation:

Analysis of RNA degradation in post-mortem tissues: Towards gene expression analysis for the investigation of death. Scottish Student Forensic Research Symposium, Glasgow, Scotland (March 2014).

List of key abbreviations

Actb	β-actin mRNA
B2m/B2M	β_2-microglobulin mRNA
DNA	Deoxyribonucleic acid
dNTP	Deoxynucleoside triphosphate
EDNAP	European DNA profiling research group
Fos	FBJ osteosarcoma mRNA
Gapdh	Glyceraldehyde-3-phosphate dehydrogenase mRNA
Hmbs	Hydroxymethylbilane synthase mRNA
mRNA	Messenger RNA
m^7G	7-methylguanosine cap
nt	Nucleotides
qPCR	Quantitative PCR, real time PCR
RIN	RNA integrity number
RNA	Ribonucleic acid
RT	Reverse transcription
RT-PCR	Reverse transcription polymerase chain reaction
Psmc4	Proteasome 26S subunit ATPase 4 mRNA
PCR	Polymerase chain reaction
RNase	Ribonuclease
rRNA	Ribosomal RNA
Sdha	Succinate dehydrogenase complex, subunit A mRNA
tRNA	Transfer RNA
UCE, UBCH5B	Ubiquitin conjugating enzyme (UBCH5B)
Ubc/UBC	Ubiquitin C mRNA
18S rRNA	18S ribosomal RNA
6-FAM	6-carbxoxyfluorescein

Contents

Chapter 1: Introduction

1.1 Thesis overview

Ribonucleic acid (RNA) analysis presents a new and unique opportunity to answer a range of as yet, unanswered questions in forensic science. Some of the potential applications of RNA analysis are summarised in Table 1.1 (1). Of these, this thesis is focused on the following research themes: detection of cell-specific gene expression, reactive changes in gene expression and quantification of RNA degradation.

Table 1.1: **Potential applications of gene expression analysis in forensic science**. Table reproduced from (1).

Type of RNA assessment	Application(s)
Detection of cell-specific gene expression	Identification of body fluid/tissue type of biological samples recovered in casework
Functional status of organs and tissues	Diagnosis of the cause and mechanism of death
Reactive changes in gene expression	Wound age determination Determination of vitality and survival time
Quantification of RNA degradation	Ageing biological stains Determination of the post-mortem interval

Identification of RNAs with expression associated with a specific tissue type could potentially provide forensic scientists with a novel tool for identification of the biological origin of crime scene specimens (2). This will be explored in Chapter 3, specifically regarding the development and validation of assays for identification of menstrual blood, vaginal secretions and contact traces in casework samples (3).

It is postulated that most external events to which an organism is exposed will leave a 'mark' on the transcriptome, reflected in the type and relative abundance of expressed RNAs (4). As a result, transcriptome analysis of post-mortem tissues has been proposed as a novel source of information regarding the cause and circumstances of death in cases where these cannot be determined using conventional methods (4). However, RNA is known to be a labile molecule. In fact, some research groups have suggested that quantification of tissue RNA degradation may serve as a novel measure of the post-mortem interval (5, 6). Unfortunately, little is known about what happens to RNA in tissues after death; information which is absolutely critical for correct interpretation of gene expression data. This will be explored in more detail in Chapters 5 through 7, with the aim of enhancing our current understanding of RNA decay behaviour. Initially, a protocol was devised and validated to permit characterisation of post-mortem tissue RNA degradation; the outcomes of which are presented in Chapter 4.

Because of the practical and ethical issues surrounding the use of human autopsy material, RNA degradation behaviour has been assessed in the tissues of mice decomposed for up to 72 hours. Three techniques were implemented: total RNA quantification by UV-visible spectrophotometry; total RNA quality analysis on the Bioanalyzer 2100 platform; and amplification of a panel of endogenous control RNAs by RT-qPCR. In addition, two post-mortem interval variables have been considered to identify their effect on tissue RNA. Ambient temperature during the post-mortem interval was altered, to determine whether this affected the time span during which RNA can be successfully analysed (Chapter 5). Secondly, the validity of an alternative *ex vivo* decomposition simulation was considered in Chapter 6, to establish whether data generated under this experimental design is directly comparable with gene expression data from tissue samples decomposed *in vivo*. Finally, in an attempt to characterise the nature and progression of the degradation of individual RNAs, Chapter 7 applied qPCR assays with specific design features to RNA extracts from partially decomposed tissues.

1.2 Molecular biology of RNA

1.2.1 Structural nature of RNA

RNA is an important cellular biomolecule with involvement in a diverse range of biological processes within the cell, often (but not always) in concert with deoxyribonucleic acid (DNA). RNA, like DNA, is a polymer of repeating monomer units called ribonucleotides (Figure 1.1) linked into linear chains by phosphodiester bonds (7). Each ribonucleotide is composed of a base (one of four incorporating uracil, cytosine, guanine or as featured in Figure 1.1, adenine), a ribose sugar and a phosphate group. RNA molecules are formed by linking adjacent ribonucleotides into long chains via phosphodiester bonds, which connect the 3' and 5' carbons of ribose sugars on adjacent ribonucleotides through the phosphate group. This gives the RNA molecule directionality; termed "5' to 3'" (7). Unlike the ribose and phosphate group, the base is not directly involved in the linear conformation of RNA but plays an important role in instigating the interaction between RNA and other nucleic acids, in the form of hydrogen bonds (7).

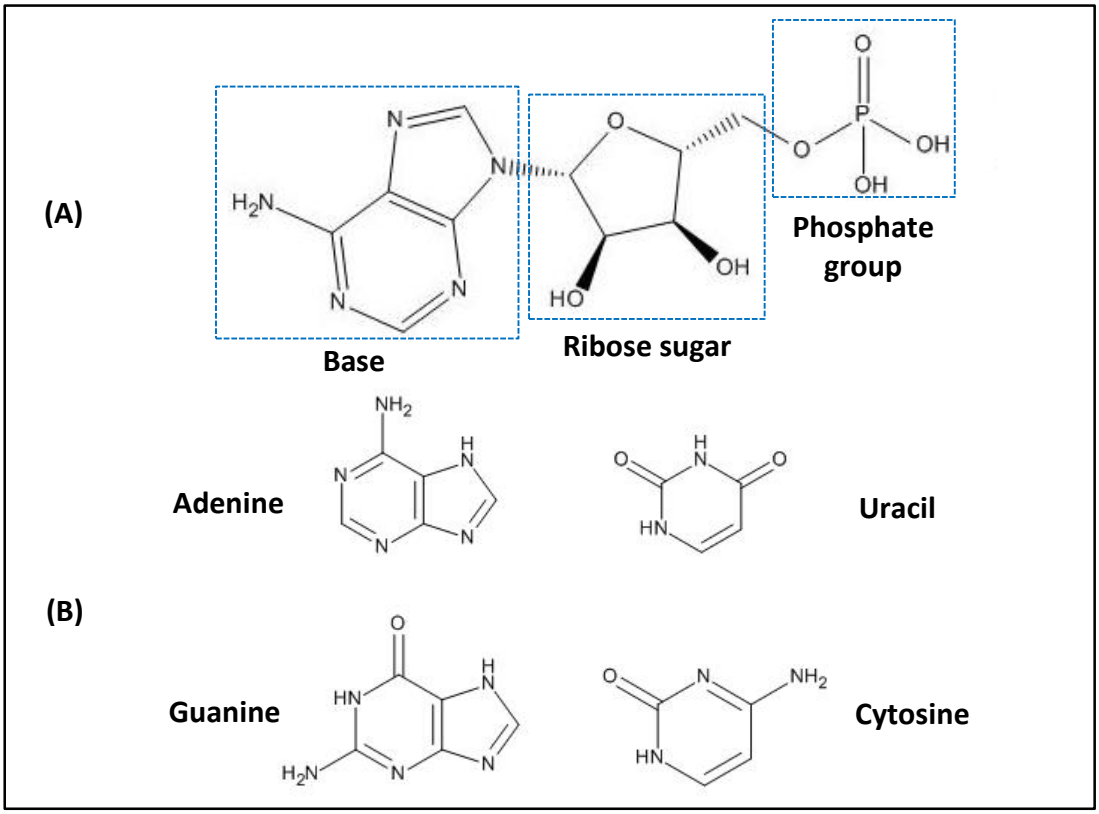

Figure 1.1: **(A) Structure of a ribonucleotide and (B) Structure of the four bases in RNA.** (**A**) Ribonucleotides are linked into chains via a phosphodiester bond linking the 3' and 5' carbons of two adjacent entities. The base is attached to the ribose sugar via a β-glycosidic linkage. (**B**) The base can be one of four: adenine, guanine, uracil or cytosine. Illustration drawn in ChemBioDraw v14.

The sequence of ribonucleotides determined by the bases at each position in the chain constitutes the primary structure of an RNA molecule. Much like proteins, RNA often possesses higher levels of structure (secondary, tertiary) making the molecules more globular in shape; mediated by intramolecular hydrogen bonding (7). RNAs can form a wide array of folded structures and may associate with numerous RNA binding proteins. Structure is one of the key distinguishing characteristics between the different classes of RNA existing in the cell.

1.2.2 The main classes of RNA

Despite having the same characteristic primary structure (i.e. nucleotide base sequence) different RNAs perform a diverse range of activities within the cell, summarised in Table 1.2. RNA classes can be differentiated based on their length, 3D configuration, function and half-life (4, 8).

Table 1.2: **Different classes of RNA.** The messenger, transfer and ribosomal RNAs are involved directly in the manufacture of proteins based on DNA sequence data. Adapted from (4).

RNA type	Function
Messenger RNA (mRNA)	Template for transfer of sequence data from nuclear DNA to the ribosome for translation
Transfer RNA (tRNA)	Amino acid carrier during translation
Ribosomal RNA (rRNA)	Ribosome structural component, comprising ~96% total cellular RNA
Small nuclear RNA (snRNA)	Component of the spliceosome, functioning in pre-mRNA processing in the nucleus
Small nucleolar RNA (snoRNA)	Functions in processing of pre-rRNA in the nucleus
Small interfering RNA (siRNA)	Regulation of gene expression
microRNA (miRNA)	
Anti-sense RNA (asRNA)	
Piwi-interacting RNA (piRNA)	

This research will focus primarily on messenger RNA (mRNA), which acts as the molecular intermediate between DNA and protein. Subsequent paragraphs will therefore detail the metabolism of mRNA in the cell: how it is synthesised, processed and exported to the cytoplasm; the function that it performs; and its degradation and how this is controlled. Essential to this overall process also are the transfer (tRNA) and ribosomal RNAs (rRNA), which work in concert with mRNA in the transfer of the genetic sequence to direct protein assembly (7). Out with these three primary RNA classes, other smaller non-coding RNAs exist and are involved in numerous other activities in the cell. These small RNAs will not be discussed in any

great detail; suffice to say that they exist and play important roles in RNA metabolism (7).

1.2.3 mRNA transcription, post-transcriptional processing and translation

Although mRNA comprises only approximately 3-5% of cellular RNA (4, 9), it plays an essential role in protein synthesis by acting as an intermediate between DNA and protein. This involves the transfer of genetic information from the nucleus to the cytoplasm whereby the ribosome can use it to assemble proteins. **Transcription** is the process by which RNA is synthesised from a template molecule of DNA. This is catalysed by the enzyme RNA polymerase II, which is recruited to transcribe a gene of interest into RNA by transcription factors. Using nucleotide triphosphates (NTPs) as an initial substrate, RNA polymerase II constructs mRNA oligonucleotide chains by catalysing the formation of new phosphodiester bonds between the 5'phosphate of a new NTP and the exposed 3'-OH of the terminal nucleotide on the nascent mRNA strand (7).

However, a significant proportion of eukaryotic genes comprise alternating coding (exonic) and non-coding (intronic) sequences, meaning that transcription in this manner results in the synthesis of a long precursor pre-mRNA molecule (7). A large macromolecular complex known as the spliceosome is able to remove the unwanted intronic sequences by **splicing**, to obtain a contiguous open reading frame. Subsequent to splicing, the 5' and 3' ends of the mRNA molecule are modified structurally to protect it against enzymatic attack (7). The 5' terminal ribonucleotide is covered by the addition of a guanosine triphosphate via a 5'-5' linkage, forming the 7-methylguanosine cap (m^7G) (7). At the opposite end, most eukaryotic mRNAs undergo polyadenylation – addition of a sequence of tens to hundreds of adjacent adenosines (As) creating a structure known as the poly (A) tail (7). The resultant **mature mRNA** molecule exhibits a structure as illustrated in Figure 1.2.

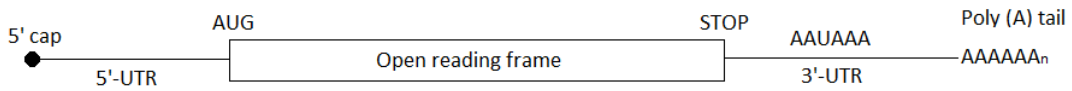

Figure 1.2: **Structure of a mature mRNA molecule.** The open reading frame contains the nucleotide sequence translated into protein by the ribosome – beginning with the start codon AUG and finishing with one of three stop codons: UAA, UAG or UGA. This coding sequence is flanked by the non-coding 3' and 5' untranslated regions (UTRs). The ends of the mRNA molecule are protected by the 3' poly (A) tail and 5' 7-methylguanosine (m^7G) cap. Information adapted from (7).

Following transcription, splicing and post-transcriptional processing the mature mRNA molecule exported into the cytoplasm, where it is used as a template for **translation**. mRNAs are transported through the nuclear envelope into the cytoplasm with the assistance of the nuclear pore complex (10). RNAs diffuse passively through the cytoplasm and can dock into the ribosome via their 5' m^7G cap. The ribosome is a protein-rRNA structure able to 'read' an mRNA, utilising the sequence of its open reading frame to direct polypeptide synthesis. Amino acids are delivered to the ribosome on the acceptor stem of a tRNA and positioned based on the complementarity between the anti-codons of tRNA and codons of the mRNA template. As the mRNA translocates through the ribosome, it catalyses the formation of peptide bonds between adjacent amino acids to form a polypeptide which is subsequently released.

1.2.4 Physiological mRNA degradation mechanisms and mRNA stability

Unlike DNA, mRNA is not a permanent fixture of the cell. The synthesis of mRNA occurs in response to transcription factor signals (7), and the mRNAs themselves only exist for a short period before degradation (11). This period varies between mRNAs most likely as a result of the functionality of the encoded protein: with mRNA half-lives ranging from as little as 15 minutes for the c-Fos transcript to well over 24 hours for that encoding β-globin (11). As the quantity of protein which can be produced from an mRNA molecule is a function of its biological half-life and transcription rate, it is hypothesised that the most stable mRNAs correspond to

constitutively expressed genes (12, 13). Such genes encode for proteins involved in essential, ubiquitous 'housekeeping' functions in the cell such as respiration, nucleotide synthesis and protein metabolism (7, 14). For example, the mRNA encoding for the cytoskeletal protein β-actin can be translated as many as 1,000 times before the degradation machinery takes hold (15).

Short lived mRNAs on the other hand, are thought to encode genes of regulatory significance (13). The short half-life of mRNAs is physiologically important to the cell and key in the control of gene expression – permitting much faster up- or down-regulation of genes in response to the cell's physiological needs (14). Interestingly, the half-life of some mRNAs is not static; and can be modified by physiological or environmental signals promoting either stability or decay (16-19). Precise control over the rate of mRNA degradation is important, given that this governs the quantity of mRNA available as a template for protein translation.

RNA is physiologically destroyed by enzymes which possess **ribonuclease** activity (RNases) (20). These can be of two types: exoribonucleases, which sequentially remove nucleotides from the free ends of the RNA molecule either in the 3' to 5' or 5' to 3' direction; or endoribonucleases, which cleave RNA internally (Figure 1.3) (21, 22).

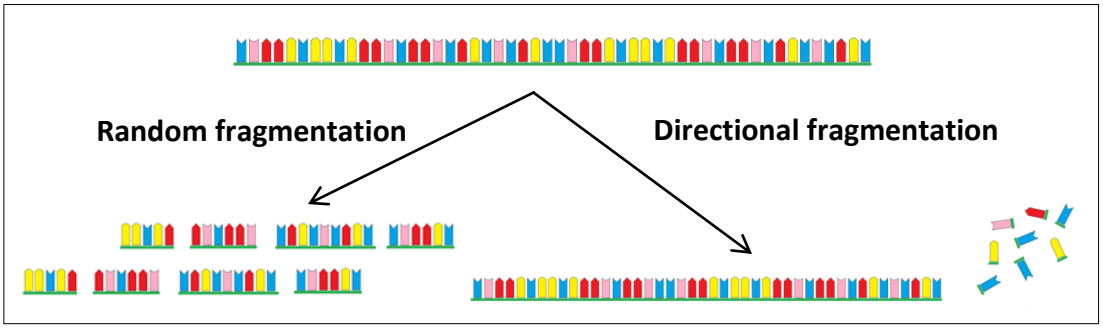

Figure 1.3: **Two key mechanisms of mRNA decay**. Messenger RNAs can either be disassembled in the 5' to 3' or 3' to 5' direction; mediated by exoribonucleases. Other endoribonucleases or chemical agents can attack the RNA molecule from within, at random points or within specific sequence motifs.

Immediately after transcription and their release into the cytoplasm, mRNAs start to undergo progressive deadenylation – shortening of the poly (A) tract at the 3' end of the molecule (20). Deadenylation is proposed to be the rate limiting step in mRNA decay (11). Nuclease complexes with poly (A) specific 3'-exonuclease activity in eukaryotic cells include PAN2/PAN3, CCR4/NOT or poly (A) specific ribonuclease (PARN). Deadenylated mRNA can either undergo degradation from the exposed 3' end, or most commonly removal of the m^7G cap ('decapping') and 5' to 3' decay (Figure 1.4) (11).

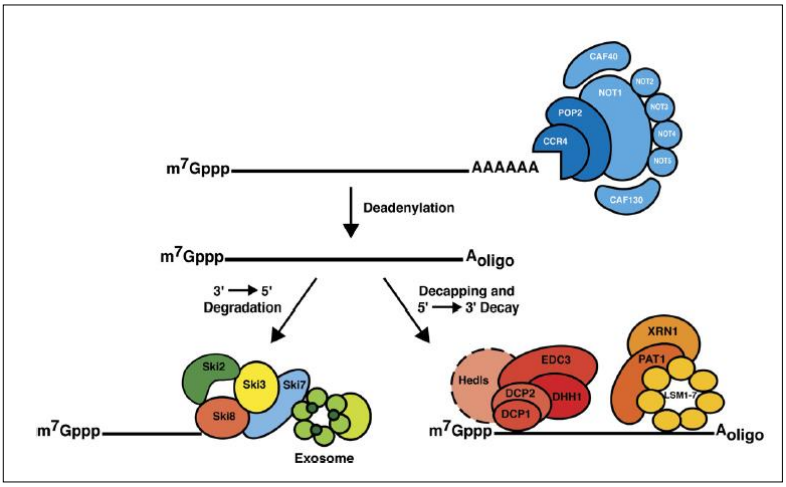

Figure 1.4: **Overview of eukaryotic mRNA decay mechanisms**. mRNA initially undergoes deadenylation, after which it may undergo two pathways: 3' to 5' degradation by the exosome, or decapping and 5' to 3' degradation by the exonuclease XRN1. Illustration from (23).

3' to 5' degradation of deadenylated mRNA is performed by the exosome, a large ring-shaped protein complex present both in the cytoplasm and nucleus (Figure 1.4). This however, is postulated to be a secondary mechanism of physiological RNA decay. In most instances, deadenylation is followed by hydrolysis of the m^7G cap by the DCP1/DCP2 decapping complex. This leaves an exposed 5' monophosphate nucleotide, which can be acted upon by the 5' exonuclease XRN1 to degrade the rest of the transcript (Figure 1.4) (11, 20, 22).

Controlling the rate of mRNA translation and degradation plays an important role in regulating gene expression. All sections of an mRNA molecule – the open reading frame, 3'-UTR, 5'-UTR, poly (A) tail and 7-methylguanosine cap – can confer stability to an mRNA molecule. However, a majority of known sequence elements influencing mRNA stability are located in the 3' untranslated region (3'-UTR), such as the AU-rich element (ARE) (24, 25). The half-life of a particular mRNA transcript is not fixed, but can vary in response to developmental, nutritional, hormonal, pharmacological and environmental (e.g. hypoxia, temperature/heat shock, UV, diurnal variation) stimuli (19, 24).

1.3 Applications of RNA in forensic science

As described in Section 1.1, this thesis is concerned with two applications of RNA analysis in forensic science: for identification of the tissue origin of a biological specimen, and to study the transcriptional changes in tissues after death. The following sections will provide a brief overview of the current state of the literature in these two areas.

1.3.1. Cell specific RNA expression: Body fluid and tissue origin identification

1.3.1.1 Cell specific RNA expression: Background

Nowadays, it is a matter of routine for DNA profiles to be obtained from biological samples recovered from a crime scene to identify an individual (1, 26). Some of the biological specimens encountered in a forensic context include blood, semen, saliva, menstrual blood, lacrimal fluid, sweat, vaginal secretions and skin cell deposits (4, 27). Establishing a DNA profile match provides a spatial link between an individual and a location of interest to a criminal investigation, but no information regarding the origin of the biological material (28). In many cases, correct identification of the tissue type from which genetic material originated can

be of immense value to a forensic investigation; most notably in cases of sexual assault (8, 29-31).

There are currently a plethora of methods commercially available for body fluid identification in forensic casework, including: biochemical colour change tests, enzymatic assays, immunoassays, crystal tests, microscopic tests, alternate light sources and spectroscopic analyses (32-39). However, these techniques have many inherent problems: most are labour intensive and time consuming, waste or damage biological samples, have poor specificity and their technological diversity prevents multiplex analysis (26, 40, 41). Moreover, there are a number of biological samples for which no effective, confirmatory identification technique exists, e.g. vaginal secretions and menstrual blood (8, 42, 43). In many forensic laboratories tissue origin identification is being bypassed solely for operational efficiency (26, 44).

This is the problem that mRNA profiling seeks to solve. Terminally differentiated cells take the form that they do following a developmentally regulated cellular program, in which specific genes are transcriptionally active (turned 'on') while others have their transcription suppressed (turned 'off') (26). As a result, each cell type has its own unique pattern of gene expression defined by the presence and relative abundance of mRNAs encoding for specific functional genes. It is proposed that characterisation of the mRNAs present in a biological specimen permits identification of its tissue origin.

Since the first article identifying menstrual blood specific mRNA markers was published in 1999 (45), many groups have contributed to the ever-expanding database of mRNA markers suitable for the identification of blood, menstrual blood, saliva, semen, vaginal secretions and skin cell deposits. A selection of important, well researched, tissue specific mRNA markers is included below in Table 1.3.

Table 1.3: **A selection of body fluid specific RNA markers utilised for the identification of blood, saliva, semen, menstrual blood and vaginal fluid in forensic casework specimens.** Information collated from (2, 27, 29, 31, 40, 46-49).

Body fluid	Gene/mRNA marker	Protein function	Site of expression
Blood	Haemoglobin A/B (HBA/B)	α/β subunits of haemoglobin, involved in oxygen transport	Blood – erythroblasts (erythrocyte precursor)
	Aminolevulinic acid synthase (ALAS2)	Enzyme in haem biosynthesis pathway	Blood – erythroblasts (erythrocyte precursor)
Saliva	Histatin 3 (HTN3)	Involved in non-immune defence against pathogens in the oral cavity	Saliva – salivary glands
	Statherin (STATH)	Inhibits calcium precipitation in oral cavity	Saliva – salivary glands
Semen	Kallikrein 3/ Prostate specific antigen (PSA)	Serine protease enzyme, liquefies semen to facilitate movement of spermatozoa	Semen – seminal plasma/ prostate gland
	Protamine 1/2 (PRM1/2)	'Histone-like' proteins, involved in chromatin condensation to fit into small spermatozoa	Semen – spermatozoa
Menstrual blood	Matrix metalloproteinases 7, 10 and 11 (MMP7/10/11)	Endopeptidase enzymes, function to break down the extracellular matrix during tissue remodelling in menstruation	Menstrual blood – endometrium
Vaginal secretions	Mucin 4 (MUC4)	Glycosylated membrane protein, functions in vaginal lubrication and protection of the vaginal epithelium against microbial invasion	Vaginal secretions – vaginal epithelium
Skin	Keratin 9 (KRT9)	Intermediate filament protein, found in terminally differentiated skin cells in the palms of hands and soles of feet only	Skin – palms and soles of feet only

1.3.1.2 Cell specific RNA expression: Evaluation

mRNA based body fluid identification overcomes many of the limitations of traditional protein-based identification procedures. As a result of their similar molecular structures, DNA and RNA can be co-extracted from biological specimens preventing sample wastage (41), and the analysis procedure mirrors that of DNA profiling (48). Unlike biochemical or serological tests, mRNA analyses can be multiplexed – i.e. in a single reaction tube, one can simultaneously test for a full panel of body fluids/tissue types (29, 50, 51). For some biological specimens such as menstrual blood, vaginal secretions and skin cell deposits, mRNA analysis presents the first method by which they can be reliably identified (43, 52-54). It can even allow the discrimination of semen from vasectomised males (55), and the identification of solid tissues (51). Unlike most current techniques, mRNA profiling has the potential to confirm the presence of a particular body fluid/tissue type rather than being solely 'presumptive' in nature (40).

Somewhat surprisingly, several studies have shown that despite the perceived instability of RNA tissue specific RNAs can still be successfully detected by PCR in biological specimens after storage periods of 2, 6, 15, 16, 23 and 28 years (50, 56-59). This instability has also formed the basis of several quantitative RNA assays for ageing biological specimens, e.g. those developed by Bauer *et al*. (56) and Anderson *et al*. (28, 60).

The panel of markers applicable to biological specimens is not only limited to mRNA. Several studies have also identified the presence of tissue specific miRNAs (61-63) and bacterial RNAs for strains of *Lactobacilli* specific to the vagina (43, 64).

In terms of sensitivity, mRNA technology has been shown to perform comparably to conventional biochemical, enzymatic or immunological body fluid identification methods (8). As each mRNA target exhibits its own unique basal expression level, the sensitivity of each body fluid identification assay is strongly variable and depends on the markers implemented (26, 65). Sensitivity also varies by body fluid type; e.g. with markers consistently amplified in 0.1 µL blood (65), 0.5 µL saliva, 0.5 µL semen (66) and 1/64th of a vaginal and menstrual blood swab

(3). It has been suggested that implementation of real time PCR rather than endpoint PCR improves sensitivity up to 40-fold (67). Haas *et al*. (8) were able to demonstrate the comparable sensitivity of their 3 blood, 2 saliva and 2 semen specific markers to four commonly used presumptive tests (Figure 1.5A).

(A)

Method, Volume blood (µL)	5	1	0.1	10^{-2}	10^{-3}	10^{-4}
Benzidine test						
Hexagon OBTI						
SPTB mRNA						
PBGD mRNA						
HBB mRNA						

Method, Volume saliva (µL)	5	1	0.1	10^{-2}	10^{-3}
Amylase test					
STATH mRNA					
HTN3 mRNA					

Method, Volume semen (µL)	5	1	0.1	10^{-2}	10^{-3}
Acid phosphatase test					
STATH mRNA					
HTN3 mRNA					

(B)

	Blood	Saliva	Semen	Vaginal secretions	Menstrual blood
SPTB	+	-	-	-	(+)
PBGD	(+)	-	-	-	(+)
HBB	+	-	-	-	+
STATH	-	+	-	-	-
HTN3	-	+	-	-	-
PRM1	-	-	+	-	-
PRM2	-	-	+	-	-
HBD-1	-	-	-	+	(+)
MUC4	-	-	-	+	+
MMP-7	-	-	-	(+)	+
MMP-11	(+)	-	-	-	+

Figure 1.5: **Sensitivity and specificity of mRNA profiling for body fluid identification**. (**A**) Shows the sensitivity of three blood, two saliva and two semen specific markers compared to conventional presumptive tests with respect to the input volume of the body fluid required to always give a positive result (dark grey) or give a positive result in 1 or 2 of 3 replicates (light grey). (**B**) Shows minimal cross-reactivity of mRNA markers with body fluids other than that with which they should be associated (shaded light grey). Illustrations adapted from (8).

Similarly, the specificity of mRNA profiling for tissue identification (i.e. the rate of false positives) is dependent on the RNAs targeted (8) (Figure 1.5B). Good human specificity has been demonstrated for blood, saliva and semen specific mRNAs – with cross-reactivity only significant for primate species (65, 66). Identifying tissue specific RNAs is more challenging for some tissue types than others; e.g. the high biochemical and histological similarity between the oral and vaginal mucosae makes marker cross-reactivity more likely (43, 68). In fact, researchers have struggled to identify markers specific to vaginal secretions, with

many of the biomarkers such as MUC4 and HBD1 detected often in saliva (44, 54, 69, 70).

The cost and labour intensive nature of mRNA profiling is likely to hinder its universal roll out to all forensic laboratories (71). Implementation of RNA profiling in forensic casework however, goes way beyond only the laboratory technique. A fundamental problem with the use of mRNA profiling for tissue origin identification is in the interpretation of the results. There are no approved, systematic strategies currently in use for unbiased data analysis and the reporting of mRNA evidence in the courtroom. These issues present the next developmental challenge for RNA analysts (33, 50, 71). Correct interpretation is particularly challenging where the results are negative or where the RNA profile is 'partial' for a particular tissue type. It is accepted that mRNAs exposed to the environment are subject to degradation by RNases (both endogenous and microbial), chemical agents, heat, UV/luminescent light irradiation or mechanical shearing (30, 42, 48). Therefore, the 'drop-out' of mRNA markers is expected, and few inferences can be made regarding the tissue type of a biological specimen in light of a negative result (30).

Chapter 3 of this thesis will present the outcomes of validation work performed to assess the efficacy of RNA profiling for the identification of menstrual blood, vaginal secretions and skin cells; using the RNA markers recommended by the European DNA Profiling (EDNAP) group. The key aim of this project was to examine a number of 'blind' mock casework specimens to try to correctly identify whether they contained menstrual blood, vaginal secretions and skin cells.

1.3.2 Transcriptome analysis in forensic pathology

For too long, the informative value of RNA in forensic medicine was ignored under a false perception that it is too unstable, and thus too short-lived to be worth investing attention in. Samples of human tissue recovered after a routine autopsy do not usually become available before a period of at least five to ten hours has passed; after which it was believed that all RNA would have been destroyed (72). Ribonuclease (RNase) enzymes are ubiquitous to the environment and can rapidly destroy RNA upon exposure. Almost every article considering the forensic applications of RNA introduce this topic with a statement professing the extreme instability of RNA, usually with no experimental evidence to back this up.

This notion has been quashed by the publication of material by Phang *et al*. (73) as far back as 1994, in the first article to illustrate successful RNA recovery from human post-mortem kidney and cardiac muscle. Using tissue samples stored in a -20 ^{o}C freezer for between three and eight months, Phang *et al*. were able to successfully demonstrate the recovery of total RNA and amplification of β-myosin mRNA, and make a primitive assessment of the quantity and quality of RNA recovered.

Successfully demonstrating the recovery of intact RNA suitable for analysis from post-mortem tissues formed the initial step in a long journey towards the application of gene expression profiling in forensic pathology. It is likely that this research has acted as a platform from which other research has stemmed and the field is slowly gaining momentum. Prior to discussing the potential applications of gene expression analysis in forensic pathology, it is necessary to briefly review current practice to provide context and highlight the areas for improvement.

1.3.2.1 Current methodology for the investigation of suspicious deaths

On presentation of a body to the forensic pathologist, two key questions which their examination aims to answer are:

- Time of death
- Cause and circumstances of death

Accurate estimation of the time of death is imperative for crime scene reconstruction, forming the centre of a timeline which can be used by investigators as a starting point; e.g. identifying or disregarding potential suspects (74). However in practice, it is exceedingly difficult to achieve despite more than a century's worth of intensive research towards this aim. Most techniques adopted are based on the rate of physicochemical changes which occur in the body immediately or shortly following death. A selection of techniques suggested as indicators of the post-mortem interval are included in Table 1.4; not all of which are routinely applied in casework.

In temperate climates such as in Scotland the single most informative indicator is *algor mortis:* the reduction in core body temperature which occurs over approximately the first day post-mortem (75). Cadaver cooling is the single most thoroughly researched topic in forensic pathology with publications stretching as far back as 150 years (66). One of the most respected methods for post-mortem interval estimation is Henssge's nomogram, based on an algorithm which takes into account rectal temperature, ambient temperature and the subject's weight to estimate the time elapsed since death (76).

Table 1.4: **Properties of the body which may serve as indicators of post-mortem interval.** Information collated from (66).

Physical property of the body	Principle	Application
Algor mortis	Based on the reduction in core body temperature on cessation of thermoregulation and heat generation at death	Useful in the first 24 hours from death Most commonly implemented method
Rigor mortis	Depletion of oxygen and energy in muscle fibres causes development of muscle rigidity	Can provide information over the first 36 hours from death
Livor mortis	Stagnant blood pools under the force of gravity causing skin discolouration	Not usually implemented for time of death, unless particularly early
Vitreous humour potassium concentration	Potassium diffuses through the retina into vitreous humour on loss of cell membrane selectivity to small molecules and ions	Not usually implemented, but can be informative after the first 24-48 hours, after which other methods fail
Electrical muscle stimulation	The muscular response to electrical stimulation can be graded, reducing with post-mortem interval	Not usually implemented, but can be informative in first 24 hours
Stomach contents examination	Examination of the digestion state of the last meal	Relatively uninformative, but may provide an indication as to the time interval between the last meal and death
State of decomposition and insect invasion	Sequential changes in the body due to bacterial and insect invasion can be categorised as a gross measurement of post-mortem interval	Only method available for longer post-mortem intervals

Despite extensive efforts to improve accuracy, all of the methods above are able at best to provide a window for the time of death. The results that they provide are confounded by numerous uncontrollable and unpredictable variables specific to each case. For example, post-mortem interval estimations made based on core temperature measurements are modified significantly by factors such as ambient temperature, humidity, air circulation, body mass/surface area ratio,

posture, starting body temperature, clothing/coverings etc. (66). The poor outcome of research to try to improve the accuracy of time of death estimations using these current technologies suggests that a change of tack is required in order to solve this problem. In recent years, quantification of nucleic acid degradation over the post-mortem interval has been considered as a potential solution (5, 6). The state of current literature with regard to this is discussed in subsequent sections.

In addition to pinpointing the time of death, it is of prime importance to determine accurately the mode, cause and circumstances of death. These three features have slightly different definitions in forensic pathology: the mode being the physiological basis of death e.g. heart failure; the cause an external event or existing pathology leading to death; and the manner implying whether death was natural, accidental, suicidal or homicidal (66).

The exact examination procedure employed by a forensic pathologist depends wholly on the circumstances of each individual case. However, Table 1.5 provides an insight into the sequence of methods currently used routinely: from an external and internal examination of the body in the autopsy theatre through to ancillary investigations requested in some instances such as histology, biochemistry, toxicology and molecular genetic tests. It has been estimated that despite this full battery of methods, an answer regarding cause of death can be established with relative certainty in 90-95% of cases (77). Gene expression analysis is currently being considered as a novel tool for determination of the cause of death. There is a significant gap between sophisticated molecular genetics analyses and the still very traditional way of conducting a forensic post-mortem examination in an autopsy theatre (1). The potential of this technology will be considered in a review in subsequent sections.

Table 1.5: **Examination procedures routinely employed for determination of the cause of death in forensic examinations**. Table adapted from (77).

Diagnostic level	Substrate for examination
External examination	Intact body
Autopsy	Organ systems Organs Injuries Macroscopic organ changes Diseases and disease related changes of organ systems
Histology and immunohistochemistry	Changes at a tissue and cellular level
Post-mortem biochemistry	Disturbances of homeostasis e.g. diabetes mellitus, uraemia, water-electrolyte metabolism
Toxicology	Substrates (drugs, poisons, toxins) Metabolites Quantification and distribution
Microbiology	Pathogen identification and quantification
Molecular pathology	Viral genetic material Genetic mutations

1.3.2.2 Potential applications of RNA in forensic pathology

1.3.2.2.1 RNA stability analysis and estimation of the post-mortem interval

The post-mortem interval can be described as the time period spanning from physiological death to discovery of the body, autopsy and tissue collection (4). As discussed, current techniques for estimation of the post-mortem interval are limited and subject to inaccuracy (Section 1.3.2.1, Chapter 1). This problem has long since plagued forensic pathologists and despite research in this area spanning over a century, no significant breakthroughs have been achieved; suggesting that a change of approach is necessary (66).

Of interest is the study of the relationship between RNA decay and the post-mortem interval. For many decades the informative value of RNA in forensic science was ignored under a false perception that it was too unstable (Section 1.2.4, Chapter 1). However, this acknowledged susceptibility of RNA to degradation could

potentially prove to be informative in itself. It has been proposed that the fragmentation state of RNA recovered from post-mortem tissues could be utilised as a novel measure of the time elapsed since death (5, 6).

This was first investigated in 2003 by Bauer *et al*. (5), who designed a multiplex PCR assay to try to track and quantify the post-mortem degradation of FASN mRNA by amplifying four target regions spaced along the transcript's length. Their use of the oligo (dT) priming technique during reverse transcription meant that in all FASN mRNAs reverse transcribed into cDNA the 3' poly (A) tail would be present, and under-representation of the 5' end implied partial degradation. The ratio of the quantity of each amplicon to the 3' proximal target amplicon was used as a measure of the degree of degradation. This assay was applied to the blood and brain tissue of cadavers with a post-mortem interval ranging between 0 to 145 hours. Bauer *et al*. were able to demonstrate a significant, time dependent reduction in the ratio of FASN1/FASN4 (the most 3' and 5' proximal amplicons respectively) in both blood and brain samples (Figure 1.6).

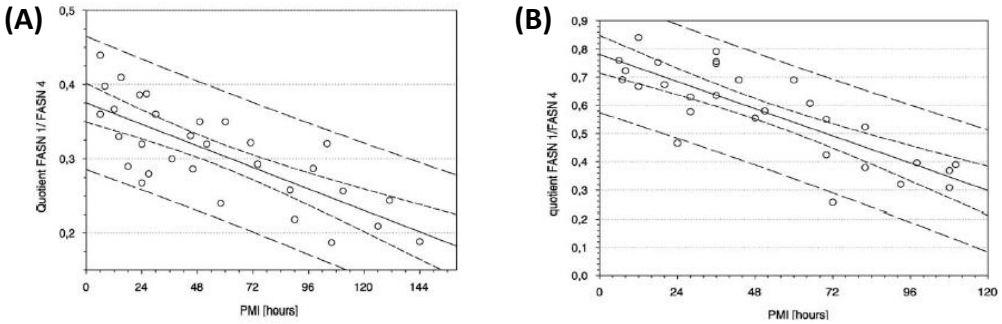

Figure 1.6: **Decline in the ratio of FASN1/FASN4 in (A) blood and (B) brain over the first 145 hours post-mortem.** Confidence and prediction intervals are also depicted. Illustration from (5).

This research shed a positive light for the first time on the potential application of mRNA expression profiling in forensic medicine. However, the outcomes have been criticised as the confidence and prediction intervals obtained using this technique are much too wide, i.e. that it would only be possible to

estimate large time ranges for the post-mortem interval, as is already possible with conventional techniques. Until this can be improved, it hinders its realistic application in casework (77).

Using the mouse as an animal model, Sampaio-Silva *et al*. similarly demonstrated a linear relationship between the degradative state of the transcriptome and the post-mortem interval over the first 11 hours following death (6). Animals were sacrificed and samples of heart, lung, spleen, skeletal muscle, liver, stomach, pancreas and skin collected immediately following death and decayed *ex vivo* (in a tube) at 21°C for up to 11 hours. They were able to illustrate a significant linear correlation between the RNA quality index (RQI) and post-mortem interval for RNA recovered from heart, skeletal muscle and liver tissue (Figure 1.7).

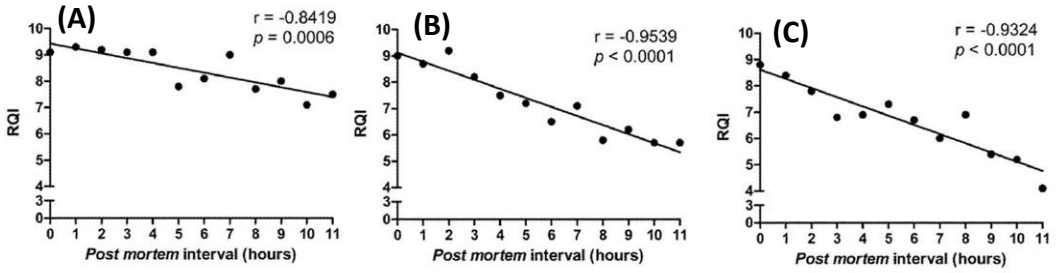

Figure 1.7: **Quality of RNA extracted from (A) heart, (B) skeletal muscle and (C) liver tissue, over an 11 hour post-mortem interval**. A significant linear correlation exists between the RNA quality index (RQI) and post-mortem interval in all three tissue types over this short duration. It can be seen that the drop in RQI over the period is most pronounced in liver tissue, indicating that RNA is least stable in this tissue type. Illustration from (6).

In addition to the RNA quality index (RQI), Sampaio-Silva *et al*. (6) were able to illustrate a significant linear relationship between the post-mortem interval and the measured quantity of a number of mRNA transcripts in skeletal muscle and liver. Six endogenous control RNAs exhibited a linear decline in their detected quantity over time (relative to that of Rps29) – Actb, Gapdh, Ppia and Srp72 in skeletal muscle, and Alb and Cyp2E1 in liver (Figure 1.8). Rps29 was selected upon

which to normalise this data by the authors who claim it to be stable in both skeletal muscle and liver tissues.

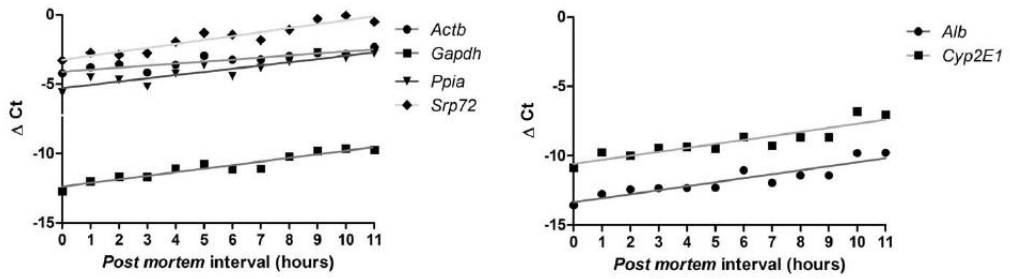

Figure 1.8: **Expression level of six RNAs in mouse (A) skeletal muscle and (B) liver tissue, over an 11 hour post-mortem interval**. The raw C_T obtained upon RT-qPCR amplification of all six transcripts (Actb, Gapdh, Ppia, Srp72, Alb and Cyp2E1) has been normalised to that of Rps29 by means of the ΔC_T. Illustration from (6).

Unfortunately, there are several issues with the experimental design adopted by Sampaio-Silva *et al*. (6) which affect the reliability of these outcomes. All tissue samples examined were recovered from the animal at the time of death and allowed to decompose *ex vivo*. Once tissue is removed and the integrity of the body is disturbed, RNA becomes exposed to external RNases and other agents. As a result, it may be expected that RNA in tissues *ex vivo* exhibits different decay behaviour to those still encased within the body. Additionally, natural decomposition exhibits a degree of inherent variability between individuals, and it is reasonable to expect that this variability is significantly reduced when decomposition is performed in a test tube separate from surrounding organs and organ systems. Obviously, this does not truly reflect the situation *in vivo*, where the corpse is allowed to decay as a whole as would occur in a practical setting. This issue will be considered in more detail in Chapter 6. Sampaio-Silva *et al*. have attempted to address this issue, by analysing a very small number of tissue samples decomposed *in vivo* and matching them up somewhat successfully with the results presented within the study.

In addition, the normalisation of real time PCR data in post-mortem tissues to a single endogenous control gene (Rps29, Figure 1.8) is a somewhat debatable procedure, given that natural degradation/decomposition is expected to affect *all* RNAs. Even studies using pristine clinical samples have expressed doubt over the existence of a 'universal' endogenous control gene for normalisation (78, 79). Sampaio-Silva *et al*. pertain that this data analysis method was suitable for their data set, and that Rps29 exhibited a high level of reproducibility across the 11 hour post-mortem interval investigated. However, this method is extremely unlikely to be acceptable long-term, and new methods of gene expression data normalisation need to be explored which are more appropriate to degraded post-mortem tissue RNA.

Li *et al*. (80) took a different approach to post-mortem interval determination by quantifying the decay of 18S rRNA and microRNA 1 (miR-1) in rat tissues over the first 7 days following death. They propose that during the first 48 hours following death, the detected quantity of 18S rRNA increases (Figure 1.9A) as a result of ribosome degradation (particularly the structural proteinaceous component) and 18S rRNA release. Following this, 18S rRNA was visibly degraded resulting in a parabolic relationship between the detected quantity of 18S rRNA and post-mortem interval. On the contrary, miR-1 was found to be relatively stable, especially over the first 96 hours following death (Figure 1.9B). Li *et al*. suggest that the extremely short length of miRNAs (21-25 nt) makes them more robust and less prone to degradation than other RNA types such as mRNA or rRNA (80). This makes them good candidates for data normalisation purposes when working with poor quality post-mortem RNA samples.

This parabolic relationship between RNA expression and post-mortem interval identified by Li *et al*. (80) is in stark contrast to the linear relationship presented by Sampaio-Silva *et al*. (6). In addition, this approach of using miRNAs seems to have more merit than Sampaio-Silva *et al*.'s approach of using a single mRNA for normalisation, which is already known to be fraught with issues (6). However, significantly more work is required to study the degradation of miRNAs in post-mortem tissue. There is much less published material evaluating the use of

miRNAs as endogenous controls in clinical samples. As such, it is essential that the expression profiles of these miRNAs is deemed to be stable and uninducible, even in response to different causes of death.

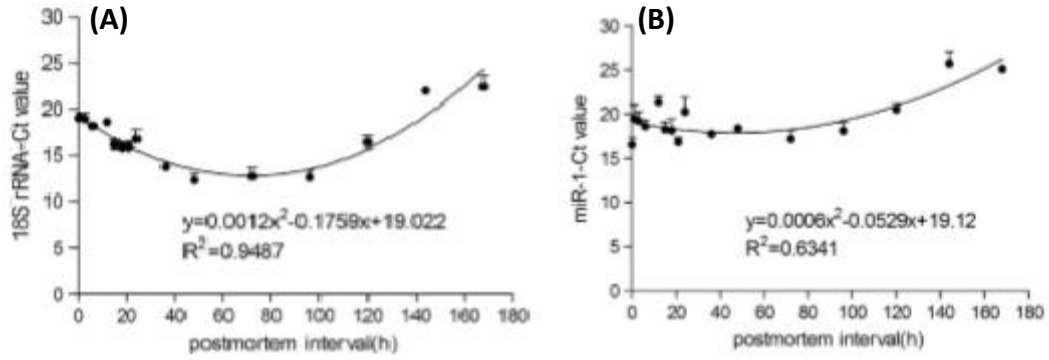

Figure 1.9: **Expression of (A) 18S rRNA and (B) microRNA 1 (miR-1) in rat heart tissue over a 7 day (168 hour) post-mortem interval**. A parabolic relationship between the quantity of 18S rRNA and miR-1 and the post-mortem interval was established. It can be seen that the quantity of 18S rRNA increased significantly during the first 48 hours post-mortem, manifesting in a reduction in C_T.

These three key studies have all shed a positive light on the use of RNA as an indicator of post-mortem interval. However, the literature in this area is not always optimistic and a number of studies conducted on human material have expressed difficulty in making a correlation between the post-mortem interval and RNA quality. One such study is that of Koppelkamm *et al*. (81), who examined the quality of RNA (defined by the RNA integrity number, RIN) recovered from human brain, heart and skeletal muscle tissue over a 42 hour post-mortem interval. They were only able to illustrate a significant linear correlation between the post-mortem interval and RNA quality in cardiac muscle tissue samples; not in brain or skeletal muscle (Figure 1.10).

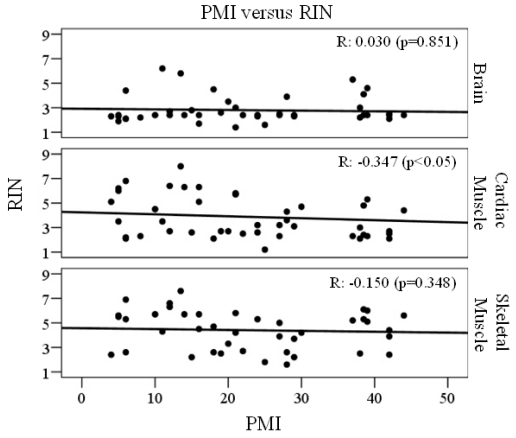

Figure 1.10: **Relationship between the post-mortem interval (PMI) and RIN in human brain, cardiac and skeletal muscle samples**. Only cardiac muscle demonstrated a significant correlation between PMI and RIN; no such relationship could be illustrated in either of brain or skeletal muscle. Illustration from (81).

Similarly, Heinrich *et al*. (72) were unable to make a correlation between the quantity of five endogenous control RNAs (ACTB, B2M, CYPA, TBP and UBC) and post-mortem interval (up to 118 hours) in human brain, heart and muscle. In a parallel study, Heinrich *et al*. (82) were also unable to demonstrate a correlation between the quantity of GAPDH mRNA and post-mortem interval (up to 118 hours) in any of human brain, heart, skeletal muscle, liver, kidney or spleen tissue. Using microarray technology, Preece *et al*. were unable to ascribe a significant relationship between the post-mortem interval and the quantity of intact ACTB mRNA in human brain tissue (83). Finally, Miller *et al*. (84) were unable with human brain tissue samples to illustrate a correlation between post-mortem interval and the results of RT-qPCR analysis for four endogenous control gene RNAs. In none of these studies were the authors able to pinpoint an exact reason for the strong variability in their data.

These outcomes clearly highlight that it is not the mere time span between death and sampling that determines the quality of the transcriptome, and that other factors must be in play influencing the rate of RNA degradation. When working with human samples, one has to accept their inherent heterogeneity with regard to: subject age, gender, BMI, ethnicity, diet/malnutrition, drug

administration, trauma, cause of death, and ambient conditions during the post-mortem interval (72).

Some of these factors have already been demonstrated to have a profound effect on RNA degradation. For example, Koppelkamm *et al*. (81) demonstrated that in the skeletal muscle of subjects with a BMI > 25 kg/m^2 (classified as overweight), post-mortem RNA quality was significantly reduced. This was proposed to be a product of the insulation provided by subcutaneous fat which slows the rate of cadaver cooling in the hours following death, contributing to increased RNase activity. Tissue type has been shown in a number of studies (6, 81, 85, 86) to be a strong indicator of RNA quality. Skeletal muscle and heart tissue consistently prove to be sources of intact, high quality RNA; whereas RNA in liver, pancreas and skin tends to be more heavily fragmented. This is proposed to be due to the high RNase content of these tissue types (liver in particular), relative to the fibrous nature of skeletal and cardiac muscle (6).

It is already accepted that the ambient conditions during the post-mortem interval strongly influence the rate of decomposition, including factors such as temperature, humidity, sunlight/UV and exposure (e.g. clothing, wrappings, burial or submersion in water). As such, it is expected that they too will have a significant effect on the rate of post-mortem RNA degradation. Elevated ambient temperature has been shown by Kuliwaba *et al*. (87) to accelerate RNA degradation in surgical bone samples stored in saline, at 4 °C and 37 °C.

It is impossible when working with autopsy tissue samples in research of this nature to keep these factors constant. As a result, the use of animal models for preliminary research has been advocated because of the ease with which these variables can be reduced/eliminated. This will be discussed in detail where it becomes relevant in subsequent chapters.

1.3.2.2.2 Gene expression analysis towards determination of the cause of death

The complement of RNAs present in a cell, referred to as the RNA 'pool' or the transcriptome, reflects the portion of a person's DNA which is actively in use to fulfil cell function. The transcriptome is not static but is a dynamic, constantly changing feature of the cell, affected for example by: cell type, cellular development, pathology, nutrition, drug intake, hormonal influences and environmental factors such as oxygen availability and temperature. Gene expression is tightly regulated at several levels; the rates of transcription and translation and also the turnover of specific mRNA transcripts modified in response to extracellular or intracellular stimuli. This flexibility in the transcriptome is essential for the sustenance of life as it allows the demands of the body to be met rapidly at a cellular and molecular level. Consequently, it is reasonable to conclude that most external events to which an organism is exposed will leave a 'mark' on the transcriptome, reflected in the **type** and **relative abundance** of expressed RNAs (4). This is anticipated to be much more sensitive to small-scale changes in cell physiology than conventional methods employed during an autopsy, which rely on the manifestation of these changes at such a level that they can be detected under a microscope or with the naked eye. If it were possible to fully characterise the effect of an 'event' on the transcriptome with reference to the expression level of specific RNA markers known to function in its response pathway, it may be possible to extrapolate back from a gene expression profile to identify the original unknown 'event' leading up to death.

As the induction and transcripion of new RNAs is an active process requiring energy input, it should cease relatively shortly after death. It is proposed that if the transcriptome is preserved in cells and tissues after death, RNA analysis at the point of a post-mortem examination should provide an insight into the activity of tissues and the conditions to which they were exposed at the time of death. Development of genetic profiling in this manner to supplement the conventional post-mortem examination has been termed loosely a '**molecular autopsy**'. To the forensic pathologist, clearly the most attractive application of gene expression profiling is in diagnosis of the cause of death, particularly in cases where conventional post-

mortem procedures are unsuccessful (88). Research considering the application of gene expression analysis to cause of death determination is in its infancy, but so far has suggested that the method holds promise.

Much of the literature available to date considers the use of transcriptome profiling for the diagnosis of death by asphyxiation (89-94). Asphyxia is a loose term used to describe deaths resulting from disturbance to oxygen supply, e.g. due to suffocation, smothering, strangling or choking. There are few universally applicable diagnostic features of asphyxial deaths, making confirmatory diagnosis difficult. mRNA analysis presents a novel means by which to assess the tissue response to oxygen deprivation at the transcriptional level. Several mRNA transcripts have been targeted and studied in both humans and animal models for this purpose, most selected on the basis of their involvement in the adaptive response to cellular hypoxia. Genes already shown to be up-regulated in response to hypoxia include: hypoxia inducible factor 1 (HIF-1), vascular endothelial growth factor (VEGF), erythropoietin (EPO) and glucose transporter 1 (GLUT-1); the immediate early genes c-fos and c-jun; the brain and atrial natriuretic peptides (BNP/ANP) and pulmonary surfactant associated proteins A1 and A2 (SPA-1/SPA-2) (89-96).

The identification of markers specifically expressed in the skin of mice killed by neck compression also displays promise that mRNA transcription also occurs during the supravital reaction; the short period between death of the organism and death of the individual component cells/tissues (97). Supravital transcription of mRNA would permit more prolonged gene regulation in response to the death 'event'. Additionally, some other works have identified the gene expression response of tissues to contusion stress (98, 99) and acute versus chronic drug (100, 101) and alcohol (102) administration. The long-term goal for this type of research would lie with construction of a gene expression database for diagnostic screening purposes (88).

1.3.2.2.3 Reactive gene expression analysis for wound ageing

Wounds can be inflicted on the body by a wide range of means, including blunt and sharp force trauma, burns, strangulation or suffocation (103). During the post-mortem examination, it is commonplace for wounds to be removed from the body for microscopic examination with the aim of estimating the age of the wound – i.e. the time interval between infliction of the wound and death (103). Wound healing is a complex but highly organised and controlled process, requiring the co-ordination of a number of inflammatory cell types in addition to growth factors, cytokines and adhesion molecules (76, 104). All of these contributors to the wound healing process are expressed at the wound site in a temporally-specific manner, and can be identified and quantified to try to estimate the age of the wound and also identify whether the wounds were pre- or post-mortem, and the order of their infliction (1).

Traditionally, this has been performed by immunohistochemistry (76). However, mRNA expression analysis poses a much more sensitive and quantitative tool by which this can be achieved (1). In the tissue surrounding the wound, new mRNAs encoding for proteins involved in the tissue response to injury are transcribed. A wide range of cytokine and growth factor mRNAs have been subject to analysis for this purpose. Those demonstrating up-regulation of their expression in wounded tissue include: interleukins 1α, 1β, 6, 8 and 10 (104, 105); basic fibroblast growth factor (105-107); keratinocyte growth factor (107); tumour necrosis factor 1α (104, 105, 108); transforming growth factors β1 and β3 (105); macrophage inflammatory proteins 1 and 2 (108); and tissue type plasminogen activator (109). Each has been demonstrated to exhibit its own unique time line of expression during the wound healing process. Characterisation of the temporal expression of these mRNAs and other, as yet uncharacterised RNAs lends itself to the development of a novel tool for wound age estimation and determination of survival time.

1.4 Practical analysis of RNA

Gene expression analysis is performed in exactly the same way regardless of whether the biological substrate is a body fluid sample, contact trace, or human/non-human solid tissue sample. Initially, RNA is extracted from the biological sample and its concentration can be quantified and its quality assessed. Following this, RNA is reverse transcribed into cDNA and the cDNA amplified either by endpoint or quantitative PCR. The following section provides background technical information on each of these stages in gene expression analysis.

1.4.1 Extraction and purification of RNA from biological samples

Prior to any nucleic acid analyses, body fluids and solid tissues must undergo **extraction** to obtain an extract of pure RNA (or DNA) with which to work. This extraction process has three main stages (9):

1. To liberate RNA-containing cells from a solid substrate (e.g. a swab) or to homogenise solid tissue samples to release their individual constituent cells
2. To break open the cell membrane, releasing RNA into solution
3. To remove unwanted components of the biological material, such as proteins and lipids

1.4.1.1 Extraction and purification of RNA: Silica column technology

A wide range of extraction techniques have been developed for this purpose and of these, silica column-based RNA purification is the most widely used in a forensic context due to its ease and speed of use, automatability and minimal reagent toxicity (110). This method is currently an accepted standard in published forensic RNA research, for example being adopted and recommended in research validation exercises arranged by the RNA branch of the European DNA Profiling Group (EDNAP) (C. Haas, personal communication) (3, 111).

As with all nucleic acid extraction protocols, under this system biological specimens first undergo lysis to solubilise RNA. For samples dried onto a surface such as a swab or swatch of fabric, the cells must be released into liquid mechanically by vigorous vortexing. Solid tissue samples on the other hand must be homogenised, using a device such as a rotor-stator disperser.

Both are achieved in a lysis buffer containing sodium dodecyl sulfate, guanidinium thiocyanate, and β-mercaptoethanol. Collectively, these dissolve the phospholipid-based cell and organellar membranes allowing the cell contents – including RNA – to be released. Additionally, they denature proteins such as DNases, RNases and other damaging enzymes to preserve nucleic acids (9, 112, 113).

The resultant cell lysate can then be passed through a silica membrane comprised of microscopic glass fibres, onto which RNA is captured (114). This process is facilitated by the chaotropic salt guanidinium thiocyanate, which forms hydrated ions with water. This disrupts the shell of hydration around both RNA and the silica membrane, making it more energetically favourable for RNA to adsorb to the silica. The actual molecular basis of this interaction is poorly understood, but it has been proposed that the guanidinium ions form a bridge between the negatively charged RNA and silica to permit their interaction by ionic bonding (112). Silica columns containing adsorbed RNA can be washed repeatedly with ethanol to remove non-nucleic acid impurities, and pure RNA subsequently eluted into water (9).

1.4.1.2 Extraction and purification of RNA: Liquid-liquid extraction

Rather than using a solid phase for immobilization of RNA, this method is a liquid-liquid extraction system which relies on the partition of nucleic acids into aqueous solvents and proteins and lipids into organic solvents (115, 116). TRI Reagent® is a proprietary mixture containing primarily phenol, Tris buffer and guanidinium thiocyanate, a potent protein denaturant and RNase inhibitor. Initially, TRI Reagent® is added to cells/tissue along with 1-bromo-3-chloropropane or

chloroform. Upon centrifugation the mixture separates into a biphasic emulsion: RNA partitioning in the aqueous phase and proteins and lipids into the organic phase. At an acidic pH, DNA partitions at the interface between the two, as demonstrated in Figure 1.11.

Upon removal of the aqueous phase, RNA can be precipitated out of solution in isopropanol and centrifuged into a solid pellet, as illustrated in Figure 1.11. This pellet of RNA is rinsed in ethanol to reduce any contamination and re-dissolved in water in pure, clean form.

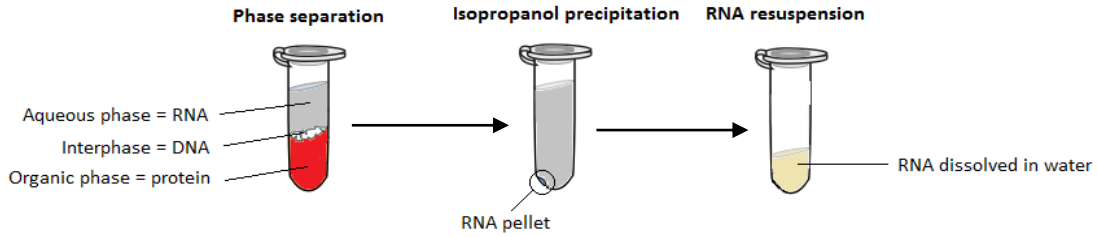

Figure 1.11: **Purification of RNA using the TRI Reagent® protocol**. Tissue samples are first homogenised in TRI Reagent®. RNA partitions into the aqueous phase, and can be precipitated out of solution with isopropanol, washed, and resuspended in water.

This technique is highly regarded in molecular biology due to its very efficient tissue lysis, resulting in high yield and high molecular weight RNA (117, 118). Silica column based methods tend to cause RNA loss due to repeated 'washing' and induce shearing of RNA into smaller fragments, making organic extraction favourable in instances where this may pose a problem (118). However, the laborious nature of the procedure, subjectivity (caused by manual phase separation) and the extremely toxic nature of chemicals such as phenol (which is flammable and strongly corrosive) make this method wholly impractical for routine use in forensic laboratories; hence the high uptake of column based systems (118).

1.4.2 Quantification of RNA: UV-visible spectrophotometry

It is important that the concentration of RNA present in a sample is quantified to ensure the success of downstream analyses. UV-visible spectrophotometry is a simple and rapid technique for gross examination of the quantity and purity of total RNA in an extract. Nucleic acids (incorporating both DNA and RNA) have a characteristic absorbance spectrum in the wavelength range from 220 to 350 nm, as illustrated below in Figure 1.12.

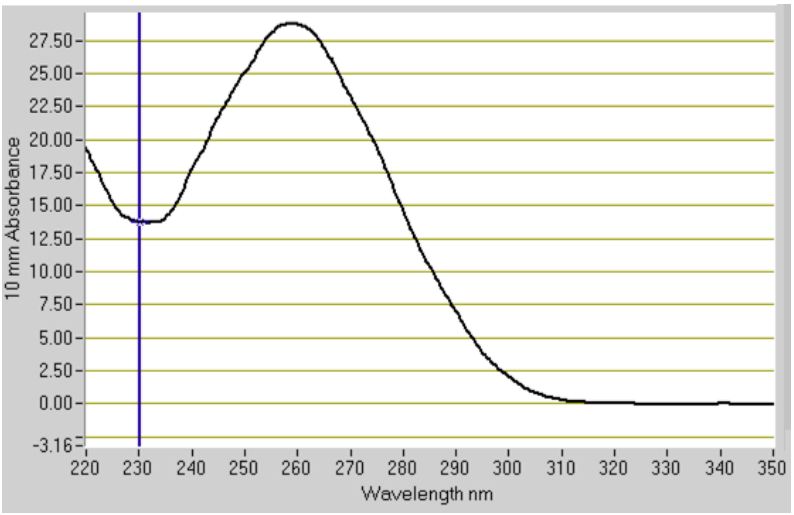

Figure 1.12: **Absorption profile of an RNA sample in the wavelength region 220 to 350 nm**. Absorption maximum of RNA occurs at 260 nm; in this case corresponding to an RNA concentration of 1148 ng/µL, an $A_{260/280}$ of 2.00 and an $A_{260/230}$ of 2.00. Graph illustrates the raw data output from a Nanodrop-1000 spectrophotometer.

Photons of UV light are absorbed by the conjugated π-systems present in the aromatic rings of the bases (adenine, guanine, cytosine and uracil) of each nucleotide in the RNA strand (119). These photons are absorbed as they match the energy required for an electronic transition within the molecule, allowing an electron to be promoted from the highest occupied molecular orbital to the lowest unoccupied one. As a result, each nucleotide base possesses its own unique absorption spectrum (119). However as a whole, RNA absorbs UV light maximally at

~260 nm wavelength, illustrated by the absorption peak at this wavelength in Figure 1.12 (120).

The absorbance of a nucleic acid sample is directly proportional to the number of absorbing molecules in the light beam, i.e. the RNA concentration. Unfortunately, the absorbance profile of RNA is practically indistinguishable from that of DNA (121) meaning that RNA extracts must be treated with DNase to remove DNA contamination prior to RNA quantification by UV-visible spectrophotometry (122). This concentration of an RNA sample can be calculated using the **Beer-Lambert law** based upon its absorbance at 260 nm (114):

$$A = log_{10}\left(\frac{I_o}{I}\right) = \varepsilon\, c\, L$$

Where ***A*** represents the absorbance of the RNA sample at 260 nm (in optical density units, or mL cm^{-1}), $\boldsymbol{I_o}$ is the incident light intensity, ***I*** the transmitted light intensity, $\boldsymbol{\varepsilon}$ the extinction coefficient for RNA (40 ng cm mL^{-1}, or 8,500 M^{-1} cm^{-1}), ***c*** the concentration of the RNA sample (in ng/µL) and ***L*** the light path length through the sample (both 1 mm and 0.2 mm measured). Although the extinction coefficient of RNA varies by base composition and is also affected by base pairing (which significantly reduces absorbance), 40 ng cm mL^{-1} is typically used as a standard value for ε for most molecular biology applications (119, 121, 123, 124).

Many other organic molecules besides nucleic acids absorb UV light in this wavelength range 220 to 350 nm, because of their strongly conjugated structures. This is useful, allowing us to make a crude assessment of RNA sample contamination by examining its larger UV spectrum. Proteins absorb strongly at 280 nm, particularly the amino acids tryptophan, tyrosine and cysteine (125). Thus, an A_{260}/A_{280} absorbance ratio of 2 ± 0.1 suggests a sample with little protein contamination (114, 126-128). In addition, contaminants such as phenol and chaotropic salts, remnants of the extraction protocol, can be identified by their absorbance at 230 nm (128).

UV-spectrophotometry however, is not able to make an assessment of the integrity or amplifiability of RNA, only to define the concentration (5, 129). The

absorbance of an RNA sample is primarily defined by the concentration of nucleotides, which occurs similarly in both intact and fragmented RNA. The absorbance of a nucleotide is known to be affected by neighbouring nucleotides (both those to which they are hydrogen bonded and those covalently attached in the RNA strand) (123).

For this research, RNA concentration has been estimated using the Nanodrop ND-1000 UV-visible microspectrophotometer (Thermo Scientific) (130). This method is favoured due to its low sample consumption, with only 1-2 µL of RNA extract required for quantification. The RNA sample is applied to a small pedestal and the instrument uses a pulsed xenon flash lamp light source to deliver UV light through it (in the wavelength range 220 to 350 nm). The transmitted light is then delivered through a fibre optic cable to a linear CCD array for assessment of the proportion of absorbed/transmitted light. The instrument computes the RNA concentration (in ng/µL) using the Beer-Lambert law, presenting this alongside the $A_{260/280}$ and $A_{260/230}$ ratios to give a straightforward and convenient results read-out.

1.4.3 Quality analysis of RNA: The RNA integrity number algorithm

RNA is rapidly degraded by RNase enzymes which are ubiquitous to tissues, bodily fluids and the general environment (Section 1.2.4, Chapter 1) (131). This fragmentation compromises our ability to reliably quantify the expression level of individual RNAs; the primary goal for most clinical and forensic analyses. It is therefore standard practice to make an assessment of the fragmentation state of a total RNA sample prior to more specific gene expression analysis. This is achieved by targeting the ribosomal RNAs (rRNAs) which form a major structural component of the ribosome and comprise more than 90% of cellular RNA.

Traditionally, assessment of RNA fragmentation has been performed using standard slab gel electrophoresis to separate out the RNA molecules in a mixed sample according to their length in bases (114). The progressive fragmentation of RNA is reflected in a gradual shift towards smaller fragment sizes. However, the low reproducibility, interpretational subjectivity and poorly quantitative nature of gel

electrophoresis has fuelled the development of more robust measures of RNA quality (131). Although several methods are available, one of the most widely used and trusted is the Bioanalyzer 2100 (Agilent Technologies) (131).

The Bioanalyzer 2100 is an automated, microfluidic electrophoresis system permitting voltage-induced size separation coupled with laser induced fluorescence detection of nucleic acids (132). Its miniaturised scale permits analysis of the degradation state of as little as 200 pg of RNA. RNA samples, acrylamide gel (mixed with a nucleic acid intercalating dye) and electrophoresis run buffer are loaded into separate wells on a microfluidic chip, as illustrated in Figure 1.13A below (132).

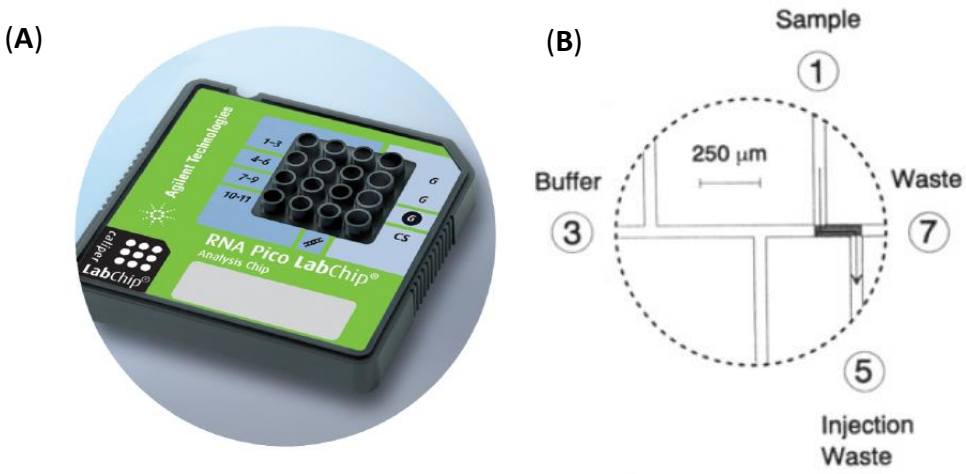

Figure 1.13: **Structure of Bioanalyzer 2100 RNA electrophoresis chip**. (**A**) The RNA sample, acrylamide gel and electrophoresis run buffer are placed into three distinct wells of the RNA 6000 Pico chip. (**B**) The microfluidic lanes of the chip are primed with acrylamide, and both buffer and the sample injected from their respective wells. Illustration from (133).

The chip is initially 'primed' with acrylamide gel using a syringe. The acrylamide gel is mixed with a proprietary intercalating dye, which inserts itself into the RNA structure to permit its indirect visualisation by laser induced fluorescence detection. During the run, individual electrodes are inserted into all RNA sample wells (of which there are 12) to create the current required for the separation of

RNA. RNA samples are electrophoresed sequentially, with each completed in 70 seconds.

A typical Bioanalyzer 2100 electropherogram output for an RNA sample is illustrated in Figure 1.14. Three primary peaks are visible in each electropherogram, the first of which is the marker: a 25 nucleotide long fragment of RNA added to all wells for quality control purposes. The two main peaks pertaining to the RNA sample are those of the 18S and 28S ribosomal RNAs, which together constitute over 90% of eukaryotic RNA (7, 9).

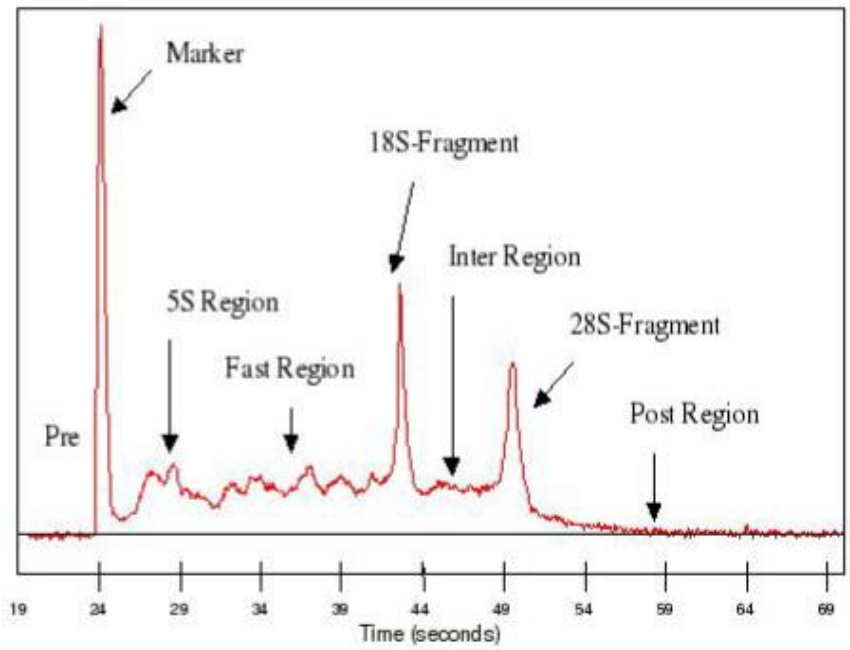

Figure 1.14: **Features of the RNA electropherogram utilised by the Bioanalyzer during calculation of the RNA integrity number (RIN).** The most notable features are the 18S and 28S rRNA fragments. mRNA degradation state can also be assessed with the baseline background level. For a detailed review of how the RIN algorithm works, read (131) from where this illustration was derived.

Using the features of this electropherogram output, the 2100 Bioanalyzer Expert Software defines the quality of an RNA sample using an algorithm known as the RNA integrity number (RIN) (131). The RIN is a predictive model measuring the quality of an RNA sample on a numerical scale between 1 (poor quality, completely

degraded RNA) and 10 (excellent quality, intact RNA) (131, 134). Although RNA degradation is a continuous process, the RIN algorithm aims to objectively and reproducibly quantify its severity and place the RNA sample into this numerical spectrum. The features of the electropherogram expected at different levels of RNA quality and the spectrum of estimated RIN values are illustrated in Figure 1.15.

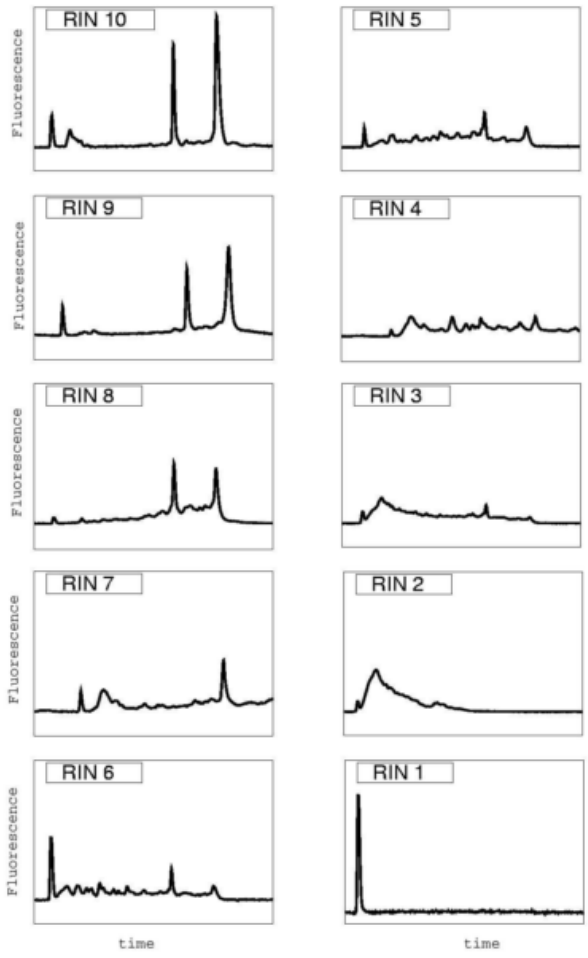

Figure 1.15: **Illustration of the spectrum of RNA degradation using the RNA integrity number (RIN) algorithm**. At the high quality end of the scale with a RIN of 10, the 18S and 28S rRNA peaks appear very distinct, with strong signal intensity and the baseline is flat. As the RNA quality reduces and thus the RIN, the rRNA peaks reduce in intensity and degraded RNA appears as a rugged or elevated baseline, and a shift to the left. Illustration from (131).

The basis of the RIN algorithm lies within a Bayesian artificial neural network which assesses a number of specific features within the RNA electropherogram, selecting those which permit the most efficient distinction between the RIN categories (131). Seven of the key features of the electropherogram used to compute the RIN of an RNA sample are summarised in Table 1.6.

Table 1.6: **Seven primary features of the RNA electropherogram used to compute RIN**. The 28S and 18S rRNA peak heights and/or areas are arguably the most important indicators of RNA quality, since they represent undegraded rRNA. Information collated from (131).

	Feature
1	Total RNA ratio: 28S + 18S rRNA peak area / total RNA area
2	28S region area / 28S peak height
3	28S area ratio
4	28S + 18S area / fast region area
5	Linear regression value at the end point of the fast region
6	Number of detected fragments in fast region
7	Presence or absence of 18S peak

Based on their structure and function in the cell, it is expected that different types of RNA (such as rRNA, mRNA, tRNA and the small RNAs) degrade at different rates in the cell. Although the RIN describes primarily rRNA because of the ease with which it can be managed (resulting from its high abundance), research has shown that the RIN is very closely correlated with the results of downstream quantitative RT-PCR targeting mRNA (81, 128) and is able to robustly identify very small changes in RNA integrity (135).

1.4.4 Reverse transcription of RNA into cDNA

The first step in gene expression analysis is reverse transcription, where RNA is converted into DNA. This type of DNA is known more specifically as complementary or 'copy' DNA (cDNA). This process is very similar to PCR in that, the reverse transcriptase enzymes which perform this step like DNA polymerases require an oligonucleotide primer on which to build the new cDNA strand complementary to the RNA template. Three priming strategies are commonly used for reverse transcription; all of which are described in Table 1.7.

Table 1.7: **Priming strategies used during reverse transcription of RNA into cDNA**. Information collated from (134, 136).

Priming strategy	Characteristics of primers	Anneals to
Random	Mixture of heterogeneous primers, usually 6-9 nucleotides in length	Wide range of target sequences in the total RNA population
Oligo (dT)	Primer consists of a tract of only nucleotides with thymine base	Poly(A) tail of mRNA
Gene specific	Designed using gene sequence databases similarly to PCR primers, to RT only specific RNA sequences	Only specific RNAs of interest

The choice of primer has a profound effect on the yield of cDNA, but there is no optimal priming strategy to use in all experimental designs (136). Random priming is most commonly implemented as it gives a more balanced covering of the entire transcriptome and improved cDNA yield (137). However, the 'randomness' of primer annealing commonly results in the production of more than one cDNA product length per RNA target – as primers of this type (hexamers – nonamers of indiscriminate sequence) can anneal anywhere along the length of the RNA molecule. Random priming is somewhat recommended when working with poor quality RNA samples (12, 137). Oligo (dT) priming is much less forgiving of RNA fragmentation, as it relies on the poly (A) tail of an RNA molecule remaining intact (138). In addition, it is unsuitable for analysis of ribosomal RNAs (such as the 18S

rRNA commonly used as an endogenous control RNA) which lack a poly (A) tail in their structure.

During the reverse transcription procedure, RNA is incubated with dNTPs, a reverse transcriptase enzyme (and the necessary buffer to provide optimal conditions for reverse transcriptase activity) and the primer type of choice. After primer annealing at low temperature (commonly 25 °C), reverse transcription of RNA into cDNA is initiated at ~37-50 ^{o}C and after a long period of primer extension, the reaction is terminated by heating at 85 ^{o}C to denature the reverse transcriptase. The process is not cyclical like PCR, but involves long periods of incubation. The outcome is that RNA is largely reverse transcribed into cDNA, which can be recognised by the *Taq* DNA polymerases employed in subsequent endpoint and real time PCR.

The efficiency of RNA to cDNA conversion during reverse transcription is extremely variable, influenced strongly by the characteristics of the reverse transcriptase type implemented and the quantity of RNA to be reverse transcribed (137). Some reports have suggested that the RNA to cDNA conversion efficiency can vary up to 100-fold, with typical measurements ranging from as little as 20% (139) up to 110% (137) for the Moloney murine leukaemia virus (MMLV) reverse transcriptases most commonly contained within commercially available kits (139). Despite the extremely poor understanding of this process, the conversion of RNA into cDNA is an essential step in gene expression studies and reverse transcription remains the only tool by which this can be achieved.

1.4.5 Gene expression analysis with the polymerase chain reaction

1.4.5.1 cDNA amplification by endpoint PCR and capillary electrophoresis

The polymerase chain reaction (PCR) is an enzyme-mediated process permitting *in vitro* replication of a specific DNA target sequence (140, 141). The boundaries of this target DNA sequence are defined using a pair of oligonucleotide

primers, which anneal to the template DNA and are extended with dNTPs by a thermostable *Taq* DNA polymerase (142).

The process is cyclical, controlled by raising or lowering the temperature of each PCR tube. Initially, DNA sequences are denatured into single-stranded form by heating the reaction mix to approximately 96 °C. Subsequently, the tubes are cooled to 55-70 °C to mediate the annealing of two oligonucleotide primers to the target sequence. At approximately 72 °C, the *Taq* DNA polymerase may replicate the target DNA, by extending the primers with dNTPs to form a contiguous DNA product. These three temperature steps are cycled often 20 to 40 times generating billions of copies of the original DNA target sequence, which can range in length from around 60 to thousands of bases. In this conventional format, PCR is termed 'endpoint' as the DNA products generated can only undergo further analysis after all PCR cycles have been completed. Endpoint PCR is not sufficiently quantitative and is generally only used as a presence/absence test for a particular DNA target. In the field of gene expression analysis, PCR is performed on the cDNA products of reverse transcription as *Taq* polymerase is specific to DNA; not RNA.

In order to analyse the resulting products of an endpoint PCR reaction they can be resolved by electrophoresis – more specifically, capillary electrophoresis – which separates out the amplified DNA fragments according to their length in bases. All data presented throughout this thesis has been generated using the Applied Biosystems 3130 Genetic Analyzer capillary electrophoresis platform. On this platform, PCR products are electrokinetically injected into a 50 µm glass capillary filled with uncrosslinked dimethylacrylamide (more commonly known as POP™) and separated through it by the application of an approximately 15 kV voltage across the capillary (143). The PCR products are detected and identified by laser induced fluorescence detection: labelled with a fluorescent dye on the 5' end (e.g. 6-carboxyfluorescein (6-FAM), 6-carboxy-4',5'-dichloro-2',7'-dimethoxyfluorescein, succinimidyl ester (JOE), 6-carboxytetrametylrhodamine (6-TAMRA)) which is covalently bound to the oligonucleotide primer. These fluorophores are excited with an Ar^+ laser and the emitted fluorescence detected with a CCD camera. The result is an electropherogram in which each fluorescently

labelled PCR product features as a peak of a specific length in nucleotides (Figure 1.16).

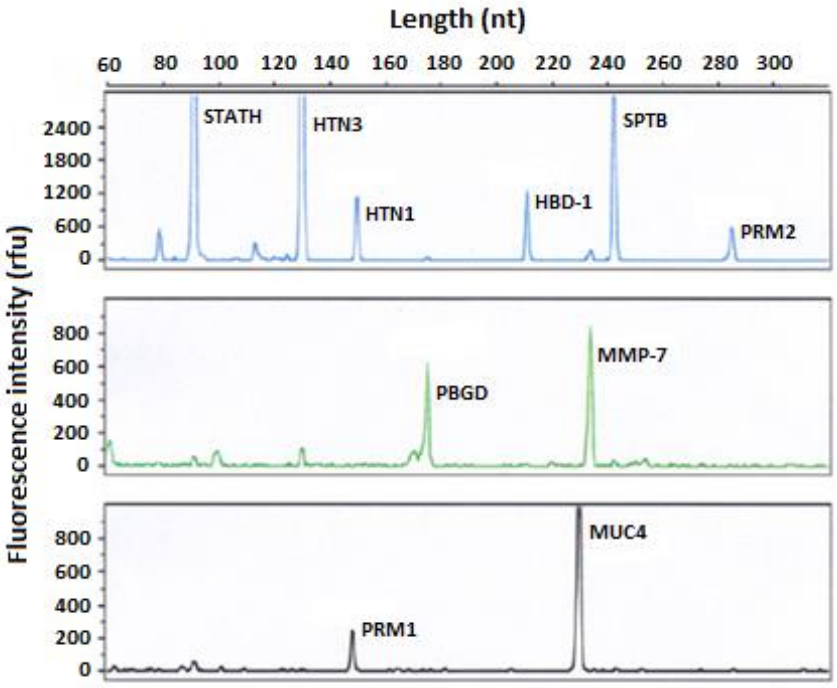

Figure 1.16: **Multiplex endpoint PCR result using RNA extracted from a blood, saliva, semen, menstrual blood and vaginal secretion mixture on a single swab**. RNA marker peaks can be seen representing all five body fluid types: SPTB and PBGD represent blood, STATH, HTN3 and HTN1 represent saliva, PRM1 and PRM2 represent semen, MMP-7 represents menstrual blood, and MUC4 and HBD1 represent vaginal secretions. Three fluorescent dyes have been used for detection of the PCR products, designated in blue, green and black. Illustration reproduced from (47).

1.4.5.2 cDNA amplification by real time PCR

Reverse transcription quantitative PCR (RT-qPCR) is currently the method of choice for most gene expression applications, forensic or otherwise (144). The kinetics of the endpoint PCR reaction do not allow for reliable quantification of the starting quantity of a nucleic acid target in a biological sample – only the presence or absence of a cDNA corresponding to a particular RNA marker (145). Real time PCR is different in that it monitors the accumulation of an amplicon throughout the duration of the PCR reaction, rather than only at the end. 'Monitoring' the progress

of a PCR reaction can be achieved using several reporting chemistries. Through this thesis two approaches have been used: the non-specific DNA binding dye SYBR® Green I, and the use of *TaqMan*® hydrolysis probes.

In real time PCR with SYBR® Green I, reactions are set up in an identical manner to endpoint PCR except that the SYBR® Green I dye is added to the PCR mixture (134). SYBR® Green I intercalates with double stranded DNA (dsDNA) by inserting itself in between the base pairs of the minor groove, stabilised by electrostatic interactions and van der Waals forces (146). As the PCR proceeds and dsDNA products are generated by *Taq* DNA polymerase, multiple SYBR® Green I dye molecules can intercalate within each PCR product as illustrated in Figure 1.17 (134). When unbound from dsDNA, SYBR® Green I has a low level of fluorescence. However, the dsDNA-SYBR® complex is strongly excited by light of wavelength 497 nm which matches the energy required for an electronic transition in the molecule, and emits at 520 nm.

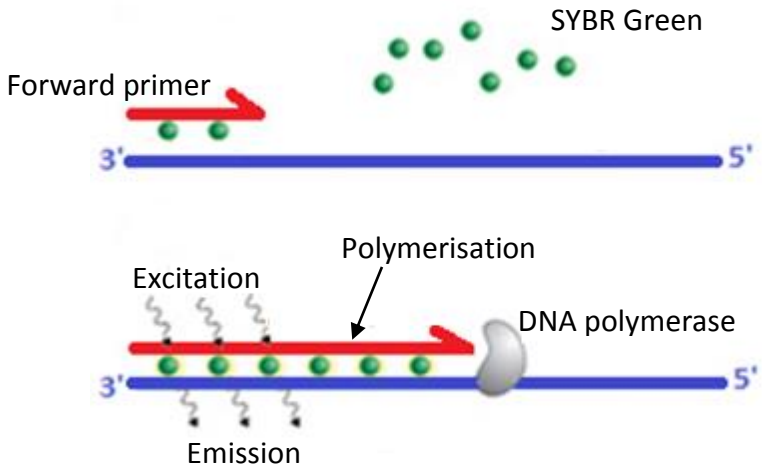

Figure 1.17: **Mechanism of SYBR Green I in monitoring the accumulation of PCR products**. Initially, SYBR® Green I is in unbound form, when no dsDNA has been generated. As DNA polymerase extends the forward primer, SYBR® Green I dye intercalates with the newly formed dsDNA. The resultant DNA-SYBR® Green I complex is excited by light of wavelength 497 nm, and emits light of wavelength 520 nm.

At the end of every PCR cycle, samples are illuminated by a lamp within the real-time PCR instrument. In the case of the Stratagene Mx3005P available for this

research, the light source is a quartz tungsten halogen lamp. Monitoring the emission of light of wavelength 520 nm by SYBR® Green I is used to quantify the accumulation of PCR products (147).

On the converse, the key distinguishing characteristic between conventional PCR assays and the *TaqMan*® assay (144) is in the addition of a dual labelled non-extendible hybridisation probe, generally 20 to 30 bases in length, to the reaction mix (148). This probe has two dyes covalently linked to/near the ends: a 5' proximal reporter dye, and a 3' proximal quencher dye (145, 149). As with SYBR® Green I, the reporter dye (6-FAM) can be excited by light of a specific wavelength generated by the real time instrument. When the probe is intact, this energy is transferred by fluorescence resonance energy transfer (FRET) to the quencher dye (6-TAMRA), whose absorption wavelength matches the emission wavelength of the reporter dye. The quencher dye emits this energy as light of a higher wavelength (144) (Figure 1.18). Quenching is dependent on the close proximity between the two dyes, assisted by secondary structure adopted by the probe (149).

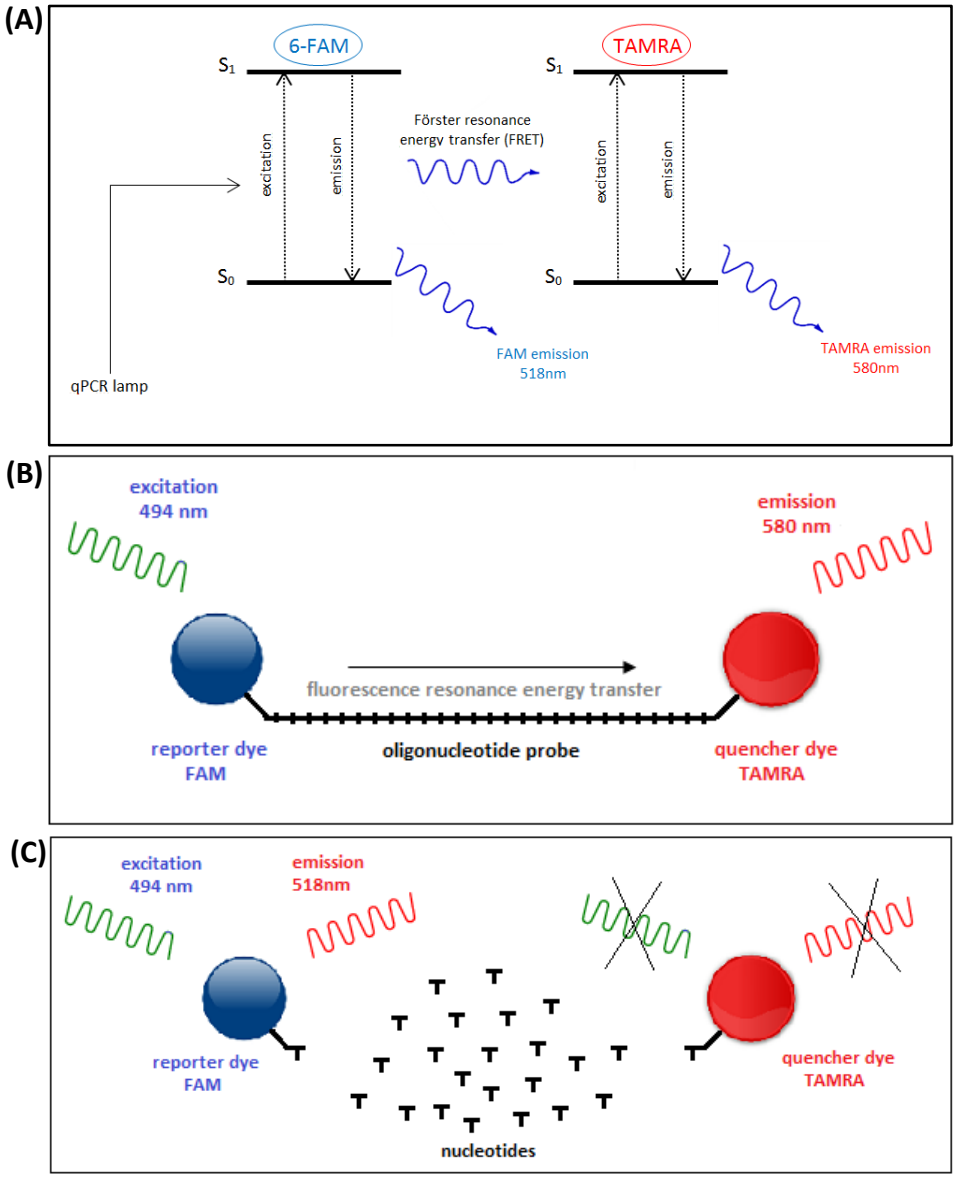

Figure 1.18: **Mechanism of Förster/fluorescence resonance energy transfer (FRET).** (**A**) Light of a specific wavelength is absorbed by the reporter dye, as this matches the energy required for an electronic transition in the molecule. In the case of 6-FAM, the excitation wavelength is 494 nm. 6-FAM's emission wavelength (518 nm) matches the excitation wavelength of the quencher dye, 6-TAMRA. (**B**) Prior to amplification and probe digestion, energy absorbed by the reporter dye is transferred to the quencher (6-TAMRA) which emits it as light of higher wavelength. (**C**) Digestion of the probe by *Taq* polymerase during amplification of a target sequence of DNA abolishes this FRET linkage between the two dyes, and fluorescence of the reporter dye can be detected.

During the annealing step of PCR, this probe is designed to hybridise to cDNA between the forward and reverse primer binding sites, as illustrated in Figure 1.19. As the primer is extended by *Taq* polymerase during the extension step of PCR, its inherent 5'-exonuclease activity (150-152) cleaves the 5' terminal of the *TaqMan®* probe in a nick-translation reaction, progressively releasing the probe as mono- and di-nucleotides ((150, 152, 153) (Figure 1.19). This removes the FRET connection between the reporter and quencher dyes, permitting emission of light of a specific wavelength determined by the reporter dye (in the case of 6-FAM, at 518 nm) (Figure 1.18). The emission of light by the reporter and quencher dyes is monitored at the end of every PCR cycle (154).

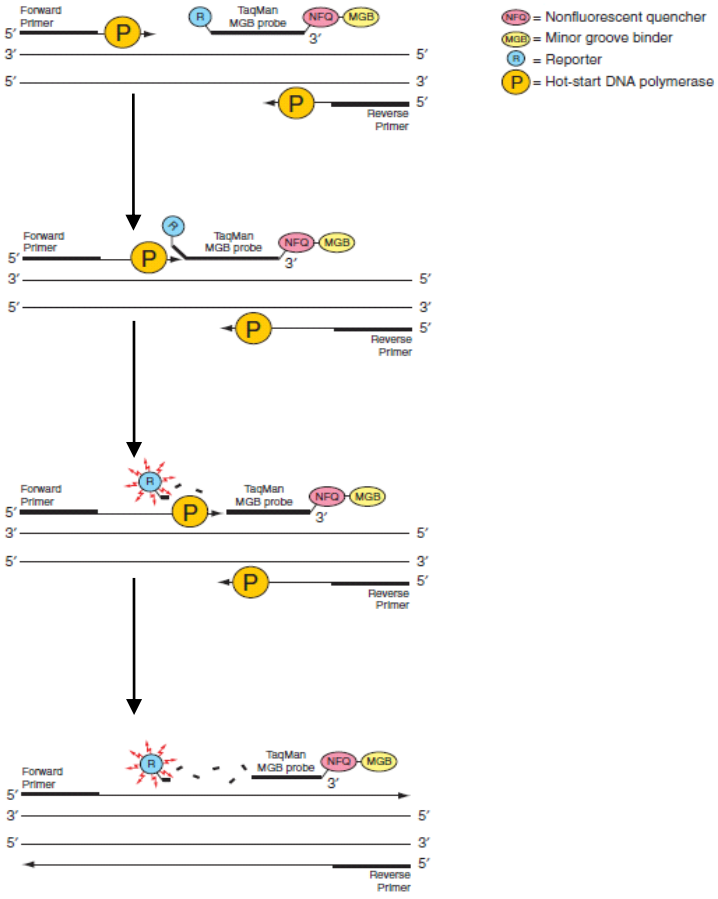

Figure 1.19: **Overview of real time PCR with *TaqMan®* 5' nuclease assay**. Amplification of the target DNA (thin black line) results in digestion of the *TaqMan* probe, so that the reporter and non-fluorescent quencher dyes are separated, and 'quenching' of fluorescence ceases. This gradual increase in fluorescence is detected by the real time PCR equipment after every cycle of amplification. Illustration reproduced from *TaqMan®* Universal PCR Mastermix Handbook (155).

The process of 'monitoring' is exactly the same, whether real time PCR is performed with SYBR® Green I or with a *TaqMan*® probe. Samples are illuminated by a quartz tungsten halogen lamp during the elongation phase of qPCR, and the real time PCR instrument measures the fluorescence emission spectrum with the use of a CCD camera (148). The fluorescence signal emitted accumulates as the PCR reaction progresses in a manner proportional to the quantity of amplification products (145). Amplification plots are typically sigmoidal in shape, as illustrated in Figure 1.20. During the initial cycles, no PCR product is detected as their concentration is below the detection threshold. This is followed by a period of exponential amplification, linear amplification and a final plateau phase in which the reaction is 'exhausted' and no significant product accumulation takes place. The threshold fluorescence is always set during the exponential phase, meaning that quantity measurements will be unaffected by limited reaction components during the plateau (156).

Quantification of the starting template of cDNA is achieved by setting a cycle 'threshold' (C_T) or cycle of quantification (C_Q) – an arbitrary fluorescence value above which the fluorescence signal is recognised as due to accumulation of the cDNA target and not as a result of background fluorescence (134, 156, 157). Several methods have been described for determination of the fluorescence threshold (157). All data described in this report has been generated using a threshold fluorescence level set automatically by the real time PCR instrumentation at ten times the standard deviation of the baseline fluorescence variation over PCR cycles 5 to 9.

The C_Q is the number of cDNA amplification cycles required for the fluorescence plot to cross this threshold level. The C_Q is inversely proportional to the starting quantity of the cDNA template of interest, permitting extrapolation back from the C_Q to an unknown starting cDNA concentration by comparison to a standard curve (148). The higher the initial copy number of the target nucleic acid the lower the number of cycles required to reach threshold and thus the further left the amplification plot (Figure 1.20).

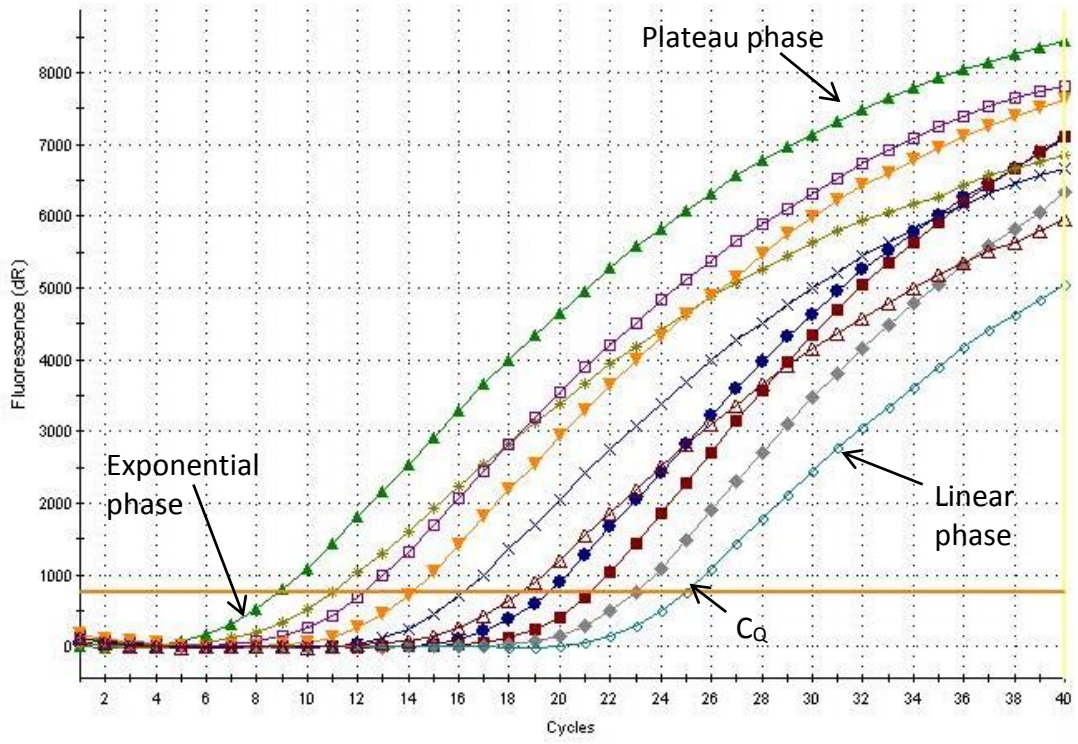

Figure 1.20: **Accumulation of qPCR products**. This illustration represents a standard curve of mouse cDNA ranging from 200 ng/µL to 0.001 ng/µL, assayed for the 18S rRNA reverse transcript. The fluorescence threshold line is denoted in orange.

One particularly unique feature of real time PCR with SYBR® Green I is that after all PCR cycles have been completed, the specificity of the PCR reaction can be assessed using a 'melt' or dissociation curve to ensure that only a single PCR product has been generated (158). The temperature of dissociation of the two strands of a dsDNA PCR product is strongly dependent on its length and sequence (particularly the GC-content). As such, by progressively heating the PCR mixture, the PCR product will eventually 'melt' at a specific temperature, causing a drastic reduction in SYBR® Green I fluorescence (158). For PCR amplifications where a single dsDNA product has been generated as is desired, the dissociation curve should be characterised by a single 'spike' in SYBR® Green I fluorescence. An example dissociation curve is included in the quality control data presented in Appendix 1, Figure A1.4, for illustrative purposes. It is standard protocol to generate a dissociation curve for all qPCR assays used with SYBR® Green I as part of strict quality assurance.

RT-qPCR in this form is a strongly favoured technique for gene expression analysis as a result of its impressive sensitivity, specificity, reproducibility and wide quantification range (72, 128, 134).

1.4.5.3 RT-qPCR data interpretation and normalisation

There are two key approaches to the analysis of gene expression data: **absolute** and **relative** quantification. Absolute quantification involves the calculation of the cDNA (and ultimately RNA) copy number present in a sample for a given target; by comparison to a standard curve generated using a serial dilution of cDNA standards (159). However, the absolute copy number of an RNA is not necessarily of direct interest in most gene expression analyses. When conducting RT-qPCR experiments, it is difficult to directly compare samples because of differences in the input quantity of tissue/cellular material, its transcriptional activity, RNA extraction efficiency, RNA to cDNA reverse transcription efficiency, and qPCR efficiency (79). The extremely high sensitivity of RT-qPCR to minute fluctuations in gene expression means that experimentally-induced variation can be easily misconstrued as due to biological activity (160). Several methods have been suggested for the normalisation of RNA expression data, summarised in Table 1.8 (79).

Throughout this study, four of the five potential normalisation strategies have been implemented to try to minimise variation in RT-qPCR data. Wherever possible, the quantity of cells or solid tissue has been standardised using its mass. Once the RNA was extracted from tissues and contaminating DNA removed, the RNA concentration was normalised to 100 ng/μL. Relative quantification was performed using both ribosomal and messenger RNAs.

Table 1.8: **Methods for normalisation of RNA expression data**. Information collated from Huggett *et al*. (79).

Normalisation strategy	Details	Advantages	Disadvantages
Similar sample size	Use similar sample volume or tissue mass	Easy to do	Can be difficult to accurately estimate, e.g. on a balance Differences in cell type and cellular content still cause unavoidable variation
Total RNA quantity	Use similar RNA input, as measured by UV-vis spectrophotometry	Easy to do Ensures similar RT behaviour, prevents overloading	Doesn't control for error at the RT and qPCR stages Mainly based on the quantity of rRNA, which comprises > 90% of RNA
Reference RNAs: rRNA	Normalisation of C_Q values to that of 18S rRNA	18S rRNA is an internal control, so is subject to the same RT and qPCR influences Measured using the same method, RT-qPCR	Must be first validated to ensure rRNA stability Resolution is defined by the error and variability in 18S rRNA expression
Reference RNAs: mRNAs	Normalisation of C_Q values to that of endogenous control mRNAs such as Gapdh, Actb, B2m	Internal controls, so are subject to the same RT and qPCR influences Measured using the same method, RT-qPCR	Must be first validated to ensure endogenous control mRNA stability Resolution is defined by the error and variability in endogenous control RNA expression
'Spiked' in RNA	Normalisation of C_Q values to that of an exogenous control, a piece of synthetic RNA introduced to samples during the RNA extraction stage	Internal controls, so are subject to the same RT and qPCR influences Measured using the same method, RT-qPCR	Must first be designed and qPCR assays designed and tested Is not extracted from cells of interest

Relative quantification calculates the fold-change in the expression level of a cDNA target by normalisation to an endogenous control gene transcript. Most commonly, this is expressed as the difference (ΔC_Q) (161) or ratio (relative expression ratio or 'RER') (156) between two RNAs: the endogenous control RNA and the target RNA of interest (145). An endogenous control gene RNA is defined by a number of inherent characteristics in its expression: it is an RNA that is thought to be ubiquitously expressed in all nucleated cell types as the function of the encoded protein is essential for cell survival; and it is thought not to be induced in response to any physiological or pathological conditions (156, 161, 162). Endogenous control RNAs commonly implemented in published gene expression studies include 18S rRNA, glyceraldehyde-3-phosphate dehydrogenase (Gapdh) mRNA, β-actin (Actb) mRNA, and β_2-microglobulin (B2m) mRNA (161). Usually, the expression of these endogenous control genes is assumed to be stable and thus acts to normalise the input quantity of RNA. However this assumption is particularly controversial following the publication of a number of studies illustrating up- or down-regulation of these RNAs in particular cellular conditions (163-166).

Under the experimental design followed in Chapters 4 through 7 the input quantity of tissue and/or RNA generated for each sample could not be confidently standardised; making absolute quantification an inappropriate data analysis technique. Therefore, the data presented herein describes the results of relative quantity analysis using the $2^{-\Delta\Delta CQ}$ method described by Livak *et al*. (161). The $2^{-\Delta\Delta CQ}$ method is able to provide an estimate in the fold-change in the quantity/expression of one RNA relative to another. It assumes a 100% qPCR efficiency for all assays used during gene expression analysis. RNAs are analysed in pairs, and the difference between the raw C_Q values for each of the two RNAs calculated for every sample individually.

Using the RT-qPCR data presented in Figure 1.21 as an example, the difference between the measured C_Q (ΔC_Q) for glyceraldehyde-3-phosphate dehydrogenase (Gapdh) mRNA and hydroxymethylbilane synthase (Hmbs) mRNA was calculated for each of the 6 time points under investigation.

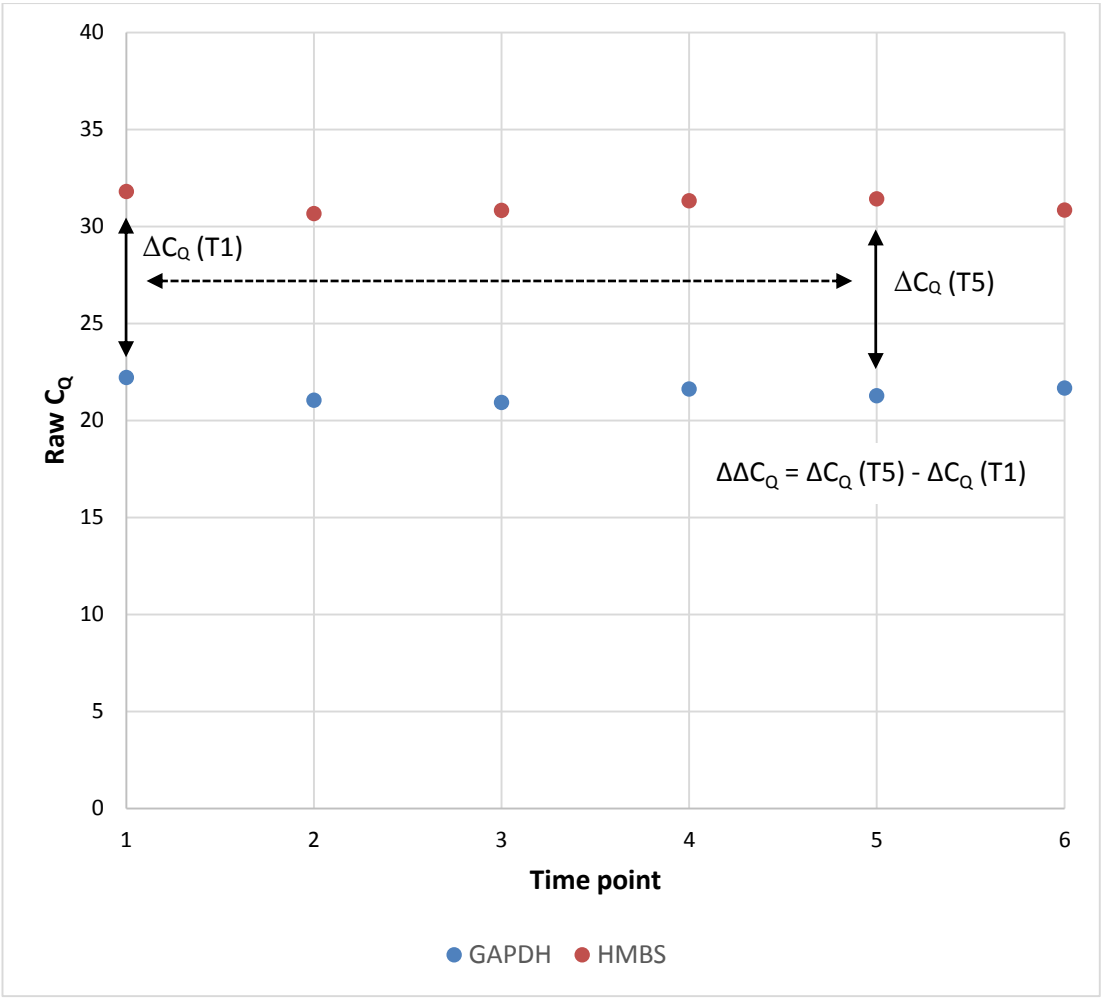

Figure 1.21: **Expression of Gapdh and Hmbs in mouse skeletal muscle tissue, raw C_Q data.** The difference in C_Q between the two genes is calculated for all six time points (Hmbs – Gapdh) – referred to as the ΔC_Q. The difference between the ΔC_Qs calculated at two time points (the $\Delta\Delta C_Q$) gives an indication of the change in the relative expression level over the intervening time interval. This can be converted into the linear scale to describe the fold-change in the expression of Gapdh relative to Hmbs using the $2^{-\Delta\Delta CQ}$ formula.

The ΔC_Q at time point 1 represents the 'control' point, prior to the onset of any RNA degradation. The ΔC_Q is then calculated for all later time points or 'experimental' groups, as displayed in Equations 1 and 2. RNA #1 and RNA #2 in this example are Gapdh and Hmbs:

$$\Delta CQ_{T1} = CQ_{T1}\ (RNA\ 1) - CQ_{T1}\ (RNA\ 2) \qquad \text{Equation (1)}$$

$$\Delta CQ_{Tx} = CQ_{Tx}\ (RNA\ 1) - CQ_{Tx}\ (RNA\ 2) \qquad \text{Equation (2)}$$

From these two equations, the $\Delta\Delta C_Q$ can be calculated as displayed in Equation 3, to measure the relative change in ΔC_Q in the duration from the control time point to any other time point, denoted "x":

$$\Delta\Delta CQ = \Delta CQ_{Tx} - \Delta CQ_{T1} \qquad \text{Equation (3)}$$

However, C_Qs are related to RNA/cDNA quantity by an exponential relationship. The $\Delta\Delta C_Q$ can be converted into an estimated fold-change in the relative expression level of the two gene targets using the following formula:

$$Fold\ change = 2^{-\Delta\Delta C_Q} \qquad \text{Equation (4)}$$

1.5 Research objectives

RNA analysis presents a unique opportunity to answer a wide range of as yet, unanswered questions in forensic science. This thesis focuses on two related research themes – detecting cell-specific RNA expression for identification of biological specimens, and quantifying RNA degradation in post-mortem tissues.

Different cell types possess their own unique transcriptome, characterisation of which is postulated to permit identification of their tissue origin (Section 1.3.1). Chapter 3 explored the use of this principle towards identification of menstrual blood, vaginal secretions and skin cell deposits. The work presented describes the development of an analytical protocol for manipulation of RNA and its application to dried biological specimens, to interpret whether or not 'blind' mock casework samples contained traces of menstrual blood, vaginal secretions or skin cell deposits. This research was carried out in collaboration with the RNA branch of the European DNA Profiling (EDNAP) group (3, 66), with the aim of validating the reliability and reproducibility of cell-specific RNA detection as a means of identifying biological specimens.

As well as exhibiting tissue type specificity, the dynamic nature of the transcriptome has led to it being suggested as a novel source of diagnostic information in forensic pathology (Section 1.3.2). Unfortunately, RNA is a labile molecule and is subjected to constant attack during the post-mortem interval. Prior to its application in any diagnostic assay, it is imperative that the degradation of RNA in tissues after death is thoroughly characterised. Chapters 5 through 7 of this thesis look at the decay behaviour of RNA in post-mortem tissues with the aim of determining for how long after death tissue RNA remains analysable; and after what point it becomes so degraded that the reliability of gene expression data is likely to be compromised. Because of the heterogeneity of human autopsy samples and legal difficulties incurred working with them, an animal model was used for this research in the form of the laboratory mouse (*Mus musculus*).

Initially, an experimental design was developed and tested; the outcomes of which are presented in Chapter 4. This appraised a number of potential protocols

for the preparation of RNA from mouse skeletal muscle, kidney, liver and heart tissue. Use of the preservative RNAlater® was evaluated, to determine its efficacy at halting tissue RNA degradation upon storage for up to 8 weeks. Two RNA purification protocols (TRI® Reagent and RNeasy®) were directly compared, to assess which provided high quantity, high molecular weight, pure RNA for downstream analysis. The optimum protocol was selected, and implemented into subsequent chapters assessing RNA decay behaviour in mouse tissues.

RNA decay behaviour was assessed in the skeletal muscle, kidney, liver and heart tissue of mice decomposed for up to 72 hours (Chapters 5 through 7). This work aimed to identify for how long after death RNA could be successfully extracted from tissues and analysed using three techniques: total RNA quantification by UV-visible spectrophotometry; total RNA quality analysis on the Bioanalyzer 2100 platform; and amplification of a panel of six endogenous control RNAs by RT-qPCR (18S rRNA, B2m, Actb, Gapdh, Hmbs and Ubc). The relationship between post-mortem interval and the RNA expression data generated with each of these three strategies was characterised.

In addition, two post-mortem interval variables have been considered to assess their effect on tissue RNA. It was postulated that reducing the ambient temperature during the post-mortem interval would preserve tissue RNA, extending the time span during which RNA remains viable. To investigate this, mouse corpses were decomposed at each of 10, 22 and 30 °C for up to 72 hours prior to tissue RNA analysis (Chapter 5). Secondly, many studies opt for using the more practical *ex vivo* decomposition simulation under which tissues are excised from the corpse and left to degrade in a test tube. The validity of this approach was considered in Chapter 6, to assess whether data generated under this experimental design is directly comparable with gene expression data from tissue samples decomposed *in vivo*.

In an attempt to characterise the nature and progression of degradation for individual RNAs, Chapter 7 applied qPCR assays with specific design features to RNA extracts from partially decomposed tissues. The quantity of sequences proximal to

the 3’ end, 5’ end and centre of target endogenous control RNAs (Hmbs, Sdha and Psmc4) was measured by RT-qPCR in an attempt to identify whether post-mortem RNA degradation is random in nature (suggestive of endoribonuclease or chemical attack) or whether RNA transcripts have a tendency to be disassembled from one end. Finally, the use of target amplicons of differing length and position was considered to identify whether this lends itself to development of an assay for quantification of the post-mortem interval.

Chapter 2: Materials and Methods

2.1 Identification of tissue origin by RNA profiling: Overview

Analysis of the RNA profile of a biological specimen recovered from a crime scene can potentially be used to estimate its tissue origin. This section describes the protocol for generation of an RNA profile from blood, saliva, semen, menstrual blood, vaginal secretions and skin cell deposits. This research was undertaken in collaboration with the RNA branch of the European DNA Profiling (EDNAP) research group. The following procedure describes a number of key steps: from the extraction of DNA and RNA from the aforementioned specimen types; through reverse transcription, cDNA amplification, DNA amplification and identification of the PCR products by capillary electrophoresis. This protocol pertains to all data presented in Chapter 3.

2.1.1 Acquisition and preparation of 'mock' crime scene specimens and controls

Samples of semen, saliva, blood, menstrual blood, vaginal secretions and skin cell deposits were prepared or received for analysis. All human body fluid samples were acquired in accordance with guidelines set forth by the University of Strathclyde's Ethics Committee. Simultaneously through all four research exercises extraction blank (dry swab), reverse transcription blank (substituting RNA for nuclease free water) and PCR blank (substituting cDNA for nuclease free water) samples were also run; the results of which can be assumed negative unless further discussed.

2.1.1.1 EDNAP exercise four: Saliva, blood, semen and menstrual blood samples

Human saliva, blood, semen and menstrual specimens were received from the co-ordinating laboratory (Institute of Legal Medicine, University of Zurich, Switzerland) (3). They consisted of four dilution series: saliva (25, 5, 1 and 0.2 µL on swabs), blood (1, 0.1, 0.01 and 0.001 µL on swabs), semen (5, 1, 0.2, 0.04 µL on swabs) and menstrual blood stains (1/4, 1/8, 1/16, 1/32 and 1/64 on cotton fabric). In addition, 8 stains of unknown origin (numbered 1 to 8) were received for analysis. Five other specimens were prepared in house. Menstrual blood was collected from two healthy volunteers using a MoonCup^{TM} device on days 1 and 2 of their menstrual cycle. For the purposes of extraction, 10 µL of each liquid menstrual blood sample was utilised and blotted on a cotton swab. A fifth circulatory blood sample, dried on cotton tissue, was utilised from the GEDNAP 2011 accreditation exercise. All samples were stored at 4 °C prior to processing.

2.1.1.2 EDNAP exercise five: Samples of vaginal secretions

Samples of human vaginal secretions were received from the co-ordinating laboratory (Institute of Legal Medicine, University of Zurich, Switzerland) (3). They consisted of a vaginal secretion dilution series (1/4, 1/8, 1/16, 1/32 and 1/64 cuttings of cotton swabs) and eight questioned stains of unknown origin (numbered 9 to 16). In addition, 3 other specimens were prepared in house: a vaginal swab, a buccal swab and a swab of an undetermined quantity of saliva, collected from a single volunteer. All samples were stored at 4 °C prior to processing.

2.1.1.3 EDNAP exercise six: Skin cell deposits

A number of specimens were received from the co-ordinating laboratory (Institute of Legal Medicine, University of Zurich, Switzerland) for the analysis of RNAs associated with skin cells. These consisted of a dilution series of cultured skin cell RNA on cotton swabs ((200, 50, 12, 3 and 0.8) ng) and eight questioned

specimens of unknown origin (numbered 17 to 24); including for example a single key from a computer keyboard, a glass slide and a piece of paper.

In addition, seven other 'touch' samples were prepared in house by swabbing: a tablet computer screen, touchscreen mobile phone screen, mug handle, steering wheel, computer keyboard, computer mouse, and the surface of an individual's hand. All swabs were dampened with 25 µL nuclease free water (Ambion, Life Technologies, Paisley, UK) prior to specimen collection, and stored at 4 °C until processing.

2.1.2 Extraction and purification of RNA from 'mock' crime scene samples

2.1.2.1 AllPrep® (Qiagen) DNA/RNA co-isolation procedure

For the co-isolation of DNA and RNA from human saliva, semen, blood, menstrual blood and vaginal fluid, the AllPrep® DNA/RNA Mini Kit was employed (Qiagen, Crawley, UK) (167). Each whole stain/swab was incubated in 350 µL RLT buffer (pre-prepared 100:1 with β-mercaptoethanol) for 3 h at 56 °C to solubilise nucleic acids. The lysate was applied to an AllPrep® DNA column, and passed through by centrifugation in a microcentrifuge at 10,000 rpm for 30 s.

To the flow through was added 1 volume of 70% ethanol (Sigma Aldrich Ltd., Gillingham, UK) and the resultant mixture applied to an RNeasy® column. This lysate was passed through the column by centrifugation at 10,000 rpm for 15 s. Under similar centrifugation conditions, the column was washed once with 700 µL buffer RW1, twice with 500 µL buffer RPE, and the column dried by centrifugation for 1 min at 10,000 rpm. RNA was eluted into 50 µL RNase-free water by centrifugation for 1 min at 10,000 rpm.

The DNA column was then washed with 500 µL buffer AW1 followed by 500 µL buffer AW2, in between centrifuging for 15 s at 10,000 rpm, and the column subsequently dried by centrifugation for 2 mins at 13,000 rpm. DNA was eluted into 80 µL buffer EB. Both DNA and RNA were transferred to -20 °C for storage.

2.1.2.2 RNeasy® (Qiagen) RNA extraction procedure

For the isolation of RNA only from human semen specimens, the RNeasy® Mini Kit (Qiagen) was implemented (168). Each whole stain/swab was incubated in 350 µL RLT buffer (pre-prepared 100:1 with β-mercaptoethanol) and 20 µL 0.1 M dithiothreitol for 3 h at 56 °C. This cell lysate was applied directly to an RNeasy® column. RNA precipitation, binding, clean-up and elution were performed as detailed in Section 2.1.2.1. RNA extracts were transferred to -20 °C for storage.

2.1.2.3 Arcturus® PicoPure® RNA isolation procedure

RNA was recovered from skin cell deposits using the high sensitivity Arcturus® PicoPure® RNA Isolation Kit (Applied Biosystems, Life Technologies, CA, USA) (169). Swabs/stains were incubated in 100 µL extraction buffer for 30 mins at 42 °C, and the buffer recovered in total from the swab by centrifugation in a spin basket. Meanwhile, the RNA purification column was pre-conditioned by incubation for 5 mins at room temperature with 250 µL conditioning buffer, and centrifuged in a microcentrifuge at 13,000 rpm for 1 min.

Recovered RNA was precipitated by the addition of 100 µL 70% ethanol to the cell extract, and the mixture applied to an RNA purification column. RNA was bound by centrifugation for 2 mins at 1,220 rpm to disperse the sample through the membrane, followed by 1 min at 13,000 rpm. The column was washed by centrifugation for 1 min at 11,000 rpm with 100 µL wash buffer 1, followed with two repeats of 100 µL wash buffer 2. The column was subsequently dried by centrifugation for 3 min at 13,000 rpm. RNA was eluted into 14 µL elution buffer, with 1 min centrifugation at 4,000 rpm followed by 2 mins at 13,000 rpm. RNA extracts were transferred to -20 °C for storage.

2.1.2.4 Removal of contaminating DNA

RNA extracts were treated with DNase to destroy any carry-over of genomic DNA using the TURBO DNA-free® Kit (Ambion, Life Technologies, Paisley, UK) following the manufacturer's guidelines (122). To each RNA extract was added 0.1 volume 10X TURBO DNase buffer and 1 µL TURBO DNase, and the RNA incubated for 30 mins at 37 °C. To this, 0.1 volume DNase inactivation reagent was added and incubated at room temperature for five mins. The DNase inactivation reagent was pelleted out by centrifugation in a microcentrifuge at 13,000 rpm for 3 mins and the supernatant (clean, DNA-free RNA extract) stored at -20 °C.

2.1.3 Reverse transcription of RNA into cDNA using SuperScript® III

Reverse transcription of RNA into cDNA was performed using the SuperScript® III First Strand Synthesis System (Invitrogen, Life Technologies, Paisley, UK), according to the manufacturer's protocol (170). 2 µL of RNA was reverse transcribed per reaction, with 1 µL random primers, 0.5 µL 10 mM dNTPs and 2 µL nuclease free water. This mixture was denatured at 65 °C for 4 mins, snap cooled, and to it added 1 µL 10X RT buffer, 2 µL 25 mM $MgCl_2$, 1 µL 0.1 M dithiothreitol, 0.5 µL RNaseOUT™ and 0.5 µL of either reverse transcriptase (RT+ control) or 0.5 µL nuclease free water (RT- control). All samples were reverse transcribed in duplicate, giving a RT+ and an RT- control to monitor for gDNA contamination.

Temperature regulation was achieved using either the Veriti® Thermal Cycler with a 0.1 mL VeriFlex™ block or the 2720 Thermal Cycler (Applied Biosystems, CA, USA). Primers were annealed by incubation at 25 °C for 10 mins, followed by 50 mins at 50 °C to permit cDNA synthesis. The reverse transcriptase enzyme was then was then denatured at 85 °C for 5 mins. 0.5 µL RNase H was added to each tube and incubated at 37 °C for 20 mins to facilitate RNA removal. cDNA RT products were then transferred for storage at -20 °C.

2.1.4 Amplification of tissue type specific markers by endpoint PCR

2.1.4.2 EDNAP exercise four: Amplification of menstrual blood specific markers

Amplification of human saliva, blood, semen and menstrual blood cDNA samples was performed using nine sets of PCR primers, targeting:

- Six menstrual blood-specific RNAs/cDNAs: MMP11, MMP7, MMP10, MSX1, LEFTY2 and SFRP4
- Three endogenous control gene RNAs/cDNAs: B2M, UBC and UCE

These were divided into three multiplex PCR assays: the matrix metalloproteinase (MMP) 3-plex, the menstrual blood (MB) 3-plex, and the 'housekeeping' gene 3-plex. Details of each of the RNA/cDNA markers targeted, the PCR primer sequences and PCR product lengths are described in Tables 2.1 and 2.2. Primers were purchased and prepared by the organising laboratory.

PCR amplification of cDNAs with the MMP, MB and housekeeping gene triplexes was performed using the Multiplex PCR Kit (Qiagen, Crawley, UK) (171), in a total reaction volume of 12.5 µL. Each reaction contained 1 µL cDNA along with 6.25 µL 2x Multiplex PCR MasterMix, 1.25 µL Q-Solution, 1.25 µL of the relevant primer triplex and 2.75 µL of water. Amplification was performed on a Veriti® Thermal Cycler using a 0.1 mL VeriFlex™ block (Applied Biosystems, CA, USA) with the following cycling conditions: denaturation at 95 °C for 15 mins, followed by 35 cycles of 94 °C for 30 s, 55 °C (increasing by 0.2 °C per cycle) for 90 s and 72 °C for 40 s, and final elongation at 72 °C for 30 mins.

Table 2.1: **Six RNA/cDNA markers amplified for the identification of human menstrual blood: MMP11, MMP7, MMP10, MSX1, LEFTY2 and SFRP4**. Primers were designed and prepared by the co-ordinating laboratory. Forward primers were labelled with the 6-FAM™ fluorophore to allow PCR product detection. Information collated from (3).

Multiplex	RNA marker identity	Primer sequence and concentration	cDNA amplicon length (nt)
Matrix metalloproteinase (MMP) 3-plex	Matrix metalloproteinase 11 (MMP11)	F: GGT GCC CTC TGA GAT CGA C R: TCA CAG GGT CAA ACT TCC AGT 2 µM	92
	Matrix metalloproteinase 7 (MMP7)	F: CAT GAG TGA GCT ACA GTG GGA ACA GGC R: CTA TGA CGC GGG AGT TTA ACA TTC CAG 2 µM	161
	Matrix metalloproteinase 10 (MMP10)	F: TCA CAG GGT CAA ACT TCC AGT R: CTG GAG AAT GTG AGT GGA GT 2 µM	230
Menstrual blood (MB) 3-plex	Msh homeobox 1 (MSX1)	F: CCC CGT GGA TGC AGA GCC CCC G R: GCT TAC GGT TCG TCT TGT GTT TGC GGA G 5 µM	96
	Left-right determination factor 2 (LEFTY2)	F:GCC CAC GTG AGG GCC CAG TAT GTA GT R: GGT GTG TGC TGG TGG CCT CCG ACG C 2 µM	130
	Secreted frizzled related protein 4 (SFRP4)	F: GCG ACG AGC TGC CTG TCT ATG ACC R: CAG TCA ACA TCA AGA GGC CTT TCC TGT AC 5 µM	136

Table 2.2: **Three 'universal' RNA/cDNA markers amplifiable from all human tissue types and body fluids: B2M, UBC and UCE**. Primers were designed and prepared by the co-ordinating laboratory. Forward primers were labelled with the ATTO550 fluorophore to allow PCR product detection. Information collated from (3).

Multiplex	RNA marker identity	Primer sequence and concentration	cDNA amplicon length (nt)
'Housekeeping' gene 3-plex	β_2-microglobulin (B2M)	F: GGC ATT CCT GAA GCT GAC A R: AAA CCT GAA TCT TTG GAG TAC G 0.2 µM	120
	Ubiquitin C (UBC)	F: GGG TCG CAG TTC TTG TTT GT R: TCC AGC AAA GAT CAG CCT CT 0.2 µM	186
	Ubiquitin conjugating enzyme UBCH5B (UCE)	F: AAT GAT CTG GCA CGG GAC C R: ATC GTA GAA TAT CAA GAC AAA TGC TGC 1 µM	241

2.1.4.3 EDNAP exercise five: Amplification of vaginal fluid specific markers

Amplification of human vaginal fluid cDNA samples was performed using seven sets of PCR primers, all targeting vaginal fluid specific RNAs/cDNAs: MYOZ1, CYP2B7P1, MUC4, Ljen, Lcris, Lgas and HBD1. These were divided into two multiplex PCR assays and a singleplex: the vaginal 3-plex, the Lacto 3-plex, and the HBD1 singleplex. Details of each of the RNA/cDNA markers targeted, the PCR primer sequences and PCR product lengths are described in Table 2.3.

Table 2.3: **Seven RNA/cDNA markers amplified for the identification of human vaginal secretions: MYOZ1, CYP2B7P1, MUC4, Ljen, Lcris, Lgas and HBD1.** Primers were designed and prepared by the co-ordinating laboratory. Forward primers were labelled with the 6-FAM™ fluorophore to allow detection. Information collated from (3).

Multiplex	RNA marker identity	Primer sequence and concentration	cDNA amplicon length (nt)
Vaginal 3-plex	Myozenin 1 (MYOZ1)	F: GGG TTG GTG AGA CAG GAT CA R: GGG TTG GTG AGA CAG GAT CA 2 µM	81
	Cytochrome P450 family 2, subfamily B, polypeptide 7 pseudogene 1 (CYP2B7P1)	F: TCC TTT CTG AGG TTC CGA GA R: TTT CCA TTG GCA AAG AGC AT 2 µM	198
	Mucin 4 (MUC4)	F: GGA CCA CAT TTT ATC AGG AA R: TAG AGA AAC AGG GCA TAG GA 2 µM	235
Lacto 3-plex	*Lactobacillus jensenii* 16S-23S rRNA intergenic spacer region (Ljen)	F: AAG TCG AGC GAG CTT GCC TAT TGA AAT R: CGC CTT TTA AAC TTC TTT CAT GAG AAA GTA GC 2 µM	171
	Lactobacillus crispatus 16S-23S rRNA intergenic spacer region (Lcris)	F: GAG AGC AGG AAT GCT AAG AG R: CCG GAT CAT TGC TTA CTT AC 2 µM	292
	Lactobacillus gasseri 16S-23S rRNA intergenic spacer region (Lgas)	F: ATG ATG GAG AGT GCG AGA GC R: CCG GAT CAT TGC TTA CTT AC 2 µM	311
HBD1 singleplex	Human beta-defensin 1 (HBD1)	F: CCT GGG TGT TGC CTG CCA GTC GC R: CAG GTG CCT TGA ATT TTG GT 2 µM	200

PCR amplification of cDNAs with the vaginal and Lacto 3-plexes was performed using the Multiplex PCR Kit (Qiagen, Crawley, UK) (171), in a total reaction volume of 12.5 µL. Each reaction contained 1 µL cDNA along with 6.25 µL 2x Multiplex PCR MasterMix, 1.25 µL Q-Solution, 1.25 µL of the relevant primer multiplex and 2.75 µL of water. Amplification was performed on a 2720 Thermal Cycler (Applied Biosystems, CA, USA) with the following cycling conditions: denaturation at 95 °C for 15 mins, followed by 35 cycles of 94 °C for 30 s, 55 °C (increasing by 0.2 °C per cycle) for 90 s and 72 °C for 40 s, and final elongation at 72 °C for 30 mins.

PCR amplification of cDNAs with the HBD1 singleplex was performed instead using the *Taq* polymerase AmpliTaq Gold® in a reaction volume of 12.5 µL. Each reaction contained 2.5 µL cDNA along with 1.25 µL GeneAmp® dNTP Blend, 1.25 µL 10x AmpliTaq® Gold Buffer II, 1.5 µL 25 mM $MgCl_2$, 0.2 µL AmpliTaq Gold® DNA Polymerase (all Applied Biosystems, CA, USA), 1 µL primers and 4.8 µL water. Amplification was performed on a 2720 Thermal Cycler with the following cycling conditions: denaturation at 95 °C for 11 mins, followed by 35 cycles of 94 °C for 20 s, 55 °C for 60 s and 72 °C for 45 s, and final elongation at 72 °C for 30 mins.

2.1.4.4 EDNAP exercise six: Amplification of skin cell specific markers

Amplification of cDNA originating from skin cell deposits was performed using eleven sets of PCR primers, targeting:

- Eight skin-specific RNAs/cDNAs: LCE1C, IL1F7, LCE1D, LCE2D, CCL27, LOR, KRT9 and CDSN
- Three endogenous control gene RNAs/cDNAs: B2M, UBC and UCE

These were divided into three multiplex PCR assays: the skin-1 5-plex, the skin-2 3-plex, and the 'housekeeping' gene 3-plex. Details of each of the RNA/cDNA markers targeted, the PCR primer sequences and PCR product lengths are described in Tables 2.2 and 2.4. Primers were purchased and prepared by the organising laboratory.

Table 2.4: **Eight RNA/cDNA markers amplified for the identification of skin cell deposits: LCE1C, IL1F7, LCE1D, LCE2D, CCL27, LOR, KRT9 and CDSN**. Primers were designed and prepared by the co-ordinating laboratory. Forward primers were labelled with the 6-FAM™ fluorophore to allow detection.

Multiplex	RNA marker identity	Primer sequence and concentration	cDNA amplicon length (nt)
Skin-1 5-plex	Late cornified envelope 1C (LCE1C)	F: GCT GAA GGA CCC TGT GCT R: CAG GAC ATC TTG GTG GCG 1 µM	56 and 58
	Interleukin 1-F7 (IL1F7)	F: CCA GTG CTG CTT AGA AGA CC R: TCA CCT TTG GAC TTG TGT GAA 2 µM	92
	Late cornified envelope 1D (LCE1D)	F: CCT GTG CTG CCT GTG ACT R: GGC ACT TAG GGG GAC ATT TA 2 µM	142
	Late cornified envelope 2D (LCE2D)	F: TCT GTG CTT TTG CAT GTG AC R: GGA CCA CAG CAG GAA GAG AC 2 µM	193
	Chemokine ligand 27 (CCL27)	F: AGC ACT GCC TGC TGT ACT CA R: TTC AGC CCA TTT TCC TTA GC 2 µM	254
Skin-2 3-plex	Loricrin (LOR)	F: CTC CTC ACT CAC CCT TCC TG R: CCA GAG GTC TTC ACG CAG TC 8 µM	114
	Keratin 9 (KRT9)	F: GCT CCT GGC AAA GAT CTC AC R: GAC TGC ACC TCC TGA CCA CT 8 µM	155
	Corneodesmosin (CDSN)	F: CCT GAG CTG CCA TCA GTC AG R: TGC TTA GGG GAG GTG ATA CG 8 µM	196

PCR amplification of cDNAs with the skin-1 5-plex, the skin-2 3-plex and the 'housekeeping' gene 3-plex was performed using the Multiplex PCR Kit (Qiagen, Crawley, UK) (171), in a total reaction volume of 12.5 µL. Each reaction contained 1 µL cDNA along with 6.25 µL 2x Multiplex PCR MasterMix, 1.25 µL Q-Solution, 1.25 µL of the relevant primer triplex and 2.75 µL of water. Amplification was performed on a 2720 Thermal Cycler (Applied Biosystems, CA, USA) with the following cycling conditions: denaturation at 95 °C for 15 mins, followed by 35 cycles of 94 °C for 30 s, 55 °C (increasing by 0.2 °C per cycle) for 90 s and 72 °C for 40 s, and final elongation at 72 °C for 30 mins. The starting annealing temperature for the skin-1 5-plex was increased to 58 °C, similarly with an increment of 0.2 °C per cycle.

2.1.5 Quantification of human DNA yield

Quantification of human DNA was performed using the Investigator® Quantiplex Kit (Qiagen, Crawley, UK), following the manufacturer's protocol in a reduced 12.5 µL reaction volume (172). Each reaction was set up with 5.75 µL each of reaction mix and primer mix, with 1 µL human DNA. Thermal cycling was performed on the Stratagene Mx3005P real time PCR platform (Agilent Technologies, CA, USA) with the following temperature conditions: 95 ^{o}C for 1 min activation step, followed by 40 cycles of 95 ^{o}C for 5 s and 60 ^{o}C for 32 s. Fluorescence threshold and standard curves were plotted by the internal MxPro software and used for automatic calculation of DNA concentration.

2.1.6 Amplification of human DNA STR loci

Amplification of STR loci in genomic DNA was performed with the Investigator® Decaplex SE PCR Assay (Qiagen, Crawley, UK). Reactions were set up and amplified as stipulated by the manufacturer (173), with a reduced 12.5 µL reaction volume. Each reaction was set up with 2.5 µL reaction mix, 1.25 µL primer mix, 0.2 µl *Taq* polymerase and up to 8.55 µL human DNA, diluted in nuclease free water (Ambion, Life Technologies, Paisley, UK). Thermal cycling was performed on a

2720 Thermal Cycler (Applied Biosystems, Life Technologies, Paisley, UK) using the following temperature conditions: 94 °C hot start for 4 mins, 5 cycles of 96 °C for 30 s, 62 °C for 2 mins, 72 °C for 1 min 15 s; 25 cycles of 94 °C for 30 s, 60 °C for 2 mins and 72 °C for 1 min 15 s; 1 h at 68 °C to permit polyadenylation; followed by a hold at 4 °C. PCR products were stored at 4 °C prior to electrophoresis.

2.1.7 Separation of PCR products by capillary electrophoresis

Separation and detection of PCR products was achieved using a 3130 Genetic Analyzer (Applied Biosystems, Life Technologies, CA, USA). For separation of amplicons generated with the RNA/cDNA multiplexes, 1 µL of each PCR product was added to 10 µL of a 1:80 GeneScan-500 LIZ internal lane standard to HiDi® Formamide mix (both Applied Biosystems). The electrophoresis conditions were programmed as follows: 10 s injection time, 3 kV injection voltage, 15 kV run voltage, 60 ^{o}C oven temperature, 21 min run time, and dye set G5. The results were analysed on GeneMapper v3.2, using a peak height threshold of 100 rfu.

For separation of human DNA amplicons generated with the Decaplex SE STR amplification system, 1 µL of each PCR product was added to 10 µL of a 1:24 BTO internal lane standard (Qiagen, Crawley, UK) to HiDi® Formamide mix. The electrophoresis conditions were programmed as recommended by the manufacturer (173), and the results analysed on GeneMapper v3.2 using a peak height threshold of 50 rfu.

2.2 Analysis of RNA in solid tissues: Overview

Much of the research presented in this thesis concerns the analysis of RNA in solid tissues, to track the degradation of RNA after death. When using solid tissues as a substrate for RNA recovery, the protocol is subtly different to that described previously for body fluid specimens. The increased RNA yield from solid tissues widens the scope for more thorough analysis of the transcriptome. Additionally, it was important when fulfilling the aims of this study that quantitative PCR was implemented as a substitute for endpoint PCR. The following Section 2.2 therefore provides a detailed protocol for the recovery and analysis of RNA from solid tissue samples.

2.2.1 Collection of animal tissue samples

All experimental steps involving live animals were performed in accordance with the ethical guidelines set out by the Biological Procedures Unit within Strathclyde Institute of Pharmacy and Biomedical Science. All animals utilised were 12 week old, male C57/BL6J laboratory mice.

A number of methods are currently permitted for euthanizing rodents under Schedule 1 of the Animals (Scientific Procedures) Act 1986 (174). For the purposes of this work, death by cervical dislocation was selected as being the quickest method and as having the least likely impact on gene expression; compared to death by injection of an anaesthetic overdose or by exposure to carbon dioxide gas in rising concentration.

2.2.2 Preservation of RNA in biological specimens using RNAlater®

Following excision from the body, all animal tissue samples were shredded with a scalpel to less than 0.5 cm in any dimension and immediately immersed in at least 5 to 10 volumes (usually 1 to 2 mL) of RNAlater® (Ambion, Life Technologies, Paisley, UK). After refrigeration at 4 °C overnight to permit penetration of the solution through tissues, samples could be frozen at -20 °C for longer term storage; though not longer than 8 weeks in any instance.

2.2.3 Extraction and purification of RNA from solid tissues

2.2.3.1 RNeasy® (Qiagen) RNA extraction procedure

Extraction and purification of RNA from a variety of RNAlater® preserved tissue types was performed using the RNeasy® Mini Kit (QIAGEN, Crawley, UK), following the manufacturer's standard guidelines (168). Up to 20 mg tissue was shredded and homogenised in 600 µL buffer RLT (prepared 1:100 with β-mercaptoethanol (GE Healthcare, Little Chalfont, UK)) using an IKA T10 basic ULTRA-TURRAX® disperser with attached S10N-5G dispersing element (IKA, Staufen, Germany). Any remaining solid tissue debris was pelleted and removed by centrifugation at 13,000 rpm for 3 mins.

To the homogenate was added and mixed 1 volume (approx. 600 µL) 70% ethanol (Sigma Aldrich Ltd., Gillingham, UK) and the resultant mixture applied to an RNeasy® column. The tissue lysate was run through the column by centrifugation at 10,000 rpm for 15 s. Under similar centrifugation conditions, the column was washed once with 700 µL buffer RW1, twice with 500 µL buffer RPE, and the column dried by centrifugation for 1 min at 10,000 rpm. RNA was eluted into 50 µL RNase-free water by centrifugation for 1 min at 10,000 rpm.

2.2.3.2 RNeasy® (Qiagen) RNA extraction procedure: Incorporating proteinase K treatment for fibrous tissue types

Extraction and purification of RNA from RNAlater® preserved skeletal muscle samples was performed using the RNeasy® Mini Kit (QIAGEN, Crawley, UK) following the manufacturer's guidelines for fibrous tissue types (175). Up to 20 mg skeletal muscle tissue was shredded and homogenised in 600 µL buffer RLT (prepared 1:100 with β-mercaptoethanol (GE Healthcare, Little Chalfont, UK)) using an IKA T10 basic ULTRA-TURRAX® disperser with attached S10N-5G dispersing element (IKA, Staufen, Germany). To the homogenate was added and mixed 1,180 µL RNase-free water (Ambion, Life Technologies, Paisley, UK) and 20 µL proteinase K (Sigma-Aldrich Ltd., Gillingham, UK). Samples were incubated at 55 ^{o}C for 10 mins to facilitate proteinase K breakdown of the abundant proteins in fibrous muscle tissue samples. Any remaining solid tissue debris was pelleted and removed by centrifugation at 13,000 rpm for 3 min.

To this lysate was mixed ½ volume (approx. 900 µL) of 96-100% ethanol (Sigma-Aldrich Ltd.) and the resultant mixture applied to an RNeasy® spin column. The tissue lysate was run through the column by centrifugation at 10,000 rpm for 15 s. Under similar centrifugation conditions, the column was washed once with 700 µL buffer RW1, twice with 500 µL buffer RPE, and the column dried by centrifugation for 1 min at 10,000 rpm. RNA was eluted into 50 µL RNase-free water by centrifugation for 1 min at 10,000 rpm.

2.2.3.3 TRI Reagent® RNA extraction procedure

Extraction of RNA from a variety of RNAlater® preserved tissue types was performed using the TRI Reagent® protocol following the manufacturer's guidelines (Sigma-Aldrich Ltd., Gillingham, UK) (176). Less than 100 mg tissue was homogenised in 1 mL TRI Reagent® and 3 µL polyacryl carrier (Molecular Research Center, Cincinatti, USA) using an IKA T10 basic ULTRA-TURRAX® disperser with attached S10N-5G dispersing element (IKA, Staufen, Germany).

To the homogenate was added and mixed 100 µL 1-bromo-3-chloropropane (Sigma-Aldrich Ltd.). After a 3 min incubation period, the mixture was centrifuged at 13,000 rpm at 4 ^{o}C for 15 mins, to partition the aqueous and organic phases. The aqueous phase was removed and to it added 500 µL isopropanol (Sigma-Aldrich Ltd.) to precipitate out RNA. Precipitated RNA was pelleted by centrifugation at 13,000 rpm at 4 ^{o}C for 10 mins, the supernatant discarded, and the RNA pellet washed in 1 mL 75% ethanol (Sigma-Aldrich Ltd.). RNA was re-pelleted by centrifugation at 10,500 rpm at 4 ^{o}C for 5 mins. The RNA pellet was re-suspended in 50 µL RNase-free water (Ambion, Life Technologies, Paisley, UK) and heated to 55 °C for 10 mins to facilitate RNA solubilisation. For liver tissue samples which provided a particularly high RNA yield, the re-suspension volume was increased from 50 to 200 µL.

2.2.3.4 Removal of contaminating DNA

RNA extracts were treated with DNase to destroy any carry-over of genomic DNA using the TURBO DNA-free® kit (Ambion, Life Technologies, Paisley, UK) following the manufacturer's guidelines (122). To each RNA extract was added 0.1 volume 10X TURBO DNase buffer and 1 µL TURBO DNase, and the RNA incubated for 30 mins at 37 ^{o}C. To this, 0.1 volume DNase inactivation reagent was added and incubated at room temperature for 5 mins. The DNase inactivation reagent was pelleted out by centrifugation at 13,000 rpm for 3 mins and the supernatant (clean, DNA-free RNA extract) stored at -20 ^{o}C.

2.2.4 Quantification of RNA by UV-visible spectrophotometry

RNA concentration was measured with the Nanodrop-1000 UV-vis spectrophotometer (Thermo Scientific, Loughborough, UK). The instrument was first blanked with a sample of RNase-free water (the same solvent as all eluted RNA samples), and 1.5 µL of sample used for calculation of RNA concentration, $A_{260/280}$

and $A_{260/230}$. All RNA extracts were quantified both before and after treatment with DNase, to assess the level of genomic DNA contamination within the RNA sample.

2.2.5 RNA quality analysis using the Bioanalyzer 2100

RNA quality was measured using the Bioanalyzer 2100 instrument coupled to the RNA 6000 Pico kit (Agilent Technologies, Wokingham, UK), following the manufacturer's instructions (132). The RNA 6000 Pico kit has an input range of up to 5 ng/µL total RNA, making it the most sensitive chip available for RNA integrity number (RIN) determination.

1 µL of Pico dye concentrate was added and mixed into 65 µL filtered Pico gel matrix and centrifuged for 10 mins at 13,000 rpm. The Pico chip was primed with 9 µL gel-dye mix in triplicate and 9 µL conditioning solution. Samples were denatured prior to use at 70 ^{o}C for 2 mins, and 1 µL added to the chip wells with 5 µL Pico marker. The fully prepared chip was vortexed for 1 min at 2,400 rpm on a chip vortex mixer (IKA, Staufen, Germany) prior to insertion into the instrument.

2.2.6 Reverse transcription of RNA into cDNA using the High Capacity cDNA Reverse Transcription Kit

Tissue RNA extracts were reverse transcribed into cDNA using either the High Capacity cDNA Reverse Transcription Kit or the High Capacity cDNA Reverse Transcription Kit with RNase inhibitor (Invitrogen, Life Technologies, Paisley, UK), following the manufacturer's guidelines (177). RNA extracts were usually reverse transcribed in a volume of 20 µL although in some instances, this was factored up to 30, 80 or 120 µL depending on the volume of cDNA required for downstream analysis.

Following the standard protocol for reverse transcription with random priming, each 20 µL reaction incorporated: 2 µL 10X RT buffer, 0.8 µL 25X dNTP mix, 2 µL 10X random primers, 1 µL reverse transcriptase, 4.2 µL RNase-free water and

10 µL RNA sample. Alternatively, following the High Capacity cDNA Reverse Transcription Kit with RNase inhibitor protocol 1 µL of RNase-free water was substituted with 1 µL RNase inhibitor. For a limited number of applications oligo (dT) priming was instead adopted for reverse transcription, in which case each 20 µL reaction incorporated: 2 µL 10X RT buffer, 0.8 µL 25X dNTP mix, 1 µL oligo $(dT)_{(20)}$ (50 µM) primers (Invitrogen, Life Technologies, Paisley, UK), 1 µL reverse transcriptase, 5.2 µL RNase-free water and 10 µL RNA sample.

The thermal cycling parameters are summarised in Table 2.5 below. Temperature controlled steps were performed on a 2720 Thermal Cycler (Applied Biosystems, Life Technologies, Paisley, UK). Prior to storage at -20 ^{o}C, all cDNA samples were diluted in RNase-free water (Ambion, Life Technologies, Paisley, UK), to minimise interference of reverse transcription components carried over into subsequent real time PCR. This dilution ranged from 1:1 to 1:12, as discussed in more detail in the relevant sections.

Table 2.5: **Temperature conditions used for reverse transcription using the High Capacity cDNA Reverse Transcription Kit, with either random or oligo (dT) priming**.

	Random priming	**Oligo (dT) priming**
Primer annealing	10 mins, 25 °C	N/A
Primer extension	2 h, 37 °C	2 h, 37 °C
Reverse transcriptase denaturation	5 mins, 85 °C	5 mins, 85 °C

2.2.7 Gene expression analysis by RT-qPCR

All cDNA samples were amplified in duplicate or triplicate using some or all of a large panel of TaqMan® assays. Reactions were set up using 5 µL TaqMan® Universal PCR Master Mix (Applied Biosystems, Life Technologies, Paisley, UK), 0.5 µL of the selected inventoried TaqMan® assay, 2.5 µL water and 2 µL cDNA. Thermal cycling was performed on a Stratagene Mx3005P real time PCR instrument (Agilent Technologies, CA, USA), with the following temperature conditions: 2 mins at 50 ^{o}C to permit uracil-N-glycosylase mediated degradation of qPCR carryover contamination; 10 mins at 95 ^{o}C to activate *Taq* polymerase, and 40 cycles of 95 ^{o}C denaturation for 15 s and 60 ^{o}C elongation for 1 min. The threshold fluorescence level was set using the baseline threshold method, following which it is defined as 10 times the standard deviation of fluorescence during cycles 5 through 9 of qPCR.

Raw C_Q data was analysed in Microsoft Excel 2010, Minitab v17 (Minitab Inc.) and GenEx Pro v5.4.3 (MultiD Analyses). Microsoft Excel 2010 was used for basic data presentation, bar charts, line graphs, etc. Minitab v17 was utilised for more detailed statistical analyses such as the Student's t-test, Anderson-Darling's test of normality, analysis of variance (one-way ANOVA), linear/non-linear regression and hierarchial cluster analysis. Assessment of endogenous control RNA stability was performed using the geNorm (178) and NormFinder (179) data analysis packages interent to GenEx Pro v5.4.3 (Chapter 5).

Chapter 3: RNA profiling of evidentiary material: Towards identification of the tissue origin of forensic specimens

3.1 Introduction: The European DNA Profiling (EDNAP) Group

The detection of RNAs with spatially restricted expression profiles can be used for identification of the tissue origin of a biological specimen recovered in casework (Section 1.3.1, Chapter 1). This field has incurred an explosion of research in recent years, with groups all over the world contributing to the database of tissue specific mRNA markers utilisable for the identification of blood, semen, saliva, menstrual blood, vaginal secretions and skin cell deposits (1, 2, 8, 26, 27, 29, 30, 43, 44, 48, 53, 54, 67, 68, 180-183).

The European DNA Profiling (EDNAP) Group, a division of the International Society of Forensic Genetics (http://www.isfg.org/EDNAP) have taken an interest in this field by co-ordinating a number of collaborative research exercises concerning the practical application of RNA analysis onto biological specimens. To date, six research exercises have been devised, distributed and published by the Institute of Legal Medicine at the University of Zürich in collaboration with distinguished research groups from all over the world, including the University of Strathclyde (3, 40, 41, 65, 66). These have involved the application of singleplex and multiplex PCR assays for identification of blood, semen, saliva, menstrual blood, vaginal secretions and skin cell deposits. A summary of the experimental design of the six research exercises completed to date is compiled in Table 3.1.

Table 3.1: **Summary of the six research validation exercises co-ordinated by EDNAP since 2011.** In addition to all tissue specific mRNAs listed, exercises 3, 4, 5 and 6 have included assays against the endogenous control mRNAs B2M, UBC and UCE. The manuscript for EDNAP exercise six is currently submitted for publication (C. Haas, personal communication).

EDNAP research exercise [reference]	Biological specimen(s) targeted	PCR assays designed	mRNA markers targeted
1 [Haas *et al*. (2011) (41)]	Blood	Assay for three blood mRNAs by singleplex PCR	HBB, SPTB, PBGD
2 [Haas *et al*. (2011) (65)]	Blood	Assay for seven blood mRNAs with two multiplex PCR assays	1) HBA, HBB 2) ALAS2, CD3G, ANK1, PBGD, SPTB
3 [Haas *et al*. (2012) (66)]	Saliva and semen	Two assays for a total of 8 mRNA markers specific to saliva and semen	Saliva: STATH, HTN3, MUC7 Semen: PSA, PRM1, PRM2, SEMG1, TGM4
4 [Haas *et al*. (2014) (3)]	Menstrual blood	Two assays for a total of 6 mRNA markers specific to menstrual blood	1) MMP11, MMP7, MMP10 2) MSX1, LEFTY2, SFRP4
5 [Haas *et al*. (2014) (3)]	Vaginal secretions	Three assays for a total of seven mRNA and rRNA markers specific to vaginal secretions	1) MYOZ1, CYP2B7P1, MUC4 2) Ljen, Lgas, Lcris 3) HBD1
6	Skin	Two assays for a total of eight mRNA markers specific to skin	1) LCE1C, IL-1F7, LCE1D, LCE2D, CCL27 2) LOR, KRT9, CDSN

Through this work, EDNAP's primary objective is in the validation of RNA profiling as a reliable method for application in future forensic casework. This aligns well with the research strategy of this thesis. Each research exercise tested the robustness, specificity and sensitivity of the RNA profiling method; when carried out by different and sometimes inexperienced laboratory operators using a wide range of analytical strategies. Research of this nature is essential if the outcomes of RNA analysis are to be accepted by the international scientific community as acceptable forensic evidence for the courtroom. The *Scientific Working Group on DNA Analysis Methods* (SWGDAM) has a list of published guidelines for developmental validation of a new genetic analysis method – summarised in Table 3.2. The EDNAP collaborative research exercises aim to fulfil a number of these validation requirements, namely: species specificity testing, sensitivity testing, repeatability and reproducibility, applicability to casework samples and mixture analysis. It is likely that the outcomes of these studies will be cited in the first cases worldwide in which RNA is utilised as a source of evidence for the courtroom, to demonstrate and strengthen its admissibility.

Of the six aforementioned research exercises, the author has contributed practical research to four in order to assist EDNAP in validating the use of RNA profiling for the identification of menstrual blood, vaginal secretions and skin cell deposits under the SWGDAM guidelines. The objectives of this research will be described in subsequent sections.

Table 3.2: **The SWGDAM developmental validation guidelines for new DNA analysis methods.** All of the required elements marked with an asterisk (*) were assessed in the RNA collaborative research exercises. Information summarised from (184).

Scientific Working Group on DNA Analysis Methods (SWGDAM) **Developmental validation guidelines for new DNA analysis methods**
• Characterise genetic markers • **Assess species specificity*** • **Sensitivity testing*** • **Stability testing (to environmental/chemical insult)*** • Assess precision and accuracy **Repeatability** – same laboratory, operator, equipment* **Reproducibility** – different laboratory, operator, equipment* • **Applicability to casework samples*** • Population studies • **Mixture studies*** • PCR studies Primer sequences Reaction conditions Effects of primer multiplexing PCR controls Detection/measurement criteria

3.2 Experimental design, aims and objectives

The aim of this work was to devise and implement an analytical protocol permitting the identification of menstrual blood, vaginal secretions and skin cell deposits in 'mock' casework samples by characterisation of their RNA expression profiles. This analytical protocol was developed in accordance with EDNAP's guidelines and included all steps in RNA analysis: RNA extraction and purification, removal of DNA contamination, reverse transcription of RNA into cDNA, PCR amplification of cDNA and product separation by capillary electrophoresis. A number of RNAs were identified from the forensic literature with expression previously demonstrated to be strongly associated with specific tissue types. Six RNAs linked to menstrual blood, seven to vaginal secretions and eight to skin cell deposits were assayed for by RT-PCR, using the protocol described in Section 2.1, Chapter 2. The identity of these RNAs is revealed in Table 3.3.

Table 3.3: **Body fluid identification mRNAs with expression profiles associated with menstrual blood, vaginal secretions and skin cell deposits**. All markers have been previously reported in the literature. Functional information collated from (3, 51, 53, 68, 181, 185-196).

Target biological specimen	RNA marker identity	Marker protein function	Previous marker reference
Menstrual blood	Matrix metalloproteinases 7, 10 and 11 (MMP7/10/11)	Zinc-dependent endopeptidase enzyme, functions in to break down the extracellular matrix during tissue degradation and remodelling in menstruation	(2)
	Msh homeobox 1 (MSX1)	Transcriptional repressor, involved in cell signalling required for embryo implantation in the endometrium	(33)
	Left-right determination factor 2 (LEFTY2)	Growth factor, thought to play an important role in endometrial bleeding	(33)
	Secreted frizzled related protein 4 (SFRP4)	Inhibits proliferation and stimulates apoptosis of the endometrium during menstruation	(33)
Vaginal secretions	Myozenin 1 (MYOZ1)	Intracellular binding protein, tethers calcineurin to the sarcomere	(68)
	Cytochrome P450 family 2, subfamily B, polypeptide 7 pseudogene 1 (CYP2B7P1)	Non-coding RNA transcribed from a pseudogene; function unknown	(68)
	Mucin 4 (MUC4)	Glycosylated membrane protein, involved in protection of epithelium against microbial invasion and vaginal lubrication	(182)
	Human beta-defensin 1 (HBD1)	Small peptides secreted by neutrophils and epithelial cells, involved in protection of epithelium against microbial colonisation	(182)

Vaginal secretions	*Lactobacillus jensenii* 16S-23S rRNA intergenic spacer region (Ljen)	Lactobacilli are bacteria present in the vaginal tract, and the intergenic spacer region is a section of RNA between the 16S (small) and 23S (large) rRNA subunits (which are transcribed as a polycistronic RNA), used for microbial identification	(64)
	Lactobacillus crispatus 16S-23S rRNA intergenic spacer region (Lcris)		(43)
	Lactobacillus gasseri 16S-23S rRNA intergenic spacer region (Lgas)		(43)
Skin cell deposits	Late cornified envelope 1C (LCE1C)	Protein family involved in epidermal cornification, the formation of a protective layer of dead keratinocytes on the surface of the skin	(181)
	Interleukin 1-F7 (IL1F7)	Cytokine involved in the skin's adaptive immune response, particularly skin hypersensitivity	(181)
	Late cornified envelope 1D (LCE1D)	Protein family involved in epidermal cornification, the formation of a protective layer of dead keratinocytes on the surface of the skin	(181)
	Late cornified envelope 2D (LCE2D)		(181)
	Chemokine ligand 27 (CCL27)	Cytokine involved in the skin's innate inflammatory response, specifically recruitment of T-cells	(181)
	Loricrin (LOR)	Key structural component of the cornified cell envelope, a tough and insoluble barrier formed inside the plasma membrane in stratified squamous epithelia that make up the stratum corneum	(53)
	Keratin 9 (KRT9)	Cytoskeletal intermediate filament protein, found only in terminally differentiated epidermal cells in the palms of the hands and soles of the feet	(53)
	Corneodesmosin (CDSN)	Epidermal adhesion molecule, reinforcing cell-cell adhesion in the upper epidermis and stratum corneum	(53)

Using the devised protocol, a total of 24 'blind' stains were analysed to try and identify whether or not they contained menstrual blood, vaginal secretions and skin cells. To prevent any bias, these 'blind' stains were prepared and shipped by EDNAP's co-ordinating laboratory, and their identity only revealed upon submission of the results and completion of the study. These 'blind' stains were designed to mimic real life casework including both fresh and environmentally compromised samples, and a wide range of biological specimen types (not restricted only to menstrual blood, vaginal secretions and skin cell deposits).

For each of menstrual blood, vaginal secretions and skin cells a dilution series was also analysed to try to identify the minimum input required for successful identification by RNA profiling – i.e., the sensitivity of the protocol described in Section 2.1, Chapter 2. For both menstrual blood and vaginal secretions, the difficulty of obtaining liquid samples meant that the two dilution series were prepared on cotton swabs: 1/4, 1/8, 1/16, 1/32 and $1/64^{th}$ of a swab. For skin samples, a dilution series of RNA extracted from cultured human skin cell lines was prepared: 200, 50, 12, 3 and 0.8 ng of RNA.

Furthermore, a number of mock casework stains were prepared in-house onto which the protocol was applied, including:

- Menstrual blood stains (10 µL liquid menstrual blood spotted onto cotton)
- Circulatory blood stains
- Vaginal swabs
- Buccal swabs
- Liquid saliva, spotted onto a swab
- Swabs of 'touched' items – a tablet computer screen, touchscreen mobile phone screen, computer keyboard, computer mouse, mug handle, car steering wheel and a simple swab of the surface of the hand

It is standard practice when working with RNA to assay for the presence of 'housekeeping' or endogenous control gene RNAs. These are RNAs that, based on their known function in the cell, are thought to be permanently and ubiquitously expressed in all cell types, necessary for cell survival. Such RNAs include those which encode for the following proteins:

- *β_2-microglobulin* (B2M), a structural component of the major histocompatibility class I complex, present on all nucleated cells to permit the presentation of foreign antigens to provoke an immune response to invasion
- *Ubiquitin C* (UBC), which is 'tagged' onto damaged/old proteins for degradation by the proteasome and recycling
- *Ubiquitin conjugating enzyme UBCH5B* (UBCH5B, referred to by EDNAP as UCE), which catalyses the ubiquitination of damaged/old proteins to target them for degradation and recycling by the proteasome

The assumed 'universal' expression of these RNAs means that they are commonly used as a positive control to confirm the presence of intact RNA in a biological specimen; irrespective of its origin.

The expression of these three RNAs was examined in known stains of blood, semen, saliva, menstrual blood and skin cell deposits to assess their efficacy as endogenous positive controls in these sample types and to determine the minimum input of each body fluid type required for their successful identification. Moreover, they were assayed for in 'blind' samples to mimic how endogenous controls would be used in a casework scenario as positive controls and how their results are interpreted.

This study incorporated RNA profiling into the standard DNA profiling workflow for biological casework specimens. By doing this, it was hoped to ascertain whether expanding the genetic analyses to include both RNA and DNA would compromise the quality of DNA profiles output. Clearly, any observed reduction in the success rate of DNA profiling would demerit the potential benefits that RNA profiling could bring to a forensic investigation.

Overall, the objectives of this chapter are three-fold – summarised for clarity in Box 3.1 below.

Box 3.1: Objectives of Chapter 3

To **develop a protocol** for successful extraction, reverse transcription and amplification of RNA from dried biological specimens.

To apply this protocol to **identify** a range of 'blind' mock casework specimens prepared by the organising laboratory – specifically to identify whether they express RNA markers associated with menstrual blood, vaginal secretions and skin cell deposits.

To assess the **sensitivity** of RNA markers (both tissue specific and endogenous controls) expressed in dilution series' of blood, saliva, semen, menstrual blood, vaginal secretions and skin cells.

In contrast to the rest of this thesis, this chapter presents the outcomes of research into the expression of RNAs in body fluids and contact traces as opposed to solid tissues. However, irrespective of the biological substrate onto which RNA analysis is applied, the experimental workflow remains the same. The bulk of this work was conducted very early during thesis preparation and contributed strongly towards early protocol development and testing. In addition, the collaborative links maintained with EDNAP researchers have proven invaluable for guidance and support. The outcomes of this work have been published in two journal articles (3, 66) and another is currently under review by *Forensic Science International: Genetics*.

3.3 Method

All aspects of the method have been described in detail in Section 2.1, Chapter 2. Initially, this includes a description of the preparation of all biological specimens, followed by a detailed protocol for:

- Extraction and purification of RNA
- Treatment of RNA with DNase to remove DNA contamination
- Reverse transcription of RNA into cDNA
- PCR amplification of cDNA: including *Taq* polymerases, primer sequences, concentrations and thermal cycling parameters
- Extraction and purification of DNA
- Quantification of DNA
- PCR amplification of DNA STRs
- Separation of cDNA/DNA PCR products by capillary electrophoresis

3.4 Results and discussion

3.4.1 EDNAP exercise four (I): Identification of endogenous control gene mRNAs

3.4.1.1 Results

The presence of three endogenous control gene RNAs – B2M, UBC and UCE – was assayed for in dilution series of semen (0.04 to 5 µL), blood (0.001 to 1 µL) and saliva (0.2 to 25 µL); the results of which are presented in Table 3.4. These results are incorporated into Table S7 of Haas *et al*. (2014) (3).

Table 3.4: **Results after amplification of a dilution series of semen (0.04 to 5 µL), blood (0.001 to 1 µL) and saliva (0.2 to 25 µL) for the presence of three endogenous control gene RNAs**. The absence of a specific mRNA marker is denoted '-', and no result upon DNA typing with 'NR'. Peak heights were designated by the GeneMapper v3.2 software.

		Electropherogram peak height (rfu)			
Sample type	**Volume (µL)**	**B2M**	**UBC**	**UCE**	**DNA profile result**
Semen	5	-	10631	1667	Full profile
	1	-	4868	2920	Full profile
	0.2	-	-	-	Full profile
	0.04	512	-	-	Partial profile (2/10 full loci)
Blood	1	8719	9112	5767	Full profile
	0.1	9152	5168	1265	Partial profile (6/10 full loci)
	0.01	-	-	-	NR
	0.001	-	-	-	NR
Saliva	25	4219	9215	-	Full profile
	5	810	3181	-	NR
	1	-	798	-	NR
	0.2	-	-	-	NR

As illustrated in Table 3.4, these RNAs were diluted out in the lowest volume samples. None of the endogenous control RNAs could be detected in 0.2 µL semen, ≤ 0.01 µL blood and 0.2 µL saliva, and only a partial RNA profile from 5, 1 and 0.04 µL semen and 25, 5 and 1 µL saliva. Only for large blood stains could a full, 3 marker RNA profile be obtained. All samples were reverse transcribed in duplicate (RT+ and an RT- control), with all RT- controls blank with the exception of one contaminating 1367 rfu peak at the B2M locus for the RT- 0.01 µL blood sample. This illustrates that the B2M, UBC and UCE primers are RNA/cDNA specific and do not amplify genomic DNA.

Additionally, the results obtained upon DNA profiling are presented adjacent in Table 3.4. This demonstrated that DNA could be detected more sensitively than RNA in semen; with a full DNA profile obtained from only 0.2 µL semen. In blood and saliva the converse was true; a full DNA profile only obtained from 1 µL blood and 25 µL saliva.

3.4.1.2 Discussion

The purpose of adding endogenous control gene RNAs to a body fluid identification assay is to confirm the presence of human RNA, irrespective of its origin. Ideally, the endogenous control gene RNAs would prove more sensitive than the body fluid specific assay to permit the correct interpretation of negative results (33). In this research however, EDNAP did not specifically request that body fluid specific assays be applied for comparative purposes.

The outcomes of this study suggest that these three endogenous control gene RNAs are not particularly sensitive markers for the detection of semen and saliva (Table 3.4). B2M was poorly expressed in high volumes of semen; and similarly UCE poorly expressed in saliva. Problems with the amplification of endogenous control gene RNAs in these two body fluid types have been previously reported. Gene expression in semen is relatively low, deemed to be due to the very small spermatozoa cytoplasm volume and low ribosome count (8). The

desquamated mucosa lining the oral cavity has virtually no metabolism, resulting also in reduced transcription and translation of RNAs (29).

Some other mRNAs such as GAPDH and ACTB have been examined as potential endogenous control genes, with the same difficulties presented upon examination of semen and saliva (71). It has been suggested that 18S rRNA might act as a more sensitive marker for difficult body fluid types, as rRNA constitutes more than 90% of cellular RNA (51). However, the extremely high abundance of 18S rRNA relative to other mRNAs makes it difficult to incorporate into a multiplex assay. As yet, no universally effective endogenous control gene exists for incorporation into forensic assays of this nature (33). This work clearly highlights that more research is required to develop an endogenous control RNA panel applicable to all body fluid types; the ideal scenario. Failing this, endogenous controls could potentially be identified which are particularly applicable to specific biological specimen types.

3.4.2 EDNAP exercise four (II): Identification of menstrual blood specific RNAs

3.4.2.1 Results

Eight 'blind' samples (numbered 1 through 8), a dilution series of known menstrual blood (1/4 to 1/64th of a menstrual blood swab) and a number of menstrual blood and circulatory blood samples prepared in-house were examined to try to identify within them six menstrual blood specific RNAs and three endogenous control RNAs. The outcomes of this analysis are displayed in Table 3.5; data presented in Tables 2, 3 and S2 of Haas *et al*. (3). A sample electropherogram illustrating the results for Stain 3 can be viewed in Figure A2.1 in Appendix 2.

Table 3.5: **Results after amplification of a menstrual blood dilution series (1/4, 1/8, 1/16, 1/32 and 1/64th of a swab), four known menstrual blood samples, eight stains of unknown identity and a blood stain for the presence of six menstrual blood specific RNAs and three endogenous control RNAs.** Those samples which failed to amplify are denoted '-'. Stains 2 and 5, marked with an asterisk (*) did not contain menstrual blood.

	Electropherogram peak height (rfu)									
	Matrix metalloproteinase assay (3-plex)			Menstrual blood assay (3-plex)			Endogenous control RNA assay (3-plex)			
Sample type	**MMP11**	**MMP7**	**MMP10**	**MSX1**	**LEFTY2**	**SFRP4**	**B2M**	**UBC**	**UCE**	**DNA profile result**
Men blood 1/4	929	-	5784	531	-	-	9920	10514	10507	Full profile
Men blood 1/8	1367	868	5360	-	-	237	10251	10218	10471	Full profile
Men blood 1/16	355	222	1946	-	-	-	10353	10164	9508	Full profile
Men blood 1/32	235	-	1286	-	-	-	10285	10261	8123	Full profile
Men blood 1/64	-	289	-	-	-	-	10450	10550	4984	Full profile
Men blood day 1A	-	-	-	-	-	-	-	-	-	Full profile
Men blood day 1B	2963	8702	3961	1642	-	-	9015	9094	5307	Full profile
Men blood day 2A	875	191	8894	-	1953	-	8925	9151	9120	Full profile
Men blood day 2B	-	234	4832	-	-	-	8156	9197	8156	Full profile
Stain 1	7310	3271	9237	503	4413	-	9414	10679	1042	Full profile
Stain 2*	-	-	683	-	-	-	9659	10366	10349	Full profile
Stain 3	7126	8097	8733	7721	8024	8422	9374	10231	10176	Full profile
Stain 4	8644	293	9077	625	1868	320	9738	10557	8572	Full profile
Stain 5*	-	2181	-	-	-	-	10084	9914	10377	Full profile
Stain 6	1620	-	1150	1525	451	-	10183	10097	8930	Full profile
Stain 7	-	-	-	-	-	-	9098	3694	-	Full profile
Stain 8	-	-	-	-	-	-	10297	10306	7260	Full profile
Circulatory blood stain	-	-	-	-	-	-	4331	-	2089	Full profile

Table 3.5 illustrates that DNA profiling does not appear to have been compromised in any way; a full DNA profile being obtained from all samples, even the smallest dilution sizes of menstrual blood. All extraction blank and RT- controls gave negative results (data not shown). The three endogenous control gene RNAs were consistently detected in almost all menstrual blood and unknown stains, with the exception of one (menstrual blood, day 1A sample). In the menstrual blood dilution series, the three matrix metalloproteinase mRNAs (MMP11, 7 and 10) were detected much more frequently and consistently than those belonging to the menstrual blood assay (MSX1, LEFTY2 and SFRP4), which exhibited particularly poor sensitivity. None of the samples in the menstrual blood dilution series gave a full mRNA marker profile; with between 1 and 4 of the 6 menstrual blood specific markers detected.

Of the unknowns, only stains 3 and 4 returned a full, 6 marker menstrual blood profile. Stains 7 and 8 returned no results, despite amplification of the endogenous control gene RNAs to confirm the successful extraction and reverse transcription of RNA. As desired, the non-menstrual blood stain returned no results for the menstrual blood specific markers.

3.4.2.2 Discussion

In the case of an alleged sexual assault, it is crucial to characterise the origin of blood recovered from evidentiary items – i.e., whether the source was circulatory (from an injury) or menstrual in nature. Menstrual blood is comprised of 30-50% circulatory blood, with the rest made up of endometrial and vascular smooth muscle (33, 182). Several methods have been previously described for the distinction of menstrual blood, such as by microscopic identification of endometrial cells, lactate dehydrogenase isoenzyme analysis and identification of fibrin degradation products such as D-dimers (197). However, all of these methods are poorly sensitive to small and degraded samples.

As can be seen in Table 3.5, the MMP markers exhibited much higher sensitivity for menstrual blood than MSX1, LEFTY2 and SFRP4, as demonstrated with

a dilution series of menstrual blood swabs. This result was confirmed across all participating laboratories in the EDNAP study, and with a set of four 'in house' prepared menstrual blood stains. At least one MMP marker could be detected by 70% of operators even in 1/64th of a menstrual blood swab. On the contrary, only MSX1 could be detected by > 50% of operators in the largest samples: 1/4 and 1/8 menstrual blood swabs. LEFTY2 and SFRP4 required significantly higher input quantities for consistent detection, which presents a serious limitation for their practical use in casework. In addition, they have been shown to drop out earlier in the menstrual flow (by day four of the menstrual cycle) than MMPs (3).

Following submission of all experimental data from the participating laboratories to EDNAP, the identity of the eight unknown stains was revealed; summarised in Table 3.6. Two non-menstrual blood samples were included (stains 2 and 5) to examine the assay specificity. Both were found to return a result for 1 of the 6 mRNA markers; MMP10 for a blood swab (stain 2), and MMP7 for a vaginal swab (stain 5). Only sporadic markers were detected for the blood stain, by a small number of operators in the EDNAP study. MMP7 was detected by 50% of operators in the vaginal swab. The presence of menstrual blood specific RNAs in a vaginal swab is not particularly surprising. Menstrual blood presents a novel challenge for the development of gene expression assays, since it relies not only on the identification of RNAs expressed in a spatially restricted manner, but also temporally during menstruation (182). Although some authors have reported the exclusivity of MMP expression only to menstrual blood (50), others have claimed that the MMPs are still detectable in vaginal swabs during the non-bleeding days 6 through 28 of the menstrual cycle; albeit at a significantly lower level than during menstruation (8).

Stains 7 and 8 were incorrectly identified as negative for the presence of menstrual blood, despite successful identification of endogenous control RNAs. This result was supported by the data submitted by other participating laboratories; with only one marker detected by > 50% of operators in stains 7 and 8. The reason for this identification failure is unclear for stain 8, but for stain 7 is most likely as a result of the small size and age (stored for approximately 5 to 6 years) of the

menstrual blood swab. Stains 1, 3, 4 and 6 all correctly returned a partial or full profile of menstrual blood specific RNAs, and were accurately identified.

Table 3.6: **Identity of the eight unknown 'mock' casework stains prepared by EDNAP, subjected to analysis for identification of menstrual blood specific RNAs**. (C. Haas, personal communication).

Stain number	Stain identity
1	Menstrual blood on sanitary towel, collected 2011
2	1/4 swab with EDTA-preserved blood
3	1/4 menstrual blood swab, collected 2011
4	Menstrual blood on sanitary towel, collected 2007
5	1/4 vaginal swab, collected 2011
6	1/4 menstrual blood swab, collected 2007
7	1/12 menstrual blood swab, collected 2007
8	1/4 menstrual blood swab, collected 2012

All samples analysed returned a full profile upon subsequent DNA profiling, indicating that DNA/RNA co-extraction appears not to have had any compromising effect on the quality of the DNA results obtained. This is clearly a beneficial outcome: obtaining a DNA match to a suspect/victim will always be of primary importance in a criminal investigation with RNA analysis providing supportive, reconstruction-led data (198).

In summary, the outcomes of this work are mixed regarding the efficacy of this method for correct identification of menstrual blood in mock casework specimens. All 24 participating laboratories were able to successfully implement their own experimental design and obtain concordant results. The three endogenous control RNAs (B2M, UBC and UCE) and the matrix metalloproteinase RNAs (MMP11, 7 and 10) exhibited reasonably good sensitivity, allowing correct identification of even small and aged menstrual blood stains. However, it has become clear that MSX1, LEFTY2 and SFRP4 are poorly sensitive markers of menstrual blood and their use should be reconsidered. This work has also highlighted the issues of correctly interpreting negative results, with false negatives

obtained for two true menstrual blood stains despite successful identification of their endogenous positive controls.

3.4.3 EDNAP exercise five: Identification of mRNAs specific to vaginal secretions

3.4.3.1 Results

Eight 'blind' samples (numbered 9 through 16), a dilution series of known vaginal secretions (1/4 to 1/64th of a vaginal swab) and a number of vaginal and non-vaginal samples prepared in-house were examined to try to identify within them the presence of seven vaginal fluid specific RNAs. The outcomes of this analysis are displayed in Table 3.7; data presented in Tables 2, 3 and S2 of Haas *et al*. (3). A sample electropherogram illustrating the results for 1/16th of a vaginal swab can be viewed in Figure A2.2 in Appendix 2.

It can be seen from Table 3.7 that all samples analysed returned a full DNA profile. The vaginal fluid specific RNA markers proved extremely sensitive except Lgas, as demonstrated with a dilution series of vaginal swabs. MYOZ1, CYP, MUC4, Ljen and Lcris were all detected even in 1/64th of a vaginal swab. Lgas was only sporadically detected in a small number of vaginal fluid samples. Analysis of the eight unknown stains permitted the identification of at least one RNA marker in each; with all seven RNAs detected in stains 12 and 14. It was possible to sporadically detect some RNAs in a buccal swab (MYOZ1, MUC4 and Ljen) and in a saliva sample (Ljen).

Table 3.7: **Results after amplification of dilution series of vaginal swabs (whole, 1/4, 1/8, 1/16, 1/32 and 1/64th of a swab), eight stains of unknown identity and a buccal swab and saliva sample for the presence of seven mRNAs specific to vaginal secretions.** Those samples which failed to amplify are denoted '-', and three DNA profiles were not done (ND). Those stains marked with an asterisk (*), the buccal swab and saliva sample did not contain vaginal secretions.

	Peak height (rfu)							
	Vaginal 3-plex			Lacto 3-plex			HBD1	
Sample type	**MYOZ1**	**CYP**	**MUC4**	**Ljen**	**Lcris**	**Lgas**	**HBD1**	**DNA profile result**
Vaginal swab	3704	8595	7821	-	7935	-	5714	ND
Vaginal swab 1/4	7248	8408	8190	5940	8177	-	5013	Full profile
Vaginal swab 1/8	3630	8372	8410	5742	8251	-	3007	Full profile
Vaginal swab 1/16	4097	8724	8763	5289	8588	830	2609	Full profile
Vaginal swab 1/32	873	8638	8703	5614	9046	-	-	Full profile
Vaginal swab 1/64	1683	8783	7948	6136	8983	-	905	Full profile
Stain 9	8394	7928	8299	-	7364	-	8876	Full profile
Stain 10	-	2029	146	6270	8859	758	3337	Full profile
Stain 11*	-	-	2169	5772	2397	552	-	Full profile
Stain 12	7759	8460	7585	314	7412	7681	2470	Full profile
Stain 13	6088	8366	9126	2396	7262	-	3379	Full profile
Stain 14	2359	8639	8049	6200	7560	6175	1318	Full profile
Stain 15*	-	-	-	8159	175	-	-	Full profile
Stain 16	-	-	-	-	2633	-	-	Full profile
Buccal swab	481	-	3043	5579	-	-	-	ND
Saliva	-	-	-	8239	-	-	-	ND

3.4.3.2 Discussion

Having the ability to definitively identify vaginal secretions on evidentiary items would significantly simplify the investigation of alleged sexual assaults. Often, a defence stance to the presence of a victim's DNA on an item is that the contact was non-sexual in nature, i.e. that the source of DNA was the victim's skin rather than their vaginal epithelium. This problem is exacerbated by the fact that methods for identification of vaginal epithelial cells are scarce. One of the only methods published to date is that of Randall, who suggested that vaginal epithelial cells could be identified by acid-Schiff staining and microscopy (199) – a method which is poorly sensitive and unspecific.

Unfortunately, the vaginal epithelium has proven to be a difficult substrate for which to identify RNAs with a restricted expression pattern. The high physiological and functional similarity between the vaginal and oral epithelia has made the distinction of vaginal secretions from saliva difficult (31). A number of RNA markers have been suggested as being indicative of the presence of vaginal secretions. Researchers have been creative with their methods to try to overcome this; for example by identifying novel RNA markers with unknown functions by whole transcriptome sequencing, or by incorporating vagina-specific bacterial RNA targets into their assays (43). The seven RNA markers selected by EDNAP for their fifth RNA research exercise, involving the identification of vaginal secretions, includes both human and bacterial specific markers as illustrated in Table 3.7.

As Table 3.7 shows, MYOZ1, CYP, MUC4, Ljen, Lcris and HBD1 exhibited extremely high sensitivity when assayed for in a dilution series of vaginal swabs. Lgas on the other hand, could only be sporadically detected. This is concordant with the results obtained by other operators; with Lgas amplified only in around 9% of vaginal swab fragments. The use of *Lactobacillal* markers for the identification of vaginal secretions was first reported by Fleming and Harbison (43), in an attempt to circumvent issues regarding the cross-reactivity of the conventional vaginal fluid markers with saliva. Some authors have reported the Lgas rRNA marker to be detectable in as little as 0.08 ng total RNA (54). However, a number of factors have

been shown to affect colonisation of the vagina with *Lactobacilli*, including health status, age, smoking, ethnicity and vaginal pH (43, 54). It seems likely that since all swabs used in this study were collected from a single volunteer, some of these factors are in play affecting the type and relative abundance of *Lactobacilli* between individuals.

In addition, *Lactobacillus jensenii* (Ljen) rRNA was amplified in an extraction negative control prepared with a blank cotton swab (data not shown). This was reported by one other operator taking part in the EDNAP study (C. Hüls and M. Vennemann, personal communication). This may be indicative of background *L. jensenii* contamination in the laboratory environment or even in the PCR reagents provided by the organising laboratory, and commands further investigation (3). Ljen rRNA was also amplified from one RT- sample (that of stain 14). However, this does not present any major issues since amplification of *L. jensenii* genomic DNA (rather than RNA) is still indicative of the presence of the bacterium.

Similarly to EDNAP exercise four, the identity of the eight unknown 'mock' casework stains was revealed following submission of data to EDNAP (Table 3.8).

Table 3.8: **Identity of the eight unknown 'mock' casework stains prepared by EDNAP, subjected to analysis for the identification of vaginal fluid specific RNAs**. (C. Haas, personal communication).

Stain number	Stain identity
9	¼ vaginal swab, collected 2010
10	5 x 5 mm cutting of a white worn underpant, collected 2012
11	½ swab urine, collected 2012
12	½ swab of vaginal secretions from a pregnant female, collected 2012
13	¼ vaginal swab, collected 2007
14	½ vaginal swab, collected 2012
15	½ buccal swab, collected 2012
16	5 x 5 mm cutting of sanitary towel, collected 2012

Two non-vaginal fluid samples were included to assess the specificity of the assay (stains 11 and 15), in addition to a buccal swab and a saliva sample prepared in house. In the urine sample (stain 11) it was possible to amplify four of the seven vaginal fluid specific markers; an outcome which was not wholly unexpected due to cross-contamination between the two body fluids. It was possible however, to amplify several markers in the buccal/saliva samples, including MYOZ1, MUC4, Ljen and Lcris. This result was concordant with the data submitted by other operators – with MYOZ1, MUC4, Ljen and HBD1 detected in > 25% of buccal swabs (stain 15). The specificity of these markers to vaginal secretions is a contentious issue. Because the epithelia of the vagina and the inside of the mouth perform very physiologically similar functions (i.e. protection against infection, secretion/transport, sensation) the identification of RNAs with exclusivity to one or the other in their expression is difficult (68). Several authors have published data demonstrating the cross-reactivity of MUC4 and HBD1 with saliva (33, 44, 54, 70, 183), an outcome which is contested by others (50, 182). This study suggests that data pertaining to MYOZ1, MUC4, Ljen and Lcris should be interpreted with caution due to cross-reactivity with saliva.

Five of the eight 'mock' casework stains provided results consistent with the presence of vaginal secretions (stains 9, 10, 12, 13 and 14). Six of the seven vaginal-fluid specific markers could be amplified even from stain 13, which had been aged for approximately 5-6 years. The survival of RNA in vaginal secretions has been doubted as a result of the high microbial load and enzyme content relative to other body fluids (such as blood or semen) (42, 44), but this outcome lends support to the long-term persistence of RNA. Unexpectedly, stain 16 (a cutting from a sanitary towel), returned a peak only for Lcris.

RNA analysis presents one of the only means by which vaginal secretions can be identified in forensic specimens. The outcomes of this work suggest that all but one of the RNAs examined are extremely sensitive indicators of the presence of vaginal secretions, even for small and aged samples. The expression of Lgas was extremely poor. It should be investigated whether this was as a donor-specific or assay-specific issue. However, some of the RNAs were not exclusively expressed in

vaginal secretions and exhibited cross-reactivity with buccal swabs and saliva; highlighting the requirement for a thorough search for new markers (70).

3.4.4 EDNAP exercise six: Identification of mRNAs specific to skin cell deposits

3.4.4.1 Results

Eight 'blind' samples (numbered 17 through 24), a dilution series of cultured skin cell RNA (200, 50, 12, 3 and 0.8 ng total RNA) and a number of 'touch' samples prepared in-house (swabs of a tablet computer, touchscreen mobile phone, mug handle, car steering wheel, computer mouse, computer keyboard and a direct swab of the surface of an individual's hand) were examined to try to identify within them the presence of eight RNAs associated with skin cells and three endogenous control RNAs. The outcomes of this analysis are displayed in Table 3.8. These results have been submitted in a manuscript to *Forensic Science International: Genetics* (September 2014). A sample electropherogram illustrating the results for 200 ng skin RNA can be viewed in Figure A2.3 in Appendix 2.

Table 3.9: **Results after amplification of a dilution series of skin RNA (200, 50, 12, 3 and 0.8 ng), eight stains of unknown origin, and a series of 'in-house' swabs for identification of eight skin-specific RNAs and three endogenous control RNAs**. Those samples which failed to amplify are denoted '-'. Those stains marked with an asterisk (*) did not contain skin cell deposits.

	Peak height (rfu)										
	Skin 1 5-plex					Skin 2 3-plex			Endogenous control RNA 3-plex		
Sample type	**LCE1C**	**IL1F7**	**LCE1D**	**LCE2D**	**CCL27**	**LOR**	**KRT9**	**CDSN**	**B2M**	**UBC**	**UCE**
Skin RNA 200 ng	7591/7703	8869	2495	2804	9054	8873	-	5767	8817	9160	9339
Skin RNA 50 ng	7508/7754	8724	3301	8893	9348	8474	-	9078	8714	9113	9228
Skin RNA 12 ng	-	-	-	-	-	-	-	-	-	-	-
Skin RNA 3 ng	-	-	-	-	-	-	-	-	-	-	-
Skin RNA 0.8 ng	-	-	-	-	-	-	-	-	-	-	-
Stain 17	686/430	-	-	-	-				-	-	-
Stain 18	-	-	-	-	-	-	-	-	-	-	-
Stain 19	-	-	-	-	-	-	-	-	-	-	-
Stain 20	-	-	-	-	-	-	-	-	-	-	-
Stain 21*	-	-	-	-	-	-	-	-	-	-	-
Stain 22	8201/5439	-	-	-	-	-	-	-	8946	-	-
Stain 23*	-	-	-	-	-	-	-	-	-	-	-
Stain 24	7301/7348	8901	3974	8970	5064	7730	-	9032	8725	9247	9063
Tablet screen	1100	-	-	-	-	-	-	-	1261	-	-
Mobile phone	1209	-	-	-	-	3060	-	-	-	-	-
Mug handle	-	-	-	-	-	-	-	2503	-	-	-
Car steering wheel	2376	820	-	-	-	-	-	-	-	-	-
Comp. keyboard	1337	-	-	-	-	-	-	-	-	-	-
Computer mouse	8444	-	-	-	-	4367	-	-	-	-	-
Surface of hand	7842	2497	2066	1025	-	8725	-	436	-	971	-

It can be seen from Table 3.9 that no samples returned a full, 11 marker RNA profile. KRT9 failed to amplify in all samples; even in those with the highest input quantity. LCE1C often returned a split peak as its mRNA exists in two alternative isoforms, amplified as two PCR products of lengths 53 and 55 nucleotides. 10 of the 11 mRNAs were detected in ≥ 50 ng skin RNA. Below this input quantity, it was not possible to characterise any of the skin-specific markers or endogenous control RNAs.

RNA could only be amplified from three of the eight 'unknowns' – stains 17, 22 and 24. All of the 'touched' objects prepared in house (swabbings of a tablet screen, mobile phone, mug handle, car steering wheel, computer keyboard and mouse) permitted detection of between 1-2 skin-specific mRNAs. The nature of the extraction system used in this study did not permit co-extraction of DNA, and thus DNA profiling was not performed. All extraction blank and RT- controls returned negative results (data not shown), indicating that the assay did not detect genomic DNA or any other form of contamination.

3.4.4.2 Discussion

Technology has advanced so far in recent years that it is often possible to identify the presence of 'touch' DNA, i.e. that deriving from the limited number of skin cells and sweat deposited on an item through direct contact which can be recovered by swabbing or tape-lifting (200, 201). Unfortunately, there are currently no methods available to identify the source of skin cell deposits, perpetuating the 'mystery' often associated with this type of invisible evidence (52). Many methods for fingerprint visualisation are detrimental to DNA analysis (50). mRNA profiling presents the first method by which this could potentially be achieved. A number of mRNAs have been identified as having expression restricted to the outermost layers of the skin.

Surprisingly, the eight skin-specific markers exhibited poor sensitivity upon examination of a dilution series of skin RNA (total RNA purchased from human skin cell lines) as demonstrated in the top half of Table 3.9. It was not possible to detect

any of the skin markers in less than 50 ng RNA. This outcome was not concordant with the data submitted to EDNAP from other operators. More than 50% of the 19 participating laboratories could successfully amplify at least four of the eight RNA markers from 0.8 ng skin RNA. Hanson *et al*. have illustrated that LCE1C, IL1F7, LCE1D, LCE2D and CCL27 are sporadically detectable in as little as 5-25 pg RNA (181). It is undeniable that assay sensitivity could have been improved by increasing the input volume of cDNA into PCR – from 1 µL (the volume recommended in EDNAP's standard protocol) up to a maximum of 3.75 µL per 12.5 µL reaction. Due to time and reagent constraints, samples were not subjected to repeat analysis by the author to try to obtain improved quality profiles.

In fact, the results presented in Table 3.9 are those obtained upon examination of a second dilution series of skin RNA swabs on behalf of EDNAP. The first set of five swabs provided (200, 50, 12, 3 and 0.8 ng RNA) returned no results, despite being processed in a single batch alongside a successful positive control (a swab of the hand surface). The reason for this complete failure of analysis is unknown, but is most likely attributed to an error in the EDNAP preparatory laboratory.

Of the eight 'unknowns', only stains 17, 22 and 24 returned a result indicating the presence of skin RNA. Following the submission of all experimental data to EDNAP, the identity of the eight 'unknowns' was revealed; summarised in Table 3.10. Stains 17 and 22 were prepared by directly swabbing the palm of the hand, and 24 by taking a skin scraping. Therefore, it appears only to have been possible to detect skin RNA in these high input samples; not in stains 18, 19 and 20 where skin cells were indirectly recovered by swabbing an intermediary object (Table 3.9). This was unexpected, as Hanson *et al*. (181) claim a 50% success rate for the amplification of some/all of LCE1C, IL1F7, LCE1D, LCE2D and CCL27 on touched objects; and Visser *et al*. (53) reported a 100% success rate for detection of some/all of LOR, KRT9 and CDSN in single fingerprints.

Table 3.10: **Identity of the eight unknown 'mock' casework stains prepared by EDNAP, subjected to analysis for the identification of skin cell specific RNAs**. (C. Haas, personal communication).

Stain number	Stain identity
17	Small swab of the palm
18	Hand print on a sheet of glossy paper
19	1 key from a computer keyboard
20	Finger print on a glass slide
21	Small swab of urine
22	Small swab of the palm, mixed with 1 µL blood
23	Small swab of saliva
24	Scraping of skin cells from the back of the hand

Stains 21 and 23 were the only samples analysed that did not directly contain skin cell deposits. Neither returned a result upon amplification of the skin specific RNAs. This outcome demonstrates the strong specificity of these RNA markers for skin and confirms previous reports by Hanson *et al*. (181) and Visser *et al*. (53); neither of whom were able to demonstrate false positives for skin upon examination of the expression of these eight markers in non-skin samples (including blood, semen, saliva, vaginal secretions and menstrual blood).

It was possible to characterise at least one skin RNA marker in all of the 'touched' objects prepared in house. LCE1C was the most consistently detected marker, present in all but one of the samples – a swab of a mug handle. This outcome mirrors a previous report by Hanson *et al*., who demonstrated LCE1C to be the most abundantly expressed and easy to detect skin marker (181). By comparison, the success rate in identifying skin RNAs in these samples was much better than in the 'unknowns' provided by EDNAP. Potentially, this could be an artefact of the storage and shipping conditions of the EDNAP samples. However, previous work has illustrated no reduction in results quality upon the first 6 months of fingerprint storage (53).

Similarly to the skin-specific RNAs, B2M, UBC and UCE exhibited poor sensitivity – only detectable in ≥ 50 ng skin RNA and sporadically in a small number of 'touch' samples (Table 3.9). Other reports have suggested that ACTB (53) and

18S rRNA (50) may serve as more sensitive and effective endogenous control markers for skin cell deposits, and these should be considered in EDNAP's future work.

This work clearly highlights the inherent difficulty in working with skin cell deposits as a source of RNA. Similar to low template DNA analysis, this method suffers from poor sensitivity and marker drop-out. Hanson *et al*. rightly advocate that skin identification assays should incorporate a large number of mRNA targets, as they acknowledge their detection in low template skin cell deposits to be inconsistent and sporadic (181). In this work, only LCE1C RNA could be consistently detected in 'touched' objects. More work is required to improve the sensitivity of these existing assays, e.g. by further optimising PCR conditions and reducing PCR amplicon lengths, or by identifying novel skin-specific markers with a higher basal level of expression. The perceived strong specificity of these assay systems for skin cell deposits is however encouraging for their potential future application.

3.5 Summary and conclusions: Cell specific gene expression profiling

The guidelines set by the *Scientific Working Group on DNA Analysis Methods* (SWGDAM) provide the minimum criteria for developmental validation of new genetic tests in forensic science. Although originally devised for DNA analyses, these same principles have been adopted by RNA researchers in their attempt to improve the credibility of evidence generated through RNA analysis. The research exercises co-ordinated by EDNAP are focused on demonstrating that RNA evidence meets these stringent criteria.

On the whole, the outcomes of this work have been positive regarding the use of RNA for identification of the origin of biological specimens, but they have highlighted the requirement for more work in some areas. A number of the assays have demonstrated excellent sensitivity to their respective tissue type, e.g. RNA markers could be successfully detected in $1/64^{th}$ of a menstrual blood and $1/64^{th}$ of a vaginal swab (EDNAP 4 and 5). On the contrary, assays for skin RNA were found to be poorly sensitive and markers were only sporadically detected (EDNAP 6). The skin identification assay (EDNAP 6) exhibited excellent specificity, with no cross-reactivity detected in non-skin samples. Some cross-reactivity was observed for the menstrual blood assay (EDNAP 4) with circulatory blood and vaginal swabs. In addition, a number of markers for vaginal fluid (EDNAP 5) were amplified from saliva, buccal swabs and urine.

When using these assays, the input quantity of RNA is critical in order to balance sensitivity and specificity. However at present, no technology exists allowing quantification of human RNA. Techniques such as UV-visible spectrophotometry, the Bioanalyzer 2100 and the use of RNA-intercalating dyes such as RiboGreen® are no use in a forensic setting because samples tend to be low quantity, low quality and contain a significant proportion of microbial RNA (e.g. especially saliva and vaginal swabs) (41, 55) (42). At too low an RNA input, peaks corresponding to tissue specific markers are lost. Excessive RNA input can actually be inhibitory to PCR, or can cause the appearance of electropherogram artefacts such as saturation peaks; which are clearly visible in some of the raw data

presented in Appendix 2. To try to overcome this problem, some laboratories have adopted a method based upon amplification of serial dilutions of cDNA but this is cumbersome, time consuming and open to bias and subjectivity.

This work also highlights issues with the use of B2M, UBC and UCE as endogenous control RNAs. Although they could be satisfactorily detected in blood and menstrual blood (EDNAP 4), their expression was low or undetectable in even high inputs of semen, saliva (EDNAP 3) and skin (EDNAP 6). Ideally, endogenous controls should be detected more sensitively than the tissue-specific RNAs to permit their use as a positive control for successful RNA purification and reverse transcription into cDNA. As this was not the case in semen, saliva or skin, the use of B2M, UBC and UCE as universal endogenous controls is discouraged and more work is required to try to identify alternative RNA targets for this purpose.

Significantly more work is required to bring the results of RNA analysis and their interpretation on par with DNA profiles. As can be seen from the raw electropherograms in Appendix 2, the PCR assays developed by EDNAP are fraught with artefacts; i.e. additional peaks other than those corresponding to an RNA marker such as dye blobs, uneven baseline and saturation peaks (65). Investment is required in optimising these PCR assays to improve the quality of their output thus simplifying their interpretation, to reduce error and subjectivity. This is made much more challenging by the differential basal expression level of RNAs in a multiplex assay, compared with DNA which for every locus always exists 2 copies per cell (71).

The number of published articles in the forensic literature regarding the use of RNA analysis for identification of the tissue origin of a biological specimen is expected to move into the hundreds in the coming months. Most of these articles identify novel RNA targets and examine sensitivity and specificity to their respective body fluid. The next challenge that EDNAP and the RNA community faces is with the interpretation of RNA data – particularly with regard to partial RNA profiles, negative results and statistical evaluation of the data. This theme will be continued throughout the rest of this thesis, focusing strongly on the interpretation of gene expression data pertaining to post-mortem tissues.

Chapter 4: Analysis of RNA in post-mortem tissues: Method development

4.1 Introduction

In accordance with the objectives outlined in Section 1.5, Chapter 1, the primary aim of this thesis was to examine the degradation behaviour of RNA in tissues after death using mice as a decomposition model. Research in this field is very much in its infancy with few published works; meaning that reliable, recommended experimental protocols and data analysis strategies are not available thus far. The exception to this is where commercially available kits/reagents have been implemented: for example, during reverse transcription and real time PCR.

It was therefore necessary to initially devise and test an effective experimental strategy; particularly with regard to tissue sample collection, the early stages of sample processing and for data analysis and presentation. This chapter reports upon the outcomes of three short experiments conducted during initial experimental design and testing.

4.1.1 Assessment of RNA stability on the bench

RNA is perceived to be an unstable molecule *in vivo* and *ex vivo*, in both settings being subjected to degradation by ribonucleases (RNases). In biological specimens such as solid tissues and body fluids, RNAs are disassembled into their constituent ribonucleotides rapidly by endogenous, intracellular RNases (202). However, exogenous RNases are also ubiquitous to the environment. The human body secretes RNases as a protective mechanism against infection, meaning that they are present in mucus, tears, saliva, skin oils and sweat, shed skin and hair (202). Exogenous RNases also can be sourced back to microbes such as bacteria and fungi. As a result, human and non-human RNases are omnipresent in our surroundings.

RNases are extremely robust (12), and can recover their activity even following autoclaving and repeated freeze-thaw cycles (9, 12). Therefore, it is necessary to take precautions when working in the laboratory with RNA to protect precious samples against RNase contamination. Such precautions include (12, 202):

- Regular changes of gloves and wearing face masks
- Having a dedicated set of clean, RNA-only pipettes
- Using only RNase-free plasticware and reagents – such as pipette tips, microcentrifuge tubes, PCR tubes, water, chemicals
- Having a dedicated 'RNA-zone' in the lab
- Cleaning down work surfaces and instrumentation with chemicals to remove RNase contamination, such as with RNase*Zap*® (203)

It was necessary to modify the analytical set up of the laboratory to implement some of these precautions for the first time.

The first stage of experimentation involved a brief study to test the effectiveness of these precautions within the current study. As the aim was to assess and quantify RNA degradation in tissues after death, it was important to initially establish that RNA could be successfully manipulated in the laboratory without inducing further, unwanted degradation. Detectable fragmentation of RNA on the bench would clearly be detrimental to the outcomes of this work. The stability of RNA (in pure form, suspended in RNase-free water) at room temperature (22 °C) was analysed, by leaving it untouched on the bench for the following time intervals: 0, 10 and 30 mins, and 1, 3, 6, 8, 24, 48, 72, 96 and 168 h.

Total RNA quality was assessed using the Bioanalyzer 2100 and RNA integrity number (RIN) algorithm. A panel of four RNAs was selected for quantification of their expression level by RT-qPCR – 18S rRNA, B2m, Gapdh and Fos. Of these, 18S rRNA, B2m and Gapdh were selected as three of the most commonly implemented endogenous control RNAs in published gene expression analyses (204). Fos on the other hand, is a member of the immediate early gene family and represents a transiently expressed, rapidly turned over RNA molecule (100).

4.1.2 Assessment of RNAlater® efficacy for stabilisation of RNA in post-mortem tissue samples

In addition to the aforementioned bench top precautions, a number of products are available on the market to safeguard the integrity of RNA in biological specimens; improving the practicality of RNA analysis. One such product is RNAlater® RNA Stabilisation Solution (205). Use of RNAlater® has been reported widely in both the forensic and clinical literature for the protection of RNA in solid tissues, body fluids, bacterial suspensions, cultured cells and plants (6, 51, 205-209).

RNAlater® is an aqueous storage reagent able to permeate cells and solid tissues, protecting RNA against the intracellular RNA degradation machinery. The primary constituent of RNAlater® is ammonium sulfate, which inactivates proteins such as RNases through a process known as *salting out* (210). Ammonium sulfate is extremely water soluble and exists in RNAlater® at high concentration; unofficial sources estimating it works best for the preservation of nucleic acids at approximately 4 M (210). When added to tissues at such a high concentration, ammonium sulfate induces the precipitation of proteins. Naturally, the charged, hydrophilic amino acids on the surface of proteins will form hydrogen bonds with surrounding water molecules in the aqueous cellular environment. Ammonium sulfate acts as a competitor in this process, reducing the availability of water to the proteins for hydrogen bonding. As a result, proteins tend to aggregate together, through the formation of hydrophobic interactions. The precipitation and inactivation of proteins such as RNases in this manner is reversible and has a minimal long-term effect on protein function (211).

According to the manufacturer, RNA in biological specimens can be completely stabilised in RNAlater® for up to 3 days at 37 °C, 1 week at 25 °C, 4 weeks at 4 °C or indefinitely at both -20 °C and -80 °C for long term storage. Tissue samples immersed in RNAlater® can be thawed and re-frozen without any significant effect on the integrity of RNA. It is stated that the preservation of biological specimens in RNAlater® is compatible with most downstream RNA

purification strategies, including the popular silica column and organic extraction protocols utilised throughout this thesis (205).

After death, it is expected that RNA is degraded by enzymes and chemicals present in decomposing tissues. To achieve the overall aim of this thesis to examine and quantify post-mortem degradation, an experimental design was devised involving the excision of tissue samples from mice at post-mortem intervals ranging from minutes to hours. This included skeletal muscle, kidney, liver and heart tissue, from which RNA was extracted. As the protocol involved the excision of tissue samples in quick succession, it was impractical for all samples to immediately undergo RNA extraction. The use of RNAlater® significantly simplified sample processing, allowing tissue samples to be stored until a convenient time for RNA extraction.

Although RNAlater® is used by RNA researchers across the fields, it was extremely important for the purposes of this study to ascertain the long-term efficacy of RNAlater® with regard to the stabilisation of RNA in mouse skeletal muscle, kidney, liver and heart tissue. In order to accurately quantify the fragmentation state of RNA at a specific post-mortem interval, it was imperative that RNAlater® halted further RNA degradation from occurring after tissue excision. The feasibility of using RNAlater® in the experimental design was initially investigated, to ascertain whether the storage of tissue samples in RNAlater® for extended periods of time would influence RNA quality.

Three mice were sacrificed and immediately following death, samples of skeletal muscle, kidney, liver and heart tissue were excised and immersed in RNAlater®. The quantity and quality of RNA recovered from these four tissues was examined after their preservation in RNAlater® for five time intervals: <1, 7, 14, 28 and 56 days. All tissue samples examined throughout this thesis were processed within 8 weeks (56 days) of excision from the animal; making this an appropriate end point.

4.1.3 Purification of RNA from partially decomposed tissues using the TRI Reagent® and RNeasy® extraction technologies: A comparison study

Following on from tissue preservation, the next stage of the experimental protocol involves the extraction and purification of RNA from solid tissue samples. As considered in detail in Section 1.4.1, Chapter 1 the RNA extraction process involves the release of RNA by tissue homogenisation and cell membrane breakdown; followed by the purification of RNA from other unwanted components such as proteins, lipids and DNA. A wide range of techniques have evolved for this purpose, including the RNeasy® silica column technology of Qiagen, and the more traditional liquid-liquid extraction using TRI Reagent®. The underlying principles of how both of these techniques work has been provided previously in Section 1.4.1, Chapter 1.

To date, there are no recent published works in the forensic literature expressing favour of a specific technique for RNA extraction – neither for forensic casework specimens (such as body fluid stains) nor for solid tissue samples. The RNA branch of the EDNAP group have adopted the RNeasy® silica column method in their validation exercises (3, 41, 65, 66), but this is most likely as a result of its automatability and reduced reagent toxicity rather than any results-based benefit.

Therefore, an investigation was undertaken to assess which of the two purification strategies provided the most favourable RNA samples with regard to: total RNA yield, extract purity, DNA contamination level and total RNA quality. These features were assessed in RNA extracted using the RNeasy® and TRI Reagent® protocols from four tissue types: skeletal muscle, kidney, liver and heart. In addition, three post-mortem intervals were considered: 0, 8 and 24 hours. These three time points were selected after pre-testing as they represented expected high, mid and low quality RNA (131). This was performed to identify which RNA purification protocol performed best, across all tissue types and also in fresh (high molecular weight, intact RNA) and partially decomposed (low molecular weight, degraded RNA) tissue samples. Based on the findings of this work, the optimal protocol will be implemented for further investigations.

4.1.4 Summary: Research objectives

Overall, the aim of this chapter was to develop and test an experimental protocol for manipulation of RNA from mouse post-mortem tissue. For clarity, Box 4.1 summarises the research questions to be answered within each of the three experiments presented.

Box 4.1: Objectives/questions to be answered within Chapter 4

Do the **anti-contamination** procedures suggested protect RNA against unwanted RNase degradation on the bench?

Is RNAlater® an effective **preservative** solution for RNA in mouse skeletal muscle, kidney, liver and heart when stored at -20 °C for up to 8 weeks; halting further progression of RNA degradation?

Which of the TRI Reagent® and RNeasy® methodologies performs most favourably with regard to RNA yield, purity and quality when utilised to **extract** RNA from mouse skeletal muscle, kidney, liver and heart tissue? Which should be incorporated into the experimental design for subsequent chapters?

4.2 Method

4.2.1 Assessment of RNA stability on the bench

Two twelve week old, male C57/BL6J mice were killed by cervical dislocation and immediately following death, skeletal muscle was harvested from the hind leg and preserved in RNAlater® (Section 2.2.2, Chapter 2). RNA was purified from skeletal muscle tissue samples (< 100 mg) using the TRI Reagent® system (Section 2.2.3.3, Chapter 2), treated with the TURBO DNA-free™ kit to remove DNA carry-over (Section 2.2.3.4, Chapter 2), quantified on the Nanodrop-1000® platform (Section 2.2.4, Chapter 2) and diluted to 5 ng/µL in RNase-free water (Ambion, Life Technologies, Paisley, UK). Diluted RNA was aliquoted into RNase-free 1.5 mL microcentrifuge tubes (Elkay Laboratory Products, Basingstoke, UK) and allowed to decay at room temperature (22 °C). All RNA samples were protected from light by wrapping in tin foil. RNA was analysed after the following time intervals: 0, 10, and 30 mins, and 1, 3, 6, 8, 24, 48, 72, 96 and 168 h.

Assessment of total RNA quality was performed on the Bioanalyzer 2100 (Section 2.2.5, Chapter 2) using the RNA 6000 Pico Kit. RNA was reverse transcribed into cDNA using the High Capacity cDNA Reverse Transcription Kit (Section 2.2.6, Chapter 2). cDNA was amplified using four pre-designed inventoried *TaqMan*® assays against the following target RNAs: 18S rRNA, B2m, Gapdh and Fos. Details of these four assays are included in Appendix 1, Tables A1.1 and A1.2. Real time PCR was performed using the protocol described in Section 2.2.7, Chapter 2.

4.2.2 Assessment of RNAlater® efficacy for stabilisation of RNA in post-mortem tissue samples

Three twelve week old, male C57/BL6J mice were killed by cervical dislocation and immediately following death, samples of skeletal muscle, kidney, liver and heart tissue were harvested and immersed in RNAlater® (Chapter 2, Section 2.2.2). Preserved tissue samples were refrigerated at 4 °C overnight to

permit penetration of the solution through the solid tissue matrix, and subsequently frozen at -20 °C for up to 8 weeks.

RNA was extracted using the TRI Reagent® system (Section 2.2.3.3, Chapter 2) from the RNAlater® stabilised skeletal muscle, kidney, liver and heart tissue samples (< 100 mg) after five time intervals: 1, 7, 14, 28 and 56 days. RNA extracts were treated with the TURBO DNA-free™ kit (Section 2.2.3.4, Chapter 2) to remove residual DNA contamination and the RNA yield quantified on the Nanodrop-1000® platform (Section 2.2.4, Chapter 2). Quality analysis was performed on the Bioanalyzer 2100 (Section 2.2.5, Chapter 2) using the RNA 6000 Pico Kit.

4.2.3 Purification of RNA from partially decomposed tissues using the TRI Reagent® and RNeasy® extraction technologies: A comparison study

Nine twelve week old, male C57/BL6J mice were killed by cervical dislocation. Of the nine, three were dissected immediately and samples of skeletal muscle, kidney, liver and heart harvested and preserved in RNAlater® (Section 2.2.2, Chapter 2). The six other mice were left to decompose intact on the bench at room temperature (22 °C). Three were dissected after a post-mortem interval of 8 h and three after 24 h, again collecting and preserving skeletal muscle, kidney, liver and heart tissue. 0, 8 and 24 h were selected as time points as the tissues were expected to present high, mid and low quality RNA.

RNA was extracted from samples of the four tissue types (< 100 mg) using the TRI Reagent® system (Section 2.2.3.3, Chapter 2). RNA extracts were quantified on the Nanodrop-1000® platform (Section 2.2.4, Chapter 2) and treated with the TURBO DNA-free™ kit (Section 2.2.3.4, Chapter 2) to remove residual DNA contamination, before re-quantification to calculate the nucleic acid loss following DNase treatment. Quality analysis was performed on the Bioanalyzer 2100 (Section 2.2.5, Chapter 2) using the RNA 6000 Pico Kit.

4.3 Results and discussion

4.3.1 Assessment of RNA stability on the bench

It was found that during the first 96 hours incubation at room temperature 22 °C, the measured quality of RNA (suspended in RNase-free water) did not visibly reduce. RNA quality was quantified in terms of the RNA integrity number (RIN) on the Bioanalyzer 2100 – the results of which are displayed in Figure 4.1. The RIN algorithm represents a very sensitive indicator of even mild degradation, as it characterises loss of the 28S (4,730 nucleotides length) and 18S (1,870 nucleotides length) rRNAs. These high molecular weight RNAs should be the first targets of degradation of the transcriptome; particularly the longer 28S rRNA.

The RIN data was examined using the Anderson-Darling test of normality and deemed not to be normally distributed, but clustered towards higher values ($p = 0.005$). As such, the data was examined with Spearman's rank order correlation, which highlighted a negative monotonic correlation between RNA quality and the storage interval ($\rho = -0.481$, $p = 0.003$). Irrespective of their storage interval on the bench, none of the RNA samples exhibited a statistically significant reduction in median RIN relative to the control, as determined by pair-wise comparison with the Mann-Whitney test (for the 0 to 168 hour time interval, $p = 0.081$).

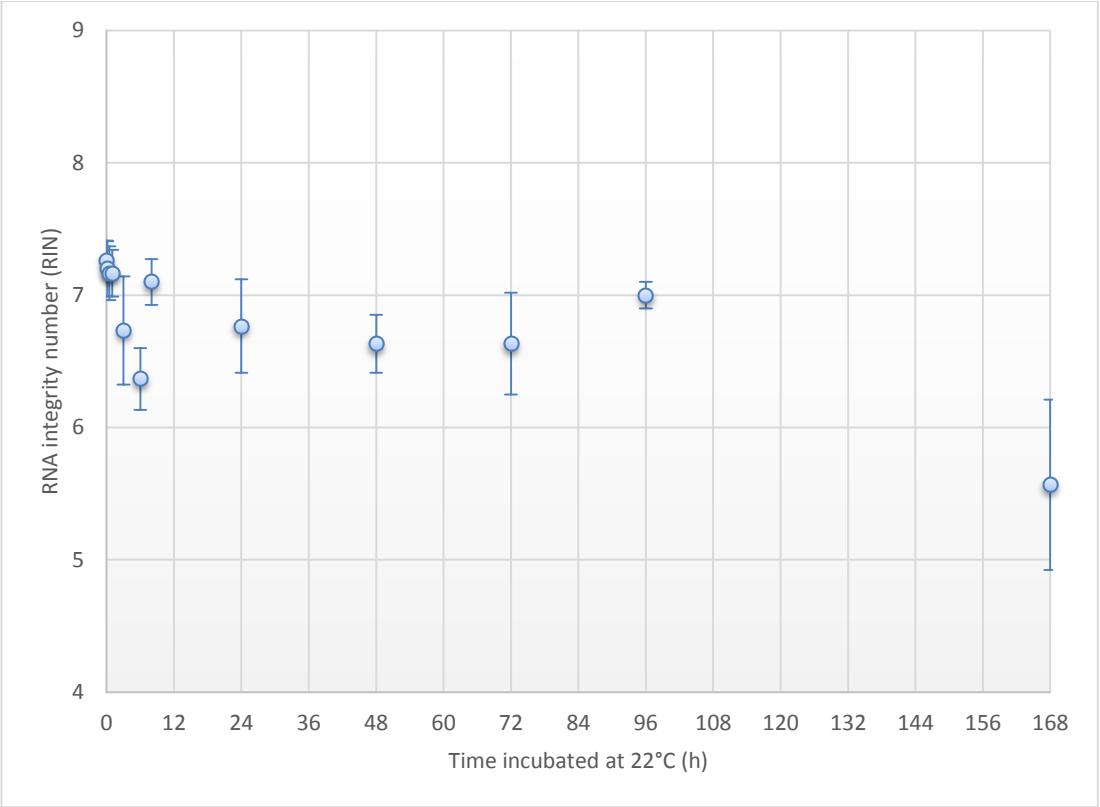

Figure 4.1: **Total RNA quality for RNA extracts left on the bench to decay at 22 °C for up to seven days.** RNA quality illustrated in terms of the mean RIN for n = 3 ± S.E.

The same set of samples was then subjected to analysis by real time PCR to measure the amplifiable quantity of four individual RNAs – 18S rRNA, B2m, Gapdh and Fos. Over the 7 day interval examined, no observable change was recorded in the quantity of these four RNAs; as illustrated in Figure 4.2. Had degradation of the target amplicon of these four RNAs occurred, this would have been characterised by an increase in C_Q. All four data sets were confirmed to be normally distributed using an Anderson-Darling normality test (18S rRNA $p = 0.058$; B2m, Gapdh and Fos $p > 0.15$). No correlation was observed (Pearson's product moment correlation) between the time incubated on the bench top and the C_Q for any of 18S rRNA ($r = -0.140$, $p = 0.534$), B2m ($r = -0.146$, 0.515), Gapdh ($r = -0.073$, $p = 0.748$) or Fos ($r = -0.123$, $p = 0.585$). Similarly, a one-way ANOVA was not able to detect any significant change in C_Q with storage interval for 18S rRNA ($p = 0.631$), B2m ($p = 0.432$), Gapdh ($p = 0.776$) or Fos ($p = 0.242$).

The target amplicon of each of these four assays is relatively short, ranging from a minimum 59 nucleotides (Fos) to a maximum 107 nucleotides (Gapdh) (Appendix 1, Table A1.1). This short target length makes real time PCR resistant to mild/moderate RNA degradation. By detecting a reduction in the measured quantity of these four RNA transcripts, this would have served as an indicator of severe sample degradation where the integrity of even these short target sequences has been compromised. This outcome is as anticipated, as total RNA quality analysis suggested that all samples contained intact (RIN 7.5 to 10) or moderate (RIN 5 through 7.5) quality RNA (212).

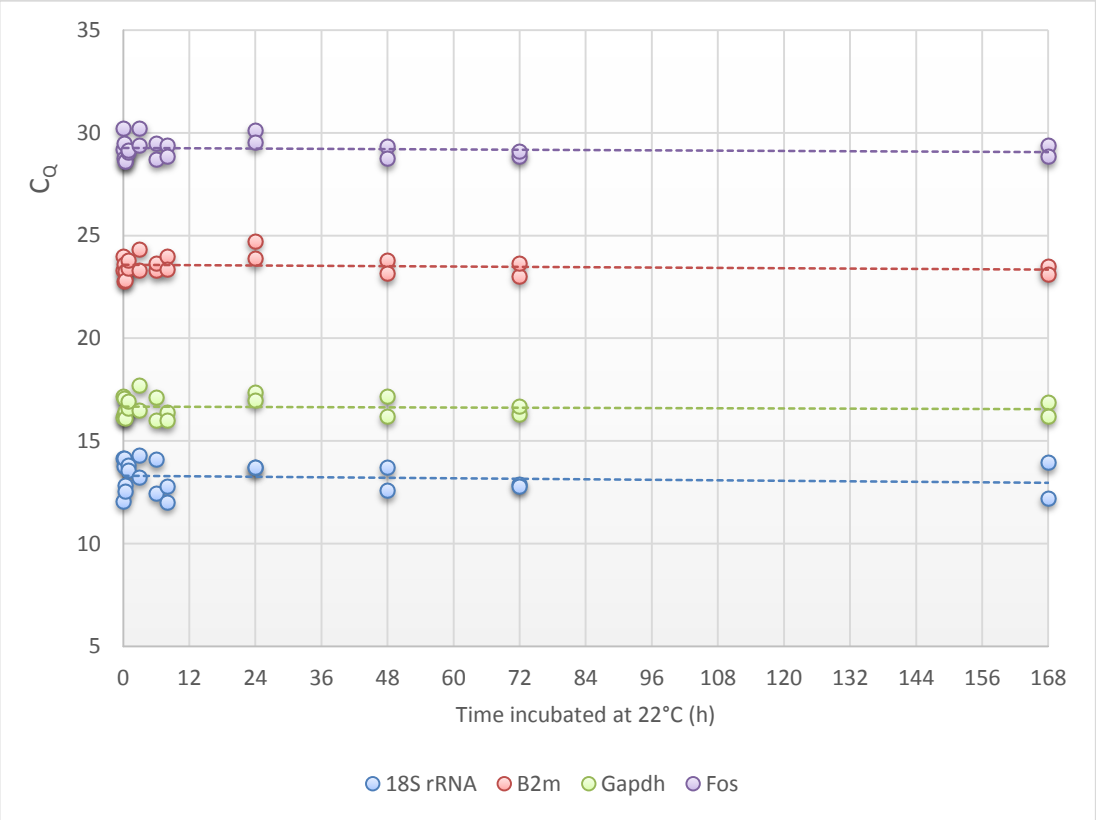

Figure 4.2: **RT-qPCR data after amplification of 18S rRNA (blue data points), B2m (red data points), Gapdh (green data points) and Fos (purple data points) from RNA samples left to degrade at 22 °C for up to 7 days**. Raw C_Q values for n = 2 are represented per time interval examined.

A high proportion of published works on the topic of gene expression analysis begin by professing the extreme fragility and instability of RNA on the bench. At a glance, one gleans the impression that many RNA scientists work with excessive 'paranoia' with regard to sample handling and interpretation. Throughout this work, most of the basic, recommended containment procedures have been implemented to reduce the risk of sample RNase contamination. Such procedures included the use of certified RNase-free plasticware and cleaning of bench surfaces with an RNase decontamination solution, namely RNaseZap®. The outcomes of this work suggest that as long as these basic procedures are followed, RNase contamination does not pose such a significant risk as the literature might lead one to think, and that additional precautions such as working continually in ice buckets seem to be superfluous.

4.3.2 Assessment of RNAlater® efficacy for stabilisation of RNA in post-mortem tissue samples

4.3.2.1 Assessment of RNAlater® efficacy: RNA quantity

To ensure the optimal tissue storage conditions were utilised, the effect of storing tissue samples in RNAlater® on the quantity and quality of RNA recovered from skeletal muscle, kidney, liver and heart was assessed following storage for 1, 7, 14, 28 and 56 days. It was found that the period of time during which tissue samples were stored in RNAlater® was found to have no consistent effect on the quantity of RNA obtained from of these four tissue types, as illustrated in Figure 4.3. The RNA yield is expressed in Figure 4.3 in terms of the quantity of RNA recovered (ng) per 1 mg tissue extracted, as the mass of tissue could not be absolutely normalised.

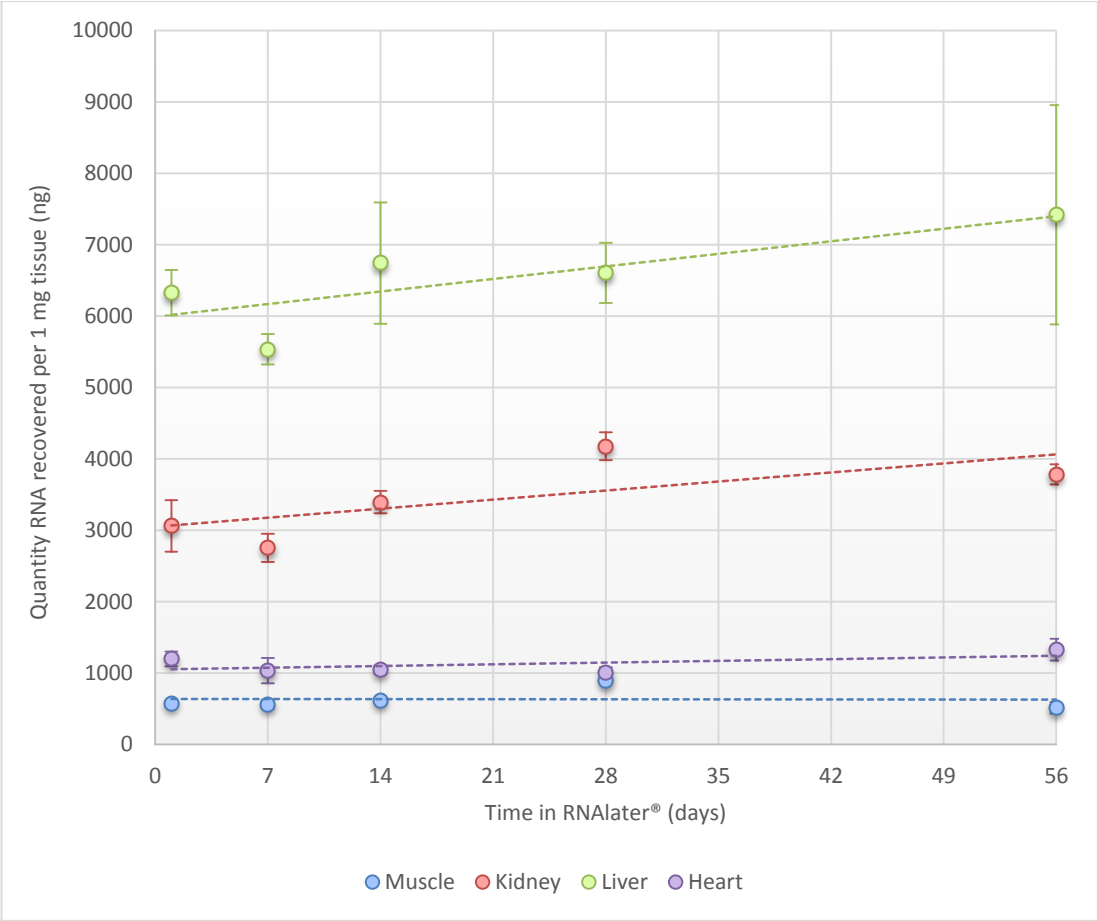

Figure 4.3: **Quantity of total RNA recovered from fresh skeletal muscle (blue data points), kidney (red data points), liver (green data points) and heart (purple data points) mouse tissue samples stabilised in RNAlater® for up to 56 days at -20 °C**. The first control point represents data from tissue samples incubated overnight in RNAlater® at 4 °C for less than 24 hours. All values represent the mean of n = 3 ± S.E.

Skeletal muscle and heart tissue provided lower yields of RNA per unit tissue. This is as expected and stems from their relatively low cellular content and abundance of contractile proteins, collagen and connective tissue (118). In both tissue types, it can be seen from Figure 4.3 that the yield of RNA remained largely unchanged over the 56 day storage interval. The four tissue type data sets were examined for normality using the Anderson-Darling normality test, which established that liver RNA quantity data was not normally distributed ($p < 0.005$) while skeletal muscle, kidney and heart RNA yield data was normally distributed ($p = 0.118$, 0.814 and 0.260 respectively).

No correlation was observed between the yield of RNA recovered from skeletal muscle ($r = -0.015$, $p = 0.957$) and heart ($r = 0.317$, $p = 0.250$) and the time interval during which they were immersed in RNAlater®, as determined using Pearson's product moment correlation. Data was analysed using a one-way ANOVA and Dunnett's Multiple Comparisons with a Control method. In RNA extracted from skeletal muscle, only the samples extracted after 28 days in RNAlater® exhibited a significantly increased yield of RNA ($p = 0.002$) relative to the control point, as observed in Figure 4.3. No such difference was observed for any heart tissue samples ($p = 0.361$). Similarly, no correlation exists between the yield of RNA from liver tissue and the storage time in RNAlater® ($\rho = 0.251$, $p = 0.367$) as determined by Spearman's rank order correlation. The quantity of RNA recovered from liver tissue was much higher than the other three tissue types, which stems from its highly cellular structure. However, the variability in RNA yield from liver tissue was much more significant; most likely as a result of this improved yield and also from sampling differences. This is illustrated by the much wider error bars in Figure 4.3, particularly at the 14 and 56 day intervals.

On the other hand, a positive linear correlation was observed between RNA yield and storage interval (up to 56 days) for kidney tissue ($r = 0.593$, $p = 0.02$) – increasing from a mean 3,061 ng RNA/1 mg tissue if extracted within 24 hours of excision from the mouse, to a mean 3,783 ng RNA/1mg tissue after 56 days storage in RNAlater®. Upon analysis with a one-way ANOVA and Dunnett's Multiple Comparisons with a Control test, only at 28 days storage was the mean RNA yield significantly elevated ($p = 0.008$) relative to the control point (< 24 hours storage). This increase in RNA yield from kidney tissue was unexpected and the reason for it is not immediately clear. To the author's knowledge, no publications to date have illustrated an increased RNA recovery from tissues stored in RNAlater®, but it could potentially be that storage of the tissue improved the release of RNA from the tissue matrix.

4.3.2.2 Assessment of RNAlater® efficacy: Total RNA quality

Storage of excised tissue samples in RNAlater® for up to 56 days was not found to strongly influence the quality of RNA in fresh tissue samples, as illustrated in Figure 4.4. All four tissue type data sets were examined using the Anderson-Darling test of normality. Skeletal muscle, kidney and heart tissue RIN data values were found not to be normally distributed ($p = < 0.005$, 0.011 and < 0.005 respectively) whereas the liver RIN data set was normally distributed ($p = 0.436$).

Following on from this, the four tissue type data sets were examined to establish whether a correlation existed between the storage interval in RNAlater® and RIN. No correlation was observed for any of skeletal muscle (Spearman's rank order correlation $\rho = -0.139$, $p = 0.623$), kidney (Spearman's rank order correlation $\rho = 0.116$, $p = 0.681$) or liver (Pearson's product moment correlation $r = -0.142$, $p = 0.614$), illustrating no consistent reduction in RNA quality upon storage in these three tissue types. On the other hand, a linear decline in heart RNA quality with storage interval in RNAlater® was confirmed using Spearman's rank order correlation ($\rho = -0.673$, $p = 0.006$). This decline however, is very subtle as illustrated in Figure 4.4. Even after 56 days storage in RNAlater®, all three heart tissue samples retained a RIN greater than 7, indicative of good quality RNA.

All RNA samples with the exception of two were assigned a RIN between 6 and 9 – indicative of reasonably high quality, intact RNA. Two samples processed on day 14 exhibited a marked reduction in RNA quality – one skeletal muscle sample returning a RIN of 4.3 and one heart sample RIN 4.2. The RINs for these two samples were not consistent with the overall trend of the data, and this reduction is proposed to be due to an error in sample handling (e.g. RNase contamination) rather than attributed to the effect of storage in RNAlater®. These samples were not subjected to repeat analysis to define the cause of the RNA degradation, as re-extraction of the same tissue sample would not have matched up with the desired '14 day' time point in Figure 4.4.

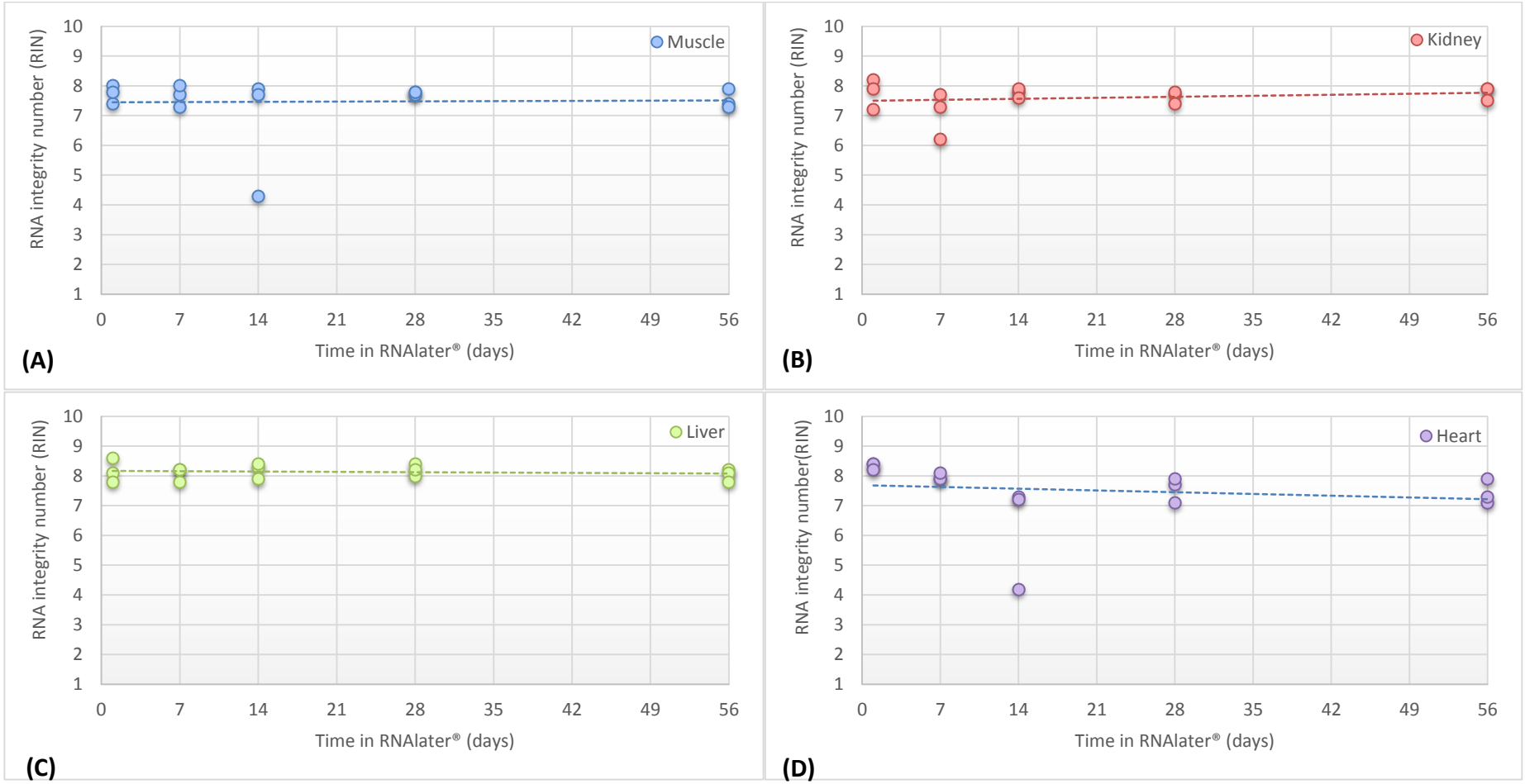

Figure 4.4: **Quality of total RNA recovered from fresh mouse (A) skeletal muscle, (B) kidney, (C) liver and (D) heart stabilised in RNAlater® for up to 56 days**. Values represent n = 3 for each time point.

4.3.2.3 Assessment of RNAlater® efficacy: Conclusions

This preliminary experiment was not intended to be a large-scale validation of the efficacy of RNAlater®. It was critical to the outcomes of this work that the fragmentation state of RNA at the time of tissue collection was preserved upon immersion in RNAlater® and storage at -20 °C, in order to reliably quantify post-mortem degradation. This short study has found no consistent decline in the quantity and quality of RNA recovered from skeletal muscle, kidney and liver tissue samples stored in RNAlater® for up to 56 days (8 weeks). Unfortunately, a negative linear correlation was observed between RIN and storage time for heart tissue samples. However, even after 56 days storage the quality of the RNA recovered from heart tissue was still on par with that of skeletal muscle, kidney and liver (Figure 4.4).

Despite the widespread adoption of RNAlater® in the clinical and forensic literature, there are only a small handful of published works in which its efficacy has been independently verified (213-218). Chowdary *et al*. demonstrated that RNAlater® was equally effective as snap-freezing tissue samples in liquid nitrogen (the traditional tissue RNA preservation technique) for the preservation of intact, high quality RNA (213). Roos van Groningen *et al*. illustrated that RNA integrity was retained in kidney tissue samples for at least 3 months upon storage in RNAlater® (214). Bachoon *et al*. demonstrated that RNAlater® effectively stabilised RNA in *Pseudomonas* and *Synechococcus spp*. Without RNAlater®, their RNA was degraded to the extent where it was unamplifiable within 24 hours (215). Grotzer *et al*. demonstrated that RNAlater® was as effective as snap-freezing for the preservation of RNA in human neuroblastoma and central nervous system tumour samples (216). Mutter *et al*. illustrated no shift in quantitative RNA expression results (using an Affymetrix microarray) upon storage of uterine myometrial tissue specimens in RNAlater® at ambient temperature for up to 72 hours (217). Micke *et al*. demonstrated no identifiable change in the shape of the Bioanalyzer 2100 electropherogram output upon storage of tonsil and colon tissue in RNAlater® for up to 16 hours at 4 °C (218). Similarly, Gayral *et al*. (118) identified no difference in

RNA integrity when comparing RNAlater®-stabilised and flash frozen whole gastropods.

Although a small number of the aforementioned studies have used the Bioanalyzer 2100 platform to assess RNA fragmentation, none measured RNA quality quantitatively using the RIN algorithm. This algorithm has only been in operation since 2006 and is currently considered the 'go-to' technique for RNA quality screening (131). Most peer-reviewed works looking at the effectiveness of RNAlater® have only established that it protects RNA by qualitatively assessing agarose gels, visually looking for RNA band smearing. Clearly, this is subject to interpretational error and is poorly sensitive to mild RNA degradation. Not even the manufacturer of RNAlater® has RIN data in the public domain to confirm its efficiency using this objective, fully quantitative technique. In addition, the author has come across no published works to date in which the efficacy of RNAlater® has been assessed in a long term time-wise study as has been achieved here, where the quality of paired tissue samples has been compared for up to 8 weeks. As such, the outcomes of this work are valuable to other RNA researchers using RNAlater® in their own experimental protocols.

In summary, this work has shown that RNAlater® is fit for purpose and as such, will be implemented into the work flow in subsequent chapters to improve the practicality of tissue processing; allowing tissue samples to be harvested and stored for up to 8 weeks until a convenient time for RNA extraction.

4.3.3 Purification of RNA from partially decomposed tissues using the TRI Reagent® and RNeasy® extraction technologies: A comparison study

4.3.3.1 Extraction methodology comparison: DNA contamination

The similar molecular structure and chemical properties of RNA and DNA makes absolute purification of one from the other extremely challenging. Irrespective of the extraction method implemented, tissue RNA extracts will

unavoidably contain low level DNA contamination. This contamination causes problems during RT-PCR analysis. Although most gene expression PCR primers are specially designed not to co-amplify the DNA gene of their target RNA/cDNA transcript (by annealing to sequences at the boundary of two exons), there are some instances where the high sequence similarity between RNA and DNA means that this is not possible. This is particularly true for RNAs with no exon-intron structure or for genes with processed pseudogenes elsewhere in the genome. Therefore, it is key to experimental success to reduce or eliminate DNA contamination.

This can be achieved by treatment of the RNA extract with DNase, which destroys DNA contamination leaving RNA intact. The proportion of an RNA extract made up of DNA contamination was estimated by measuring the concentration of RNA by UV-visible spectrophotometry (on the Nanodrop-1000® platform) both before and after DNase treatment. UV-visible spectrophotometry is unable to properly discriminate between RNA and DNA, as it performs nucleic acid quantification by quantifying the absorption of nucleotide bases present in both. The % reduction in measured nucleic acid concentration following DNase treatment was assumed to be the proportion of the RNA extract made up of DNA.

It was found that DNA contamination was a more significant problem in extracts prepared using the RNeasy® technology. Figure 4.5 illustrates the proportion of each RNA extract attributed to DNA contamination for a total of 36 tissue samples.

As observed from Figure 4.5, the median DNA contamination proportion was lower for the RNA extracts prepared with TRI Reagent® at 21.4%; compared with 28.8% for RNeasy®. Although the TRI Reagent® data set was confirmed to be normally distributed with an Anderson-Darling normality test ($p = 0.353$), the RNeasy® data set was not ($p < 0.005$). Following on from this, the difference in median % DNA contamination was deemed to be statistically significant by analysis with the non-parametric Mann-Whitney test ($p = 0.000$). In addition, the % contamination was much more variable when using the RNeasy® extraction

protocol, illustrated by the wide interquartile range (24.2% to 44.8%) in Figure 4.5. This outcome is supported by similar data published by Bustin (144). Using a bank of human surgical biopsy samples, Bustin demonstrated that on average, RNA only constitutes 50 to 80% of the end RNeasy® nucleic acid extract. Bustin also found that the extract purity was also strongly dependent on operator experience/training; a factor which was not examined here.

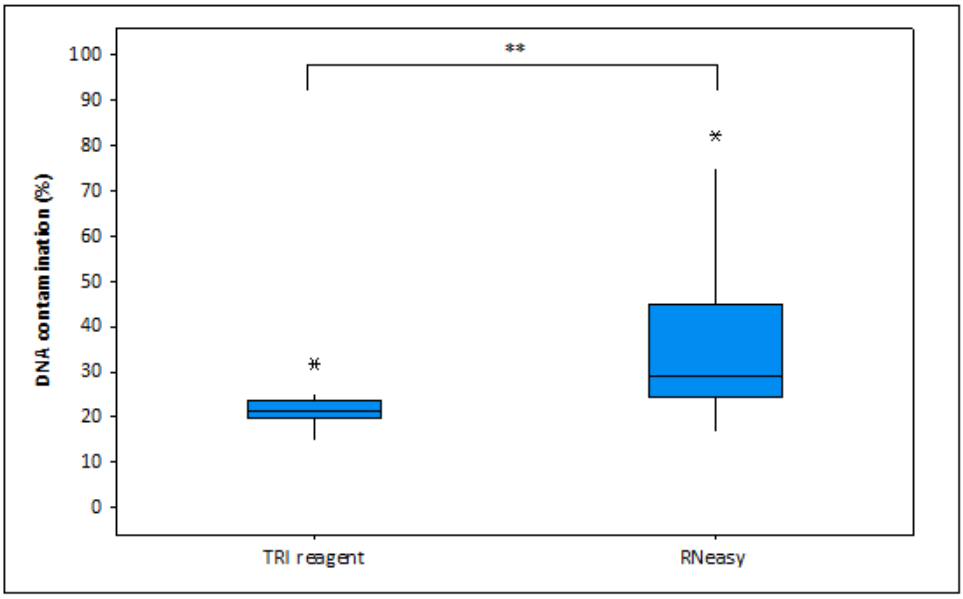

Figure 4.5: **Reduction in RNA concentration after treatment of extracts with DNase to remove residual DNA contamination**. Boxplot represents data for n = 36 per extraction method, with n = 9 for each of skeletal muscle, kidney, liver and heart tissue. RNeasy® extracts exhibited a significantly higher proportion of DNA contamination, as determined with a Mann Whitney test (p = 0.000**).

4.3.3.2 Extraction methodology comparison: Yield of RNA

The second feature to be compared between the TRI Reagent® and RNeasy® extraction methodologies was the total quantity of RNA recovered from samples of skeletal muscle, kidney, liver and heart tissue. It was found that the RNA purification method had a statistically significant effect on RNA yield, as illustrated from the data presented in Figures 4.6A, 4.6B, 4.6C and 4.6D.

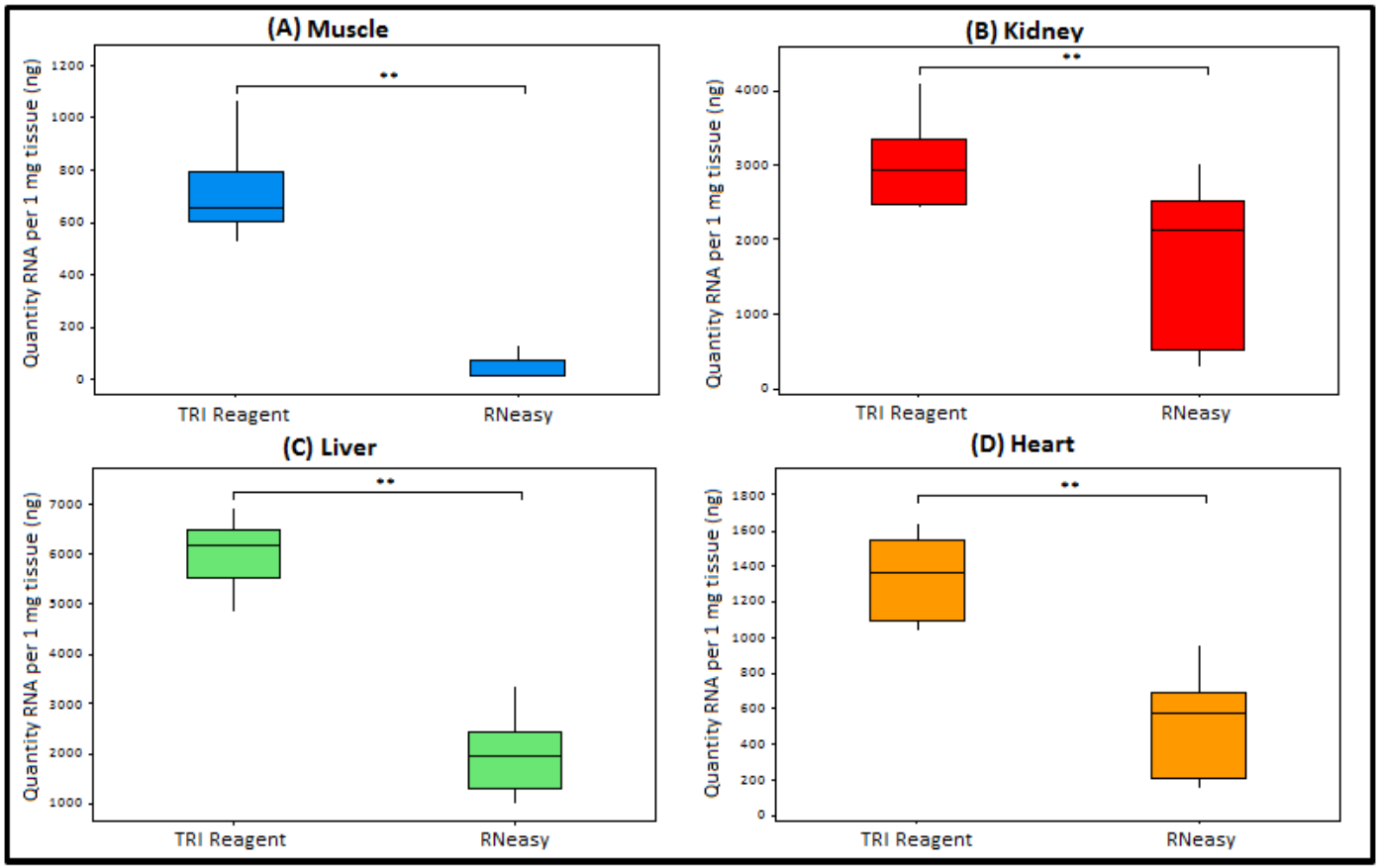

Figure 4.6: **Quantity of RNA recovered from mouse (A) skeletal muscle, (B) kidney, (C) liver and (D) heart tissue using one of two RNA purification methodologies: TRI Reagent® and RNeasy®**. Boxplot represents values for n = 9. TRI Reagent® provided a significantly higher yield of RNA in all four tissue types as determined with either a Mann Whitney (skeletal muscle) or 2 sample t-test (kidney, liver and heart), where $p < 0.01$**.

RNA yield was quantified in terms of the quantity of RNA (in ng) recovered per 1 mg tissue, as the input quantity of solid tissue could not be absolutely normalised. Quantification was performed after treatment of the RNA extracts with DNase to remove residual DNA contamination. All data sets were assessed for normality using the Anderson-Darling normality test. It was found that although the RNA yield data for skeletal muscle was not normally distributed (TRI Reagent® p = 0.155, RNeasy® p = 0.012*), all data sets for kidney (TRI Reagent® p = 0.069, RNeasy® p = 0.204), liver (TRI Reagent® p = 0.751, RNeasy® p = 0.772), and heart (TRI Reagent® p = 0.637, RNeasy® p = 0.433) were normally distributed. As such, the median quantity of extracted RNA using TRI Reagent® and RNeasy® was compared for skeletal muscle using the Mann Whitney test, and the mean quantity of extracted RNA compared for all three other tissue types using a 2 sample t-test. Using these tests, TRI Reagent® was confirmed to recover a significantly higher quantity of RNA from all of skeletal muscle (p = 0.000), kidney (p = 0.007), liver (p = 0.000) and heart (p = 0.000).

Qiagen, the manufacturer of the RNeasy® RNA purification system, acknowledges its poor performance when working with fibrous tissue types such as muscle as a substrate. They attribute this to their high protein content (168). This has been confirmed here, with an extremely poor mean RNA yield of 12.1 ng/1 mg tissue (Figure 4.6A). Qiagen advocate an additional pre-treatment with proteinase K during the lysis step for muscle samples, which has been confirmed as effective by Gayral *et al*. (118) using hare and penguin muscle as a tissue substrate. This was found to substantially improve muscle RNA yield from a median of 15.9 ng/1 mg tissue (Figure 4.6A) to 568.5 ng/1mg tissue (n = 6, data not shown in Figure 4.6A). This was still, however, substantially lower than the median RNA quantity recovered from skeletal muscle using TRI Reagent® – 653.4 ng/1mg (p = 0.037) (Figure 4.6A).

Overall, these outcomes demonstrate that TRI Reagent® provides a consistently higher yield of RNA than RNeasy® across all four tissue types examined. This is confirmed by a number of other published works. Deng *et al*. extracted RNA from porcine kidney, liver and heart tissue using the RNeasy® and TRIzol® (a similar product with a different manufacturer brand name to TRI Reagent®) methodologies

and quantified it by UV-visible spectrophotometry as has been achieved here. For these three tissue types, they were able to illustrate 274%, 298% and 515% improved RNA yield respectively when using TRIzol® relative to RNeasy® (219). Similarly poor results were obtained upon extraction of RNA from blood, tonsil, spleen, bladder and lymph node using RNeasy®. Roos van Groningen *et al*. demonstrated an approximately 10-fold improvement in RNA yield from kidney tissue with TRI Reagent® relative to RNeasy® (214). Data published by Wang *et al*. suggested that RNA yield from human brain tissue was improved 169% through the use of TRI Reagent® rather than RNeasy® (220).

In addition, some other authors have expressed concerns regarding the use of RNeasy® columns for the extraction of RNA from unusual or particularly poor quantity/quality substrates. Bohmann *et al*. (2009) demonstrated that when using severely degraded formalin fixed paraffin embedded tissues as a substrate for RNA extraction, RNeasy® provides poorer and more inconsistent RNA yield (221). Santiago-Vasquez *et al*. illustrated a massive ~1,900% improvement in RNA yield from coral (*P. elisabethae*) when using TRI Reagent® rather than RNeasy® (222). Xiang *et al*. demonstrated that the RNeasy® column extraction method is unsuitable for the recovery of small quantities of RNA from sputum (for viral screening), and that RNA yields were improved almost 100-fold when instead using TRIzol® (223). Heinrich *et al*. (82) and Carlsson *et al*. (224) both have highlighted substantial loss of RNA when using RNeasy® columns for 'clean up' of RNA samples – 50% and 30% in the two studies respectively. This loss may occur through one of three mechanisms: that the RNA is washed through the silica membrane uncaptured, that the RNA is dislodged through repeated washing of the silica membrane with buffer, or that the RNA is not successfully eluted from the silica column.

The outcomes of all of these studies are concordant with the data presented here, which demonstrates improved tissue RNA recovery when using TRI Reagent® relative to RNeasy®.

4.3.3.3 Extraction methodology comparison: Total RNA quality

So far, it has been established that tissue RNA extracts prepared using TRI Reagent® exhibit improved yield and purity compared with RNeasy®. However, it is also important to establish the quality of these RNA samples, i.e. how degraded the recovered RNA actually is. In order to achieve this, samples of skeletal muscle, kidney, liver and heart tissue with post-mortem intervals of 0, 8 and 24 hours were extracted using the two methodologies and their quality quantified on the Bioanalyzer 2100. 0, 8 and 24 hours were selected following pre-testing to provide high, mid and low quality RNA (on the RIN scale) to compare the two methods on samples of varying expected qualities.

On the whole, it was found that tissue samples extracted using the RNeasy® methodology exhibited a higher quality score than those prepared using TRI Reagent®. Figure 4.7 illustrates the raw RIN data upon quality analysis of RNA prepared using the two methods. The only exception to this trend was in skeletal muscle, where RNeasy® provided extremely poor results for tissue samples extracted at 0 and 8 hours post-mortem. These poor RIN values stem from the extremely low quantity of RNA recovered from these tissue samples, which prevented accurate quality scoring. As discussed earlier, this is attributed by the manufacturer to the high protein content of muscle which prevents RNA release/solubilisation and binding to the silica membrane (168). Surprisingly, the quantity and quality of RNA obtained from skeletal muscle tissues recovered after a 24 hour post-mortem interval was satisfactory. This improvement in RNA recovery with increasing post-mortem interval is suggestive of proteolysis during the early stages of decomposition, enhancing the release of RNA from the fibrous skeletal muscle tissue matrix.

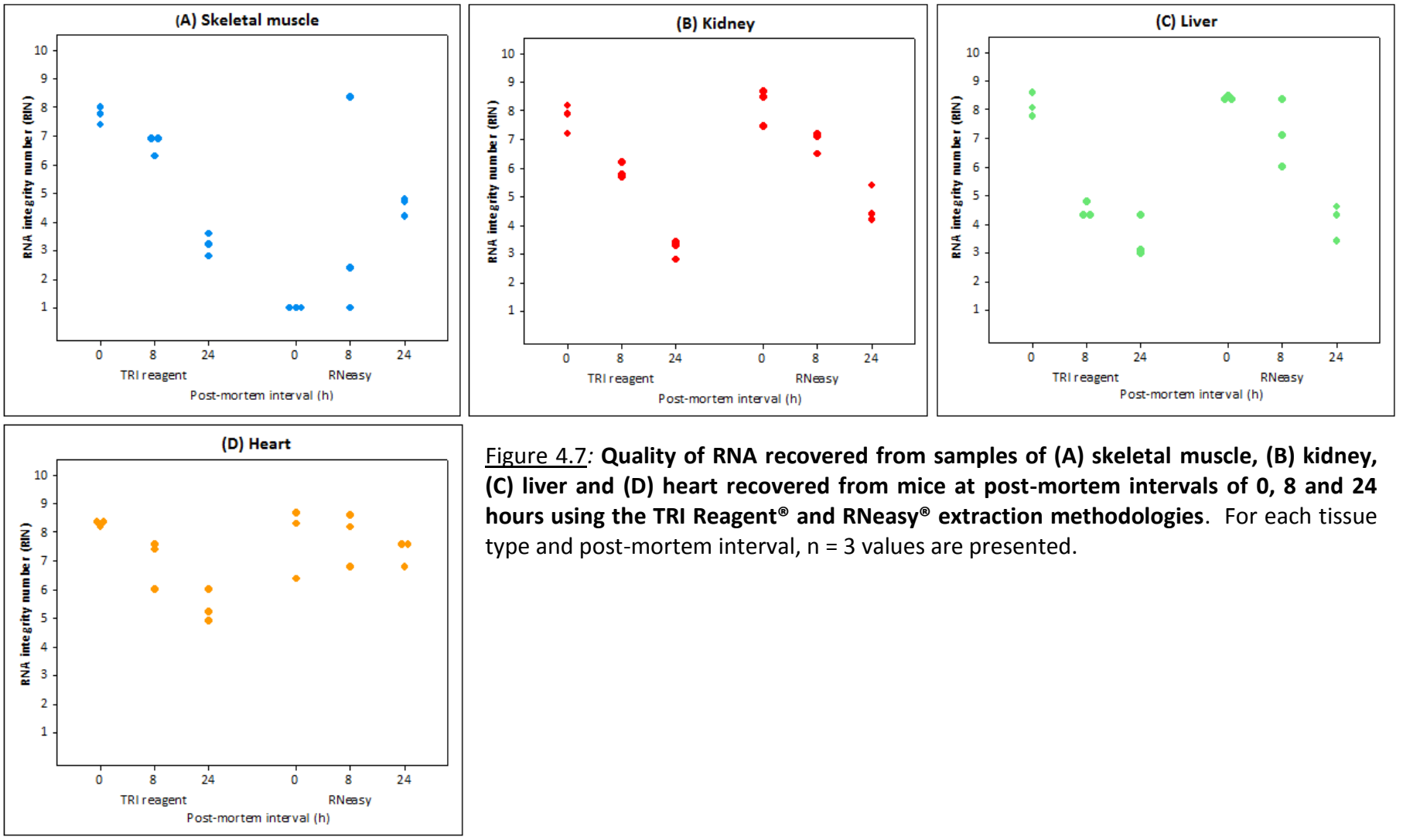

Figure 4.7*:* **Quality of RNA recovered from samples of (A) skeletal muscle, (B) kidney, (C) liver and (D) heart recovered from mice at post-mortem intervals of 0, 8 and 24 hours using the TRI Reagent® and RNeasy® extraction methodologies**. For each tissue type and post-mortem interval, n = 3 values are presented.

As illustrated in Table 4.1, for kidney, liver and heart tissue RNeasy® provided a higher mean RIN for samples extracted at almost all post-mortem intervals, indicative of superior measured RNA quality. This improvement in RNA quality was confirmed to be statistically significant in many instances (Table 4.1). Using an Anderson-Darling normality test the distribution of RINs was deemed to be normal for all data sets (data not shown) and as such, a 2 sample t-test was used to compare the mean RIN of those tissue samples extracted with TRI Reagent® and RNeasy®.

Table 4.1: **Mean RIN for RNA recovered from skeletal muscle, kidney, liver and heart tissue excised from mice at post-mortem intervals of 0, 8 and 24 hours using the TRI Reagent® and RNeasy® extraction methodologies**. RNA quality was compared between the two methods using a 2 sample t-test. Those with a detected significant difference are shaded in grey ($p < 0.05$*, $p < 0.01$**).

		Mean RIN		
Tissue type	**PMI (h)**	**TRI Reagent®**	**RNeasy®**	**Significance: p-value**
Skeletal muscle	**0**	7.73	1.00	0.001**
	8	6.70	3.93	0.349
	24	3.20	4.57	0.019*
Kidney	**0**	7.77	8.23	0.398
	8	5.90	6.93	0.030*
	24	3.17	4.67	0.069
Liver	**0**	8.17	8.43	0.375
	8	4.47	7.17	0.063
	24	3.47	4.10	0.334
Heart	**0**	8.33	7.80	0.532
	8	7.00	7.87	0.327
	24	5.37	7.33	0.019*

It is unlikely that this difference in the measured quality of RNA recovered using TRI Reagent® and RNeasy® is attributed to RNase-induced degradation during the extraction process. Following both methodologies, tissue samples initially remain impregnated with RNAlater® and once homogenised, remain in buffers

containing potent RNase inhibitors such as the protein denaturant guanidine thiocyanate (168, 176).

The two extraction procedures use completely different chemical features of RNA in order to purify it from other cellular components: TRI Reagent® relying on its solubility in the aqueous environment, and RNeasy® on its ability to adsorb onto a silica membrane. Consequently, it is reasonable to expect that that the size distribution of RNA molecules recovered may be different in each instance, giving rise to different quality scores for the extracted RNA. It is known that the RNeasy® silica membrane struggles to capture small RNAs (such as miRNA, tRNA, and 5S rRNA) and RNA fragments. The manufacturer acknowledges that RNA of length < 200 nucleotides will most likely be washed through the column uncaptured (168). In tissue samples with a long post-mortem interval, it is probable that this will result in the loss of low molecular weight fragments of degraded RNA.

Clearly, the loss of degraded RNA fragments during the extraction process may cause an 'artificially' high tissue RNA quality score when working with the RNeasy® protocol. The filtering out of very small RNA fragments can be seen in the raw data outputs from the Bioanalyzer 2100. Figure 4.8 compares the size distribution of RNA fragments upon extraction of RNA from a single sample – a skeletal muscle tissue sample, extracted after a post-mortem interval of 24 hours – using the TRI Reagent® and RNeasy® methodologies. In the sample extracted with TRI Reagent®, a strong intensity 'flare' signal can be seen observed in Figure 4.8A (circled green). This corresponds to fragments of RNA in an approximate size range 50 to 200 nucleotides (corresponding to an electrophoresis time of 24 to 27 seconds). On the other hand, the RNA signal intensity in this size range in the extract prepared with RNeasy® is very low (Figure 4.8B).

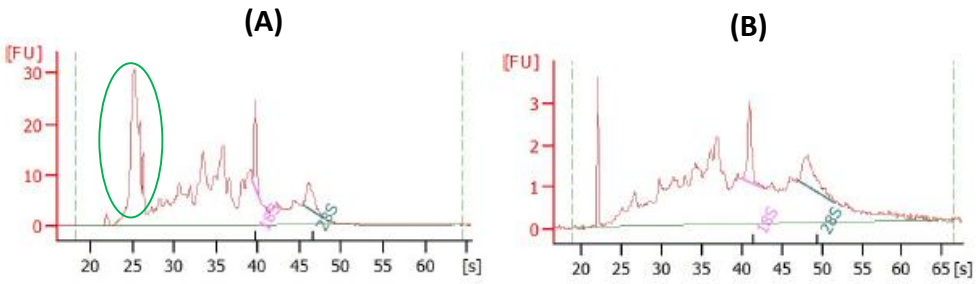

Figure 4.8: **Raw data outputs after RNA quality analysis of skeletal muscle samples (PMI 24 hours) extracted using the (A) TRI Reagent® (RIN 3.6) and (B) RNeasy® (RIN 4.8) methodologies**. The strong peak at around 22 seconds electrophoresis time in both outputs is the 25 nucleotide marker peak.

The RIN algorithm uses the signal in this region as part of its calculation to quantify RNA integrity. As a result, the inability of the RNeasy® protocol to capture small fragments of RNA is the likely cause of the improved RIN scores observed for tissue samples extracted after longer post-mortem intervals. This same phenomenon has been previously illustrated by Haimov-Kochmann *et al*. (225). Using placenta as a tissue substrate, they were able to demonstrate that additional RNeasy® 'clean up' of TRI Reagent®-extracted RNA samples caused a reduction in the detection of small RNAs, and a 23% increase in the 28S/18S ratio. These outcomes suggest that high molecular weight RNA is preferentially bound to the silica column, and small RNAs are washed straight through. Similar to the outcomes presented here, they suggest that RNeasy® 'cleaned up' extracts exhibit an artificial improvement in RNA quality, and that using this method causes under-estimation of the degree of RNA degradation. Similarly, Eldh *et al*. illustrated that TRI Reagent® gives a significantly improved yield for small RNAs, including miRNA (226).

4.3.3.4 Extraction methodology comparison

Gayral *et al*. (118) produced a useful review table summarising the features of liquid-liquid and silica column technologies from a generic perspective, included in Table 4.2. In agreement with Gayral *et al*.'s conclusions, it has been confirmed that the TRI Reagent® RNA purification system recovers a significantly higher yield

of RNA than RNeasy® for all tissue types examined, and that this RNA is purer with a lower proportion of DNA contamination. Although the measured quality of RNA samples prepared using TRI Reagent® was on the whole lower than that of RNeasy®, this has been attributed to its ability to recover even small, heavily fragmented RNA molecules. The use of TRI Reagent® does have its inherent limitations, such as the toxicity of the required reagents and labour intensive nature of the protocol (118). However, this work has provided enough experimental data to opt for TRI Reagent® as the superior RNA extraction method in all subsequent work.

Table 4.2: **Features of the liquid-liquid and silica column RNA extraction methodologies**. Information adapted from Gayral *et al*. (118).

Method	**Liquid-liquid extraction TRI Reagent®**	**Silica column RNeasy®**
Advantages	Very efficient tissue/cell lysis High RNA yield High RNA molecular weight Cost-effectiveness	Rapid procedure Purer RNA, less salt and chemical contamination
Disadvantages	Harmful chemicals involved e.g. phenol, chloroform Labour intensive, long procedure Possible residual contaminants e.g. phenol Subjectivity, incorrect phase separation causes DNA and protein contamination Non-automatability	Harmful chemicals e.g. beta-mercaptoethanol Lower RNA yield Loss of genetic material, through repeated membrane washing and incomplete elution of RNA Expensive Automatability

4.4 Summary and conclusions

Subsequent chapters of this thesis aim to characterise and quantify the degradation of RNA in post-mortem tissues. Therefore, it was crucial to confirm that the tissue processing and RNA purification procedure selected would not induce further RNA degradation; complicating data interpretation. In this sense, this chapter has validated the experimental protocol as 'fit for purpose', answering the three research questions presented in Box 4.1.

Do the anti-contamination procedures suggested protect RNA against unwanted RNase degradation on the bench?

It has been shown that aqueous RNA does not exhibit significant decay behaviour if manipulated on the bench at 22 °C for up to 96 hours. This suggests that the anti-contamination procedures adopted have successfully prevented further degradation of RNA on the bench.

Is RNAlater® an effective preservative solution for RNA in mouse skeletal muscle, kidney, liver and heart when stored at -20 °C for up to 8 weeks; halting further progression of RNA degradation?

RNAlater® was demonstrated to stabilise RNA effectively in skeletal muscle, kidney, liver and heart tissue when stored at -20 °C for up to 8 weeks. As a result, stabilisation of tissues in RNAlater® has been adopted in subsequent work to improve the practicality of tissue processing.

Which of the TRI Reagent® and RNeasy® methodologies performs most favourably with regard to RNA yield, purity and quality when utilised to extract RNA from mouse skeletal muscle, kidney, liver and heart tissue?

TRI® Reagent was shown to generate tissue RNA extracts with improved yield and purity relative to RNeasy®, and was able to more efficiently capture RNA molecules representing a wider distribution of fragment lengths. Accordingly, all data presented throughout Chapters 5, 6 and 7 of this thesis was generated using the TRI® Reagent extraction system.

Chapter 5: Assessment of RNA degradation in post-mortem tissues

5.1 Introduction

5.1.1 Tissue gene expression analysis in forensic pathology

RNA expression profiling has been suggested as a novel technique to supplement the conventional post-mortem examination, colloquially termed a '*molecular autopsy*' (Section 1.3.2, Chapter 1). Since transcription of new RNAs is an active process requiring energy input, it is expected to cease in the minutes/hours following death. As such, it has been hypothesised that examination of RNA expression in the tissues collected during an autopsy could provide an insight into gene activity at the time of death.

5.1.2 RNA behaviour post-mortem

Unfortunately, the degree to which the transcriptome is preserved in tissues post-mortem is very poorly understood. In practice, it is inevitable that a time lag exists between death and discovery of the body and tissue sampling/preservation, and what happens to RNA during this time is unknown (72). In living cells, RNA molecules have a closely regulated lifespan and when no longer required, they are degraded into their constituent nucleotides by enzymes with ribonuclease activity (RNases) as discussed in Section 1.2.4, Chapter 1. Although it is not yet fully understood, the mechanism of RNA degradation in post-mortem tissues is likely similar. Additionally, it is likely that as yet unknown microbial, chemical and physical factors further complicate post-mortem RNA degradation.

In order to correctly interpret gene expression data obtained from post-mortem tissues, it is essential to study the natural mechanisms and patterns of RNA decay after death. This is necessary to determine how closely the RNA profile of

post-mortem tissue actually reflects that present in the tissue at the time of death, and for how long after death gene expression analysis is likely to provide informative and reliable data. A time line of the stages ante-mortem (before death), peri-mortem (during/around the time of death) and post-mortem (after death) reflected in the gene expression profile obtained from autopsy tissue are summarised in Figure 5.1 (88). Of specific interest to the pathologist is alteration of the transcriptome in live cells; due to normal physiology, trauma, disease and the process of death itself. These however could be 'masked' by subsequent post-mortem degradation; highlighting the fundamental work required to study RNA behaviour post-mortem.

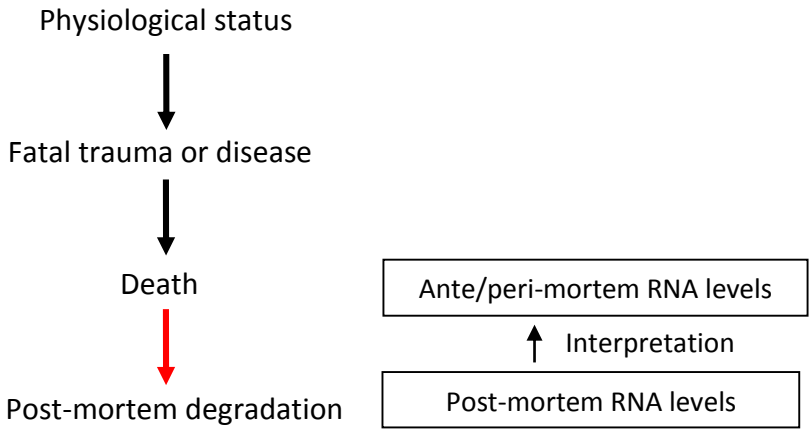

Figure 5.1: **Processes impacting upon the transcriptome detected by post-mortem gene expression profiling**. The transcriptome in tissues immediately following death has been altered by physiological/pathological factors ante- and peri-mortem. However, it is necessary for reliable interpretation of post-mortem RNA measurements to determine what happens to the transcriptome during the post-mortem interval (red arrow). Illustration adapted from (77).

Although our current understanding of human RNA decay post-mortem is extremely limited, a number of factors have been proposed in the literature as being likely/confirmed to influence RNA behaviour. This includes ante-, peri- and post-mortem elements, as summarised in Table 5.1.

Table 5.1: **Summary of factors proposed to influence gene expression results obtained from post-mortem tissue**. Information collated from (4, 12, 83, 227-230).

Summary of factors proposed to influence post-mortem gene expression	
Physiological status	Gender Age Body mass index Ethnicity Diet, malnutrition Time of day at which death occurred
Pathology/ Fatal trauma Death	Cause of death Agonal state and duration (time between disease onset and death) Stress Seizures Dehydration Tissue pH (acidity, caused by lactic acid accumulation) Toxin accumulation Pyrexia Oxygen deprivation – hypoxia/ischaemia/anoxia Coma Pharmacological treatments Drug and alcohol abuse
Post-mortem storage environment	Sunlight/ UV exposure Humidity Temperature Exposure e.g. covering, clothing, burial
Tissue collection	Sample preservation method e.g. snap-freeze, RNAlater® Post-mortem interval Tissue type Tissue integrity Freezer storage time and freeze-thaw cycling
RNA chemistry	Secondary structure Stability controlling sequence motifs

On the whole, experiments utilising human autopsy tissue material have been largely unsuccessful in ascribing a relationship between the post-mortem interval duration and the degradation state of the transcriptome (72, 81-83). Researchers in the field working with human tissue stumble across the problem of sample heterogeneity with regard to some/all of these factors (12). This makes for a large number of variables in experimentation, which are impossible to control or even to account for in data analysis. This prevents the attribution of any

identifiable differences in gene expression to one specific variable: such as time since death (4, 231). To account for this, when working with human tissue large numbers of biological replicates are essential to make statistically valid conclusions (154).

The use of animal models for preliminary work in the field has been advocated because of the ease with which these sources of biological variance can be controlled compared with human samples (12, 81, 229). Accordingly, some success has been gleaned by Sampaio-Silva *et al*. (6) and Li *et al*. (80) who were able with rodents to demonstrate a consistent relationship between RNA quality/quantity and the duration of the post-mortem interval. Both Sampaio-Silva *et al*. and Li *et al*. work towards the future aim that the decay state of the transcriptome in human tissues could be used as a novel indicator of the time since death. However, these works have been generated by decomposing rodents under strictly controlled laboratory conditions. Their outcomes clearly highlight that much more research is required to characterise the peri-, ante- and post-mortem variables influencing RNA decay behaviour before their success can be replicated in human tissues and under non-controlled situations.

5.1.3 Experimental design, aims and objectives

This research aims to take a broad look at RNA behaviour post-mortem, rather than narrowing down the analyses to a search for some 'predictive' element of post-mortem interval. The key objective of this work was to determine for how long after death tissue RNA remains analysable; and after what point it becomes so degraded that the quality and reliability of gene expression analyses is likely to be compromised.

Laboratory mice (*Mus musculus*) were selected as a mammalian model to achieve this due to their ease of use and to suit financial constraints. RNA was examined in the skeletal muscle of mice allowed to decompose intact under controlled laboratory conditions for up to 72 hours. From each mouse six samples of skeletal muscle were collected, at various time intervals up to this maximum.

Tissue samples were subjected to extraction to provide pure RNA, which was analysed for degradation using a panel of three key techniques.

Although skeletal muscle is not of specific interest from a clinical perspective (rarely will the cause of death be attributed to an issue with skeletal muscle), it was selected as the first tissue substrate for examination in response to work by Heinrich *et al*. (82), Koppelkamm *et al*. (81), and Bahar *et al*. (85); all of whom have demonstrated it to provide RNA of favourable quantity and quality compared with other tissue types. Also, its position close to the skin surface means its natural decomposition is more likely to reflect the ambient conditions to which the mouse corpse was exposed; which is of interest in Section 5.1.3.3.

An *in vivo* decomposition model was adopted; i.e., tissues were allowed to decompose in the organism as a whole. The integrity of each mouse corpse was maintained to the highest possible standard, to best simulate a natural setting where a corpse would be allowed to decompose uninterrupted. A number of recent publications have used the alternative *ex vivo* simulation, in which the animal is dissected immediately following death and tissue types are separated and allowed to decompose individually in a test tube (6, 87). Although this is clearly practically advantageous, there is very little data to confirm that RNA behaviour is consistent across both settings. The implications of this alternative experimental design are discussed in more detail in Chapter 6.

5.1.3.1 Analysis of tissue RNA yield and quality

Initially, tissue RNA extracts were quantified by UV-visible spectrophotometry to provide a gross assessment of the yield of RNA recovered. UV-visible spectrophotometry is commonly implemented in RNA research to confirm successful extraction of clean RNA and to allow normalisation of the input quantity of RNA to downstream analyses, as discussed in more detail in Section 1.4.2, Chapter 1. Therefore, the purpose of this step was to determine whether a reduction in total RNA yield due to degradation could be observed over the 72 hour post-mortem interval under investigation. In addition, this step intended to

determine whether the quantity of RNA recoverable from tissues at any point post-mortem fell to such a level that the success of downstream analyses would be compromised.

Subsequently, the quality of RNA samples was assessed with the Bioanalyzer 2100 (as described in Section 1.4.3, Chapter 1) to examine the fragment size distribution of RNA molecules recovered. This also allows quantification of the degree of RNA degradation in the form of an RNA integrity number (RIN). Several minimum RIN thresholds have been suggested in the literature, below which authors claim that RNA samples should be discarded as too fragmented to be of informative value upon gene expression analysis (138, 212). Such recommended thresholds vary depending on author opinion, but two of the most commonly referenced are a minimum of RIN 5 suggested by Fleige *et al*. (128, 212), or 3.95 as suggested by Weis *et al*. (138). This work will examine after what post-mortem interval tissue RNA quality falls below these thresholds, and whether the measured RNA quality correlates with the success of subsequent gene expression analysis by RT-qPCR.

5.1.3.2 Assessment of individual transcript decay behaviour by RT-qPCR

It is clearly not possible to characterise the degradation of each of the tens of thousands of mammalian RNAs in existence. Therefore, six RNAs were selected for analysis by RT-qPCR to quantify their abundance in mouse tissues post-mortem: 18S rRNA, B2m, Actb, Gapdh, Hmbs and Ubc. These six RNAs were chosen as they are commonly implemented throughout the clinical and forensic literature as endogenous control or 'housekeeping' genes (204). This means that based upon the known/presumed function of their encoded protein, they are expected to be ubiquitously expressed in all cell types, continuously, for cell survival. As such, they may be amongst the most stable RNAs in the transcriptome and their expression is not thought to be strongly inducible (232).

The expression of these six RNAs was quantified by RT-qPCR implementing the *TaqMan*® hydrolysis probes technology (Section 1.4.5, Chapter 1) over the first

72 hours post-mortem in mouse skeletal muscle tissue. This work was undertaken to track the progressive loss of these six transcripts through degradation. Several previous studies have suggested that RNAs can exhibit their own unique degradation behaviour post-mortem (80, 87, 93, 233, 234). In living tissues, the half-life of every RNA transcript is tightly regulated. Their lifespans vary most likely as a result of the functionality of their encoded protein, with RNA half-lives ranging from as little as 15 minutes for the c-Fos transcript to well over 24 hours for that encoding β-globin (11, 13). Precise control over the rate of RNA degradation in living cells is important, given that this governs the quantity of RNA available as a template for protein translation.

As yet, it is largely unknown whether this level of control still exists in tissues after death, or whether RNA degradation proceeds at 'random' and all transcripts are decayed in a similar fashion and at a similar rate. However, Zhao *et al*. (93), Inoue *et al*. (233), Kuliwaba *et al*. (87) Li *et al*. (80) and Pardue *et al*. (234) all have published data suggesting that this is most likely not the case, and that RNAs exhibit differential decay behaviour in post-mortem tissues or in surgical/biopsy specimens.

Clearly, if RNAs of interest in forensic medicine exhibit their own unique degradation behaviour this poses an interpretational obstacle upon gene expression analysis of tissues with an extended time interval between death and sample collection. The six endogenous control RNAs selected for analysis here should in theory, based upon their function, be amongst the most stable and long-lived RNAs in the murine transcriptome. A key objective of this work was to examine whether they degrade in parallel during post-mortem decomposition, or whether even this class of apparently 'stable' RNAs exhibit differential post-mortem behaviour.

5.1.3.3 Examining the effect of ambient temperature on tissue RNA decay

It is already known that the decompositional changes occurring in the body following death are strongly influenced by the environmental conditions to which the corpse is exposed (235), and RNA degradation is expected to be no different. Factors such as temperature, sunlight/UV, humidity, and exposure (i.e. clothing,

wrapping or burial) are anticipated to influence the rate of RNA decay as they do for decomposition as a whole. However as yet, little conclusive experimental evidence exists to support this inference.

Ambient temperature is one of the most strongly influential environmental conditions on decomposition. A number of research articles in clinical and veterinary medicine have suggested that the rate of RNA degradation can be slowed upon refrigeration of solid tissue samples, as one might expect (86, 87, 127). Fontanesi *et al*. (127, 236) illustrated that porcine muscle tissue samples were preserved against degradation for at least 24 hours upon refrigeration at 4 °C. Kuliwaba *et al*. demonstrated with human surgical bone samples that their refrigeration in saline for up to 72 hours improved the detected quantity of two bone RNAs: CTR and OCN (87). Additionally, Marchuk *et al*. (86) demonstrated that the RNA within lupine connective tissues was preserved against visible degradation for up to 96 hours upon refrigeration at 4 °C. However, neither Kuliwaba *et al*. nor Marchuk *et al*. used a fully quantitative RT-PCR system in their research, meaning that the value of these outcomes have been diminished by the advancement of RT-qPCR technology (86, 87).

The second phase of this work extended the analysis to assess tissue RNA degradation upon alteration of the ambient temperature to which the mouse corpses were exposed. Mice were left to decompose naturally at one of three ambient temperatures: refrigerated at 'cool' conditions of 10 °C, at a standard room temperature of 22 °C and in an incubator at 30 °C to simulate 'warm' conditions. Tissue sample collection, processing and RNA analysis proceeded as discussed previously.

This study examined the influence of ambient temperature on the rate of tissue RNA degradation. As refrigeration of the corpse slows down natural decomposition as a whole, this was predicted to slow down the onset of RNA fragmentation and reduce its severity. Accordingly, corpses stored in cooler conditions were expected to provide RNA in sufficient quantity and quality for reliable gene expression analysis for a longer post-mortem interval. On the

converse, the time interval during which corpses stored in warm ambient conditions gave reliable results upon RT-qPCR analysis was expected to be markedly shorter.

5.1.3.4 Examining tissue gene expression during the supravital reaction

The supravital reaction is defined as the time between two types of death:

- Clinical death, characterised by cessation of brain, heart and lung function;
- Biological death, characterised by death of individual cells/tissues (237)

During this time, tissues are expected to remain transcriptionally active. However, the length of time during which cells continue to transcribe RNA is completely unknown. It is reasonable to expect it may lie within the region of minutes to hours; however, research on the subject is sparse. Induction of gene expression immediately before, during and after the death 'event' is that which forensic pathologists hope holds the key to diagnosis (238). This 'event' should cause precise up- or down-regulation of RNAs known to be involved in the tissue response, which can be measured in terms of the type and relative abundance of detected RNAs.

The gene expression activity of mouse skeletal muscle in the first three hours following death was examined to try and quantify the time interval during which they remained transcriptionally active. A panel of nine RNAs were selected for assessment, as summarised in Table 5.2. The immediate early gene RNAs Fos and Jun were selected in response to previous work by Ikematsu *et al*. (239), who demonstrated them to be significantly up-regulated in the tissues of mice killed by asphyxia. The cytokine Tgfb1 was selected in response to the work of Kuliwaba *et al*. (87), who demonstrated it to exhibit a fast degradation rate (relative to Gapdh) in human surgical bone specimens. In addition, six RNAs (Casp3, FasR, Fadd, Dff40, Casp6 and Apaf1) were selected as markers of cell death; in particular the apoptotic signalling cascade. This was in response to the work of Sanoudou *et al*. (240), who demonstrated the up-regulation of a number of apoptosis-related genes in post-mortem skeletal muscle using microarray technology.

Clearly, the exact RNAs induced in response to a specific death 'event' strongly depend on the cause of death. These nine RNAs (Table 5.2) were selected not because they specifically are associated with death by cervical dislocation, but as an attempt to characterise a more 'general' gene expression response to death.

Table 5.2: **RNA targets selected for gene expression analysis during the supravital reaction.** Protein function information summarised from the National Center for Biotechnology Information (www.ncbi.nlm.nih.gov).

RNA target	Protein function
FBJ murine osteosarcoma oncogene (Fos)	Immediate early gene pair, rapidly expressed by cells in response to a wide variety of cell stimuli Form the heterodimer AP-1, a key transcription factor
Jun proto-oncogene (Jun)	
Transforming growth factor beta-1 (Tgfb1)	Inducible cytokine secreted from many cell types, controls cell growth, proliferation, differentiation and apoptosis
Caspase 3 (Casp3)	Member of apoptotic signalling cascade, activated by caspases 8, 9 and 10 and itself activates caspases 6 and 7 in both the extrinsic and intrinsic apoptosis activation systems
Fas receptor (FasR)	Cell membrane receptor accepting signals from the Fas ligand, may stimulate cell death through apoptosis
Fas associated death domain (Fadd)	Adaptor protein, bridging the Fas receptor to caspases 8 and 10, inducing apoptosis via the extrinsic activation system
DNA fragmentation factor 40 (Dff40)	DNase enzyme, induces chromatin condensation and DNA degradation in response to activation by caspase 3
Caspase 6 (Casp6)	Downstream effector caspase, activated by caspases 7, 8 and 10
Apoptotic protease activating factor 1 (Apaf1)	Upon binding of cytochrome C and dATP, forms the apoptosome to signal apoptosis (by activation of caspase 9) through the intrinsic apoptosis activation system

This work attempts to: 1) to identify whether any of these nine genes are switched 'on' during the supravital reaction resulting in novel RNA transcription, and 2) for those which are, to try to estimate for how long after death they continue to be transcribed. In order to achieve this, mice were killed by cervical dislocation (n = 3) and six samples of skeletal muscle were collected within the first three hours following death, at: <0.25, 0.5, 1, 1.5, 2 and 3 hours. During these time

periods, mice were left untouched on the bench at 22 °C. The expression of these nine RNAs was quantified in all samples by RT-qPCR using *TaqMan*® technology.

5.1.3.5 Summary: Research objectives

Overall, the purpose of this chapter is to try and answer a wide range of questions regarding RNA behaviour in tissues over the first 72 hours post-mortem. These questions have been summarised for clarity in Box 5.1.

Box 5.1: Objectives/questions to be answered within Chapter 5

For **how long** after death can RNA still be successfully extracted from tissues?

What **quantity** of RNA can be extracted from post-mortem tissue, and can the RNA yield be correlated with the post-mortem interval?

How good is the **quality** of RNA extracted from post-mortem tissue, can this quality be correlated with the post-mortem interval and after what post-mortem interval does RNA quality fall below published guidelines for gene expression analysis?

Can the expression level of **individual RNA transcripts** (as measured by RT-qPCR) be correlated back to the RNA quality?

How does the **ambient temperature** to which the corpse is exposed during the post-mortem interval affect RNA behaviour, with respect to tissue RNA quantity, quality, and the expression of individual RNAs?

Do distinct RNA transcripts decay at the same rate in post-mortem tissue, or does each RNA transcript have its own unique degradation behaviour as is true in live cells?

Is RNA expression induced during the **supravital reaction**, and if so, for how long after death does transcription still occur?

5.2 Method

5.2.1 Post-mortem tissue sample collection

All experimental steps involving live animals were performed in accordance with the ethical guidelines set out by the Biological Procedures Unit within Strathclyde Institute of Pharmacy and Biomedical Science. The animals utilised were 12 week old, male C57/BL6J laboratory mice. As discussed in Section 2.2.1, Chapter 2, mice were euthanised by cervical dislocation to minimise any potential effect on gene expression.

A total of 16 mice were killed and left to decompose in a ventilated plastic box (Figure 5.2) at one of three ambient conditions: refrigerated at 10 °C (n = 3), on the bench at a room temperature of 22 °C (n = 10) or in an incubator at 30 °C (n = 3). These temperatures approximate the typical ambient conditions to which the mouse corpses were exposed over the post-mortem interval, given that small fluctuations of a few °C were inevitable (e.g. by opening the refrigerator or oven door, slight day/night variations in room temperature). At various time intervals following death, samples of hind leg skeletal muscle were collected by making a small incision and collecting tissue from immediately under the skin (Figure 5.3).

Figure 5.2: **Decomposition of three mice.** Mice were left to decompose in a ventilated plastic box at room temperature in a fume cupboard.

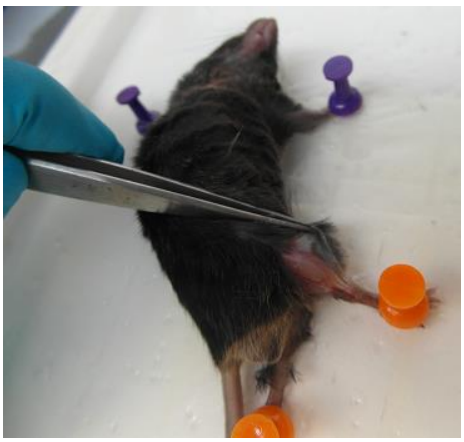

Figure 5.3: **Dissection of a mouse's hind leg to expose skeletal muscle**. A total of three tissue samples could be collected from each hind leg, by extending the incision back towards the hip bone.

From an experimental point of view, it would have obviously been advantageous for only a single muscle tissue sample to be collected from each mouse and for the corpse to be otherwise untouched prior to sample excision. This would more accurately simulate a natural setting where a corpse would be left to decompose uninterrupted. However, this experimental design would have caused a six-fold increase in the number of mice required for this study, which was neither ethically nor financially favourable. Following pre-testing, it was determined that a total of six samples of skeletal muscle could be collected from each mouse (three from each of the hind legs), whilst maintaining an appropriate gap between skin incisions. The six sampling time intervals for mice decomposed at ambient temperatures of 10, 22 and 30 °C are summarised in Tables 5.3, 5.4 and 5.5 respectively.

Under each of the three experimental conditions examined, it can be observed from Tables 5.3, 5.4 and 5.5 that a total of three or four mice were used as biological replicates. It should be noted that this small sample size was a consequence of the limited resources available for this project, rather than a conscious choice during the experimental design and planning stage.

Table 5.3: **Post-mortem interval (in hours) for six samples of skeletal muscle excised from mice decomposed at an ambient temperature of 10 °C in a refrigerator**.

Sample ID	1	2	3	4	5	6
Post-mortem interval (h) n = 3	<0.25	12	24	36	48	72

Table 5.4: **Post-mortem interval (in hours) for skeletal muscle tissue samples excised from three sets of mice decomposed at room temperature (22 °C).** Initially, RNA degradation was assessed over a 72 hour time interval (row 4). Two additional sets of mice were subsequently added (rows 2 and 3) in order to look more closely at RNA behaviour over the first 3 and 24 hours post-mortem.

Sample ID	1	2	3	4	5	6
Post-mortem interval (h) n = 3	<0.25	0.5	1	1.5	2	3
Post-mortem interval (h) n = 3	<0.25	3	6	9	12	24
Post-mortem interval (h) n = 4	<0.25	12	24	36	48	72

Table 5.5: **Post-mortem interval (in hours) for six samples of skeletal muscle excised from mice decomposed at an ambient temperature of 30 °C in an incubator**.

Sample ID	1	2	3	4	5	6
Post-mortem interval (h) n = 3	<0.25	3	6	12	24	36

Under the initial experimental design, mice were left to decompose for up to 72 h at all three ambient conditions, and samples of skeletal muscle were excised at six time intervals up to this maximum (Table 5.3, 5.4). However, some subsequent modifications were made to provide additional data points and eliminate those which did not prove to be informative. As can be seen in the results in Section 5.3, most RNA degradation was found to occur over the first 24 h post-mortem in the mice decomposed at room temperature. In response, two additional data sets were included to more closely look at RNA degradation during this immediate post-mortem period (Table 5.4). The time period during which RNA degradation was examined in the tissue of mice decomposed at 30 °C was reduced from 72 hours to 36 h. It was found that after 36 hours this mouse set exhibited signs of severe decomposition characterised by skin slippage, abdominal distension, leakage of the gastrointestinal contents, and significant tissue liquefaction through autolysis and/or putrefaction. The latter made the distinction of skeletal muscle from other tissue types increasingly difficult. As such, the maximum decomposition period after which tissue samples were collected was reduced to 36 h (Table 5.5).

5.2.2 RNA purification, quantification and quality analysis

A detailed protocol for the analysis of RNA in solid tissue samples has been included in Section 2.2, Chapter 2, which will be referred back to. Samples of skeletal muscle were collected after a range of post-mortem intervals and immediately preserved in RNAlater®, using the protocol described in Section 2.2.2, Chapter 2. RNA was purified using the TRI Reagent® procedure (Section 2.2.3.3, Chapter 2) and RNA samples subjected to DNase treatment to remove residual DNA contamination (Section 2.2.3.4, Chapter 2). RNA was quantified by UV-visible spectrophotometry (Section 2.2.4, Chapter 2) and quality analysis performed on the Bioanalyzer 2100 platform (Section 2.2.5, Chapter 2).

5.2.3 Gene expression analysis by RT-qPCR

Following RNA quantification, samples were diluted in RNase-free water (Ambion, Life Technologies, Paisley, UK) to a concentration of 100 ng/µL and reverse transcribed into cDNA with the High Capacity cDNA Reverse Transcription Kit (Applied Biosystems, Life Technologies, Paisley, UK) (Section 2.2.6, Chapter 2). The resultant cDNA products were diluted further 1:12 in RNase-free water to prevent qPCR inhibition through carryover of high concentration buffers and reverse transcriptase.

cDNA samples were amplified to quantify the presence of six endogenous control RNAs: 18S rRNA, B2m, Actb, Gapdh, Hmbs and Ubc; or nine 'supravital reaction' genes: Fos, Jun, Tgfb1, Casp3, FasR, Fadd, Dff40, Casp6 and Apaf1. Section 2.2.7.1 describes the protocol for amplification of cDNAs by real time PCR and the *TaqMan*® technology. Details of the PCR assays used against these target cDNAs (i.e. assay ID, target transcript function, amplicon site and length) are included in Tables A1.1 and A1.2, Appendix 1. Gene expression data was analysed in Microsoft Excel 2010, GenEx Pro v5.4.3 (MultiD Analyses) and Minitab v17 (Minitab Inc.) statistical softwares, using the $2^{-\Delta\Delta CQ}$ relative expression calculations described in Section 2.2.7.2, Chapter 2.

5.3 Results and discussion

5.3.1 Macroscopic examination of post-mortem decomposition

Following the aforementioned experimental design, mice were decomposed for up to 72 hours exposed to one of three ambient temperatures: 10, 22 and 30 °C. As expected, the onset of visible decomposition and its rate of progression were strongly variable between these temperature categories. Mice decomposed at 30 °C experienced putrefaction, green discolouration of the skin (caused by the formation of sulfhaemoglobin in settled blood (241)), skin slippage, gaseous abdominal distension and leakage of the gastrointestinal contents within as little as 24 hours. In particular, the liquefaction of tissues by autolysis/putrefaction made the recognition and collection of specific tissue types (notably skeletal muscle) difficult beyond a 36 hour post-mortem interval. For this reason, the collection and analysis of tissues from this set of mice was limited to 36 hours post-mortem.

Mice decomposed at 22 °C room temperature also experienced skin discolouration, skin slippage and abdominal distension within the 72 hour post-mortem interval examined; albeit at a lower severity. None of these features significantly affected the dissection and tissue collection process, and potentially this sample set could have been continued to examine longer post-mortem intervals. This however, was deemed to be out with the scope of this study.

The preservation state of mice decomposed at the cooler ambient temperature of 10 °C was significantly better than their counterparts left at 22 and 30 °C. The progression of *rigor mortis* was slowed, with it lasting for 48 to 72 hours post-mortem in some mice. None of the mice exhibited any severe macroscopic changes associated with decomposition; all mice remaining intact. Even after 72 hours post-mortem, the visible quality of tissue samples excised from this mouse set was deemed to be good.

5.3.2. Total RNA yield: UV-visible spectrophotometry

In order to determine whether the total RNA content of tissues drops appreciably post-mortem through degradation, tissue RNA yield was estimated by UV-visible spectrophotometry. Skeletal muscle tissue RNA yield was assessed for mice left to decompose at an ambient temperature of 10 and 22 °C for up to 72 hours, and at 30 °C for up to 36 hours. RNA yield was defined as the quantity of RNA obtained (in nanograms) per 1 mg of tissue subjected to extraction.

After decomposing mice at ambient conditions of 10 and 22 °C, no consistent and significant decline in skeletal muscle tissue RNA yield could be observed over the 72 hour post-mortem interval under examination – as illustrated in scatter plot form in Figure 5.4. The yield of RNA per unit tissue was strongly variable between replicates, as illustrated by the wide error bars in Figure 5.4; most notably for the 22 °C data set (red data points). This is likely caused by differences in the cellular content of individual tissue samples. Skeletal muscle is known to be a strongly fibrous, protein rich tissue type with a significantly reduced number of cells relative to other tissue types. Differences in the ratio of RNA-containing cells to fibrous tissue causes strong variability in RNA yield despite normalisation of the input tissue mass. In addition, the efficiency of RNA extraction using TRI Reagent® is very user-dependent, enhancing variability between replicates. RNA recovery is affected by the completeness of tissue matrix homogenisation and adequate separation of the aqueous and organic phases.

Both data sets were examined with the Anderson-Darling normality test to determine whether or not the data were normally distributed. With this procedure it was established that the RNA yield data for mice decomposed at 10 °C was normally distributed ($p = 0.395$), but the RNA yield data for mice decomposed at 22 °C was not normally distributed ($p = 0.016$).

Although a slight downward trend is visible for the 10 °C data (Figure 5.4), no statistically significant correlation was characterised between the post-mortem interval and total RNA yield upon storage of the corpse at an ambient temperature of either 10 or 22 °C: the 10 °C data set having been examined using Pearson's

product moment correlation (r = -0.425, p = 0.079) and the 22 °C data set using the non-parametric Spearman's rank order correlation (ρ = -0.033, p = 0.850); in accordance with the outcomes of Anderson-Darling's normality test. Further analysis of the RNA yield data for corpses stored at 10 °C with a one-way ANOVA identified no significant difference between the mean RNA yield of tissue samples extracted after any post-mortem interval (p = 0.369). Similarly, no significant difference was found in mean RNA yield after any post-mortem interval after analysis of the 22 °C data set with the non-parametric Kruskal-Wallis test (p = 0.540).

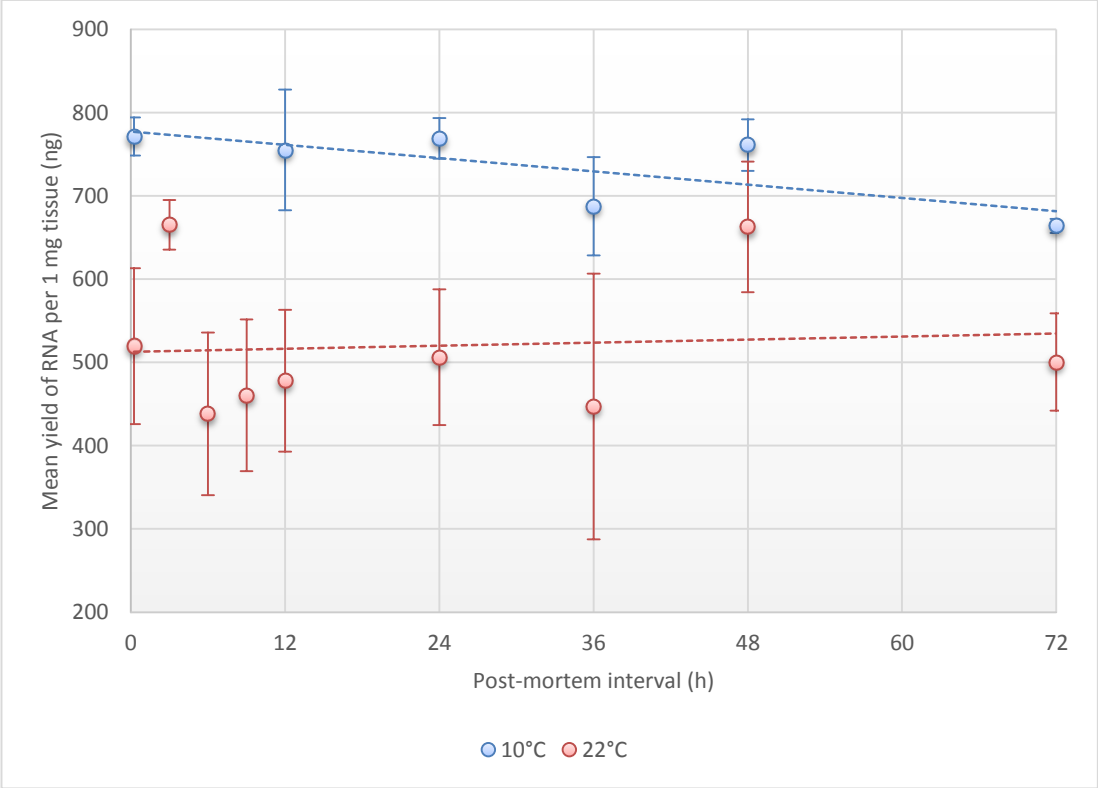

Figure 5.4: **Yield of RNA from mouse skeletal muscle tissue collected until 72 hours post-mortem, for animals stored refrigerated at 10 °C (blue data points) and at room temperature 22 °C (red data points).** Points represent total RNA quantity determined by UV-vis spectrophotometry (in ng) per 1 mg of tissue extracted. Data represents mean ± S.E. for n = 3, and n = 6 for selected data points.

This result likely represents the expected outcome of this investigation. The UV-visible spectrophotometry system employed for RNA quantification relies solely

on the absorbance of ultraviolet light (at 260 nm) by the aromatic rings of nucleobases in the RNA structure – both purines and pyrimidines (120). Photons of light in this wavelength range provide the energy required for an electronic transition in the nucleobase; their absorption inducing the promotion of an electron from the highest occupied molecular orbital to the lowest unoccupied molecular orbital. As such, RNA of mixed nucleobase composition (ACGU) should absorb light in a largely identical manner regardless of whether it exists as short (low molecular weight, fragmented RNAs) or long (high molecular weight, intact RNAs) oligonucleotide chains. UV-visible spectrophotometry is not commonly used as an indicator of RNA sample quality; rather as a screening technique for successful extraction of a sufficient quantity of RNA for downstream analyses.

The TRI Reagent® protocol used for extraction and purification of tissue RNA is not known to be strongly biased towards recovery of low or high molecular weight RNAs. This means that regardless of whether tissue RNA has been fragmented during decomposition, the measured total yield of RNA should be similar. UV-visible spectrophotometry is therefore not a sensitive indicator of mild/moderate RNA degradation, and in such samples does not provide a measure of sample integrity and/or amplifiability (129).

On the contrary, mice left to decompose at an ambient temperature of 30 °C to enhance the rate of decomposition exhibited an approximately linear decline in total RNA yield, as illustrated in scatterplot form in Figure 5.5. As before, it was determined with the Anderson-Darling normality test that the RNA yield data was normally distributed ($p = 0.550$). This outcome permitted the identification of a statistically significant, negative linear correlation between the post-mortem interval duration and RNA yield using Pearson's product moment correlation: $r = -0.791$, $p = 0.000$. Analysis of the data with a one-way ANOVA confirmed the presence of a significant difference in mean RNA yield between the post-mortem interval categories ($p = 0.012$). Upon pair-wise comparison of the data using Dunnett's Multiple Comparisons with a Control method, it was found that only after passage of a 36 hour post-mortem interval was the mean yield of skeletal muscle RNA significantly reduced relative to the control point (<0.25 hours).

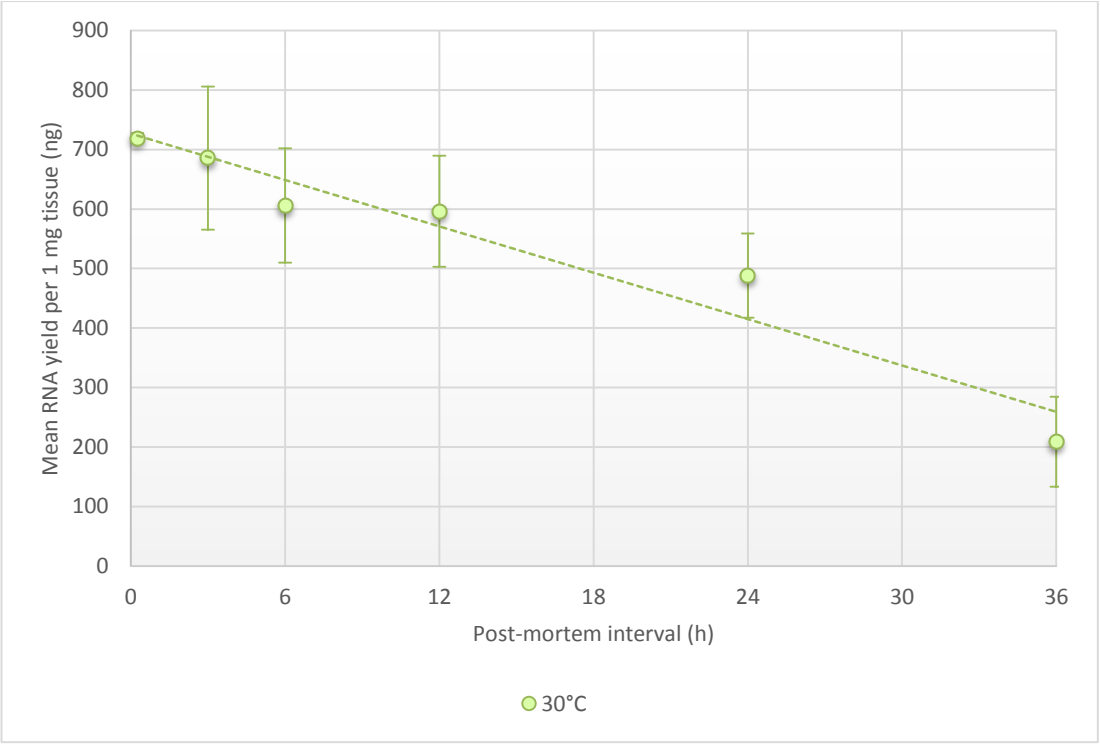

Figure 5.5: **Yield of RNA from mouse skeletal muscle tissue collected until 36 hours post-mortem, for animals stored in an incubator at 30 ºC**. Points represent total RNA quantity determined by UV-vis spectrophotometry (in ng) per 1 mg of tissue extracted. Data represents mean ± S.E. for n = 3.

This data mirrors the findings of Kuliwaba *et al*. (87), who assessed the effect of ambient temperature on the rate of RNA degradation in human bone samples (recovered after surgery, rather than post-mortem specimens) stored in saline at each of 4, 20 and 37 °C. Kuliwaba *et al*. aimed to develop a storage method for bone samples to study the molecular basis of bone pathology. They found that storage of bone tissue at each of 4 and 20 °C for up to 72 hours caused no observable reduction in the measured quantity of RNA by UV-visible spectrophotometry. On the other hand, the RNA yield from bone samples stored at 37 °C exhibited a significant linear decline with storage interval, causing the recovered quantity of RNA to fall below the minimum for Northern blot analysis. Similarly, Marchuk *et al*. (86) found no observable decline in RNA yield from lupine connective tissues (tendon, ligament and cartilage) over a 96 hour post-mortem interval when corpses were stored at 4 °C. In addition, Fitzpatrick *et al*. (242) identified no decline in total RNA yield from bovine reproductive tissues

decomposed for up to 96 hours post-mortem, where tissues were stored *ex vivo* at room temperature.

To assess in more detail the relationship between post-mortem interval and skeletal muscle RNA yield the data set was subjected to linear regression analysis; the results of which are presented in Figure 5.6. The obtained linear regression model estimates that approximately 62.6% of the variation in RNA yield is attributed to the post-mortem interval duration (unadjusted R^2). The resulting 37.4% of variation is accounted for by strong inter-sample and inter-mouse variation in skeletal muscle tissue RNA yield.

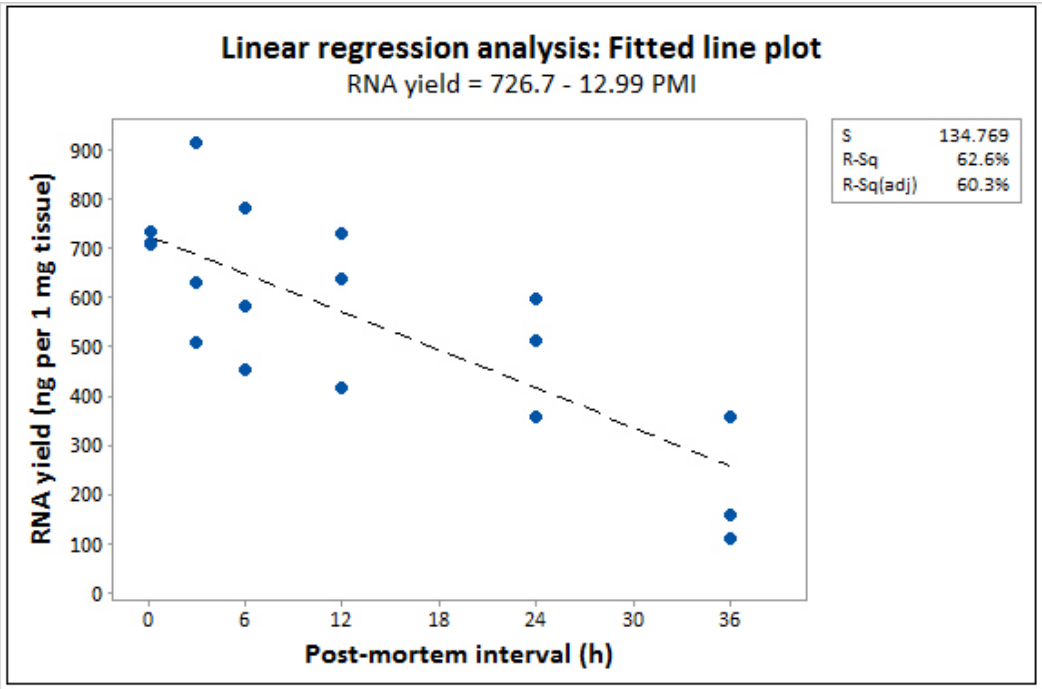

Figure 5.6: **Assessment of the relationship between post-mortem interval duration and the yield of RNA recovered by linear regression analysis.** Skeletal muscle tissue samples were examined (n = 3 per time point, n = 6 time points), recovered from mice decomposed at an ambient temperature of 30 °C for up to 36 hours.

What can be inferred from this reduction in skeletal muscle tissue RNA yield is unclear, and difficult to assess at a molecular level. As discussed, UV-visible spectrophotometry is an insensitive indicator of mild/moderate RNA degradation;

relying primarily on the nucleobases remaining intact. This outcome may indicate that RNA is being degraded to the extent that the molecular structure of individual nucleotides and nucleobases is being compromised. This proposition however, is difficult to verify from a practical perspective as these degradation products cannot easily be identified and quantified in a biological mixture. Even after a 36 hour post-mortem interval, the quantity of RNA recovered is still more than sufficient for downstream analyses such as RNA quality assessment and gene expression analysis by RT-qPCR. However, this does indicate that in the following hours/days the quantity of RNA recovered from tissues will likely fall below the sensitivity of these technologies.

5.3.3 Total RNA quality: Bioanalyzer 2100

The second feature of the transcriptome examined in post-mortem tissue was the total RNA quality. As before, skeletal muscle tissue RNA quality was assessed for mice left to decompose at an ambient temperature of 10 and 22 °C for up to 72 hours, and at 30 °C for up to 36 hours. Tissue RNA quality was measured on the Bioanalyzer 2100 platform and quantified using the RNA integrity number (RIN). After electrophoretic separation of each RNA sample, the RIN is calculated by an algorithm using a scale from 1 (poor quality) to 10 (excellent quality) (discussed in more detail in Section 1.4.3, Chapter 1). RIN is a highly sensitive and quantitative screening indicator for RNA sample degradation.

This work was undertaken to identify whether a relationship exists between the time since death and total RNA quality and if so, to try to characterise the nature of this relationship. In addition, the influence of ambient temperature on the onset and rate of RNA degradation was examined. Figure 5.7 illustrates the measured RNA quality of skeletal muscle tissue samples over a 72 hour post-mortem interval, combining data from mouse corpses stored at 10, 22 and 30 °C. In all three data sets it can be seen that the decline in RNA quality is not linear, but follows a sigmoidal shape. In the immediate hours post-mortem, the decline in tissue RNA quality is slow. This is followed by a period of rapid decline in RNA

quality. Eventually, the decay profiles level out at the lower end of the RNA integrity spectrum, at approximately RIN 2. The post-mortem interval at which each of these three stages is reached was strongly dependent on ambient temperature.

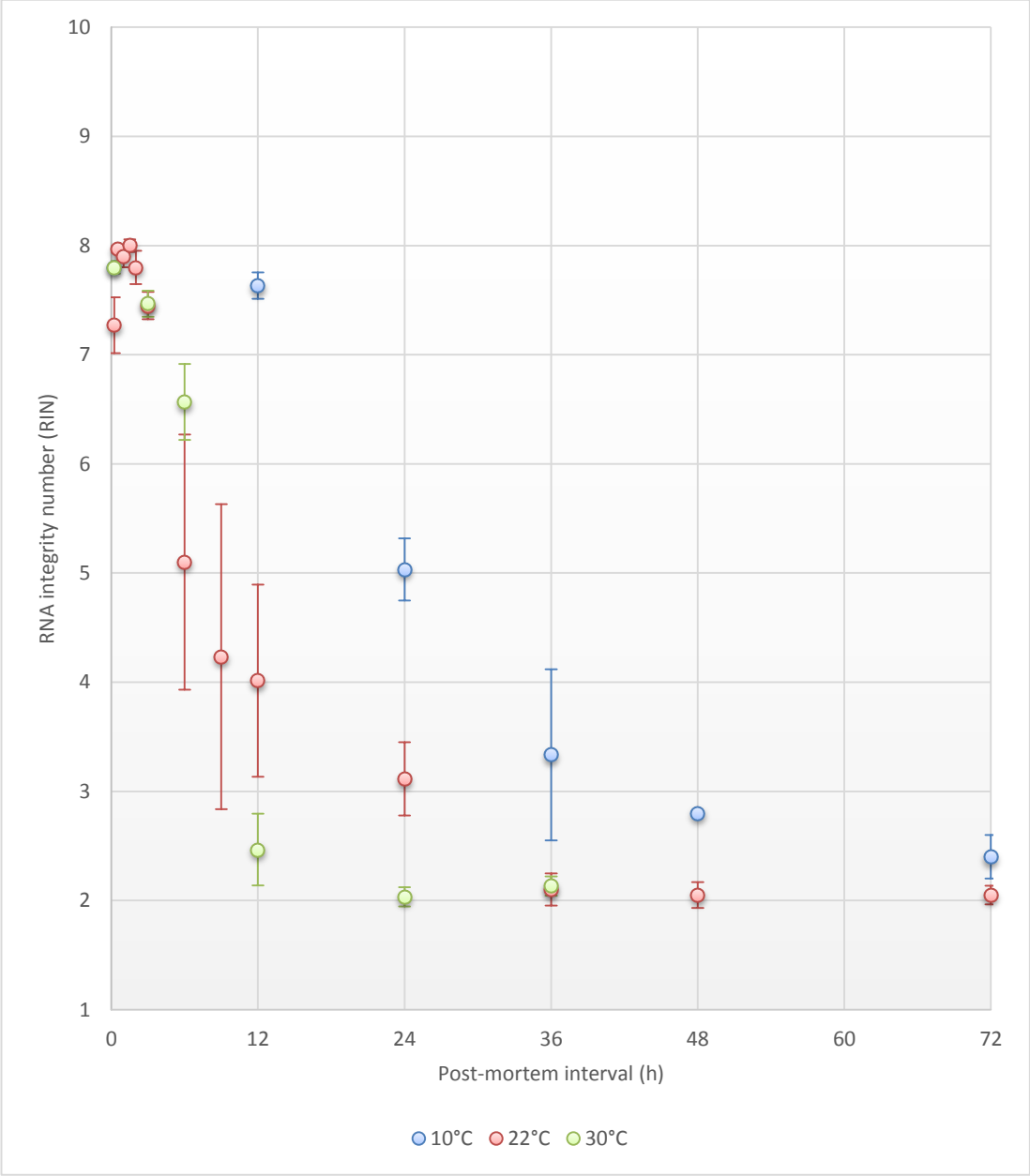

Figure 5.7: **Quality of RNA from mouse skeletal muscle collected until 72 hours post-mortem from mice exposed to ambient conditions of 10 °C (blue data points), 22 °C (red data points) and 30 °C (green data points).** Points represent RNA quality as quantified by the Bioanalyzer 2100 using the RIN algorithm. Data represents mean ± S.E. for n = 3, apart from a few exceptions where n = 4 or 6.

Prior to further analyses, data was examined for distribution using the Anderson-Darling normality test, the results of which suggested that all three data sets were normally distributed (data not shown). This facilitated the use of parametric tests for subsequent data analysis.

It can be seen in Figure 5.7 that the onset of RNA degradation is much slower in the tissues of mice refrigerated at 10 °C, as would be expected. RNA quality remains high at a mean RIN of 7.6 at 12 hours post-mortem, after which the RNA quality starts to decline. A one-way ANOVA with Dunnett's Multiple Comparisons with a Control suggested that RNA quality did not significantly reduce in this tissue set until 24 hours post-mortem ($p = 0.000$). In the tissue of mice decomposed at 22 °C, degradation onsets more quickly and a significant reduction in RNA integrity can be detected after only 9 hours ($p = 0.000$). As expected, degradation is further accelerated under the aggressive decomposition conditions at 30 °C, with RNA quality significantly reduced after only 6 hours post-mortem ($p = 0.000$).

In order to more clearly visualise the fragmentation of RNA and what these RINs actually infer, Figures 5.8, 5.9 and 5.10 display a number of raw electropherogram outputs along with their associated RNA integrity number (RIN). Figure 5.8 illustrates the degradation of RNA in the tissues of mice decomposed at 10 °C, with RNA quality presented at six time intervals up to the maximum 72 hours. Initially, in Figure 5.8A the 28S and 18S rRNAs remain intact with a fairly smooth and flat baseline. As fragmentation onsets, the intensity of signal for the 28S and 18S rRNAs reduces, and electropherogram 'shifts' to the left as small, fragmented RNA molecules elevate the baseline. It is these features of the electropherogram which are used as the basis of the RIN algorithm.

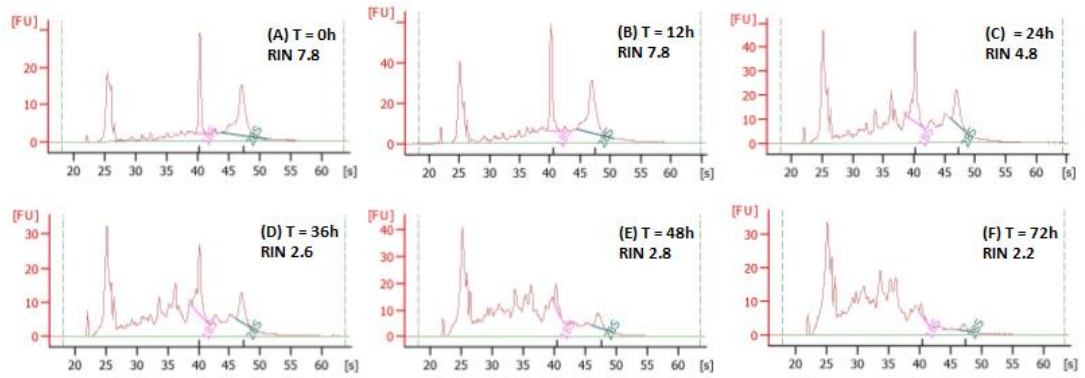

Figure 5.8: **Total RNA quality of tissue samples collected over a 72 hour post-mortem, after storage of the corpse refrigerated at 10 ºC**. Electropherograms present the Bioanalyzer 2100 output for RNA extracted from tissue samples recovered from mouse T, at six post-mortem intervals: (A) 0 hours, (B) 12 hours, (C) 24 hours, (D) 36 hours, (E) 48 hours and (F) 72 hours.

In the tissues of mice decomposed at 22 °C it can be seen in Figure 5.9 that the onset of RNA fragmentation starts earlier, and is of higher severity. After 72 hours, the 28S and 18S rRNAs have been almost lost and all that remains is small, fragmented RNA products.

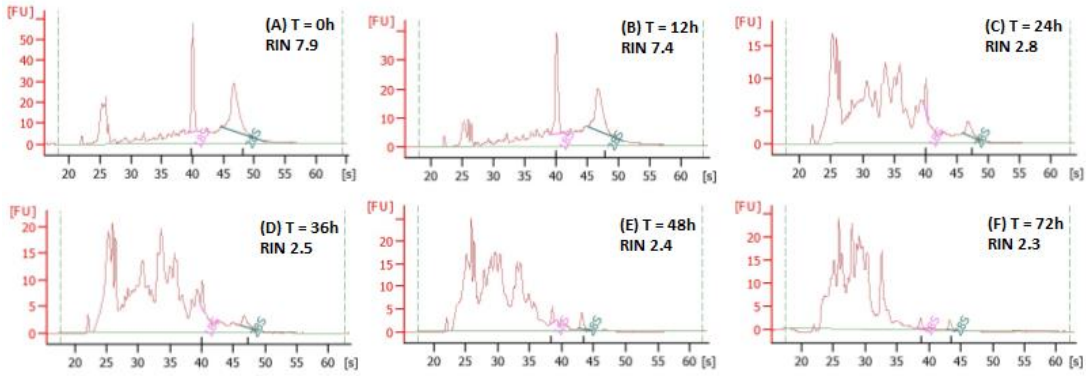

Figure 5.9: **Total RNA quality of tissue samples collected over a 72 hour post-mortem, after storage of the corpse at room temperature 22 °C.** Electropherograms present the Bioanalyzer 2100 output for RNA extracted from tissue samples recovered from mouse AA, at six post-mortem intervals: (A) 0 hours, (B) 12 hours, (C) 24 hours, (D) 36 hours, (E) 48 hours and (F) 72 hours.

Similarly, at 30 °C the onset of RNA degradation is even earlier with the 28S and 18S rRNAs all but lost within 12 hours (Figure 5.10). After 36 hours, the highest molecular weight RNAs remaining in the tissue correspond to an approximate length of less than 750 bases (estimated by comparison with an RNA ladder). It can be seen that at these latter stages (e.g. 5.10D-F), RIN remains unaffected by further RNA degradation. With such extreme degradation at the lower end of the RIN spectrum, the RIN algorithm appears to lose its sensitivity to detect and quantify further degradation.

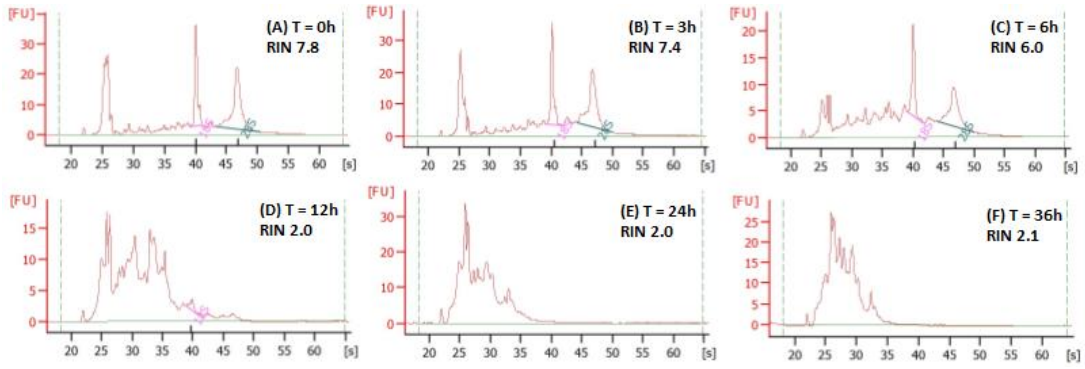

Figure 5.10: **Total RNA quality of tissue samples collected over a 72 hour post-mortem, after storage of the corpse incubated at 30 °C.** Electropherograms present the Bioanalyzer 2100 output for RNA extracted from tissue samples recovered from mouse X, at six post-mortem intervals: (A) 0 hours, (B) 3 hours, (C) 6 hours, (D) 12 hours, (E) 24 hours and (F) 36 hours.

Data published by Sampaio-Silva *et al*. (6) suggested that during the first 11 hours after death, the relationship between post-mortem interval and RNA quality (as quantified using the RNA quality index, a similar competitor to the RIN utilised throughout this work) exhibits a linear profile in mouse skeletal muscle. This was only examined for the tissues of mice decomposed at room temperature, for up to 11 hours post-mortem. The outcomes presented here demonstrate that the reduction in RNA quality is not linear with time, but follows a sigmoidal profile as illustrated in Figure 5.7. Although RIN did exhibit a sharp decline over the first 11 hours following death mirroring the data presented by Sampaio-Silva *et al*. (6),

beyond this point RNA quality tails off towards the bottom of the RIN spectrum and RNA quality is no longer useful as an indicator of post-mortem interval.

A one-way ANOVA with Fisher's Least Significant Difference test was implemented to assess whether the effect of post-mortem ambient temperature on RNA integrity was deemed to be statistically significant; focusing particularly on the comparable 12, 24 and 36 hour time intervals. After 12 hours, the quality of RNA was significantly higher in the tissue of corpses decomposed at 10 °C ($p = 0.015$) relative to 22 and 30 °C. This can be clearly observed in the data presented in Figure 5.7. A similar outcome was apparent after 24 hours post-mortem, with RNA quality significantly higher in the tissue of corpses decomposed a 10 °C ($p = 0.002$) relative to 22 and 30 °C. At and after 36 hours however, the RNA quality scores begin to converge at the lower end of the RIN scale, and this statistically significant difference is lost ($p = 0.132$ at 36 hours).

Variability in RNA quality between replicates is high, illustrated by the large error bars in Figure 5.7. This is especially visible at intermediary levels of RNA quality; i.e. between RIN 3 and 6. In order to look more closely at the source of this variability, a short assessment was conducted to look at the consistency of skeletal muscle tissue RNA quality between mice (inter-mouse variation), relative to that between a number of skeletal muscle tissue samples recovered from a single mouse (intra-mouse variation). This assessment was limited only to triplicates for mice decomposed at an ambient temperature of 22 °C, to glean an idea of whether RNA quality measurements exhibit improved consistency when sampling from a single mouse. As can be seen from the results of this analysis in Table 5.6, the variance in RNA quality (RIN) between these two categories differed only at a 12 hour post-mortem interval, where the variance was lower for intra-mouse replicates relative to inter-mouse replicates.

Table 5.6: **Assessment of variability in mouse RNA quality (quantified in terms of RIN) both within and between individual mice (n = 3 for each), as performed with the Test of Equal Variances**. Only at 12 hours post-mortem was a significant difference observed between the variance of the two categories, marked with an asterisk **.

PMI (h)	Intra-mouse RIN variance	Inter-mouse RIN variance	Test of equal variances: Multiple comparisons p-value
	3 tissue samples examined from the same mouse	3 tissue samples examined from 3 different mice	
0	0.023	0.303	0.112
12	0.010	1.470	0.004**
24	0.223	0.213	0.97
36	0.003	0.023	0.204
48	0.023	0.003	0.204
72	0.003	0.003	1

This indicates a discrepancy in the consistency of RNA quality within and between mice during the early post-mortem interval. Stronger variability between mice may be suggestive of wider influences on the rate of tissue RNA degradation; for example, from other tissues and organ systems. From a macroscopic perspective, it was clear that not all mice decomposed in a similar fashion. Some exhibited signals such as skin slippage and abdominal distension slightly earlier/later than their counterparts. However overall, the data suggests that this is not a major factor in the long-term. Intra- and inter-individual variability in RNA degradation will also be discussed in more detail in subsequent sections with respect to the decay profile of individual RNAs.

5.3.4 Degradation of endogenous control RNAs: RT-qPCR

5.3.4.1 Tracking the degradation of individual RNA transcripts

Both RNA quantification by UV-visible spectrophotometry and RNA quality analysis on the Bioanalyzer 2100 are used as indicators of the state of the transcriptome as a whole. This section presents RT-qPCR data for six endogenous control RNAs commonly used for normalisation purposes in gene expression studies

in forensic and clinical medicine – 18S rRNA, B2m, Actb, Gapdh, Hmbs and Ubc (160, 204). Fulfilling their purpose as endogenous controls, these RNAs are expected to be amongst the most stable and uniformly expressed RNAs in the transcriptome (204). Their expression was quantified by RT-qPCR in the skeletal muscle of mice decomposed for up to 72 hours at an ambient temperature of 10 and 22 °C, and for up to 36 hours at 30 °C.

As expected, it was found that the measurable quantity of each of the six examined RNA transcripts reduced through post-mortem degradation. The data illustrated in Figures 5.11, 5.13 and 5.15 demonstrates the raw C_Q data for 18S rRNA, B2m, Actb, Gapdh, Hmbs and Ubc, when RNA concentration was normalised to a 100 ng/μL input into reverse transcription and the resultant cDNA was diluted 1/12 in water prior to qPCR amplification.

It was found that in the tissues of mice decomposed at 10 °C, the magnitude of RNA loss through degradation was relatively mild as illustrated in Figures 5.11A and 5.11B. Each of the RNAs examined had a different basal expression level in the control samples (post-mortem interval < 0.25 hours) – with 18S rRNA exhibiting the strongest expression (visualised as the lowest C_Q) and Hmbs and Ubc the lowest basal expression level (visualised as the highest C_Q). This outcome is in accordance with data published by Vandesompele *et al*. (178), who illustrated that in most tissue types, Gapdh and Actb exhibit the highest basal level of expression, followed closely by B2m.

The degradation of RNA is characterised by a gradual increase in C_Q with time post-mortem (Figure 5.11A). When quantifying the expression of an RNA by RT-qPCR, the assay detects not the whole transcript (which can be thousands of nucleotides long) but a small portion of its length. In this work, the assays designed amplified a section of the RNA in the size range of 61 to 107 nucleotides (Appendix 1, Table A1.1). Successful amplification of this target sequence relies on it remaining intact; it takes only a single 'break' to render it unamplifiable and thus, undetectable (60). As such, the increase in raw C_Q visualised in Figure 5.11A indicates a reduced amplifiable quantity of each RNA.

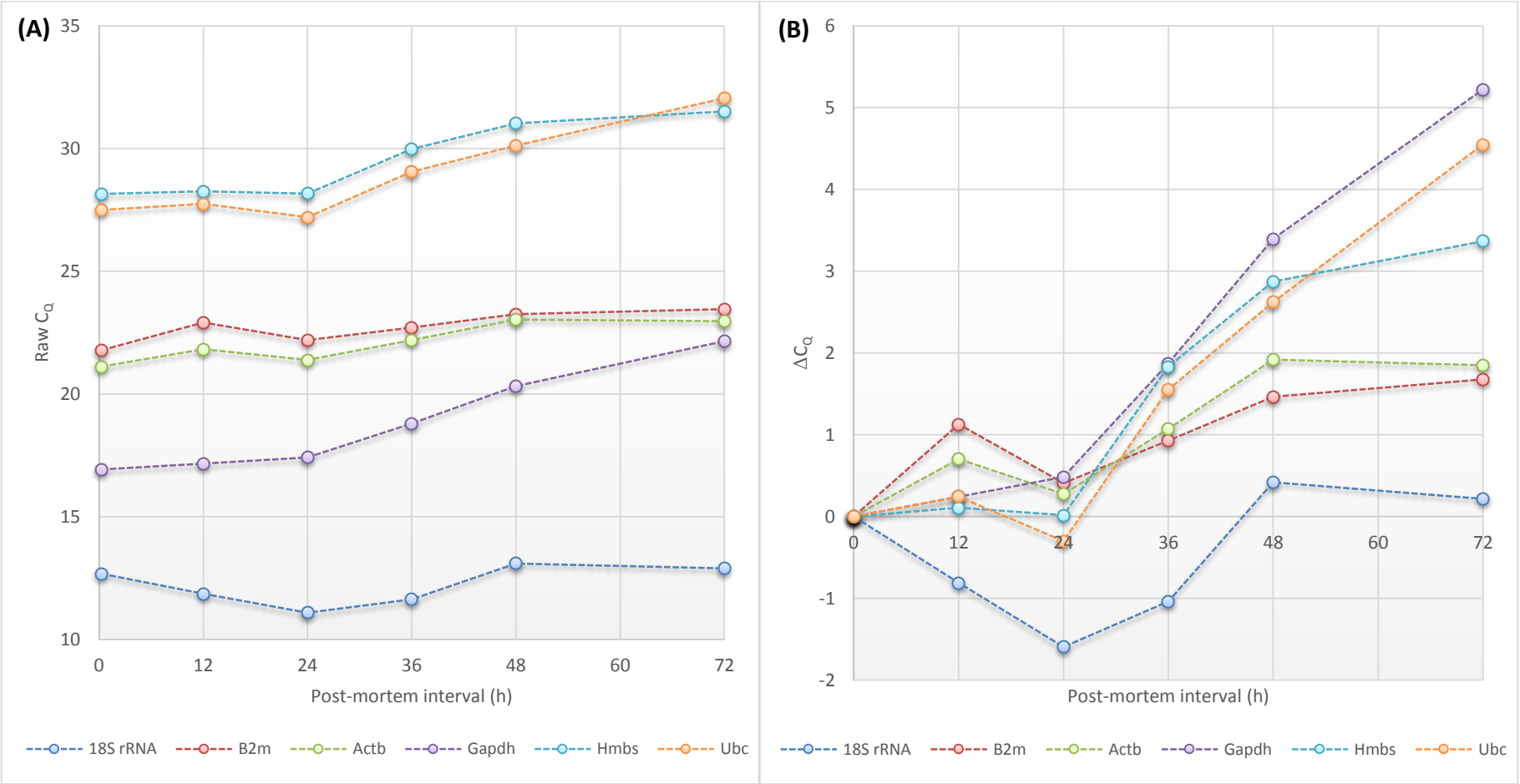

Figure 5.11: E**xpression of 18S rRNA, B2m, Actb, Gapdh, Hmbs and Ubc in the skeletal muscle tissue of mice decomposed at an ambient temperature of 10 °C for up to 72 hours.** (A) Describes the raw C_Q data for each of the six endogenous control RNAs. (B) Describes the raw data in the form of a ΔC_Q. Data points represent the mean of n = 3 mice. Error bars have been omitted for clarity.

Loss of an RNA through degradation can be more clearly visualised for each target in Figure 5.11B, which illustrates the difference in C_Q (ΔC_Q) for each post-mortem interval time point relative to the control point (time < 0.25 hours). It can be seen that during the first 24 hours post-mortem, the ΔC_Q for each of B2m, Actb, Gapdh, Hmbs and Ubc remains on or around zero, indicating no significant reduction in their measured quantity. However, between 24 and 72 hours post-mortem it can be seen that the ΔC_Q for each of these five RNAs rises in an almost linear fashion. The magnitude of increase in ΔC_Q varied between RNAs – with Gapdh exhibiting the most marked reduction in quantity (mean ΔC_Q 5.2, corresponding to an approximately 36.8-fold reduction in Gapdh quantity) and B2m the smallest reduction in quantity (mean ΔC_Q 1.68, corresponding to only a 3.2-fold reduction in B2m quantity). B2m and Actb exhibited very similar decay behaviour, as did Hmbs and Ubc.

A quick visual assessment of the data presented in Figure 5.11B suggests that RNA degradation in this sample set 'kicks in' between 24 and 36 hours. This was confirmed by performing multivariate cluster analysis on this data set, the results of which are demonstrated in the dendrogram in Figure 5.12. Cluster analysis was performed to group the ΔC_Q data into six categories, to estimate the six post-mortem intervals examined. Figure 5.12 clearly demonstrates that the ΔC_Q data for 0, 12, and 24 hours tends to cluster together, with a very strong distinction between this and the ΔC_Qs measured after a post-mortem interval of 36, 48 and 72 hours.

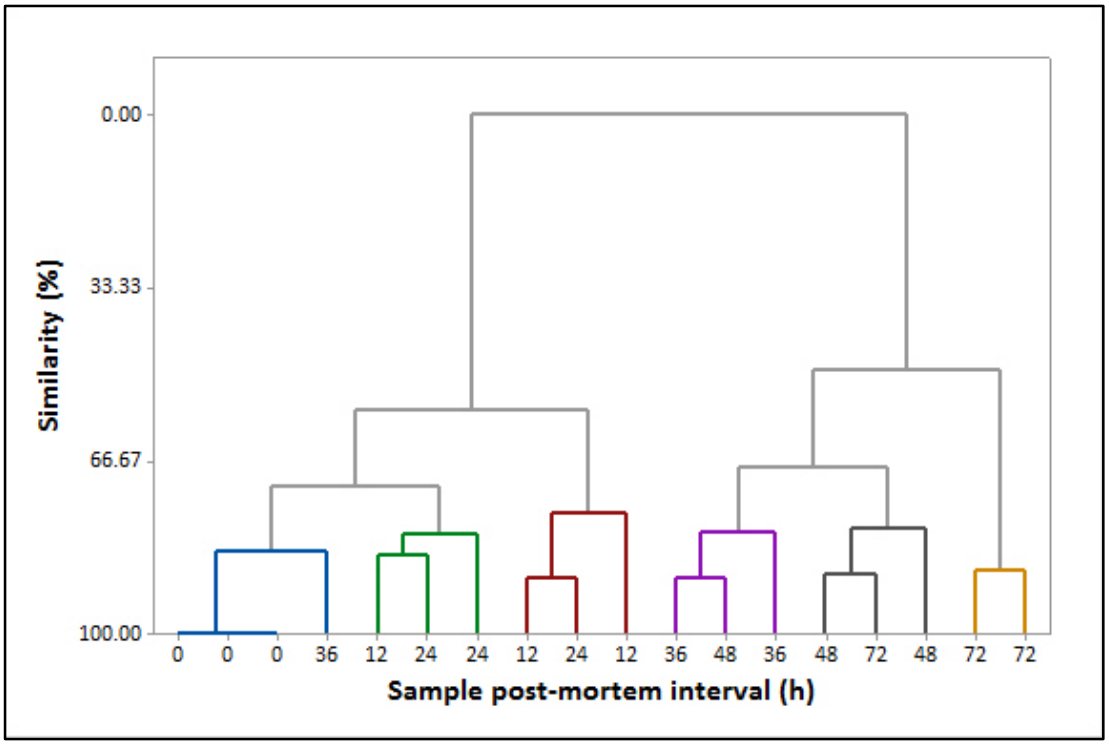

Figure 5.12: **Results of cluster analysis in the form of a dendrogram, describing the similarity of ΔC_Q data for all of 18S rRNA, B2m, Actb, Gapdh, Hmbs and Ubc**. Six post-mortem intervals were examined (0, 12, 24, 36, 48 and 72 hours) for skeletal muscle tissue collected from mice decomposed at 10 °C. Cluster analysis was performed in Minitab v17 using the complete linkage, Euclidean distance method, and six groups to reflect the six post-mortem intervals examined.

18S rRNA exhibited some very unique behaviour in skeletal muscle in the first 36 hours following death. Illustrated by a reduction in C_Q in Figure 5.11A and a marked reduction in ΔC_Q in Figure 5.11B, the measured quantity of 18S rRNA actually increased during this time period. This phenomenon is not unknown, and has been acknowledged in alternative sample types by other authors. Data generated by Anderson *et al*. (28), Alrowaithi *et al*. (243) and Hampson *et al*. (244) illustrates that in blood stains and hair samples, 18S rRNA exhibits an unusually high level of stability. This has been attributed to the protection conferred on 18S rRNA by the protein structure of the ribosome, which acts as a physical barrier against RNases (28). Fleige *et al*. (212) illustrated that ribosomal RNAs were more resistant to artificially-induced degradation in the form of UV-C irradiation, looking at 28S rRNA rather than 18S rRNA.

In addition, Li *et al*. (80) very recently published a similar outcome using rat heart as a post-mortem tissue substrate. They demonstrate a parabolic relationship between 18S rRNA C_Q and post-mortem interval (Figure 1.9, Section 1.3.2.2.1, Chapter 1). Their data suggests that the quantity of detectable 18S rRNA peaks in rat heart at 96 hours post-mortem, after which it starts to decline through degradation. This was proposed to result from proteolysis during the early post-mortem period through the action of endogenous and exogenous (microbial) enzymes causing a breakdown of the ribosome structure. In turn, this improves 18S rRNA yield by liberating it during the RNA extraction phase of the experimental workflow. The data presented in Figure 5.11 illustrates similar behaviour of the 18S rRNA in mouse skeletal muscle to that observed by Li *et al*. (80), except that the onset of 18S rRNA degradation was earlier at 24 to 36 hours post-mortem. This is most likely a tissue-type dependent effect. Chapter 6 of this thesis will examine the effect of tissue type on the onset and rate of post-mortem RNA degradation, confirming that RNA degradation is slower and less pronounced in heart tissue relative to skeletal muscle.

Analysis of the expression of 18S rRNA, B2m, Actb, Gapdh, Hmbs and Ubc in the tissues of mice decomposed at 22 °C for up to 72 hours presented similar outcomes, as illustrated in Figure 5.13.

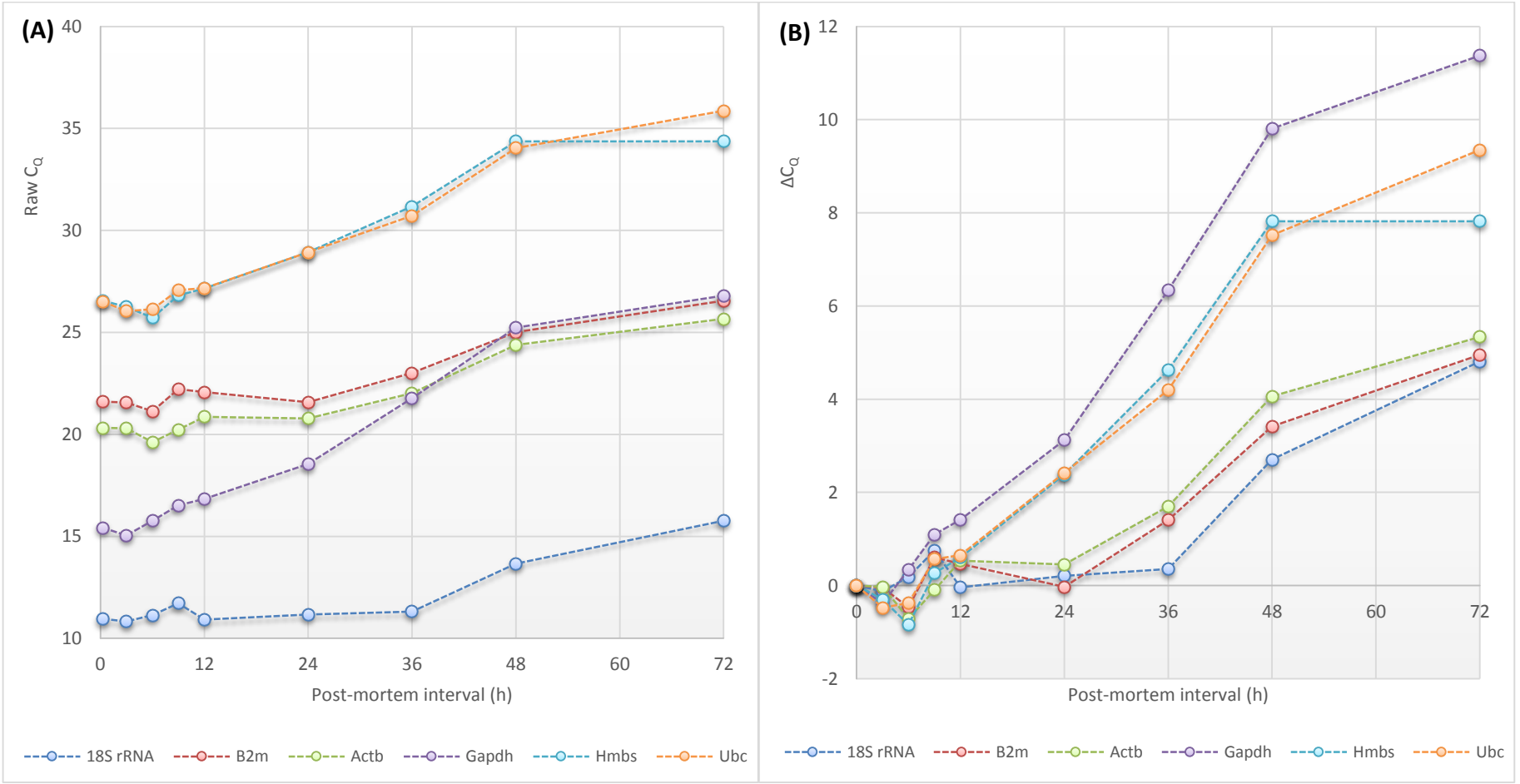

Figure 5.13: **Expression of 18S rRNA, B2m, Actb, Gapdh, Hmbs and Ubc in the skeletal muscle tissue of mice decomposed at an ambient temperature of 22 °C for up to 72 hours.** (A) Describes the raw C_Q data for each of the six endogenous control RNAs. (B) Describes the raw data in the form of a ΔC_Q. Data points represent the mean of n = 3 mice. Error bars have been omitted for clarity.

Figure 5.13 illustrates that in the tissues of mice decomposed at 22 °C, the 'order' of stability for the six analysed RNAs is identical to the 10 °C data set – with 18S rRNA exhibiting the smallest increment in ΔC_Q followed by B2m, Actb, Hmbs, Ubc and lastly Gapdh, exhibiting the poorest level of stability. Over the first 12 hours post-mortem, most of these six RNAs exhibited no substantial increase in ΔC_Q; with the exception of Gapdh. As before, B2m and Actb exhibit a similar degradation profile; degradation manifesting as a visible increase in ΔC_Q between 24 to 36 hours post-mortem. Similarly, Hmbs and Ubc exhibit almost parallel RNA degradation during the first 48 hours, after which Hmbs degradation slows and plateaus.

The key difference in this data set however, lies in the magnitude of increase in ΔC_Q. In the tissue of mice decomposed at 22 °C, the increase in ΔC_Q is much greater than at 10 °C; indicative of more severe degradation. For example, the demonstrated increase in mean Gapdh ΔC_Q over 72 hours at 10 °C of 5.2 (corresponding to an approximately 36.8-fold reduction in Gapdh quantity) is much greater in the tissues of mice decomposed at 22 °C at a mean ΔC_Q of 11.4. This corresponds to an approximately 2,700-fold reduction in the measured quantity of Gapdh over the first 72 hours following death.

The results of multivariate cluster analysis illustrated in Figure 5.14 demonstrate that ΔC_Q data exhibits strong similarity during the first 24 hours post-mortem. In particular, the 0, 3, 6, 9 and 12 hour time points exhibited strong similarity in the magnitude of RNA degradation as measured in terms of the ΔC_Q, and the 24 hour post-mortem interval data points were more loosely clustered alongside. This is most likely due to the strong similarity in 18S rRNA, B2m and Actb ΔC_Q data up to 24 hours post-mortem (Figure 5.13), indicating their stability during this time. The strongest distinction in degradation state is between 24 hours to 36 hours post-mortem, with these exhibiting strong dissimilarity in Figure 5.14. The 36, 48 ad 72 hour ΔC_Q data is well ordered in the dendrogram, indicating the progressive nature of RNA degradation during this time.

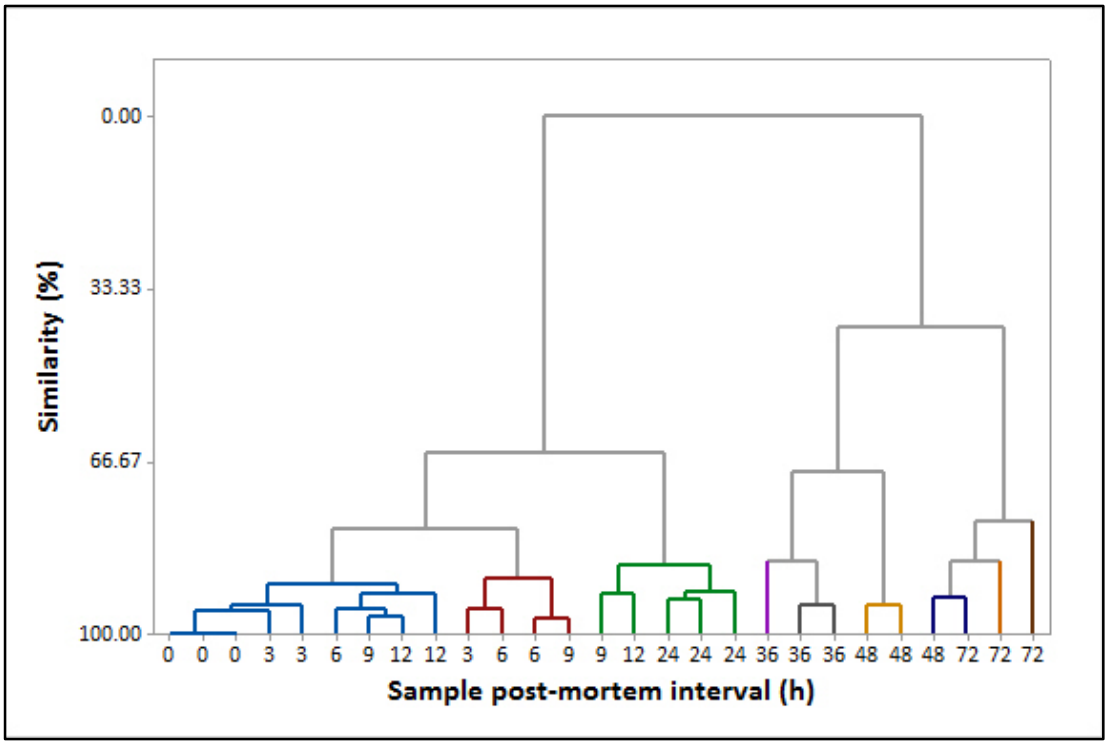

Figure 5.14: **Results of cluster analysis in the form of a dendrogram, describing the similarity of ΔC_Q data for all of 18S rRNA, B2m, Actb, Gapdh, Hmbs and Ubc**. Nine post-mortem intervals were examined (0, 3, 6, 9, 12, 24, 36, 48 and 72 hours) for skeletal muscle tissue collected from mice decomposed at 22 °C. Cluster analysis was performed in Minitab v17 using the complete linkage, Euclidean distance method, and nine groups to reflect the nine post-mortem intervals examined.

Unlike the 10 °C data set, 18S rRNA expression does not increase appreciably in the immediate period following death; rather it remains stable during the first 36 hours post-mortem, after which the ΔC_Q increases as a result of degradation. Following the previous hypothesis that proteolysis liberates 18S rRNA from the ribosome (28) this suggests that during this time, RNA degradation destroys as much RNA as is freed from the ribosome and its quantity remains unchanged.

As expected, accelerating decomposition by placing the corpses at 30 °C during the post-mortem interval in turn increased the rate of RNA degradation, as illustrated in Figure 5.15. Beyond 3 hours post-mortem, B2m, Actb, Gapdh, Hmbs and Ubc all exhibited a consistent increase in ΔC_Q, indicative of the earlier onset of RNA degradation. 18S rRNA expression was fairly stable over the first 12 hours post-mortem, before it too started to degrade.

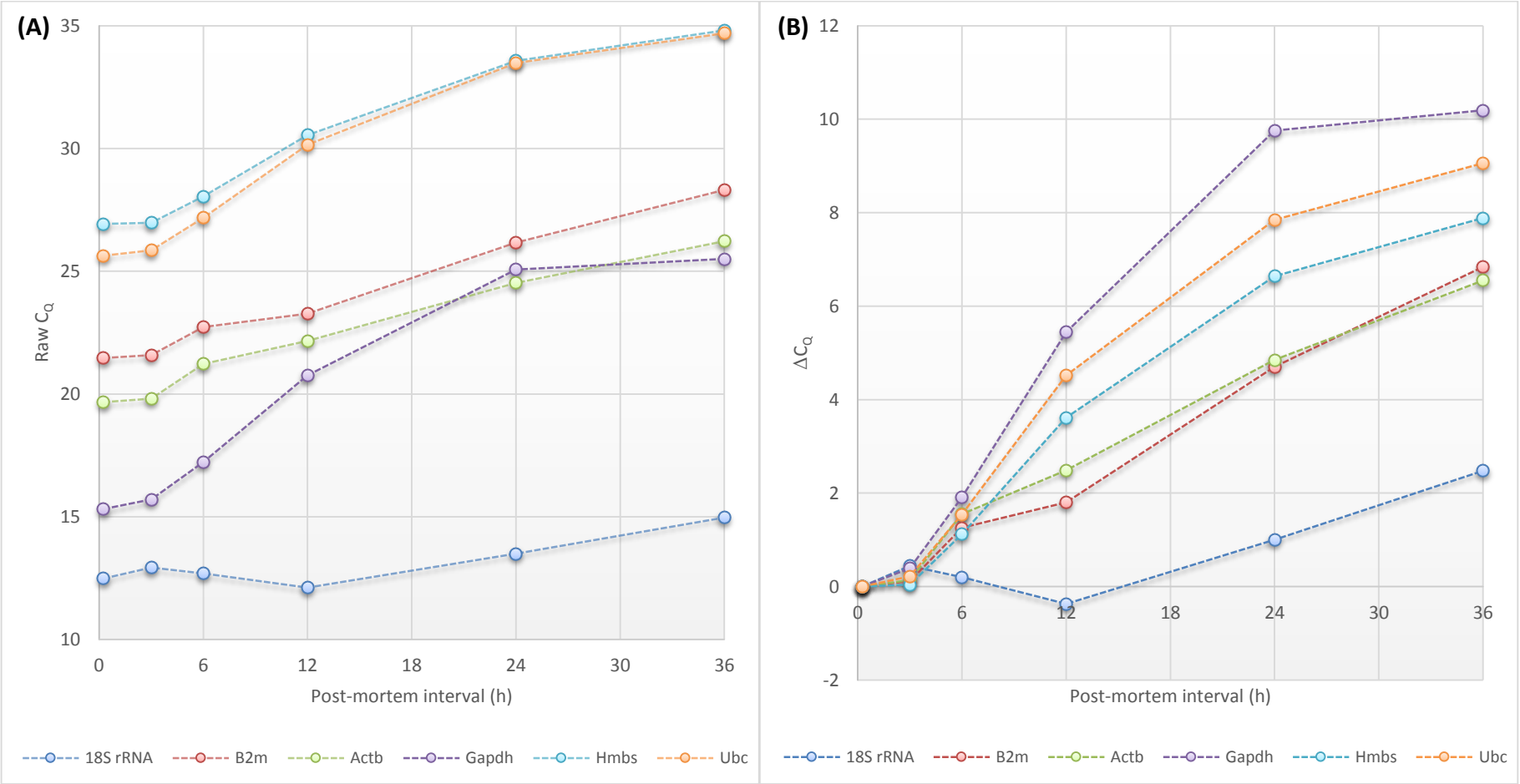

Figure 5.15: **Expression of 18S rRNA, B2m, Actb, Gapdh, Hmbs and Ubc in the skeletal muscle tissue of mice decomposed at an ambient temperature of 30 °C for up to 36 hours.** (A) Describes the raw C_Q data for each of the six endogenous control RNAs. (B) Describes the raw data in the form of a ΔC_Q. Data points represent the mean of n = 3 mice. Error bars have been omitted for clarity.

Comparing the ΔC_Q data presented in Figures 5.13 and 5.15, the magnitude of the reduction in the expression of 18S rRNA, B2m, Actb, Gapdh, Hmbs and Ubc may seem fairly similar. However, it is important to highlight the discrepancy in the total post-mortem interval (x-axis scale) examined at each of 22 and 30 °C – with the latter much shorter in duration. Using Gapdh again as an example, it was observed that Gapdh exhibited a mean ΔC_Q of 11.4 over 72 hours decomposition at 22 °C. In the tissues of mice decomposed at 30 °C, a similar mean ΔC_Q of 10.2 (corresponding to an approximately 1,180-fold reduction in the measurable quantity of Gapdh) is achieved after only 36 hours post-mortem.

The results of multivariate cluster analysis on this data set suggest that the state of RNA degradation (as measured in terms of the ΔC_Q for the six examined RNAs) is similar over the first 6 hours (Figure 5.16). 12 hours post-mortem is fairly well defined in its own cluster with a single 6 hour tissue sample. The distinction between the 24 hour and 36 hour post-mortem interval samples is much less clear, most likely as a result of the apparent plateau in the degree of RNA degradation during this time (Figure 5.15).

The 'order' of stability of the six RNAs examined in this data set again is similar to that at 10 and 22 °C, with the exception of a slight overlap of B2m and Actb as illustrated in Figure 5.15. This demonstrates that even across very different environmental conditions, the six RNAs examined exhibited their own consistent, predictable and reproducible rate of decay which was apparently unaffected by external factors. This is in contrast to the findings of Perez-Novo *et al*. (204), who found that the rank order of stability for a panel of 10 endogenous control RNAs (including B2m, Actb, Gapdh, Hmbs and Ubc) was completely different when compared between intact and degraded clinical specimens of ethmoidal and maxillary sinus samples.

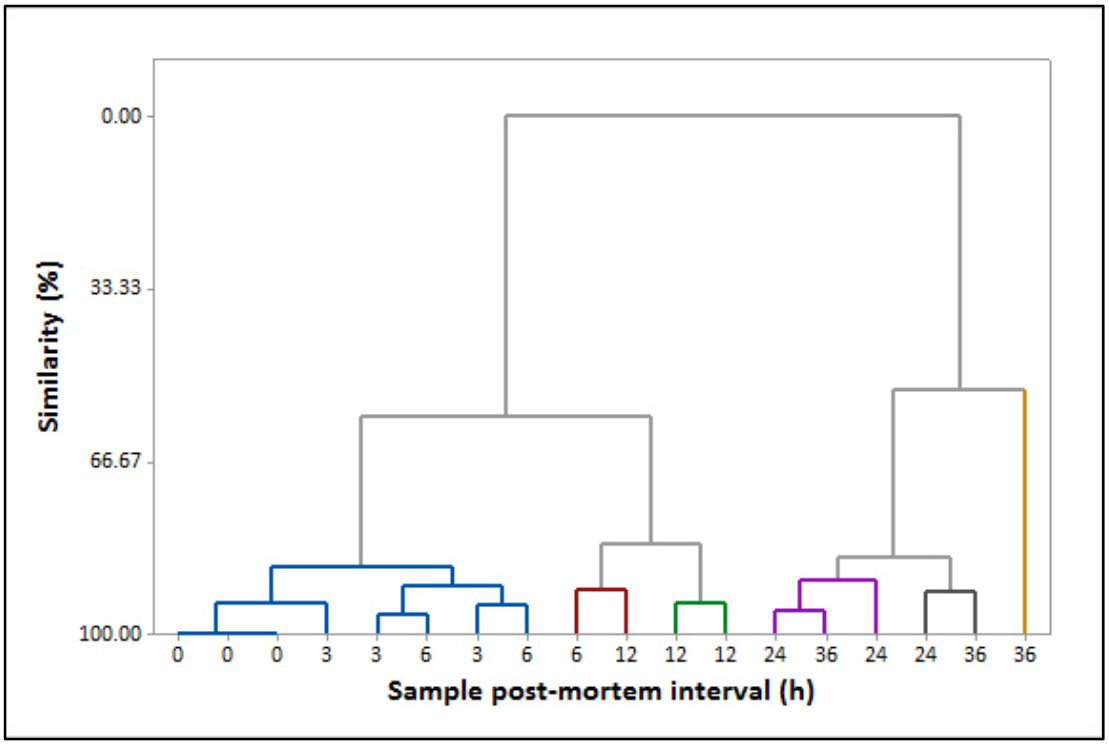

Figure 5.16: **Results of cluster analysis in the form of a dendrogram, describing the similarity of ΔC_Q data for all of 18S rRNA, B2m, Actb, Gapdh, Hmbs and Ubc**. Six post-mortem intervals were examined (0, 3, 6, 9, 12, 24, 36, 48 and 72 hours) for skeletal muscle tissue collected from mice decomposed at 30 °C. Cluster analysis was performed in Minitab v17 using the complete linkage, Euclidean distance method, and six groups to reflect the six post-mortem intervals examined.

What is abundantly clear even from this raw data is that these six RNAs do not degrade at the same rate post-mortem. The following sections will look more closely at the relationship between their expression levels. This work will investigate the implications this differential degradation has upon the selection of appropriate endogenous control RNAs and upon normalisation/interpretation of gene expression data pertaining to post-mortem tissues with an extended time interval between death and sampling.

5.3.4.2 Differential transcript stability of endogenous control RNAs

5.3.4.2.1 geNorm and NormFinder

In future gene expression studies anticipated in forensic pathology, the primary focus is to identify up- or down-regulation of an RNA associated with a particular disease state or cause of death. Endogenous control genes such as 18S rRNA, B2m, Actb, Gapdh, Hmbs and Ubc are used to provide a 'baseline' measurement to remove sampling variation (178) (Section 1.4.5.3, Chapter 1). This is theorised to allow normalisation of RNA quantity input, RNA extraction efficiency, RNA quality and RNA to cDNA reverse transcription efficiency, to identify biological changes in gene expression rather than those induced by experimental procedures (156, 204, 245). In addition, to fulfil this function successfully and obtain biologically meaningful data it is essential that the expression of endogenous control RNAs is unaffected by 'experimental treatments' (160, 179).

A desirable endogenous control RNA is one that is universally expressed (in all nucleated cell types, all of the time) and not induced in response to any physiological or pathological conditions (156, 161, 162). Unstable or variably expressed endogenous controls will introduce novel uncertainty to gene expression data (178), and could cause incorrect identification of an up- or down-regulation of an RNA of clinical or pathological interest (160). However, making this assumption is particularly controversial following the publication of a number of studies illustrating up- or down-regulation of these RNAs in particular cellular conditions (163-166).

In post-mortem analyses which aim to identify pathology associated with the death event, it is obviously desirable that the expression of an endogenous control RNA is unaffected by factors such as: age, gender, diet, environment, ethnicity, disease, administration of pharmacological treatments, cause of death, and post-mortem factors. In the current study, all factors other than post-mortem interval duration and ambient temperature have been controlled. Post-mortem samples are particularly challenging substrates with which to work because degradation of endogenous control RNAs must be managed, and cannot be avoided

(160). As such, this section will discuss which of 18S rRNA, B2m, Actb, Gapdh, Hmbs and Ubc are deemed most applicable for normalisation of gene expression data for tissue samples with an extended time interval between death and sampling.

Various software packages exist to allow assessment of endogenous control RNA expression variability, allowing researchers to select the most stable and uniformly expressed RNAs for normalisation in their particular experimental design. Two of the most commonly referenced software packages for this purpose are geNorm (178) and NormFinder (179). Both permit assessment of the stability level of a panel of potential endogenous control RNAs, identifying:

- The most stably expressed RNAs, either a single RNA or a pair of RNAs
- The optimum number of RNAs which should be used for data normalisation

Essentially, both of these statistical programs are specialist forms of analysis of variance (ANOVA). They look at the variability of raw C_Q data for several putative endogenous control RNAs between replicates and between 'experimental categories' (in this case, different post-mortem intervals), and identify which of the RNAs exhibit the lowest variability (246).

Vandesompele *et al*. (178) developed a gene stability measure called 'M', which is calculated by the geNorm program. geNorm identifies the most stably expressed endogenous control RNA using pair-wise comparisons. Using the raw C_Q data, the expression ratio for all pairings is converted using a logarithmic transformation ($\log_2$) for each sample individually (246). The variability in this ratio is then calculated using a simple standard deviation (178). The M-value denotes the average stability for each pair-wise comparison, and RNAs exhibiting the highest M-value are sequentially excluded from analysis until the user is left with the most stable RNA pair exhibiting the lowest measured M-value. These are deemed to be the most favourable endogenous control RNAs.

Andersen *et al*. (179) followed this up with the NormFinder software in 2004. Using the raw C_Q data, NormFinder calculates a 'global' average gene expression factor to which the expression of all putative endogenous control RNAs

is compared individually (179). After the C_Q data for each individual RNA target has been normalised to this 'global' gene measure, the standard deviation across all samples is calculated (246). In addition, the accumulated standard deviation provides an assessment of the optimum number of endogenous control RNAs to reduce data variability.

5.3.4.2.2 Identification of the most stable endogenous control RNA in post-mortem tissue using geNorm and NormFinder

All raw C_Q data for 18S rRNA, B2m, Actb, Gapdh, Hmbs and Ubc was collated and input to the geNorm software. Data was categorised in accordance with the ambient temperature and post-mortem interval duration for each individual sample. It was found that over the whole data set, Actb and B2m exhibited the most stable pair-wise relationship: as shown in Figure 5.17 with an M-value of 0.69. They were followed by Hmbs (M-value 1.14), Ubc (M-value 1.25), Gapdh (M-value 1.37) and 18S rRNA (M-value 1.58).

As shown in Section 5.3.4.1, the degradation behaviour of B2m and Actb at all of 10 °C (Figure 5.11), 22 °C (Figure 5.13) and 30 °C (Figure 5.15) was almost identical. In all three graphs, B2m and Actb were shown to exhibit a parallel reduction in RNA template quantity with increasing post-mortem interval, measured in terms of their ΔC_Q. This uniform decay behaviour is confirmed in Figure 5.18, which illustrates their relative expression level in terms of the $2^{-\Delta\Delta CQ}$ (B2m – Actb). Throughout the 72 hour post-mortem for which data is presented, the mean fold change in their expression level never exceeds 2. This indicates no biologically significant change in their relative expression, suggesting that the two degrade at an almost identical rate.

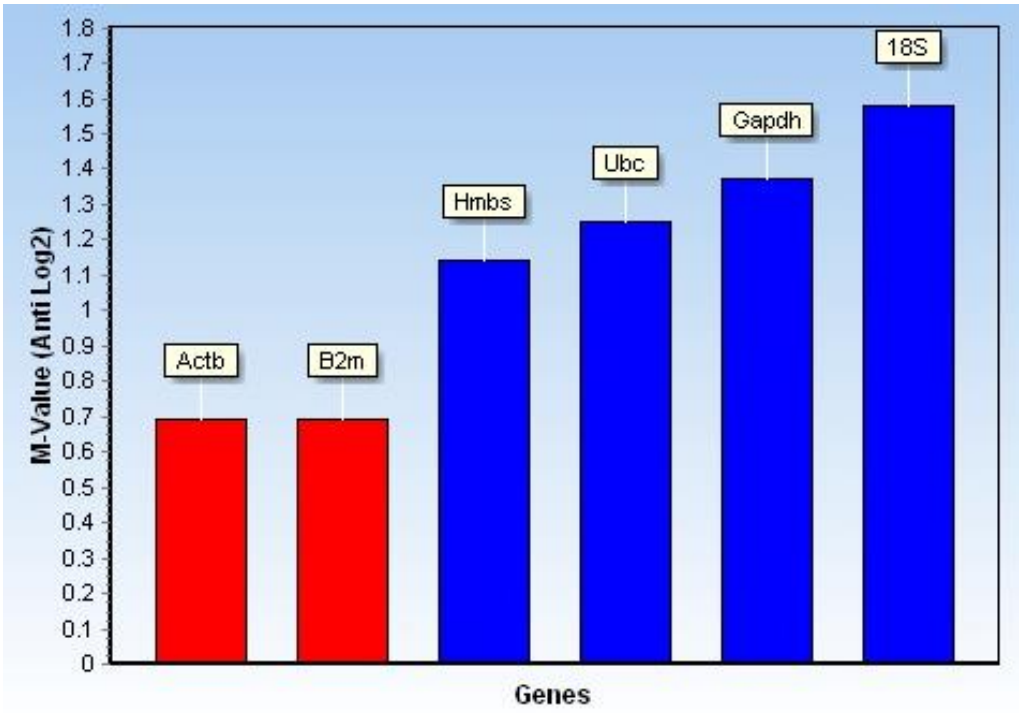

Figure 5.17: **Identification of the two most stable endogenous control RNAs across all mouse post-mortem skeletal muscle data using geNorm**. Actb and B2m were identified as the most stable RNA pair, exhibiting the lowest M-value.

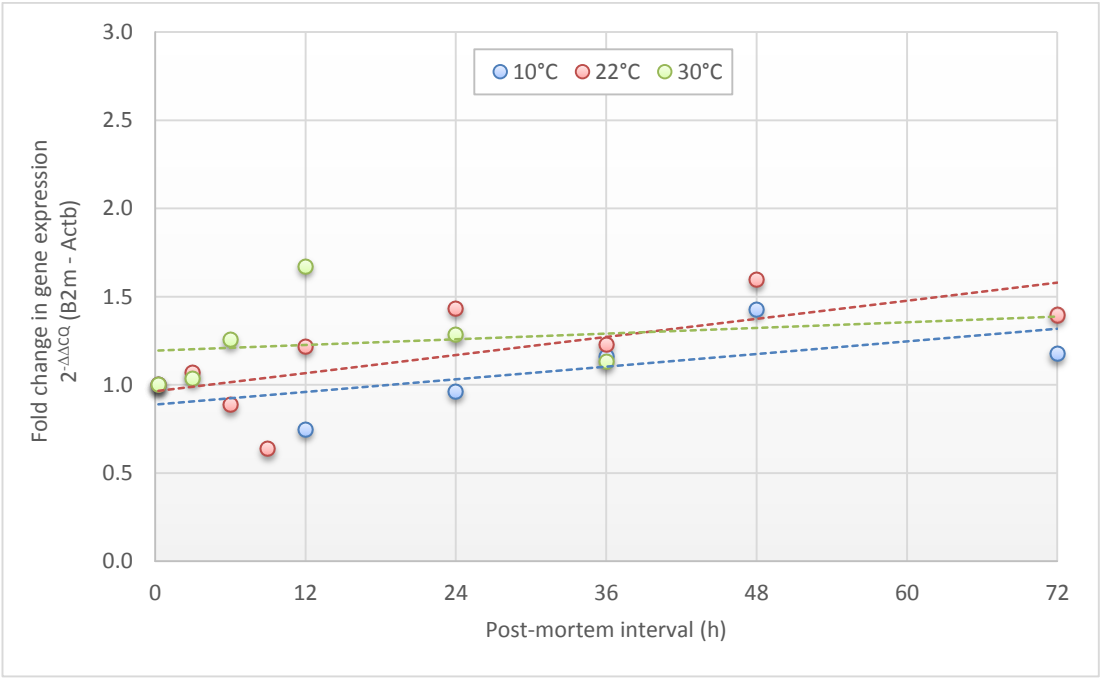

Figure 5.18: **Relative expression relationship for B2m and Actb in the skeletal muscle tissue of mice.** Mice were decomposed for up to 72 hours at 10 °C (blue data points), 22 °C (red data points) and 30 °C (green data points). Relative expression was calculated using the $2^{-\Delta\Delta CQ}$ (B2m – Actb). All data points represent the mean of n = 3. Error bars have been omitted for clarity.

Hmbs and Ubc were ranked as having an intermediary stability level, and Gapdh a very poor stability level. This concurs with the raw data presented in Section 5.3.4.1. Gapdh consistently exhibited the largest reduction in template quantity over a 72 hour post-mortem interval, followed closely by Ubc and then Hmbs (Figures 5.11, 5.13 and 5.15).

Surprisingly, 18S rRNA was deemed to have the most unstable expression level post-mortem. According to the raw data presented in Section 5.3.4.1, 18S rRNA consistently exhibited the lowest reduction in expression with progressing post-mortem interval – with a mean ΔC_Q of 0.22 (Figure 5.11), 4.81 (Figure 5.13) and 2.48 (Figure 5.15) over the maximum time period examined at each of 10, 22 and 30 °C. As such, its perceived instability was unexpected. However, the geNorm (and NormFinder) software is not designed to specifically identify the down-regulation of RNA expression, caused here by post-mortem degradation. It also identifies up-regulation of endogenous control RNA expression, for example caused by disease or drug administration in clinical samples. Throughout this experimentation it is assumed that after death, cellular depletion of ATP and other essential resources/nutrients causes cessation of novel RNA transcription, and that the apparently higher relative quantity of 18S rRNA is an artefact of its improved stability rather than *de novo* synthesis (28). It is reasonable to conclude that this unusually high stability of 18S rRNA in tissues is perceived as an up-regulation in its expression by the software. This makes 18S rRNA 'stick out' as exhibiting very different expression behaviour relative to all of the other mRNAs examined simultaneously.

The rank order of stability of 18S rRNA, B2m, Actb, Gapdh, Hmbs and Ubc was somewhat similar when examined using the NormFinder software. Again, Actb came out on top, with a standard deviation of 0.66 as illustrated in Figure 5.19A. Unexpectedly, Hmbs was deemed next most stable (StDev 0.68), followed by B2m (StDev 0.91), Ubc (StDev 0.93), Gapdh (StDev 1.66) and lastly 18S rRNA (StDev 1.85). The reason for this switch is unknown, but could stem from the central position of Actb and Hmbs in the stability order determined from the raw ΔC_Q data presented in Section 5.3.4.1.

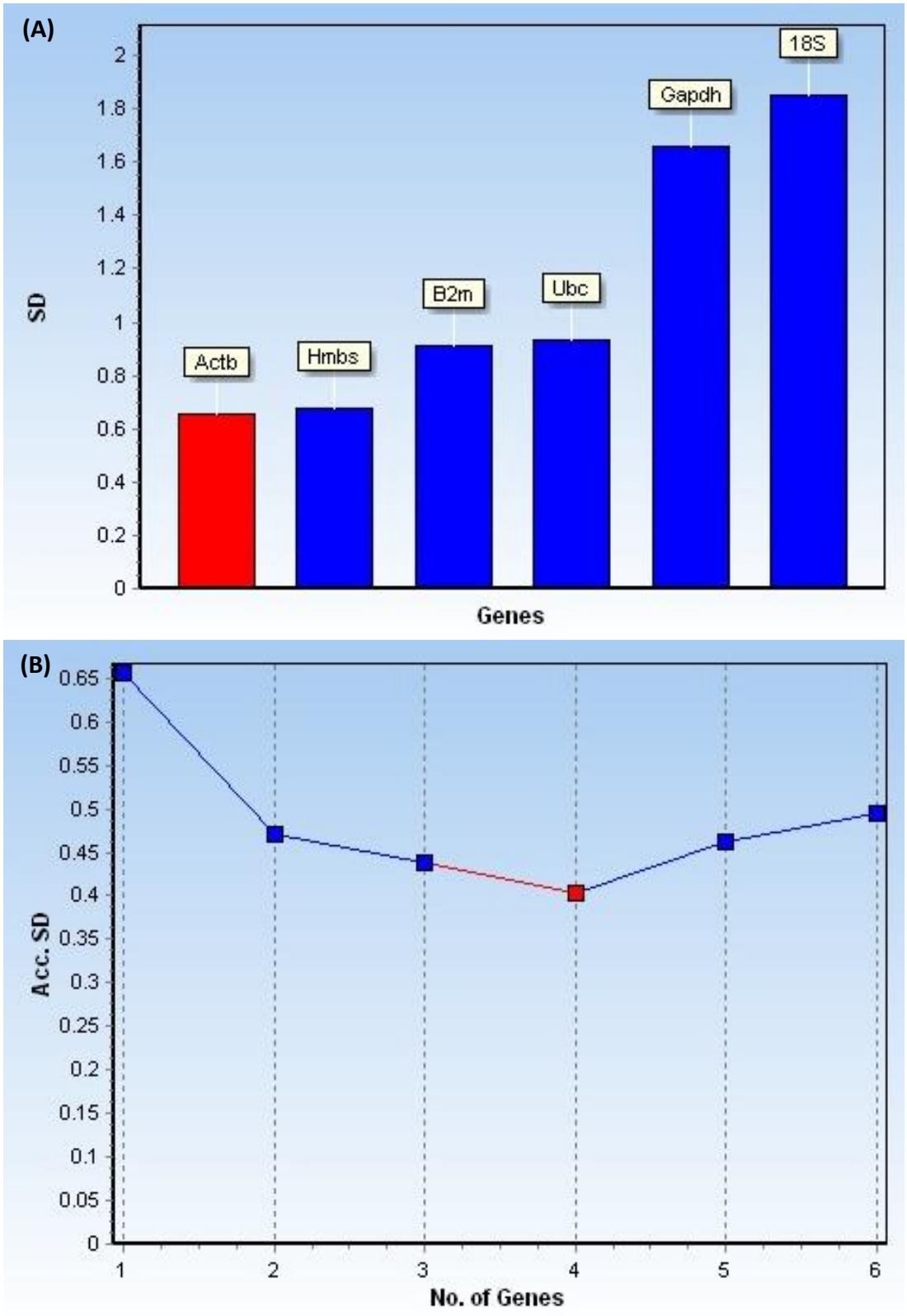

Figure 5.19: **Identification of the most stable endogenous control RNA across all post-mortem skeletal muscle data using NormFinder**. (A) Actb was identified as the most stable RNA, exhibiting the lowest standard deviation in expression. (B) The use of 4 RNAs (Actb, Hmbs, B2m and Ubc) was suggested for optimal normalisation of target RNA data. The strong variability in 18S rRNA and Gapdh expression made their inclusion as endogenous controls detrimental.

The scale of the standard deviation data presented in Figure 5.19A represents the variability of C_Q data in terms of the number of cycles (246). Even for technical replicates, the variability of C_Q is almost never less than 0.1 (246). Variability in this data is much higher than might be expected during gene expression analyses. This stems from the compromised quality of post-mortem RNA samples. This is especially true for the most degraded samples processed (with the longest post-mortem intervals), as stochastic effects during qPCR become apparent when working close to the sensitivity of these qPCR assays. This is known as the 'Monte Carlo' effect, and the scattering of C_Q values is caused by the reduced probability of primer annealing in the early stages of qPCR when the template cDNA quantity is very low (134, 247).

As illustrated in Figure 5.19B, NormFinder deemed the optimum number of endogenous control RNAs to be four – Actb, Hmbs, B2m and Ubc. The accumulated standard deviation in gene expression reduced from 0.66 with just Actb, to 0.47 including Hmbs, 0.44 including B2m and 0.40 including Ubc (Figure 5.19B). The addition of Gapdh and 18S rRNA incorporated more variability into the 'global' normalisation factor. As such, their use as endogenous control RNAs is discouraged, due to their unusual post-mortem decay behaviour – 18S rRNA being exceptionally stable, and Gapdh remarkably prone to degradation.

Overall, the outcomes of the geNorm and NormFinder analyses suggest that Actb consistently performs best as a potential endogenous control RNA for post-mortem analyses. It exhibits an intermediary level of degradation (Section 5.3.4.1), which is more representative of the expression of the RNA panel. However, several issues have already been highlighted in the literature with the use of Actb as an endogenous control RNA in clinical studies. Previous research has demonstrated altered Actb expression in response to hormonal exposure (248), viral infection (249), hyperglycaemia (250), dietary intake (251), hypoxia (163), exercise (252), asthma (253), Alzheimer's disease (254), heart disease (255) and cancer (256, 257). Some of these, particularly the altered expression of Actb in human tissues exposed to hypoxia, are concerning for the use of Actb as an endogenous control gene in forensic pathological analyses.

This outcome concurs with the findings of Bahar *et al*. (85), who found Actb to be the most stably expressed endogenous control RNA in bovine skeletal muscle (of post-mortem interval up to 22 days) using the geNorm and NormFinder softwares. Similarly, Heinrich *et al*. (72) demonstrated that in human brain tissue collected at autopsy (of post-mortem interval up to 118 hours), ACTB and B2M RNAs exhibited the lowest variability in raw C_Q values and UBC the highest.

In a more comprehensive study, Koppelkamm *et al*. (160) examined the rank order of stability (using geNorm) of ten commonly used endogenous control RNAs in human tissues collected during a post-mortem examination – brain, skeletal muscle and heart tissue. This included the six RNAs examined here, for which they found the following order from least to most stable: 18S rRNA, Gapdh, Actb, Ubc, Hmbs and B2m. Of the ten potential control RNAs they examined, 18S rRNA and Gapdh came out as the most poorly stable in both skeletal muscle and heart tissue. This concurs with the outcomes of this study, which has also demonstrated 18S rRNA and Gapdh to be the two most unsuitable RNAs for normalisation purposes. Koppelkamm *et al*. instead found B2m to be consistently one of the most stable RNAs, rather than Actb as the outcomes of this study suggest.

Koppelkamm *et al*. (160) were not able to provide any assessment as to why 18S rRNA and Gapdh consistently performed poorly as potential endogenous control RNAs, according to the geNorm software. The human tissue samples used in their study were heterogeneous with regard to factors such as age, gender, cause of death, etc. In addition, no control samples (collected at the time of death) were available for comparison purposes; a significant limitation for work of this kind on human tissue substrates. As such, RNA expression was examined in individual, unmatched samples; not 'tracked' as has been achieved here. This study has identified why Gapdh and 18S rRNA exhibit particularly unique post-mortem behaviour – because Gapdh exhibits extreme instability, whereas 18S rRNA is very resistant against degradation.

5.3.4.2.3 Differential transcript degradation

Using the $2^{-\Delta\Delta CQ}$ calculation of Livak *et al*. (161), it was possible to highlight the magnitude of difference in the degradation rates of 18S rRNA, B2m, Actb, Gapdh, Hmbs and Ubc. The $2^{-\Delta\Delta CQ}$ provides a measure of the fold-change in expression of two RNAs across two experimental 'groups'. Traditionally, it has been used for normalisation purposes when a single endogenous control RNA is to be used to calculate the fold up-regulation or down-regulation of an RNA of diagnostic interest. In this study, the two compared experimental 'groups' are the control tissue sample (collected within 15 minutes of death) and each post-mortem interval time point. Computation of the $2^{-\Delta\Delta CQ}$ for two gene products has been presented in Section 1.4.5.3, Chapter 1, and thus will not be discussed further.

Based on the raw C_Q data presented in Figures 5.11, 5.13 and 5.15 (Section 5.3.4.1) the following rank order of stability of the endogenous control RNAs is suggested from most to least stable: 18S rRNA, B2m, Actb, Hmbs, Ubc and Gapdh. As such, the magnitude of difference between 18S rRNA and Gapdh expression should provide the highest fold-change as expressed by the $2^{-\Delta\Delta CQ}$ (18S rRNA – Gapdh). Note that throughout this thesis, $2^{-\Delta\Delta CQ}$ is always calculated using the C_Q data for the most unstable RNA subtracted from that of the most stable RNA. This generates $2^{-\Delta\Delta CQ}$ values which rise rather than fall into decimal values, improving the ease of interpretation at a glance.

Figure 5.20 shows that the fold-change in the relative expression of 18S rRNA and Gapdh after some post-mortem intervals was vast. Figure 5.20 presents the mean $2^{-\Delta\Delta CQ}$ (18S rRNA – Gapdh) for skeletal muscle tissue samples excised from mice decomposed at 10, 22 and 30 °C for up to a maximum 72 hours. It can be seen that the magnitude of fold-change, as expected, is strongly affected by both post-mortem interval duration and the ambient temperature conditions.

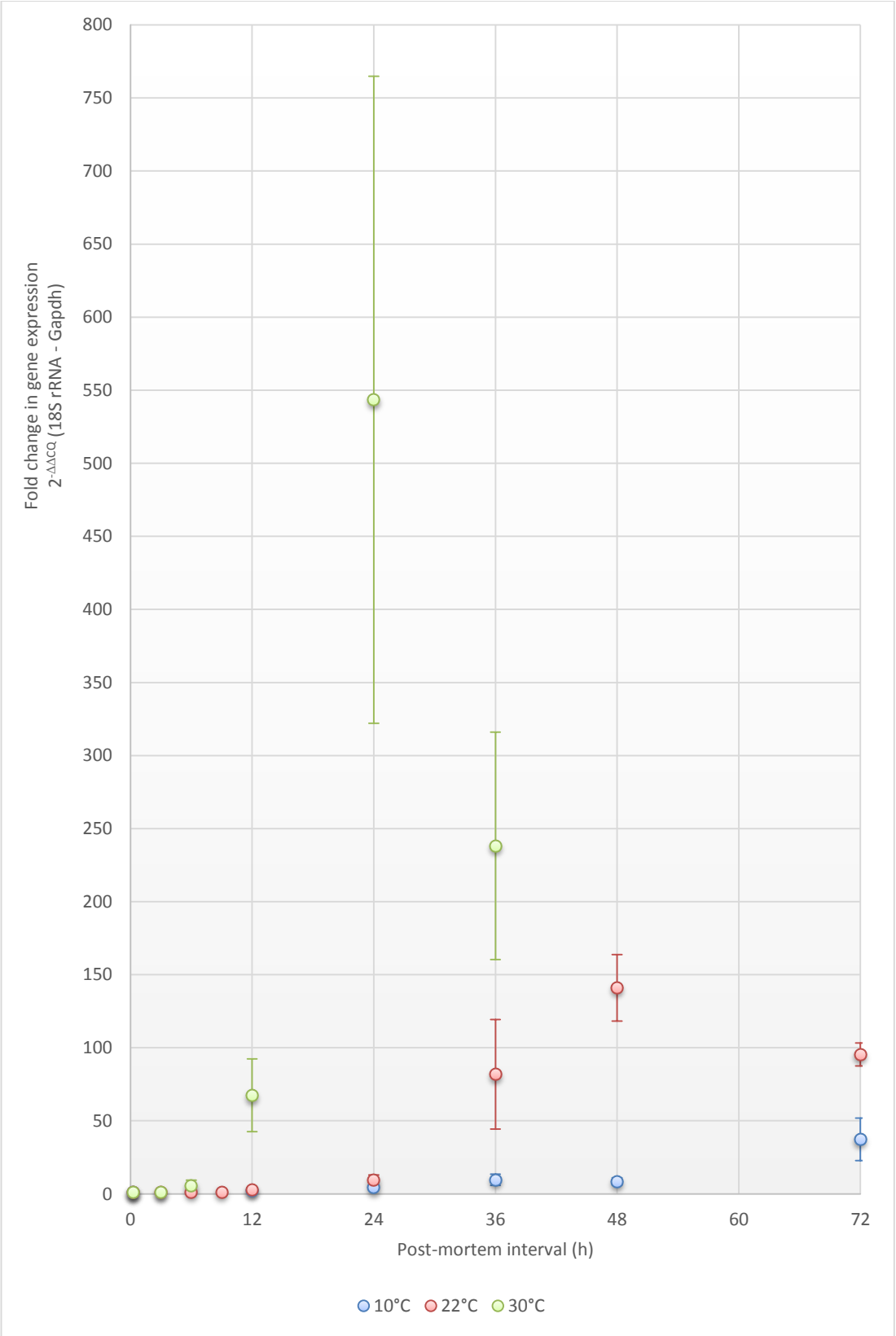

Figure 5.20: **Relative expression relationship for 18S rRNA and Gapdh in the skeletal muscle tissue of mice.** Mice were decomposed for up to 72 hours at 10 °C (blue data points), 22 °C (red data points) and 30 °C (green data points). Relative expression was calculated using the $2^{-\Delta\Delta CQ}$ (18S rRNA – Gapdh). All data points represent the mean of n = 3 ± S.E.

In the tissues of mice decomposed at 10 °C, mean $2^{-\Delta\Delta CQ}$ (18S rRNA – Gapdh) rises only minimally through the first 24 hours, up to a 4.26-fold increase in the quantity of 18S rRNA relative to Gapdh. After this point the mean $2^{-\Delta\Delta CQ}$ rises steadily, reaching its maximum after 72 hours at 37.34. In the tissues of mice decomposed at 22 and 30 °C however, the increase in $2^{-\Delta\Delta CQ}$ (18S rRNA – Gapdh) is not gradual but reaches a 'peak', after which it plateaus and begins to reverse. In the tissues of mice decomposed at 22 °C, this peak is reached after 48 hours when the mean $2^{-\Delta\Delta CQ}$ indicates a 141.01-fold reduction in the quantity of Gapdh relative to 18S rRNA. This peak is earlier still in the tissues of mice decomposed at 30 °C, where at 24 hours the $2^{-\Delta\Delta CQ}$ indicates a 543.42-fold reduction in Gapdh quantity.

Clearly, the relationship between 18S rRNA and Gapdh expression is not linear, but follows a partially sigmoidal profile where little preferential degradation happens in the first few hours, followed by a period of rapid change in the $2^{-\Delta\Delta CQ}$ and a subsequent plateau/reversal. Although this section only presents the $2^{-\Delta\Delta CQ}$ data for a small number of interesting RNA pairings (the whole set of $2^{-\Delta\Delta CQ}$ data for all RNA pairings and post-mortem intervals has been included in Appendix 3, Table 3.1), this sigmoidal shaped profile is representative of almost all of the data generated. This is in stark contrast to the findings of Sampaio-Silva *et al*. (6), who illustrate a linear expression relationship between Rps29 expression and that of Actb, Gapdh, Ppia, Srp72, Alb and Cyp2E1 in mouse skeletal muscle and liver tissue (presented previously in Figure 1.8, Section 1.3.2.2.1, Chapter 1). This study however, has several inherent limitations. Their stability assessment was limited only to the first 11 hours post-mortem, in tissues excised from the mouse and decomposed *ex vivo*, and only at room temperature. Therefore, the outcomes of this work provide a much more thorough examination of tissue RNA degradation behaviour: in a more natural setting (decomposed in an intact corpse) and over a significantly longer and more variable post-mortem interval duration.

When Gapdh expression was normalised to that of B2m and Actb by means of the $2^{-\Delta\Delta CQ}$ the degradation profile followed a very similar trend as illustrated in Figures 5.21A and 5.21B, albeit with a slightly reduced magnitude of fold-change in relative expression.

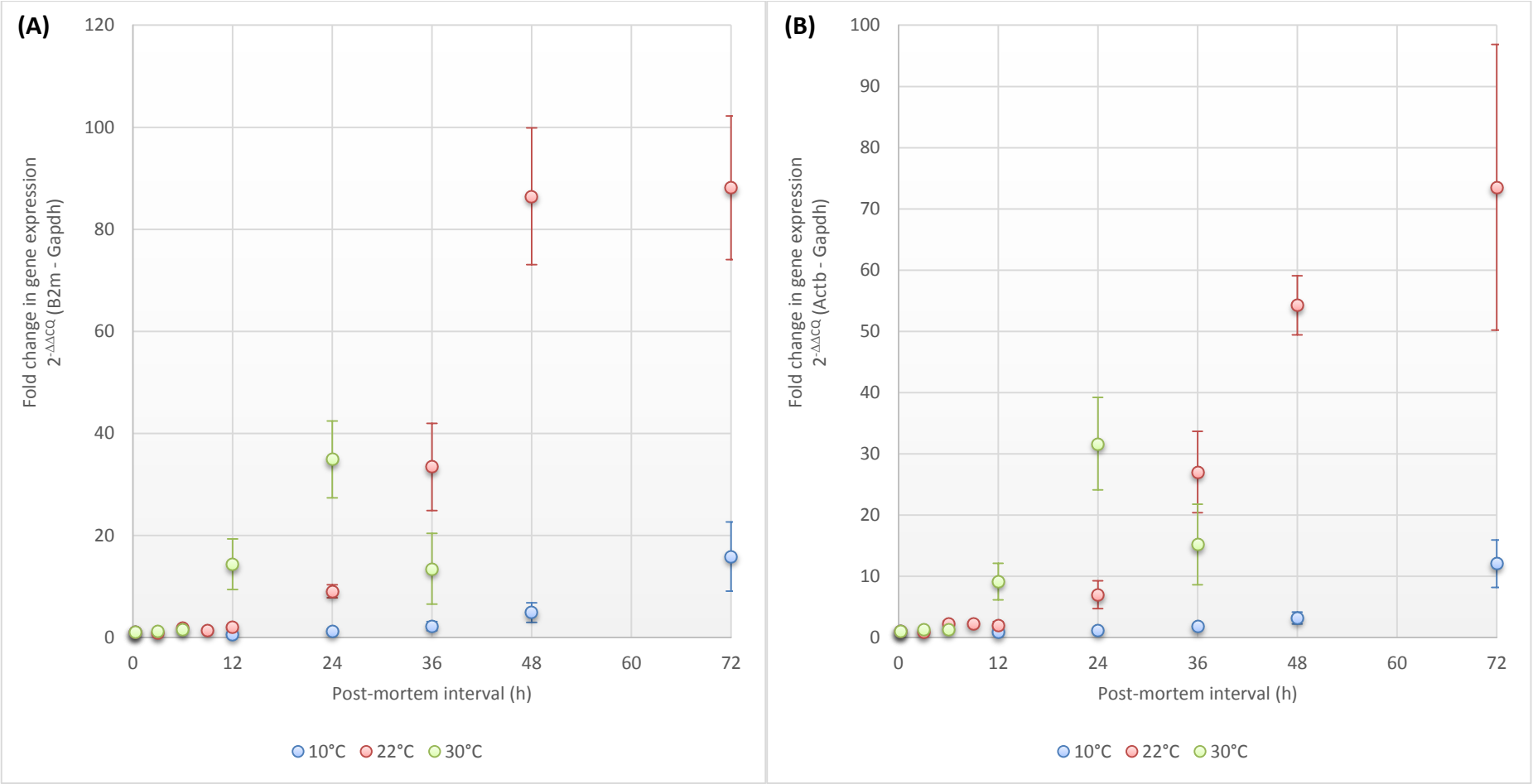

Figure 5.21: **Relative expression relationship for (A) B2m and Gapdh and (B) Actb and Gapdh in the skeletal muscle tissue of mice.** Mice were decomposed for up to 72 hours at 10 °C (blue data points), 22 °C (red data points) and 30 °C (green data points). Relative expression was calculated using the $2^{-\Delta\Delta CQ}$ (B2m - Gapdh) and $2^{-\Delta\Delta CQ}$ (Actb - Gapdh). All data points represent the mean of n = 3 ± S.E.

Figures 5.21A and 5.21B illustrate that the mean $2^{-\Delta\Delta CQ}$ (B2m – Gapdh) and $2^{-\Delta\Delta CQ}$ (Actb – Gapdh) again exhibit a small and steady increment in the tissues of mice decomposed at 10 °C – up to a maximum mean $2^{-\Delta\Delta CQ}$ (B2m – Gapdh) of 15.87 and $2^{-\Delta\Delta CQ}$ (Actb – Gapdh) of 12.06 after 72 hours post-mortem. The $2^{-\Delta\Delta CQ}$ rises much earlier in the tissues of mice decomposed at 22 and 30 °C, and is more pronounced in magnitude. In the 22 °C data set, mean $2^{-\Delta\Delta CQ}$ (B2m – Gapdh) plateaus out at 88.14 after 72 hours, and rises to $2^{-\Delta\Delta CQ}$ (Actb – Gapdh) at 73.524 after the same time interval. In the 30 °C data set a reversal in the $2^{-\Delta\Delta CQ}$ can be seen as before, where the maximum $2^{-\Delta\Delta CQ}$ (B2m – Gapdh) of 34.88 and $2^{-\Delta\Delta CQ}$ (Actb – Gapdh) of 31.64 exist after 24 hours post-mortem.

The reason for this reversal in $2^{-\Delta\Delta CQ}$ (18S rRNA – Gapdh), $2^{-\Delta\Delta CQ}$ (B2m – Gapdh) and $2^{-\Delta\Delta CQ}$ (Actb – Gapdh) is not immediately clear. This consistent outcome even when the expression of Gapdh is normalised to multiple RNAs suggests that at some point, the rapid degradation of Gapdh is exhausted somehow and the degradation of other RNAs 'catches up'. This may simply be a probabilistic issue, where the chance of contact between a Gapdh mRNA molecule and some enzymatic/chemical agent inducing RNA degradation is reduced when the number of Gapdh molecules has dropped dramatically after these long post-mortem intervals. This could explain why this reversal is most prominent in the more severely degraded samples decomposed at 22 and 30 °C, but not in those mildly degraded RNA samples at 10 °C. Alternatively, it may be an indicator of some altogether unknown physiological factor, dramatically changing the decay behaviour of Gapdh. Similar RNA behaviour was published by Inoue *et al*. (233), who demonstrated that in rat liver, the degradation of Actb, Gapdh and Hprt mRNA proceeds linearly during the first three days post-mortem, after which it plateaus and the rate of RNA degradation slows to a halt between 3 and 7 days where no further degradation was observed.

Section 5.3.4.2.2 identified Actb as potentially being the RNA of choice for endogenous control purposes in post-mortem tissues where an extended time interval between death and sampling is apparent. Figure 5.18 (Section 5.3.4.2.2) demonstrated the remarkably close relationship between B2m and Actb expression

in tissues, even in tissue samples where RNA quality had been severely compromised by degradation. On the other hand, Actb and Gapdh exhibited a very strong fold-change in expression over 72 hours post-mortem (Figure 5.21B). Similarly, Figure 5.22 illustrates that the expression relationship of Actb relative to Hmbs and Ubc is not stable.

In agreement with previous results, the increment in mean $2^{-\Delta\Delta CQ}$ is steady and gradual in the tissues of mice decomposed at 10 °C, peaking after 72 hours post-mortem at a $2^{-\Delta\Delta CQ}$ (Actb – Hmbs) of 2.95 and a $2^{-\Delta\Delta CQ}$ (Actb – Ubc) of 7.12. In the 22 °C data set, mean $2^{-\Delta\Delta CQ}$ (Actb – Hmbs) peaks after 48 hours at 14.20 and then exhibits a reversal. The mean $2^{-\Delta\Delta CQ}$ (Actb – Ubc) instead rises steadily and peaks at 21.58 after 72 hours. In the 30 °C data set a reversal in the $2^{-\Delta\Delta CQ}$ can be seen in both Figure 5.22A and 5.22B, where the maximum $2^{-\Delta\Delta CQ}$ (Actb – Hmbs) of 4.01 and $2^{-\Delta\Delta CQ}$ (Actb – Hmbs) of 10.64 exist after 24 hours post-mortem. In summary, this data demonstrates that Actb mRNA is much less susceptible to degradation than Hmbs and Ubc, and that the relative quantity of Hmbs and Ubc can reduce as much as 14.2 and 21.58-fold relative to that of Actb because of this preferential Hmbs and Ubc degradation.

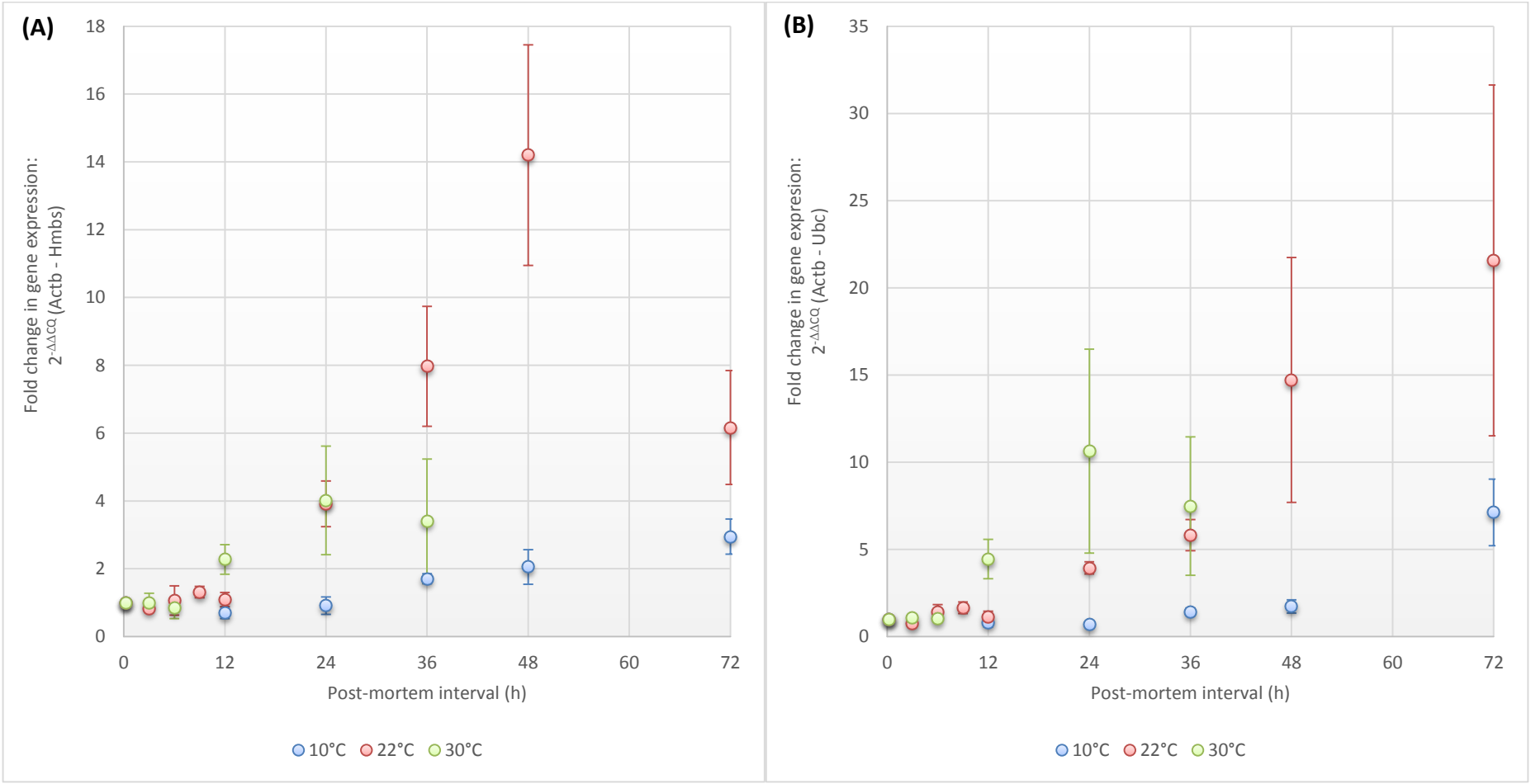

Figure 5.22: **Relative expression relationship for (A) Actb and Hmbs and (B) Actb and Ubc in the skeletal muscle tissue of mice.** Mice were decomposed for up to 72 hours at 10 °C (blue data points), 22 °C (red data points) and 30 °C (green data points). Relative expression was calculated using the $2^{-\Delta\Delta CQ}$ (Actb - Hmbs) and $2^{-\Delta\Delta CQ}$ (Actb - Ubc). All data points represent the mean of n = 3 ± S.E.

In all of the data presented, it is clear that the ambient temperature to which the corpse was exposed has a very profound effect on the rate of RNA degradation; the outcomes of RT-qPCR concurring with the previous RNA integrity number scores (Sections 5.3.3 and 5.3.4.3). This is reflected both in the speed of onset of visible differential degradation between RNAs and in the magnitude of change in the $2^{-\Delta\Delta CQ}$ for each RNA pairing. As one may expect, visible RNA degradation onsets earlier and is more severe in the tissues of mice exposed to warmer conditions, which advances decomposition. This supports the findings of Fontanesi *et al*. (127, 236), Kuliwaba *et al*. (87) and Marchuk *et al*. (86) (Section 5.1.3.3), all of whom have suggested that the refrigeration of animal meat and clinical tissue samples is beneficial for preservation of RNA quality. It has been proposed that by cooling the corpse down during decomposition, this either maintains RNases in an inactive state or keeps them sequestered in intracellular vesicles (87). In addition, both Itani *et al*. (258) and Riggsby *et al*. (259) demonstrated temperature to be a major factor controlling the rate of DNA degradation in post-mortem tissue and bone.

Clearly, the differential stability of RNAs presents a severe interpretational obstacle for tissue samples with an extended time interval between death and sampling. Even amongst these commonly implemented endogenous control RNAs which are perceived to be amongst the most stably expressed in the transcriptome (204), their resistance level to degradation was found to be extremely variable. 18S rRNA seems to be heavily protected against degradation by its structural ribosome shell (28). B2m and Actb exhibited a higher level of survivability than Hmbs and Ubc. Gapdh mRNA was depleted unusually rapidly, across all experimental conditions.

Differential degradation of RNAs in post-mortem tissue is not a completely new concept. Zhao *et al*. (93) identified unusually high stability of EPO mRNA in human tissues, relative to GAPDH. Inoue *et al*. (233) identified more rapid reduction of IL-1β mRNA in rat tissues relative to three endogenous controls, Actb, Gapdh and Hprt. Kuliwaba *et al*. (87) demonstrated preferential degradation of TGFB1 mRNA in human surgical bone specimens, and Pardue *et al*. (234) the

enhanced degradation of Hsp70 mRNA. It is known that *in vivo*, RNAs exhibit their own unique degradation characteristics determined by sequence motifs and their interaction with RNA binding proteins (86). The half-lives of different RNA species are known to vary widely (11). On the whole, inducible RNAs have the shortest half-lives (233). However, post-mortem RNA degradation is poorly understood, and it has been proposed that controlled *in vivo* mechanisms of RNA degradation account only for a small proportion of post-mortem RNA decay (260). For example, a similar degradation rate has been characterised for the highly stable endogenous control RNA cyclophilin, and the labile COX-2 mRNA in human brain (260).

To the author's knowledge, the outcomes of this study represent the first time that differential stability has been demonstrated solely between putative endogenous control RNAs. This poses a serious problem for RT-qPCR data normalisation in post-mortem tissues. As such, thorough assessment of an RNA's degradation behaviour is an absolute prerequisite for their implementation into diagnostic assays in forensic pathology (93). The ideal endogenous control RNA has a degradation rate mirroring that of the diagnostic gene it is designed to normalise (93, 233). If an endogenous control with an unusually high level of post-mortem stability (e.g. 18S rRNA) is used to normalise C_Q data pertaining to a gene of diagnostic interest, this might 'skew' the results to suggest that expression of the diagnostic gene is being biologically suppressed (232). On the contrary, where an endogenous control with a particularly low level of post-mortem stability (e.g. Gapdh) is used to normalise the data from a diagnostic gene, this may again 'skew' the results to suggest a biological up-regulation in its expression where this doesn't exist. It is likely that the use of a single RNA for normalisation purposes will lead to a large margin of error (72). Therefore, it is absolutely crucial that the degradation behaviour of all RNAs in a diagnostic assay (endogenous control RNAs and diagnostic RNAs) is characterised thoroughly prior to its application to degraded RNA samples from post-mortem tissues.

5.3.4.3 Variability in RNA degradation behaviour

Across all of Figures 5.11, 5.13, and 5.15, it is abundantly clear that the variability in $2^{-\Delta\Delta CQ}$ data is very strong between biological replicates. For each chart data was plotted using the mean data obtained from n = 3 mice, with the standard error represented in the error bars. In many instances, the margin for error between replicates was significant. Figure 5.23A below represents the $2^{-\Delta\Delta CQ}$ (18S rRNA – Gapdh) gene expression data for skeletal muscle tissue recovered from mice decomposed at 22 °C only. This duplicates the data presented in Figure 5.13, but demonstrating the $2^{-\Delta\Delta CQ}$ trend for 3 mice individually rather than collectively.

Figure 5.23A demonstrates that the general trend of $2^{-\Delta\Delta CQ}$ (18S rRNA – Gapdh) over the 72 hour post-mortem interval is similar between biological replicates – beginning with a period of little change, followed by a rapid increase in $2^{-\Delta\Delta CQ}$ between 24 to 48 hours and a subsequent plateau/reversal. However, the magnitude of fold-change between the 3 mice – named A, B and C – is substantially different, most notably at the 36 and 48 hour post-mortem interval time points.

To examine more closely the source of this variability, the experiment was repeated using intra-mouse replicates, rather than inter-mouse replicates. The experimental design was identical to that described in Section 5.2.1, other than that every tissue sample excised from the mouse corpse was divided into 3 approximately equal parts – named here AA, AB and AC – prior to RNA extraction. RNA quantity and quality analysis proceeded as before (data for which has been presented in Table 5.6, Section 5.3.3). RT-qPCR data was analysed using the $2^{-\Delta\Delta CQ}$ formula for all pair-wise combinations of 18S rRNA, B2m, Actb, Gapdh, Hmbs and Ubc, the results of which are presented in Table 5.7 alongside those for the inter-mouse replicates.

Figure 5.23B presents the data obtained from three intra-mouse replicates, describing the expression relationship of 18S rRNA and Gapdh. What is clear is that the degradation profiles of multiple tissue samples from the same mouse mirror one another more closely, with less variability in the values for $2^{-\Delta\Delta CQ}$ (18S rRNA – Gapdh) between replicates.

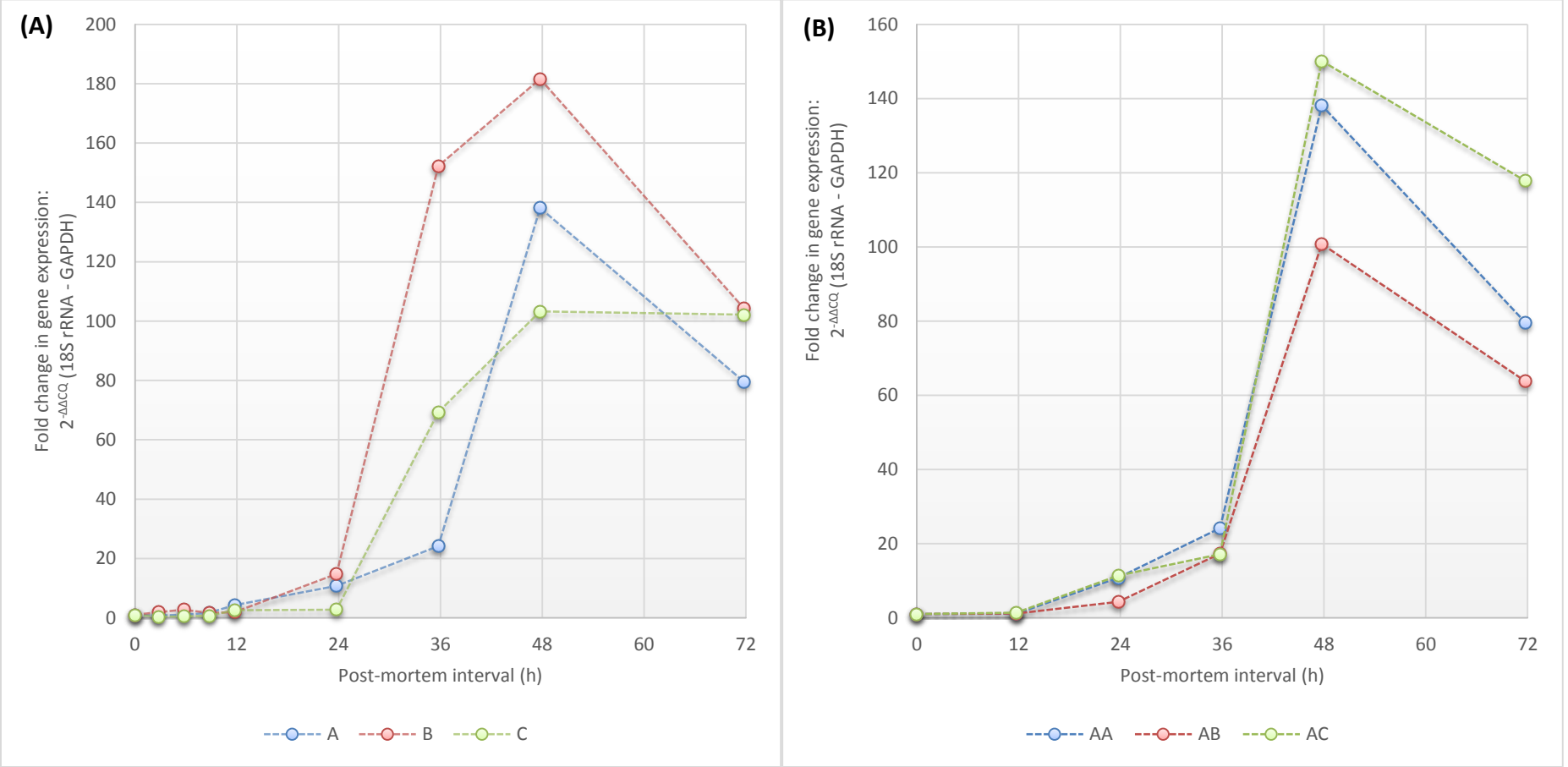

Figure 5.23: (A**) Inter-mouse variation and (B) Intra-mouse variation in the $2^{-\Delta\Delta CQ}$ (18S rRNA – Gapdh) expression relationship**. (A) Represents $2^{-\Delta\Delta CQ}$ data from three mice: A, B and C. (B) Represents $2^{-\Delta\Delta CQ}$ data for three tissue samples from the same mouse: AA, AB and AC. Data was obtained from the skeletal muscle tissue of mice decomposed at 22 °C only.

A similar outcome was observed for most pair-wise comparisons of 18S rRNA, B2m, Actb, Gapdh, Hmbs and Ubc, in that the $2^{-\Delta\Delta CQ}$ variability was much less pronounced when repeatedly sampling from the same mouse. Data to this effect is presented in Table 5.7, which lists the mean $2^{-\Delta\Delta CQ}$ for all RNA pairings and all post-mortem intervals when analysing three tissue samples from different mice (inter-mouse variation) or from the same mouse (intra-mouse variation). The variability in $2^{-\Delta\Delta CQ}$ between replicates is quantified in terms of the coefficient of variation (CV %) (standard deviation/mean x 100). Note that the control point is not presented, because its $2^{-\Delta\Delta CQ}$ is always equal to one.

In the vast majority of cases, the variation in $2^{-\Delta\Delta CQ}$ was substantially lower in replicates from the same mouse. This is presented in bar chart form in Figure 5.24 below for one particular RNA pairing: illustrating the intra- and inter-mouse variation in $2^{-\Delta\Delta CQ}$ (Ubc – Gapdh) in terms of the coefficient of variation.

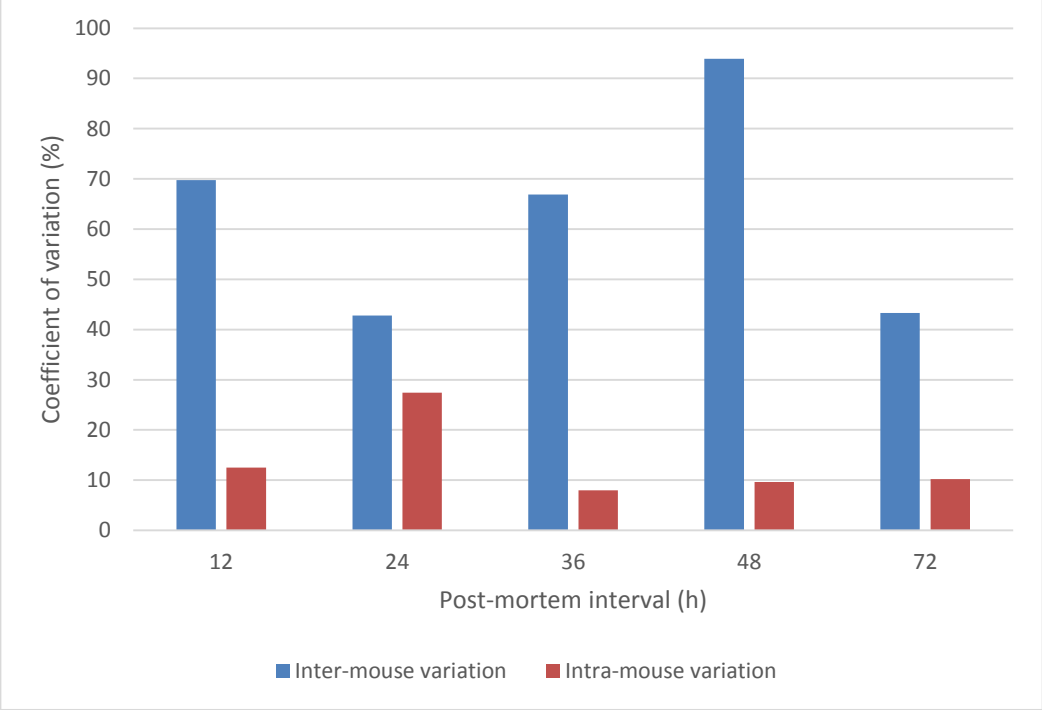

Figure 5.24: **Inter-mouse (blue bars) and intra-mouse (red bars) variability in the fold change in gene expression of Ubc and Gapdh in post-mortem tissue**. Data was plotted as the $2^{-\Delta\Delta CQ}$ (Ubc – Gapdh) and the coefficient of variation calculated using the mean of n = 3, for mice decomposed at 22 °C for up to 72 hours following death.

Table 5.7: **Raw $2^{-\Delta\Delta CQ}$ data for all endogenous control RNA pairings**. Table illustrates the mean $2^{-\Delta\Delta CQ}$ (for n = 3) and coefficient of variation (CV %) describing the variability of gene expression data between mice (inter-mouse variation) and within replicate samples of the same mouse (intra-mouse variation), after decomposition for 72 hours at 22 °C. Lowest CV % marked with an asterisk (*).

		Inter-mouse variation		Intra-mouse variation	
$2^{-\Delta\Delta CQ}$ (Gene 1 – Gene 2)	**Post-mortem interval (h)**	**Mean $2^{-\Delta\Delta CQ}$**	**Coefficient of variation (%)**	**Mean $2^{-\Delta\Delta CQ}$**	**Coefficient of variation (%)**
18S rRNA – B2m	12	1.45	26.25	1.49	24.99*
	24	0.99	54.72	1.04	38.11*
	36	2.23	50.47	1.01	41.15*
	48	1.69	32.44*	1.82	39.50
	72	1.15	36.67*	1.54	52.99
18S rRNA – Actb	12	1.65	54.00	1.41	7.62*
	24	1.34	55.33	1.57	34.67*
	36	2.72	47.73	1.54	13.02*
	48	2.68	35.21*	3.22	39.34
	72	1.71	67.66*	1.57	79.31
18S rRNA – Gapdh	12	2.90	43.26	1.23	13.58*
	24	9.43	65.24	8.84	44.56*
	36	81.90	79.30	19.55	20.47*
	48	141.01	27.85	129.68	19.85*
	72	95.38	14.35*	87.06	31.89
B2m – Actb	12	1.22	70.19	0.97	17.14*
	24	1.43	26.34	1.54	13.45*
	36	1.23	7.95*	1.64	25.62
	48	1.60	24.82	1.84	24.63*
	72	1.40	40.01	0.94	26.69*
B2m – Gapdh	12	1.96	22.24*	0.86	26.60
	24	9.04	24.37	8.33	12.98*
	36	33.43	44.27	20.53	22.06*
	48	86.48	26.87*	76.95	28.25
	72	88.14	27.69*	62.38	35.71
Actb - Gapdh	12	2.02	47.33	0.88	15.46*
	24	7.00	56.16	5.53	27.26*
	36	27.01	42.59	12.72	13.55*
	48	54.24	15.44*	42.45	19.99
	72	73.52	54.94	72.28	54.38*
18S rRNA – Hmbs	12	1.59	22.32	1.41	11.49*
	24	5.18	52.32	6.20	38.52*
	36	20.89	42.69	7.24	41.12*
	48	40.81	68.39	26.12	31.97*
	72	12.08	84.65	4.12	62.65*

		Inter-mouse variation		Intra-mouse variation	
$2^{-\Delta\Delta cq}$ (Gene 1 – Gene 2)	**Post-mortem interval (h)**	**Mean $2^{-\Delta\Delta cq}$**	**Coefficient of variation (%)**	**Mean $2^{-\Delta\Delta cq}$**	**Coefficient of variation (%)**
B2m – Hmbs	12	1.15	37.67	0.97	20.64*
	24	5.33	5.10*	6.03	15.07
	36	9.97	47.13	7.31	23.07*
	48	24.11	65.59	14.94	17.91*
	72	9.65	67.44	2.58	14.75*
Actb - Hmbs	12	1.09	33.68	1.00	8.79*
	24	3.92	29.74	3.99	27.10*
	36	7.97	38.46	4.68	33.22*
	48	14.20	39.70	8.54	33.01*
	72	6.17	47.22	2.83	18.02*
Hmbs – Gapdh	12	1.85	41.07	0.89	24.08*
	24	1.71	25.96	1.39	14.76*
	36	3.60	54.92	2.85	21.10*
	48	4.23	42.00	5.14	18.25*
	72	18.10	110.42	25.50	52.99*
18S rRNA – Ubc	12	1.68	35.32	1.14	11.85*
	24	5.09	46.04*	7.35	65.55
	36	14.56	20.73	9.43	16.98*
	48	31.80	52.08	37.05	27.69*
	72	23.98	28.04*	27.15	32.95
B2m – Ubc	12	1.26	53.82	0.79	15.59*
	24	5.53	20.51*	6.73	45.78
	36	7.18	30.98	9.95	21.50*
	48	21.31	77.20	21.65	25.32*
	72	23.81	50.54	19.84	46.45*
Actb – Ubc	12	1.16	45.87	0.81	7.21*
	24	3.94	15.27*	4.60	60.35
	36	5.82	26.58	6.31	6.46*
	48	14.71	82.64	11.86	11.23*
	72	21.58	80.77	23.16	64.36*
Ubc – Gapdh	12	1.96	69.78	1.08	12.48*
	24	1.73	42.82	1.35	27.41*
	36	5.20	66.91	2.07	8.00*
	48	6.55	93.94	3.55	9.62*
	72	4.32	43.29	3.24	10.19*
Hmbs – Ubc	12	1.06	23.91	0.82	16.50*
	24	1.04	16.63*	1.10	33.70
	36	0.77	32.44	1.40	29.33*
	48	1.31	95.97	1.46	23.70*
	72	5.77	127.67	8.20	63.62*

Overall, the data suggests that RNA degradation behaviour is more predictable and less subject to variability in multiple tissue samples from the same animal, compared with tissue samples from different animals. Between individuals, the general trend of the data is similar but the magnitude of change in $2^{-\Delta\Delta CQ}$ is much less predictable. This indicates that RNA decay behaviour in skeletal muscle may be subject to external influences such as from other tissue types and organ systems, and is unique to each individual.

It has been noted (Section 5.3.1) that the macroscopic decomposition characteristics of mice used in this study did not progress identically over the course of the post-mortem interval. Some exhibited more severe characteristics than others, such as: green skin discolouration, hair loss, skin slippage, *rigor mortis*, gaseous abdominal distension and leakage of the gastrointestinal contents. This could be due to inter-mouse differences in the rate of autolysis (breakdown of tissue structure by intracellular enzymes such as proteases, lipases and amylases) and putrefaction (colonisation and spread of bacteria, fungi and protozoans) (261). Irrespective of the potential cause, this work suggests that there is a strong element of unpredictability in post-mortem RNA decay behaviour between individuals which is rather concerning for future diagnostic application of gene expression analysis.

5.3.5 Characterising the relationship between RNA quality and qPCR performance

In the previous sections, the degradation behaviour of RNA has been assessed in tissues from three perspectives: total RNA quantity (UV-visible spectrophotometry), total RNA quality (Bioanalyzer 2100) and the expression of a panel of six endogenous control RNAs (RT-qPCR). However, for diagnostic analyses in forensic pathology the technique of primary interest is RT-qPCR. This allows characterisation of the up- or down-regulation of genes of pathological interest. Total RNA quantification and quality analysis are used as screening indicators, to identify samples which are suitable for RT-qPCR and which should be analysed with caution or even discarded.

In particular, the measured RNA integrity number (RIN) of a tissue RNA sample is used to identify whether the results of RT-qPCR are likely to be compromised by RNA fragmentation. Although the manufacturer stipulates no minimum 'cut off' RIN below which samples are deemed too fragmented for further analysis, several thresholds have been suggested in the literature. Weis *et al*. (138) suggested an optimum minimum RIN of 3.95, prior to further analysis by microarrays. Fleige *et al*. on the other hand, suggested the higher RIN 5 as being a more appropriate minimum threshold where gene expression analysis is to be performed by RT-PCR (212).

When working with post-mortem tissue samples, it is impossible to obtain pristine, high quality RNA samples with which to work. Therefore, it is important to understand after what point post-mortem RNA fragmentation is likely to compromise the reliability and reproducibility of gene expression data. This section aims to ascertain whether a relationship exists between RIN and the results of RT-qPCR, and whether RIN can be used as a predictor of the credibility of C_Q data.

Figure 5.25 presents the collated data from all mouse skeletal muscle tissue samples used in this study, describing the relationship between total RNA integrity and the fold-reduction (ΔC_Q) in the measured quantity of each RNA: 18S rRNA, B2m, Actb, Gapdh, Hmbs and Ubc. A strong relationship exists between the two features, with the lowest RNA integrities associated with the largest ΔC_Q.

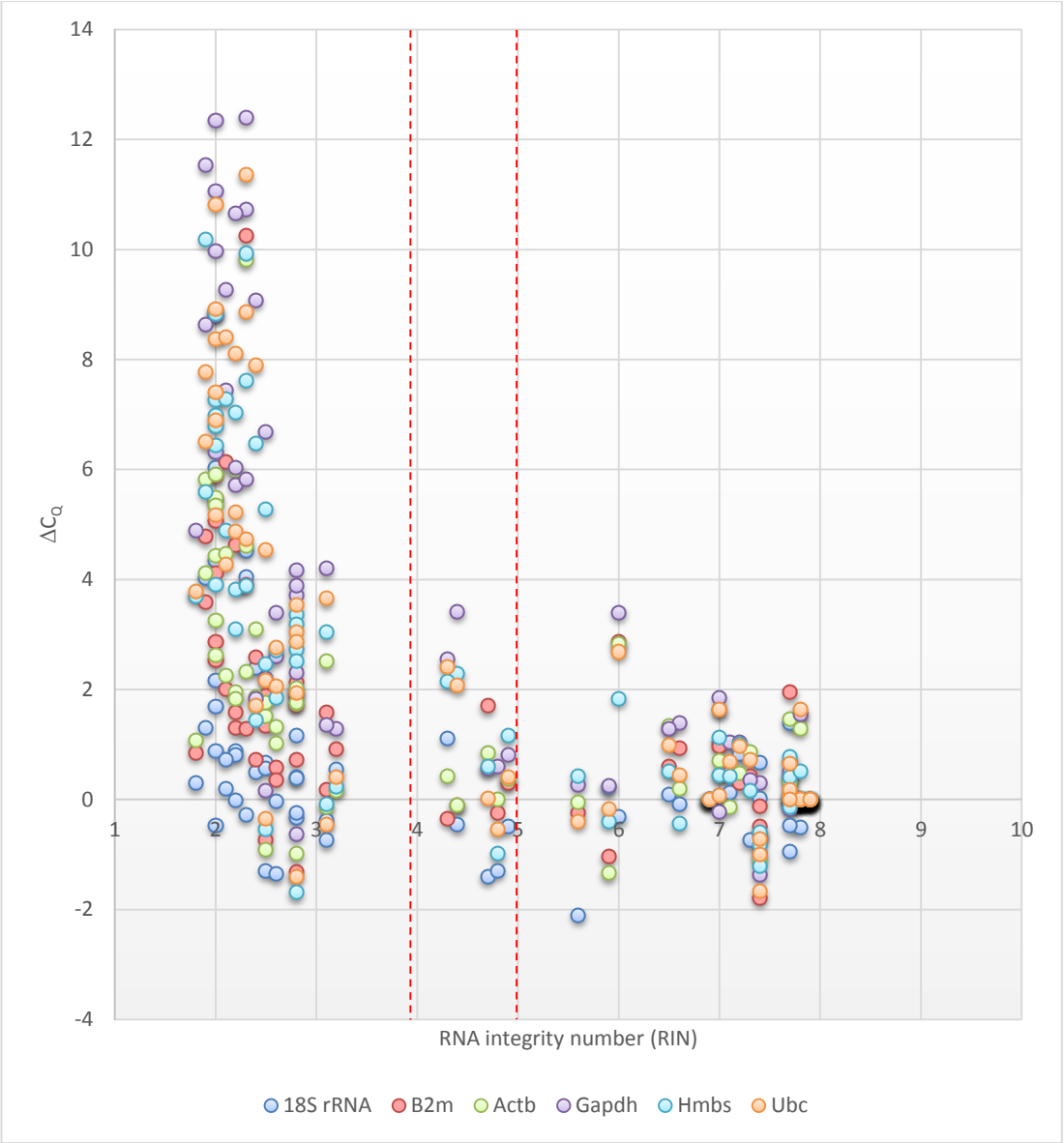

Figure 5.25: **Relationship between RNA integrity (RIN) and the RT-qPCR results upon amplification of 18S rRNA, B2m, Actb, Gapdh, Hmbs and Ubc**. Results represent the whole spectrum of post-mortem intervals and data pertaining to the skeletal muscle tissue of mice decomposed at 10, 22 and 30 °C. For illustrative purposes, the two published RIN thresholds of 3.95 (138) and 5 (212) have been added to the chart in the form of a red dotted line.

This trend was identical for all of the six RNAs when plotted individually against RIN (data shown only for collated results). It is clear however, that the relationship between RIN and ΔC_Q in post-mortem tissues is not linear. Depicted in red in Figure 5.25 are the two minimum RIN thresholds of Weis *et al*. (138) and Fleige *et al*. (212). Variation in gene expression is most prominent at the far left of

Figure 5.25, where RNA integrity falls below 3.95. Between 3.95 and 5, the magnitude of change in ΔC_Q is much less significant, and is relatively similar to good quality RNA samples above RIN 5.

In order to examine more closely the reproducibility of gene expression data at these different levels of integrity, RNA samples were split into three categories: 'high' quality (RIN > 5, n = 26); 'medium' quality (3.95 < RIN < 5, n = 5); and 'low' quality (RIN < 3.95, n = 32). The boundaries of these categories were selected in response to the two published RIN thresholds depicted in Figure 5.25. Figure 5.26 below illustrates the results of this analysis, in which the raw C_Q for each of 18S rRNA, B2m, Actb, Gapdh, Hmbs and Ubc is depicted in boxplot form for each of the three RIN categories. It can be seen that for all of the six RNAs, median C_Q was lowest in high quality RNA samples with a RIN > 5; indicating improved target RNA quantity. Median raw C_Q increased with reducing RNA quality, confirming that the fragmentation of RNA was associated with a reduction in the measurable quantity of each RNA. In the poorest quality RNA samples (RIN < 3.95) the median C_Q was at its highest for all six RNAs. Variability in C_Q was also much wider in this sample set, indicating that the reproducibility of RT-qPCR data was compromised in poor quality RNA samples. This strong variability was particularly prominent for B2m (Figure 5.26B), Gapdh (Figure 5.26D), Hmbs (Figure 5.26E) and Ubc (Figure 5.26F), demonstrated in the wider interquartile range.

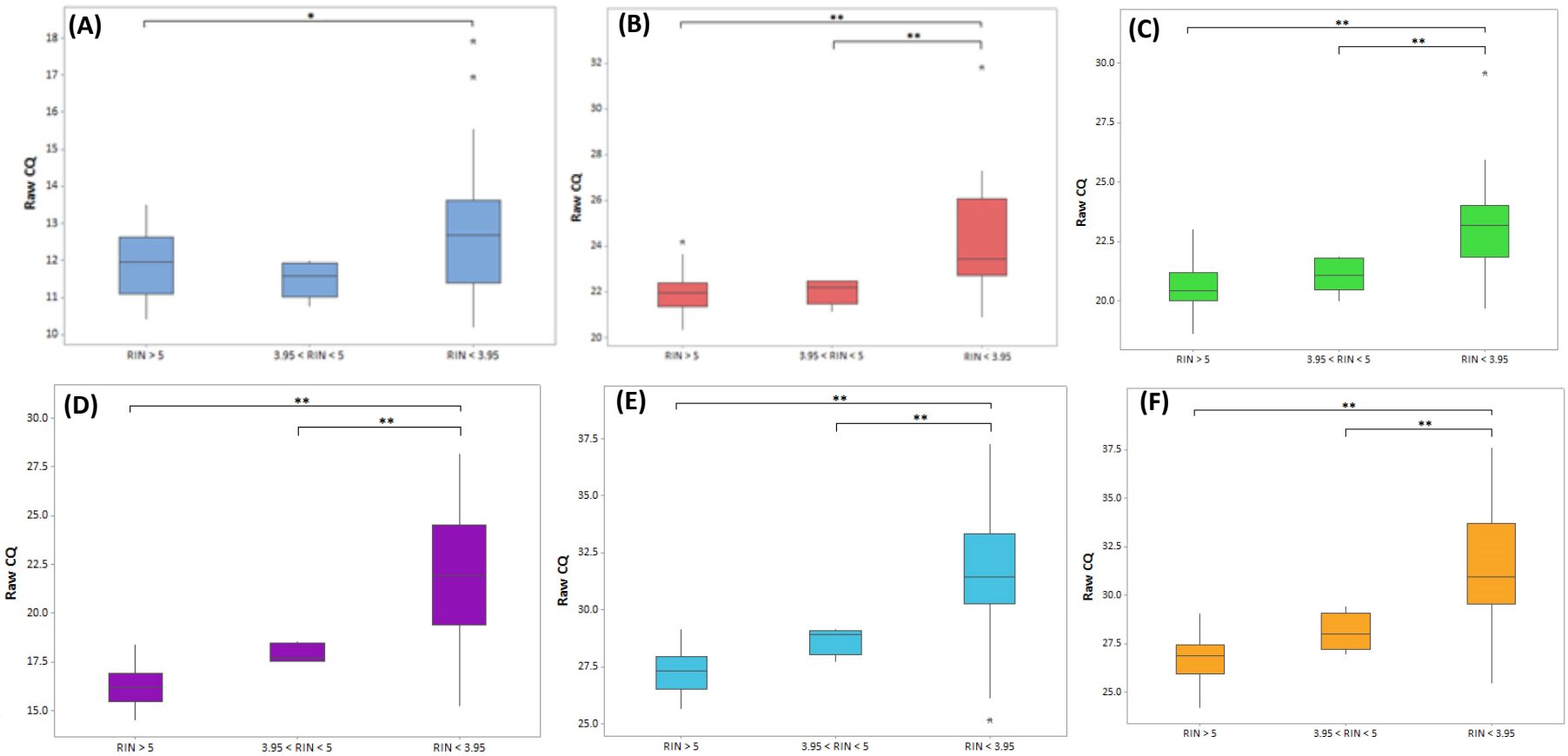

Figure 5.26: **Relationship between RNA quality and raw C_Q for each of (A) 18S rRNA, (B) B2m, (C) Actb, (D) Gapdh, (E) Hmbs and (F) Ubc for three RIN categories**. The three categories were defined as 'high' (RIN > 5); 'medium' (3.95 < RIN < 5); and 'low' quality (RIN < 3.95). Results represent data for n = 26, 5 and 32 respectively. Mean C_Q was compared between the three RIN categories using a one-way ANOVA and Fisher's Least Significant Difference test (*$p < 0.05$, **$p < 0.01$).

All six data sets were confirmed to exhibit a normal distribution using Anderson-Darling's normality test (data not shown). As such, the data was analysed using a one-way ANOVA and Fisher's Least Significant Difference test, the results of which have been incorporated into Figures 5.26A through 5.26F. It was found that for all of B2m (Figure 5.26B), Actb (Figure 5.26C), Gapdh (Figure 5.26D), Hmbs (Figure 5.26E) and Ubc (Figure 5.26F), RNA samples with a RIN < 3.95 (categorised as 'low' quality) exhibited a significantly higher mean C_Q than in the 'medium' and 'high' quality RNA samples ($p = 0.000$). Although for many RNAs (Gapdh, Hmbs and Ubc in particular) a small increment in C_Q was observed upon reduction of RNA quality from RIN > 5 to 3.95 < RIN < 5, in no instances was this deemed to be statistically significant. For 18S rRNA, a statistically significant difference in mean C_Q was only observed between the 'high' and 'low' RNA quality categories ($p = 0.019$, Figure 5.26A).

Overall, the results of the one-way ANOVA suggest that there is no statistically significant change in mean C_Q upon decline of the RNA quality from RIN > 5 to RIN > 3.95. However, further RNA fragmentation causing RIN to fall below 3.95 induced a statistically significant increase in C_Q, indicative of measurable loss of the 18S rRNA, B2m, Actb, Gapdh, Hmbs and Ubc RNAs. As such, it has been concluded that for this data generated with a mouse decomposition model the minimum RIN threshold of 3.95 suggested by Weis *et al*. (138) more accurately provides a 'cut off' below which the results of RT-qPCR are compromised; more so than the RIN 5 threshold suggested by Fleige *et al*. (212). This is a positive outcome, as use of this lower RIN threshold improves the proportion of post-mortem tissue samples which are deemed appropriate for RT-qPCR analysis – from 32/63 (50.8%) to 37/63 (58.7%).

Fleige *et al*. (128, 212) also demonstrated that the size of the qPCR target amplicon had a significant effect on the relationship between RIN and ΔC_Q. Although they recommended a minimum RIN of 5 to improve the reproducibility of qPCR data, Fleige *et al*. (212) acknowledged that very short target sequences of RNA are more robust against degradation; with the C_Q for those less than 200 nucleotides in length remaining largely unaffected until the RIN dropped below 3.5.

This outcome is supported by Antonov *et al*. (262), using data from chemically hydrolysed RNA. All of the qPCR target sequences used in this study ranged between 61 (18S rRNA) and 107 (Gapdh) nucleotides in length; well within this recommended size range for improved amplification from poor quality RNA samples. The effect of qPCR amplicon length on the results of RT-qPCR when analysing post-mortem tissues will be addressed in Chapter 7, and thus will not be discussed further.

It has been shown already that the RIN algorithm loses sensitivity and its ability to quantify further RNA degradation at the lower end of the RIN scale (Section 5.3.3). This accounts for the very wide variability in ΔC_Q at around RIN 2 to RIN 3 (Figure 5.25). Continued RNA degradation is characterised by the gradually increasing ΔC_Q for all six RNAs, but the RIN remains static. To date, the author is unaware of any published study demonstrating this 'saturation' of the RIN in extremely poor RNA quality samples, although attempting to work with such samples is particularly unusual in the field of RNA analysis.

The non-linearity of the observed relationship between RIN and RT-qPCR C_Q contradicts the findings of Fleige *et al*. (212). They demonstrated that by artificially degrading human RNA the relationship between RIN and the change in C_Q (for all of 18S rRNA, 28S rRNA, ACTB and IL-1β) exhibited a strongly linear trend. However, this study used a substantially different methodology than has been applied here – where RNA samples were artificially degraded *in vitro* by illumination with UV-C radiation or by treatment with purified RNase. This makes for much more predictable and consistent RNA decay behaviour than would be expected in a biological system, and likely accounts for this difference.

5.3.5 Induction of RNA expression during the supravital reaction

It is of significant interest to determine for how long after death tissue samples remain transcriptionally active. To try to identify this, a short study was conducted to examine the expression of nine RNAs in skeletal muscle tissue during the first 3 hours following death. These nine targets were selected in an attempt to characterise RNAs whose expression was likely to be up-regulated as a response to the extreme stress to which tissues are exposed during/after death.

Unfortunately, analysis of Jun had to be abandoned due to technical difficulties in quantifying the expression of this target by RT-qPCR. Despite being 3,187 nucleotides in length the Jun transcript has no intron-exon structure, i.e. the transcript does not undergo splicing to remove non-coding introns; meaning that the DNA gene has an identical sequence to its transcribed RNA. This makes for difficulty in designing RT-qPCR primers, which would normally span an exon-exon boundary to prevent amplification of contaminating DNA. Only one Jun assay was commercially available from Life Technologies, and this was found to have an unexpectedly poor qPCR efficiency and strong amplification of DNA contamination in negative controls. As a result, this target was removed from further analysis.

Of the other eight RNA targets, seven were not found to be up-regulated to any biologically significant degree in tissues in the minutes/hours immediately following death as illustrated in Figure 5.27: Tgfb1, Casp3, Fas, Fadd, Dff40, Casp6 and Apaf1. Figure 5.27 illustrates their expression normalised to that of the endogenous control gene B2m. Similar results were obtained upon normalisation of the data sets to two other endogenous control RNAs, 18S rRNA and Actb (data not shown). As Figure 5.27 illustrates, the fold-change expression of each of the seven RNAs does not conform to any particular trend post-mortem, as none deviates appreciably from 1. Surprisingly, none of the six apoptosis-associated RNAs were found to be up-regulated in post-mortem skeletal muscle. This is in contention with the outcomes of Sanoudou *et al*. (240), who named apoptotic cell death as one of the major gene families to exhibit up-regulation in skeletal muscle after death.

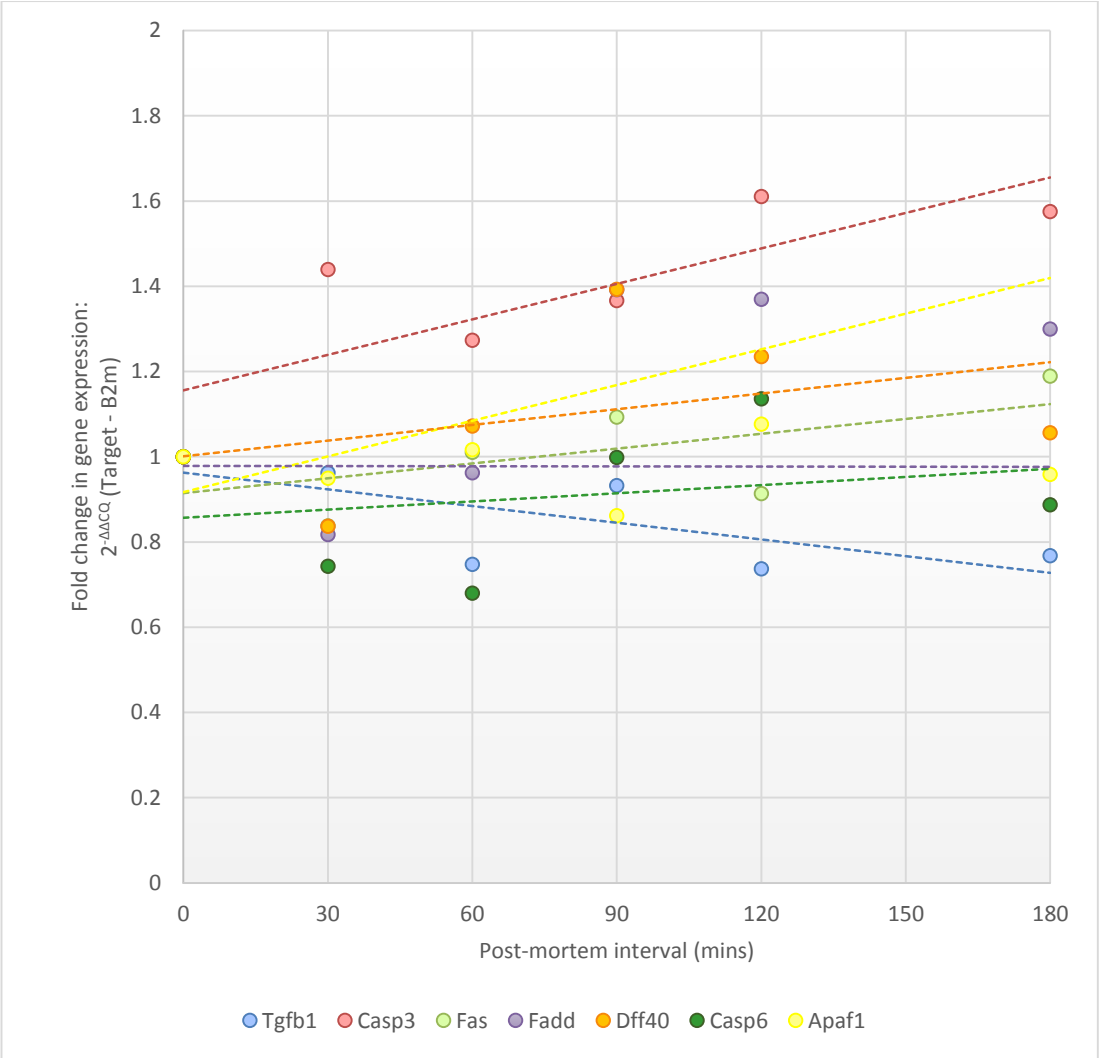

Figure 5.27: **Expression of Tgfb1 (blue data points), Casp3 (red data points), Fas (green data points), Fadd (purple data points), Dff40 (orange data points), Casp6 (dark green data points) and Apaf1 (yellow data points) in mouse skeletal muscle tissue during the first 3 hours post-mortem, normalised to the endogenous control gene B2m by means of the $2^{-\Delta\Delta CQ}$ method**. Data represents mean of n = 3. Error bars have been omitted for clarity.

On the other hand, Fos expression was increased approximately 2.8, 2.3 and 2.9-fold when normalised to the three endogenous control gene RNAs 18S rRNA, B2m and Actb respectively (Figure 5.28). The expression of these three control RNAs is assumed to be stable during this time. As can be seen in Figure 5.28, induction of Fos expression is strongest during the first 30 minutes post-mortem. After this point, up-regulation in Fos expression appears to reverse itself, most likely resulting from the strong instability of the Fos transcript itself (11). It has been

previously estimated that the Fos transcript degrades in live cells with an approximate half-life of only 15 minutes (263). This instability is conferred by sequence elements in the Fos transcript. Rapid turnover of Fos is physiologically important as the gene product is only transiently required in short bursts in response to specific extracellular signals; unnecessary expression of Fos can be detrimental to cell development and survival.

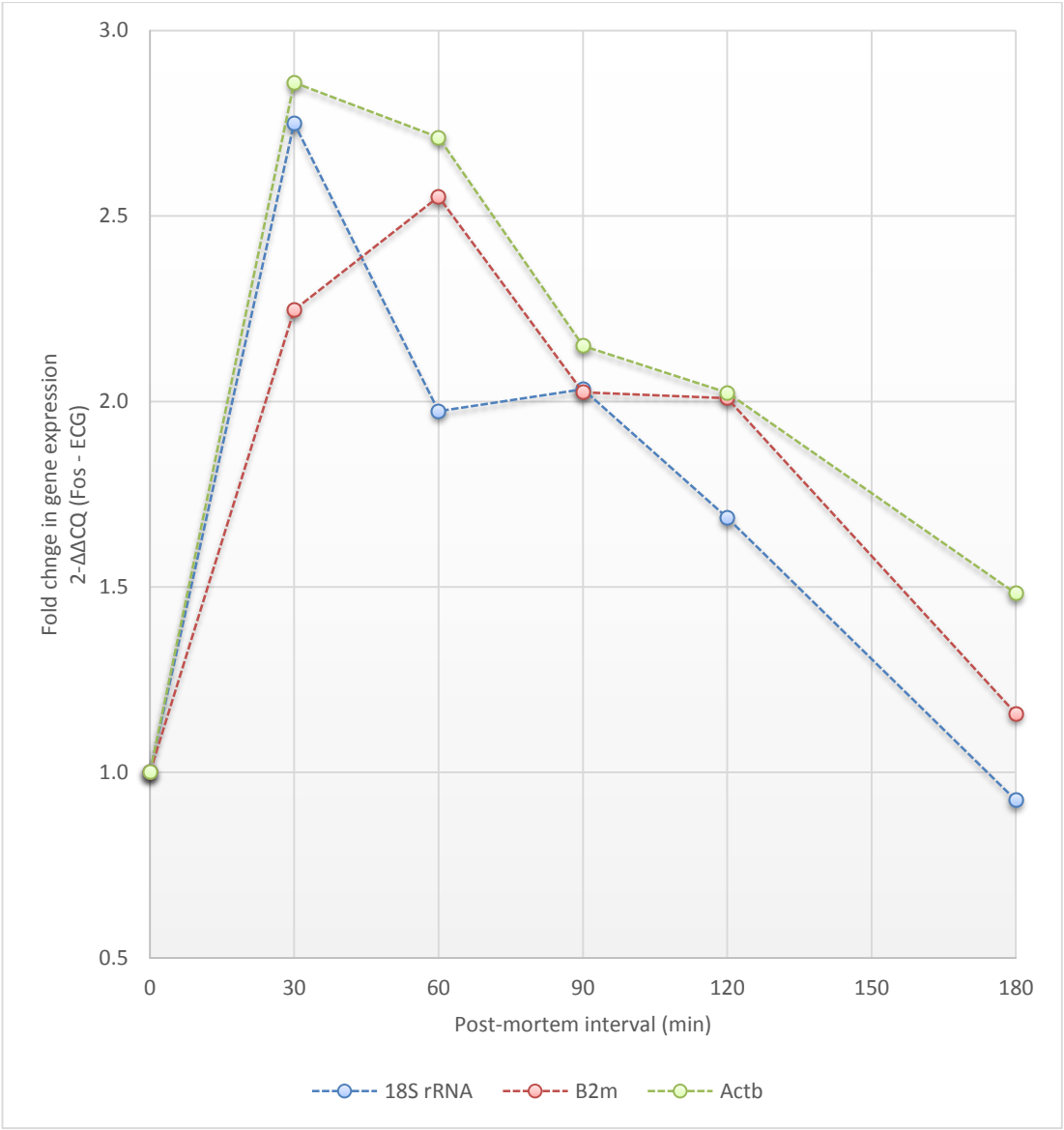

Figure 5.28: **Expression of Fos mRNA in mouse skeletal muscle tissue during the first 3 hours post-mortem, normalised to the endogenous control genes 18S rRNA (blue data points), B2m (red data points) and Actb (green data points) by means of the $2^{-\Delta\Delta CQ}$ method).** Data represents mean of n = 3. Error bars have been omitted for clarity.

This data provides evidence of strong transcription of Fos mRNA during the first 30 minutes post-mortem. However by three hours, any detectable increase in Fos expression is diminished through degradation; degradation that appears to follow a linear profile. This in part mirrors the findings of Ikematsu *et al*. (97), who identified four RNA transcripts (named S1 – S4) whose expression was induced in the first 30 minutes post-mortem in the skin of mice killed by compression of the neck. Unfortunately, Ikematsu *et al*. did not examine any subsequent time points making it unclear whether this effect on gene expression was maintained beyond 30 minutes. In addition, in a subsequent article Ikematsu *et al*. (239) illustrated that Fos and FosB expression were up-regulated in the lung tissue of mice killed by mechanical asphyxiation. However by 60 minutes, this effect was lost similar to the outcomes of this study.

In summary, the outcomes of this short piece of work suggests that the transcription of new RNAs stops somewhere between 30 and 60 minutes post-mortem. Clearly, this work is limited in that the expression of only a small number of RNAs has been considered, and only in a single tissue type (skeletal muscle). However, this type of work is probably more effectively achieved using larger-scale technologies such as microarrays and RNA sequencing; both of which can screen for the expression of hundreds or even thousands of RNA transcripts simultaneously. Both of these technologies are out with the time frame and the financial restrictions of this project. Such large-scale screening technologies are vital for identification of RNAs with expression profiles restricted to specific causes of death.

5.4 Summary and conclusions

The focus of this chapter has been to try and identify a time span during which gene expression analysis of post-mortem tissues provides data which reflects that at the time of death, and to identify any factors which might stretch/shorten this time span. Towards this aim, Box 5.1 at the beginning of this chapter presented seven research 'questions' which this work endeavoured to answer. To conclude, these questions will be revisited to contextualise the original aims with the data presented in this chapter.

For how long after death can RNA still be successfully extracted from tissues?

Over the maximum 72 hour post-mortem interval examined, and even under the most aggressive decomposition conditions, no skeletal muscle tissue sample yielded a quantity of RNA that was insufficient for downstream analyses. As a result, this study has not identified a time span during which RNA can still be successfully extracted from tissues. This demonstrated long-term survivability of total RNA in tissues after death is a positive outcome for the future of gene expression analysis in forensic pathology.

What quantity of RNA can be extracted from post-mortem tissue, and can the tissue RNA yield be correlated with the post-mortem interval?

In the tissues of mice decomposed at 10 and 22 °C, no decline was observed in tissue RNA content with increasing post-mortem interval. Under more aggressive decomposition conditions at 30 °C however, an approximately linear decline in RNA yield was observed with passing time post-mortem. Regardless of the post-mortem conditions, RNA yield was found to exhibit strong variability between replicates making it a very poor predictor of RNA degradation.

How good is the quality of RNA extracted from post-mortem tissue, can this quality be correlated with the post-mortem interval and after what post-mortem interval does RNA quality fall below published guidelines for gene expression analysis?

The decline in skeletal muscle RNA quality with increasing post-mortem interval was not linear but exhibited a sigmoidal profile: with RNA degradation slow to 'kick in', and plateauing out at the lower edge of the RIN spectrum. A significant reduction in mean RNA quality was detected after 24, 9 and 6 hours in mice decomposed at 10, 22 and 30 °C respectively. RNA quality fell below the minimum RIN of 3.95 suggested by Weis *et al*. (138) after 36, 24 and 12 hours upon decomposition at 10, 22 and 30 °C respectively.

Can the expression level of individual RNA transcripts (as measured by RT-qPCR) be correlated back to the RNA quality?

A strong relationship was observed between the expression level of 18S rRNA, B2m, Actb, Gapdh, Hmbs and Ubc and the RNA quality (RIN). This relationship however, was not linear. As anticipated, the lowest quality samples (low RIN, heavily fragmented RNA) were associated with a significantly reduced measurable quantity of these six RNAs using RT-qPCR. The published minimum RIN threshold of 3.95 suggested by Weis *et al*. (138) was deemed to be the most appropriate 'cut off' point; below which RT-qPCR data exhibited high C_Qs and poor reproducibility.

How does the ambient temperature to which the corpse is exposed during the post-mortem interval affect RNA decay behaviour, with respect to tissue RNA quantity, quality, and the expression of individual RNAs?

It has been shown that the ambient temperature conditions in which the corpse is decomposed have a very profound effect on the rate of RNA degradation and upon its severity. As one might have expected, total RNA yield and quality are significantly improved when decomposition is slowed at low ambient temperatures. The post-mortem interval during which RNA quality remained above published minimum RIN guidelines (138) was stretched to 36 hours by refrigeration of the corpse at 10 °C. Individual RNAs were also preserved (18S rRNA, B2m, Actb, Gapdh, Hmbs and Ubc) at low temperatures: with visible onset of degradation restricted to 24 – 36 hours, 12 – 24 hours and 6 – 12 hours in the tissues of mice decomposed at 10, 22 and 30 °C respectively. This strong dependency of RNA degradation on ambient temperature is problematic for post-mortem gene expression analysis,

particularly where the ambient conditions are unknown (as is true in most casework), or where it is to be used for post-mortem interval estimation (Section 1.3.2.2.1, Chapter 1).

Do distinct RNA transcripts decay at the same rate in post-mortem tissue, or does each RNA transcript have its own unique degradation behaviour as is true in live cells?

It was found that the six endogenous control RNAs examined exhibited wide variability in their stability. The rank order of stability was consistent across all tissue samples: with 18S rRNA exhibiting the highest level of stability and Gapdh the lowest. 18S rRNA in particular exhibited very unusual decay behaviour; with some post-mortem tissue samples actually presenting improved 18S rRNA yield in the early stages of decomposition. Both geNorm and NormFinder deemed Actb to be the most stably expressed endogenous control RNA for normalisation purposes. The relative levels of 18S rRNA, B2m, Actb, Gapdh, Hmbs and Ubc changed drastically over the course of the post-mortem interval, up to 500-fold. This differential stability of RNAs presents a serious interpretational issue for gene expression data derived from tissue samples with a long post-mortem interval, highlighting the requirement for thorough characterisation of an RNA's decay behaviour prior to its use in any diagnostic assay.

Is RNA expression induced during the supravital reaction, and if so, for how long after death does transcription still occur?

Of the RNAs examined in this study, Fos was the only target RNA found to have up-regulated expression in mouse skeletal muscle tissue (2.3 to 2.9-fold) in the minutes immediately following death. When the RT-qPCR data was normalised to that of the endogenous controls 18S rRNA, B2m and Actb, new transcription of Fos RNA appeared to cease somewhere between 30 to 60 minutes post-mortem. This is a positive outcome, indicating that cells seem to retain transcriptional activity during the first 30 minutes following death. It is therefore reasonable to expect that the death 'event' itself leaves an identifiable mark on the transcriptome as a whole.

Chapter 6: Is *ex vivo* tissue decomposition a valid simulation for post-mortem RNA analyses?

6.1 Introduction

6.1.1 Using an *ex vivo* decomposition model to study RNA decay behaviour

Throughout the experimentation presented thus far, an *in vivo* decomposition model has been adopted to study the degradation of RNA in tissues. Following this experimental design, RNA-containing tissues were allowed to decompose in the organism as a whole after death (Section 5.2.1, Chapter 5). The integrity of each mouse corpse was maintained to the highest possible standard, to best simulate a natural setting where a corpse would be allowed to decompose uninterrupted.

However, it is clear that the use of an alternative *ex vivo* simulation is becoming ever popular in this area of research. Under this experimental design, the organism is dissected immediately following death and tissue types are separated and allowed to decompose individually in a test tube. To illustrate this problem, Table 6.1 presents a summary of the experimental design strategy of a number of key studies in the field categorising them based on whether they followed an *in vivo* or *ex vivo* design for decomposition.

Table 6.1: **Summary of published post-mortem RNA expression studies, illustrating differences in experimental design particularly with regard to *in*/*ex vivo* tissue decomposition**. Included are the species, tissue substrate and details of the post-mortem interval duration and conditions examined.

***In vivo* decomposition model**	***Ex vivo* decomposition model**
Heinrich *et al*. (82) Human; many tissue types; up to 118 hours post-mortem interval in unknown conditions	Sampaio-Silva *et al*. (6) Mouse; many tissue types; up to 11 hours post-mortem interval at room temperature
Heinrich *et al*. (72) Human; brain, heart and skeletal muscle; up to 118 hours post-mortem interval in unknown conditions	Li *et al*. (80) Rat; heart; up to 168 hours post-mortem interval at room temperature
Marchuk *et al*. (86) Rabbit; connective tissues (tendon, ligament and cartilage); up to 96 hours post-mortem interval at 4 °C	Fitzpatrick *et al*. (242) Cow; reproductive tissues (ovary, oviduct and uterus); up to 96 hours post-mortem interval at room temperature
Bauer *et al*. (5) Human; blood and brain; up to 145 hours post-mortem interval at 4 °C	Seear *et al*. (206) Fish; kidney, brain, liver and skeletal muscle; up to 24 hours post-mortem interval at room temperature
Koppelkamm *et al*. (81, 160) Human; brain, skeletal muscle and heart; up to 48 hours post-mortem interval in unknown conditions	Kuliwaba *et al*. (87) Human; bone (autopsy and surgical); up to 72 hours post-mortem interval at 4, 22 and 37 °C
Inoue *et al*. (233) Rat; brain, lung, liver and heart; up to 7 days post-mortem interval at 20 °C	Fontanesi *et al*. (127, 236) Pig; skeletal muscle; up to 48 hours post-mortem interval at 4 °C
Catts *et al*. (264) Mice; brain tissue only; up to 48 hours at 25 °C	Bahar *et al*. (85) Cow; skeletal muscle, liver and adipose tissue; up to 22 days at 4 °C

Clearly, an *ex vivo* simulation has many practical advantages. It eliminates the requirement to store whole animals for extended periods of time, and reduces the number of animals required for experimentation. In addition, in some settings *ex vivo* decomposition is actually favourable – for example, studying the decay of RNA during the processing of animal meat in veterinary research (127, 236).

However, there is a paucity of data available in the public domain to confirm that RNA decay behaviour is consistent across both settings and that direct comparisons can be made between the two. When tissues are maintained within

the corpse as a whole, it is reasonable to expect that RNA degradation is influenced by enzymatic, chemical and microbial factors from surrounding tissues and organ systems which might enhance RNA degradation. On the converse, it has been proposed that in intact tissue RNA is protected against enzymatic attack through the sequestering of RNases within intracellular vesicles such as lysosomes (87). Interruption of the integrity of the tissue structure (e.g. by dissection and tissue processing) is likely to disturb these delicate membrane bound structures, releasing degradative enzymes and thus accelerating RNA damage (87). Additionally, removal of tissues from the body is likely to bring them into contact with exogenous RNases which might further hasten RNA decay (87). Taking all of these competing propositions into account, it is extremely difficult to hypothesise whether RNA degradation is likely to proceed faster or slower when tissues are removed from the body.

Very few studies to date have actually acknowledged the problems which exist surrounding the direct comparison of RNA expression data generated using these two opposing methodologies. Sampaio-Silva *et al*. (6) recognised the issue with regard to their experimental design. They developed a predictive model for post-mortem interval using gene expression data generated from mouse skeletal muscle, decomposed in an *ex vivo* fashion for up to 11 hours post-mortem. With this model, they subsequently attempted to estimate the post-mortem interval for a small number of skeletal muscle tissue samples decomposed *in vivo* (for 1, 4 and 10 hours post-mortem). Sampaio-Silva *et al*. claim high predictive accuracy for their model: with post-mortem interval estimates of 1.9 ± 0.01 hours, 4.1 ± 0.87 hours and 9.8 ± 1.87 hours for skeletal muscle tissue samples decomposed *in vivo* for 1, 4 and 10 hours respectively. Although this preliminary outcome is clearly promising in demonstrating that RNA behaviour is consistent across both settings, a small handful of samples are not sufficient to make reliable conclusions with regards to the validity of this experimental design. Much work still has to be done to endorse this *ex vivo* simulation as providing utilisable gene expression data.

6.1.2 Experimental design, aims and objectives

This chapter will compare the decay characteristics of RNA in mouse post-mortem tissue under two settings:

1) *In vivo*, where the mouse is left to decompose intact and tissue samples are harvested from the corpse after passage of a specific post-mortem interval

2) *Ex vivo*, where the mouse is dissected to remove tissue types immediately after death and decomposed for a specific time period in a tube

The tissue types examined in this chapter were expanded from solely skeletal muscle, utilised in previous chapters, to include kidney, liver and heart. This allowed a more comprehensive analysis of RNA decay behaviour across both settings, and in tissue types localised to different areas of the body. For example, it is reasonable to expect that the degradation of RNA in organs protected within the abdominal cavity (and in close proximity to the microbe-rich gastrointestinal tract) might differ from skeletal muscle, which is located just under the surface of the skin.

The literature available to date supports the contention that RNA behaves differently across post-mortem tissue types (6, 81, 85, 86, 206, 233, 242). Physiologically, some tissue types are known to have a high RNase content based upon their functionality making RNA more prone to rapid degradation; e.g. liver, pancreas and stomach (127, 242). On the converse, RNA is known to be particularly stable in brain, lung and fibrous tissue types such as heart, skeletal muscle, tendon and ligament (6, 81, 85, 86, 127, 206, 233). This chapter will examine the effect of tissue type (skeletal muscle, kidney, liver and heart) on the onset and rate of post-mortem degradation. This will be followed by direct comparison of *in vivo* and *ex vivo* RNA decay behaviour in these four tissue types.

RNA was examined in the skeletal muscle, kidney, liver and heart tissue of mice allowed to decompose for up to 48 hours. Mice in the *in vivo* category were killed and allowed to decompose for 8, 24 or 48 hours; after which the mice were dissected and tissues harvested. On the other hand, mice in the *ex vivo* category

were stripped of skeletal muscle, kidney, liver and heart immediately following death. These tissue types were left to decompose individually for 8, 24 or 48 hours in a sterile microcentrifuge tube. All tissue samples were subjected to extraction to provide pure RNA, which was analysed for degradation using a panel of three techniques as before.

Total RNA quantity was assessed by UV-visible spectrophotometry (Section 1.4.2, Chapter 1), to determine whether a reduction in total RNA yield due to degradation could be observed in any of the four tissue types. Total RNA quality was assessed using the Bioanalyzer 2100 (Section 1.4.3, Chapter 1) to examine the fragment size distribution of RNA molecules recovered. The degree of RNA degradation was quantified using the RNA integrity number (RIN) algorithm. Finally, the expression of two endogenous control RNAs was quantified by RT-qPCR: 18S rRNA and Gapdh (Sections 1.4.4 and 1.4.5.2, Chapter 1). These two target RNAs were selected in response to the outcomes of Section 5.3.4, Chapter 5, which illustrated them to exhibit decay behaviour of two opposing extremes in skeletal muscle: 18S rRNA exhibiting very high stability and Gapdh mRNA poor stability.

For clarity, Box 6.1 below summarises the questions to be answered through the research presented in Chapter 6.

Box 6.1: Objectives/questions to be answered within Chapter 6

Does RNA (total RNA and 18S rRNA/Gapdh) degrade at the same rate in skeletal muscle, kidney, liver and heart, or is the decay behaviour **tissue specific**?

Does **removal of tissues** (skeletal muscle, kidney, liver and heart) from the mouse corpse affect RNA (total RNA and 18S rRNA/Gapdh) degradation behaviour? Is this 'test tube' **simulation** an appropriate experimental design for studies in post-mortem gene expression analysis?

6.2 Method

6.2.1 Tissue sample preparation

All experimental steps involving live animals were performed in accordance with the ethical guidelines set out by the Biological Procedures Unit within Strathclyde Institute of Pharmacy and Biomedical Science. The animals utilised were 12 week old, male C57/BL6J laboratory mice. A total of 16 mice were killed by cervical dislocation and processed in three categories: control mice, *ex vivo* decomposed mice and *in vivo* decomposed mice. It should be noted that this small sample size (n = 4 per time point) was a consequence of the limited resources available for this project, rather than a conscious choice during the experimental design and planning stage.

For the control and *ex vivo* tissue samples, four mice were dissected immediately after death, harvesting from each skeletal muscle, kidney, liver and heart tissue. Each tissue type was divided into four aliquots:

- A *control* tissue sample, preserved immediately in RNAlater® and used for reference purposes to assess the quality of RNA in tissues at the time of death (within the first 15 minutes)
- An 8 h tissue sample, left to decompose *ex vivo* in a 1.5 mL tube for 8 h at room temperature (22 °C) prior to the addition of RNAlater®
- A 24 h tissue sample, left to decompose *ex vivo* in a 1.5 mL tube for 24 h at room temperature (22 °C) prior to the addition of RNAlater®
- A 48 h tissue sample, left to decompose *ex vivo* in a 1.5 mL tube for 48 h at room temperature (22 °C) prior to the addition of RNAlater®

All 1.5 mL tubes used were certified as DNA, DNase, RNase and pyrogen free (Elkay Laboratory Products, Basingstoke, UK). Of the other 12 mice, four were decomposed for each of 8, 24 and 48 h at room temperature (22 °C). After the relevant post-mortem interval, these mice left to decompose intact (*in vivo* tissue decomposition) were dissected to harvest skeletal muscle, kidney, liver and heart

tissue. These tissue samples were preserved and stored in RNAlater® as before (Section 2.2.2, Chapter 2) until a convenient time for RNA extraction.

6.2.2 RNA purification, quantification and quality assessment

RNA was purified from skeletal muscle, kidney, liver and heart tissue samples with the TRI Reagent® extraction system using the protocol described in Section 2.2.3.3, Chapter 2. RNA extracts were treated with TURBO DNA-free® to remove residual DNA contamination, as described in Section 2.2.3.4, Chapter 2. RNA was quantified by UV-visible spectrophotometry using the Nanodrop-1000 platform (Section 2.2.4, Chapter 2) and then subjected to quality analysis on the Bioanalyzer 2100 instrument using the RNA Pico 6000 kit, following the protocol described in Section 2.2.5, Chapter 2.

6.2.3 Gene expression analysis by RT-qPCR

Following RNA quantification, samples were diluted in RNase-free water (Ambion, Life Technologies, Paisley, UK) to a concentration of 100 ng/μL and reverse transcribed into cDNA with the High Capacity cDNA Reverse Transcription Kit (Applied Biosystems, Life Technologies, Paisley, UK) (Section 2.2.6, Chapter 2). The resultant cDNA products were diluted 1:12 in RNase-free water to prevent qPCR inhibition through carryover of high concentration buffers and reverse transcriptase.

cDNA samples were amplified to quantify the presence of two endogenous control RNAs: 18S rRNA and Gapdh. Section 2.2.7, Chapter 2 describes the protocol for amplification of cDNAs by real time PCR and the *TaqMan*® technology. Details of the PCR assays used against 18S rRNA and Gapdh (i.e. assay ID, target transcript function, amplicon site, length and all quality control data) are included in Tables A1.1 and A1.2, Appendix 1. Gene expression data was analysed in the Microsoft Excel 2010 and Minitab 16 (Minitab Inc.) statistical softwares.

6.3 Results and discussion

6.3.1 Differential degradation of RNA in accordance with tissue type (*in vivo*)

6.3.1.1 Total RNA quantity: UV-visible spectrophotometry

The outcomes of Section 5.3.2, Chapter 5 suggest that in skeletal muscle, the yield of recovered RNA from tissues does not decrease appreciably over the first 72 hours post-mortem unless under particularly aggressive decomposition conditions (at 30 °C). To assess whether this is the case also for kidney, liver and heart tissue, the quantity of RNA recovered from these three tissue types (per 1 mg tissue) was measured by UV-visible spectrophotometry for mice decomposed at 22 °C for up to 48 hours (<0.25, 8, 24 and 48 hours) post-mortem; the results of which are presented in Figure 6.1.

Figure 6.1 demonstrates that the mean yield of RNA obtained from muscle and heart tissue is much less than that of kidney and liver. This results from their relatively low cellular content and high abundance of contractile proteins, collagen and connective tissue (118). No particular trend is observable for either skeletal muscle or heart tissue, with the mean RNA yield remaining reasonably static over the course of the post-mortem interval.

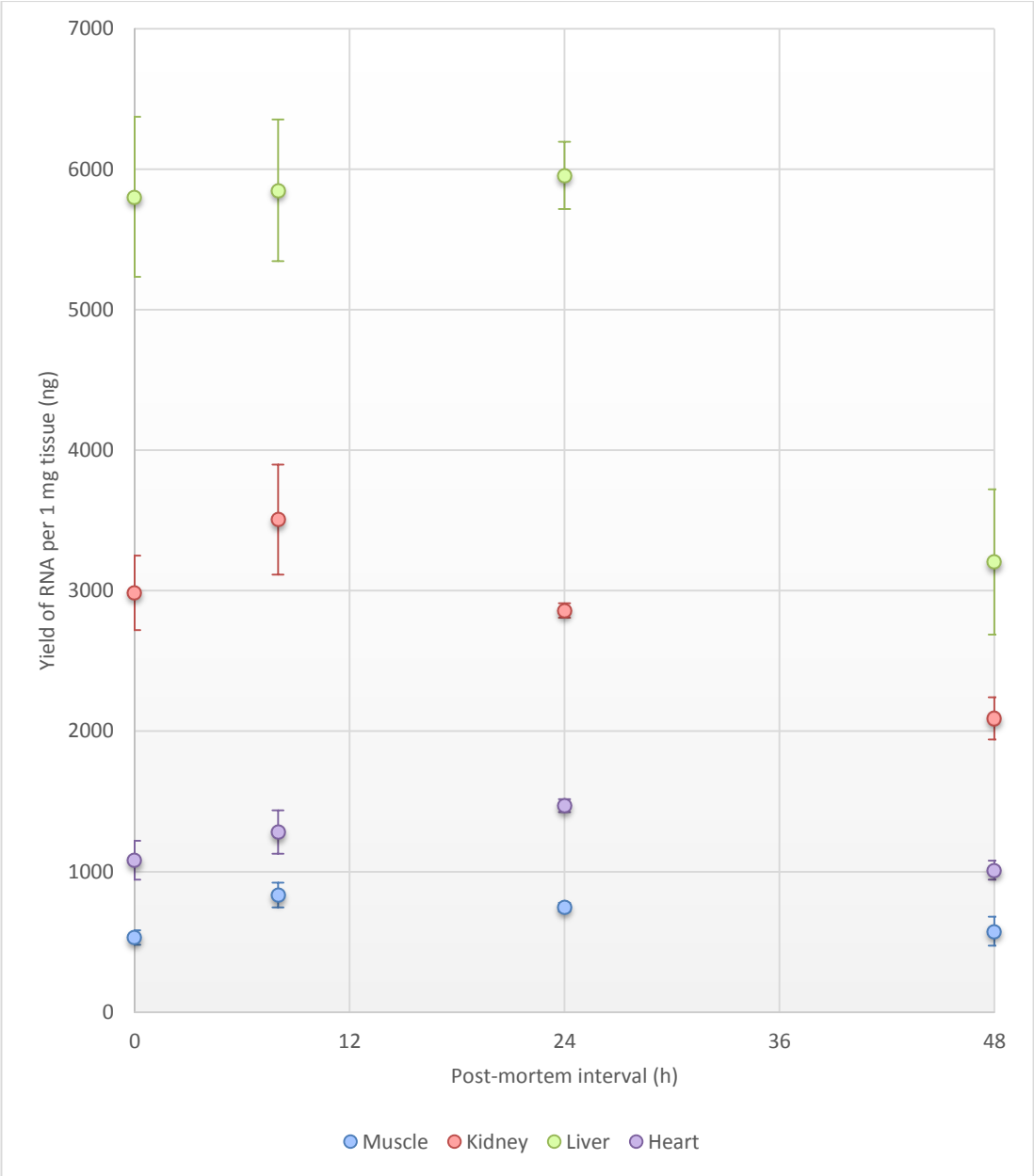

Figure 6.1: **Yield of RNA from mouse skeletal muscle (blue data points), kidney (red data points), liver (green data points) and heart (purple data points) tissue samples collected until 48 hours post-mortem, for animals stored at 22 °C.** Points represent total RNA quantity determined by UV-vis spectrophotometry (in nanograms) per 1 milligram of tissue extracted. Data represents mean ± S.E. for n = 4.

On the other hand, after a 48 hour post-mortem interval kidney and liver both yield a visibly reduced quantity of RNA. The RNA yield data for all four sample sets was deemed to be normally distributed using the Anderson-Darling normality test (p = 0.539, 0.463, 0.163 and 0.286 for each of skeletal muscle, kidney, liver and

heart respectively). As such, the data sets were assessed using Pearson's product moment correlation to establish whether a linear relationship exists between post-mortem interval and the yield of RNA recovered from any of the four tissue types. A statistically significant, negative linear correlation between post-mortem interval and RNA yield was observed for kidney ($r = -0.652$, $p = 0.006$) and liver ($r = -0.699$, $p = 0.003$), but no such correlation was apparent for skeletal muscle ($r = -0.115$, $p = 0.671$) or heart ($r = -0.148$, $p = 0.585$).

Analysis of kidney and liver RNA yield with a one-way ANOVA in both tissue types characterised a significant difference in mean RNA yield when compared between post-mortem intervals (kidney $p = 0.013$, liver $p = 0.004$). Fisher's Least Significant Difference test was able to illustrate a statistically significant reduction in mean kidney RNA yield at 48 hours post-mortem interval relative to 0 and 8 hours only; and similarly in liver, a statistically significant reduction in mean RNA yield after 48 hours post-mortem relative to all other post-mortem intervals examined. These differences can be clearly visualised in Figure 6.1.

6.3.1.2 Total RNA quality: Bioanalyzer 2100

In addition to RNA yield, the relationship between post-mortem interval duration (up to 48 hours, at 22 °C) and the quality of tissue RNA was examined for each of skeletal muscle, kidney, liver and heart tissue. Tissue RNA quality was measured on the Bioanalyzer 2100 platform and quantified using the RNA integrity number (RIN) algorithm. The outcomes are presented in Figure 6.2.

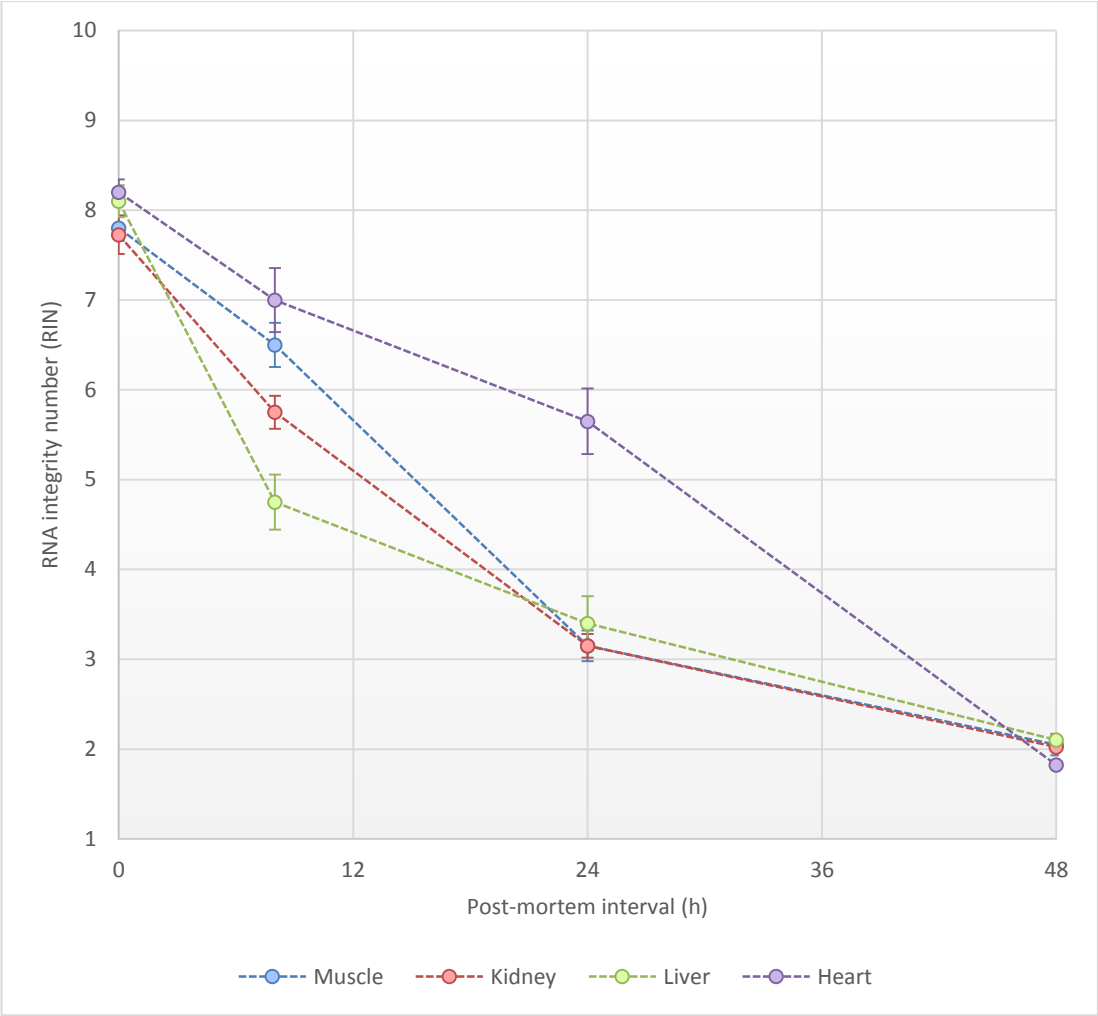

Figure 6.2: **Quality of RNA extracts from mouse skeletal muscle (blue data points), kidney (red data points), liver (green data points) and heart (purple data points) tissue samples collected until 48 hours post-mortem, for animals decomposed at 22 °C.** Points represent RNA quality as quantified by the Bioanalyzer 2100 using the RNA integrity number (RIN) algorithm. Data represents mean ± S.E. for n = 4.

Figure 6.2 illustrates that the rate at which RNA quality declines after death through degradation is not consistent across all tissue types. Liver tissue RNA quality declines most rapidly during the first 8 hours post-mortem: from mean RIN 8.1 at the control point, to 4.8 after only 8 hours. In contrast, heart tissue retains reasonably high quality RNA over the first 24 hours post-mortem during which time the mean RIN did not fall below 5.7. By 48 hours post-mortem, the RNA quality falls to approximately RIN 2 in all four tissue types, indicative of extremely poor quality RNA.

As a whole and encompassing all time points, the RIN data for muscle, liver and heart were deemed not to be normally distributed using the Anderson-Darling test of normality ($p = 0.012$, 0.037 and 0.013 respectively), with RINs skewed towards high and low values. On the other hand, the kidney RIN data was normally distributed ($p = 0.068$). A strong negative correlation was characterised between post-mortem interval and RNA quality in all four tissue types. For skeletal muscle, liver and heart, using Spearman's rank correlation coefficient: $\rho = -0.972$, -0.962 and -0.956 respectively and $p = 0.000$; and for kidney, using Pearson's product moment correlation coefficient: $r = -0.938$, $p = 0.000$.

Regression analysis of these four data sets indicated that the degradation profile of RNA, in most cases, was not linear. For muscle, kidney and liver tissue RNA degradation best fitted with a quadratic profile, as illustrated in Figures 6.3A-C. These quadratic profiles provided an excellent fit to the data, with post-mortem interval deemed to be responsible for 97.2, 98.5 and 90.9% of the variation in RNA quality for each of skeletal muscle, kidney and liver respectively (non-adjusted R^2). The slower rate of heart RNA degradation meant that the RNA quality data closely fitted with a linear profile, as illustrated in Figure 6.3D. This linear degradation profile attributed 95.0% (non-adjusted R^2) of the variation in RNA integrity as down to post-mortem interval duration.

Further analysis of the data using a one-way ANOVA and Fisher's Least Significant Difference test was conducted to examine whether the mean quality of skeletal muscle, kidney, liver and heart RNA differed at each of the four post-mortem intervals investigated. At the < 0.25 hours control point ($p = 0.202$) and after 48 hours ($p = 0.082$), no statistically significant difference was detected between the mean RIN for each of the four tissue types. This can be visualised in Figure 6.2, where the RINs remain consistently high at the < 0.25 hours control point, and converge at a very poor RIN 2 after 48 hours. After an 8 hour post-mortem interval, heart RNA exhibited a significantly higher mean RNA quality than kidney and liver RNA, and muscle RNA a significantly higher RIN than liver RNA ($p = 0.001$). After a 24 hour post-mortem interval, mean heart RNA quality was deemed to be significantly higher than all three other tissue types ($p = 0.000$).

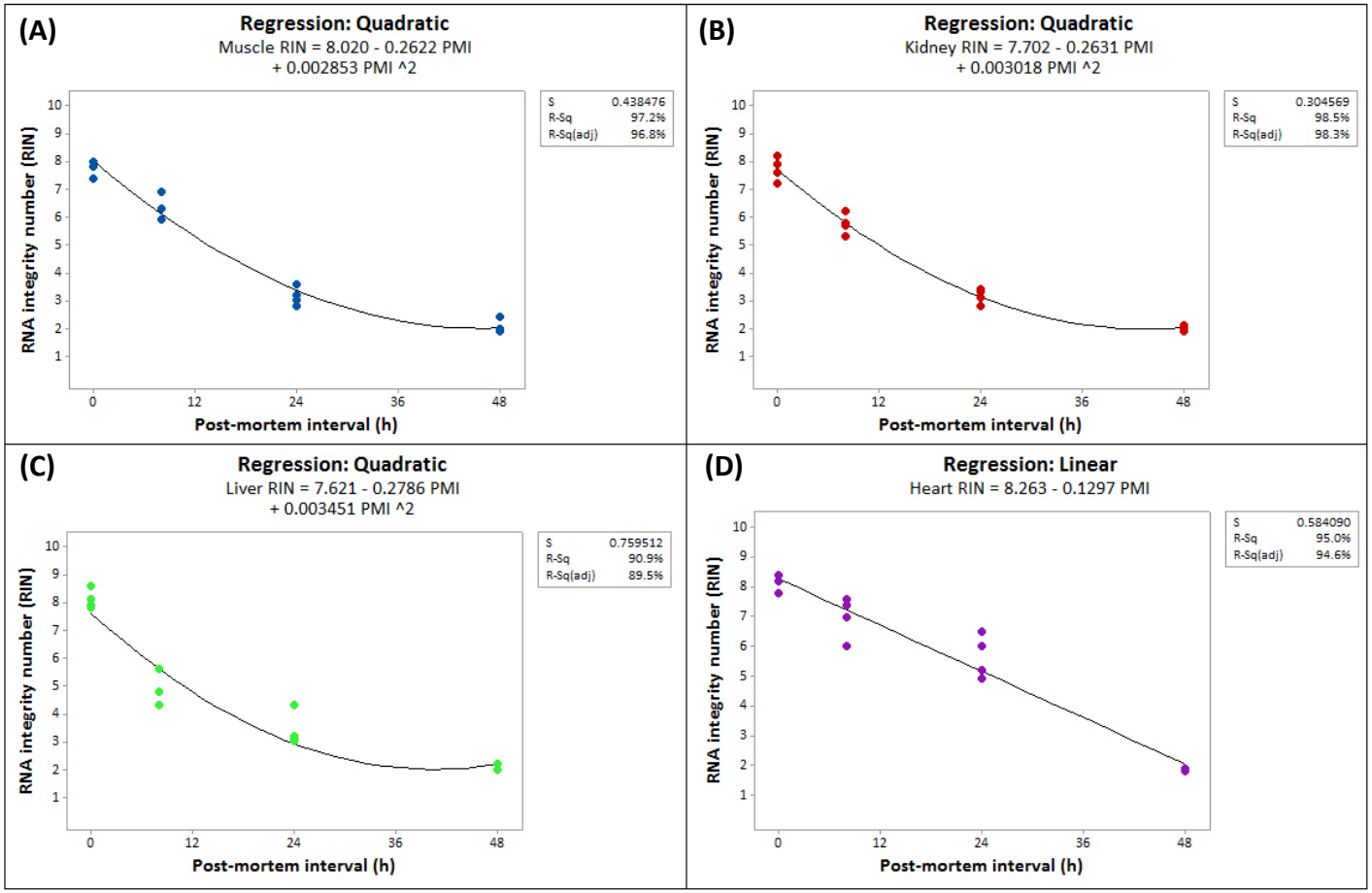

Figure 6.3: **Regression analysis of post-mortem RNA quality data for (A) skeletal muscle (blue data points), (B) kidney (red data points), (C) liver (green data points) and (D) heart (purple data points).** Tissue samples were collected until 48 hours post-mortem for animals decomposed at 22 °C. Data illustrates RNA quality as measured by the RIN algorithm on the Bioanalyzer 2100 for n = 4 per time point.

6.3.1.3 Degradation of endogenous control RNAs: RT-qPCR

The third feature of the transcriptome to be assessed in post-mortem skeletal muscle, kidney, liver and heart tissue samples was the expression of two endogenous control RNAs: 18S rRNA and Gapdh. The data presented in Section 5.3.4, Chapter 5 demonstrated that of a panel of six endogenous control RNAs, 18S rRNA was the least susceptible to degradation; determined by quantification of its expression in skeletal muscle collected after post-mortem intervals of up to 72 hours.

Using a new set of mouse subjects, this has been confirmed in the data presented in Figure 6.4. Figure 6.4 shows that the mean C_Q for 18S rRNA did not increase significantly (as determined by means of a one-way ANOVA) over the first 48 hours post-mortem in either of skeletal muscle ($p = 0.776$) or heart ($p = 0.989$). In kidney and liver, the mean 18S rRNA C_Q did not increase appreciably over the first 24 hours through degradation. A significant increase in mean C_Q could only be detected after 48 hours post-mortem in kidney and liver (one-way ANOVA with Fisher's Least Significant Difference test, $p = 0.013$ and 0.000 respectively).

Similarly, Table 6.2 demonstrates this data in the form of a ΔC_Q for each post-mortem interval relative to the control point (post-mortem interval < 0.25 hours), to improve the ease with which the increment in C_Q can be visualised. Only the 48 hour post-mortem interval duration in the kidney and liver tissue types gave a ΔC_Q indicative of a biological reduction in their expressed quantity. All other ΔC_Q points were within normal qPCR data variability.

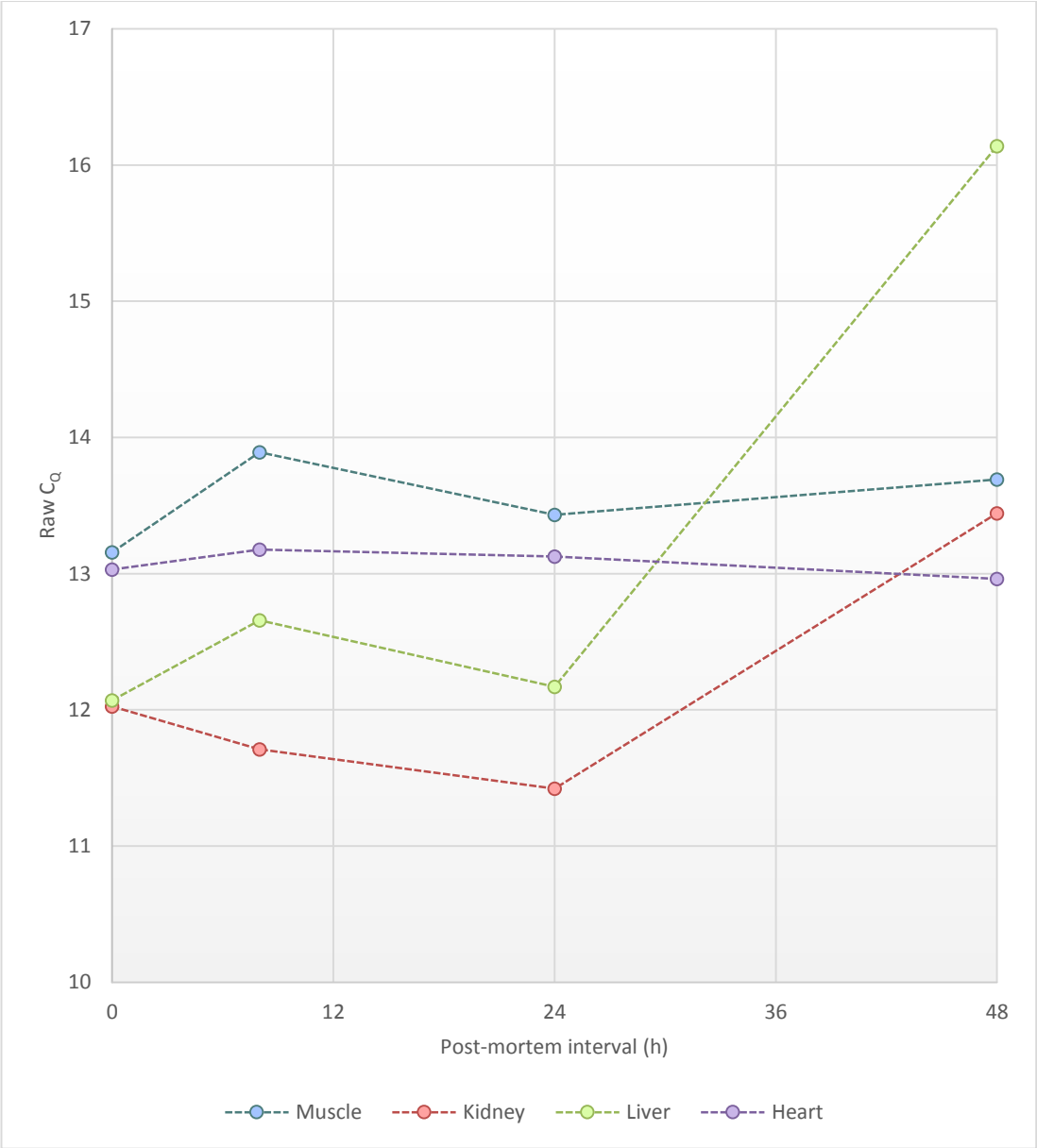

Figure 6.4: **Degradation of 18S rRNA in skeletal muscle (blue data points), kidney (red data points), liver (green data points) and heart (purple data points).** Tissue samples were collected until 48 hours post-mortem for animals decomposed at 22 °C. Data represents the mean C_Q for n = 4. Error bars have been omitted for clarity.

Table 6.2: **Mean ΔC_Q for 18S rRNA in skeletal muscle, kidney, liver and heart tissue decomposed *in vivo* at 22 °C for up to 48 hours**. Data represents the mean ΔC_Q for n = 4.

Post-mortem interval duration (hours)	Skeletal muscle	Kidney	Liver	Heart
8	0.73	-0.32	0.59	0.15
24	0.27	-0.61	0.10	-0.10
48	0.53	1.41	4.07	-0.07

Overall, this data provides evidence that 18S rRNA degradation is more prominent in post-mortem kidney and liver than it is in skeletal muscle and heart.

Gapdh mRNA was selected for analysis in response to its high level of instability, demonstrated in Section 5.3.4, Chapter 5. As presented in Figure 6.5, the degradation profile of Gapdh mRNA in mouse skeletal muscle, kidney, liver and heart is very different from that of 18S rRNA. Gapdh mean C_Q exhibits a steady increase over time in all four tissue types (Figure 6.5). This reproduces the outcomes of Section 5.3.4, Chapter 5 which demonstrated differential stability of 18S rRNA in Gapdh in skeletal muscle only. As such, it can be concluded that this differential stability is likely to be an organism-wide phenomenon, and not restricted to specific tissue types. The data was analysed using a one-way ANOVA and Fisher's Least Significant Difference test. For skeletal muscle and liver, mean Gapdh C_Q exhibited a significant increase at 24 and 48 hours ($p = 0.000$ and 0.000 respectively). This significant increase was not seen for heart until 48 hours post-mortem ($p = 0.000$), but occurred earlier at only 8 hours for kidney ($p = 0.000$).

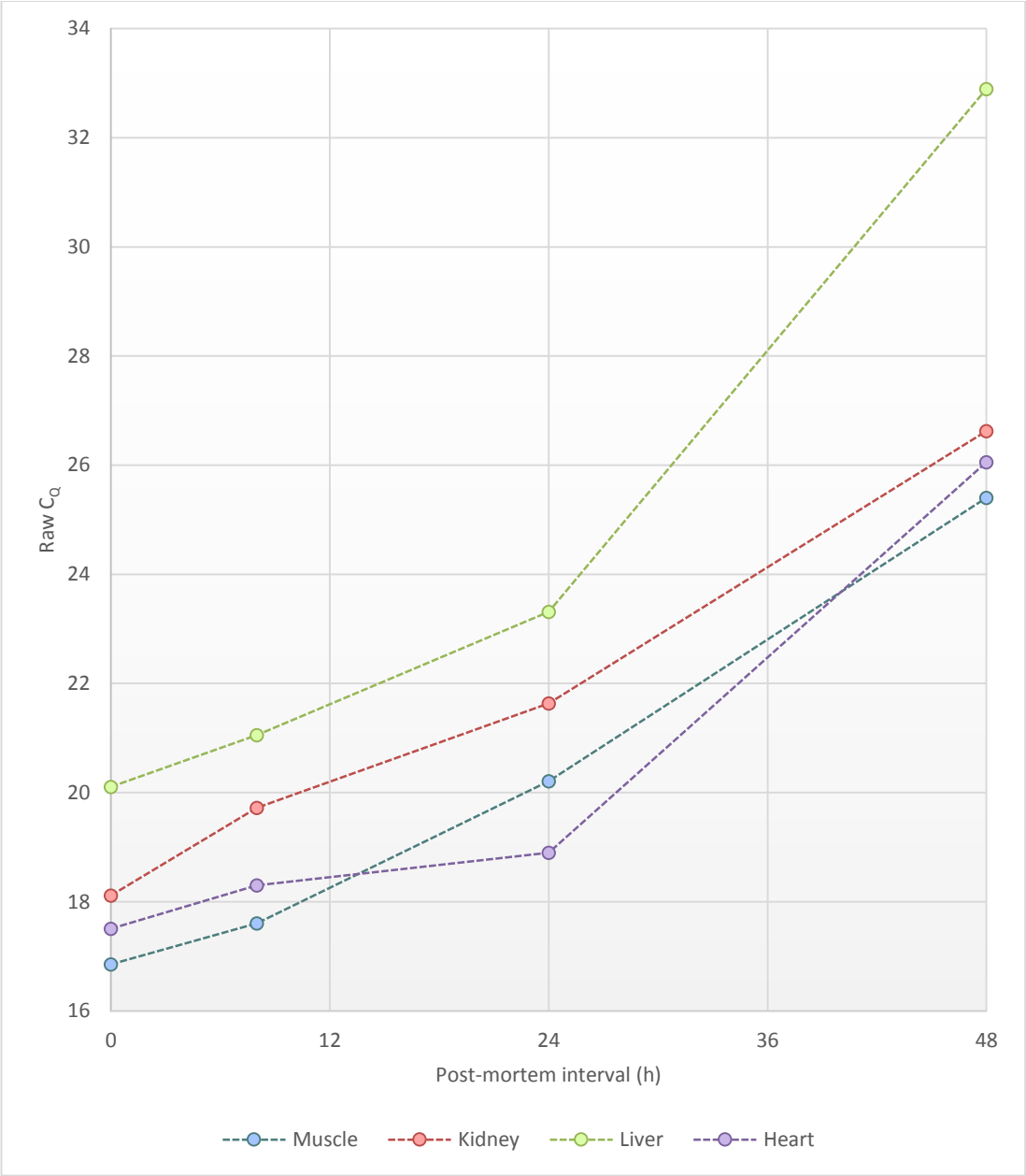

Figure 6.5: **Degradation of Gapdh mRNA in skeletal muscle (blue data points), kidney (red data points), liver (green data points) and heart (purple data points).** Tissue samples were collected until 48 hours post-mortem for animals decomposed at 22 °C. Data represents the mean C_Q for n = 4. Error bars have been omitted for clarity.

In order to more clearly visualise the increase in C_Q relative to the control point (post-mortem interval < 0.25 hours), the mean increment in C_Q (ΔC_Q) for all four tissue types is displayed in Table 6.3. This shows that the magnitude of increase in Gapdh C_Q over the maximum 48 hour post-mortem interval is most

notable for liver, followed by skeletal muscle and kidney. Heart tissue exhibited the lowest ΔC_Q at all three time points examined (Table 6.3).

Table 6.3: **Mean ΔC_Q for Gapdh mRNA in skeletal muscle, kidney, liver and heart tissue decomposed *in vivo* at 22 °C for up to 48 hours**. Data represents the mean ΔC_Q for n = 4.

Post-mortem interval duration (hours)	Skeletal muscle	Kidney	Liver	Heart
8	0.95	1.60	0.96	0.79
24	3.36	3.51	3.22	1.39
48	8.85	8.71	12.79	8.55

6.3.1.4 Discussion: Effect of tissue type on RNA degradation

In summary, this work has illustrated that RNA is best protected against degradation in heart and skeletal muscle tissue. In both tissue types, the yield of RNA was found not to decline over the 48 hour post-mortem interval investigated. Their decline in RNA quality as quantified using the RNA integrity number was slower in onset and of reduced severity. In both tissue types, 18S rRNA exhibited no reduction in yield during this time. Although Gapdh did exhibit a marked reduction in yield over the 48 hour post-mortem interval this reduction was less pronounced than for other tissue types; Gapdh mRNA being best preserved in heart tissue. It is likely that RNA is more stable in fibrous tissue types such as skeletal and cardiac muscle because of their reduced metabolic activity in this sense, with much of their enzyme activity focused on energy release.

On the other hand, both kidney and liver RNA exhibited a significant decline in RNA yield, particularly between 24 to 48 hours post-mortem. Liver RNA displayed earlier onset of RNA degradation than all other tissue types. In addition, the loss of amplifiable 18S rRNA and Gapdh mRNA was most pronounced in liver. This outcome is not surprising; liver RNA is proposed to be highly susceptible to degradation because of the high abundance of RNases in hepatocytes (85, 127).

On the whole, these outcomes are in agreement with previous publications which have touched upon the topic of tissue-specific RNA degradation. Heinrich *et al*. (72, 82) identified skeletal muscle as the source of the highest quality RNA from human tissues, followed by heart and brain tissue. Bahar *et al*. (85) also ascertained that skeletal muscle was the best bovine tissue source, with liver and adipose tissue exhibiting quicker onset and more severe RNA degradation post-mortem. Inoue *et al*. (233) concluded that rat brain tissue exhibited the slowest rate of decay, followed closely by heart and lung. Their work identified liver RNA as most susceptible to RNA degradation. Similarly, Itani *et al*. (258) confirmed that DNA is degraded most quickly in liver and kidney.

Unfortunately, none of these studies have used the RNA integrity number as a fully quantitative and sensitive measure of RNA quality to make these inferences, meaning that their conclusions are largely subjective. One of the only studies to do so is that of Sampaio-Silva *et al*. (6), who categorised mouse tissue types based upon their RNA decay behaviour using the RNA Quality Index (RQI, a competitor to RIN). In their study limited only to the first 11 hours post-mortem heart RNA was deemed most stable, followed by liver and muscle (kidney was not examined). During this time, Sampaio-Silva *et al*. pertain that RNA degradation follows a linear profile. By extending the post-mortem interval from 11 hours up to 48 hours the outcomes of this work refute this, with skeletal muscle, kidney and liver tissue RNA decaying instead in a sigmoidal (Section 5.3.3, Chapter 5) or polynomial fashion. This is as one might expect, where the quality of RNA drops most significantly in the immediate period after death, and tails off near the end of the RNA integrity number scale after extended post-mortem intervals. This type of relationship between RNA quality and post-mortem interval is not nearly as informative for estimating the time since death.

RNA quality analysis on the Bioanalyzer 2100 platform is used as a key screening technique to determine whether RNA samples are sufficiently intact to merit gene expression analysis. As discussed at length in Section 5.3.2.4, Chapter 5, several minimum RIN thresholds have been suggested in the literature. Weis *et al*. (138) suggested an optimum minimum RIN of 3.95. Fleige *et al*. on the other hand,

suggested RIN 5 as being a more appropriate minimum threshold (128, 212). Applying these two suggested minimum RIN thresholds to the data illustrates a wide spectrum of possible post-mortem intervals after which the RNA may be considered too fragmented to be of informative value – shown in Table 6.4.

Table 6.4: **Estimated post-mortem intervals during which RNA quality remains sufficient for gene expression analysis using the minimum RIN thresholds suggested by Weis *et al*. (138) and Fleige *et al*. (128, 212).** Post-mortem intervals have been derived from the equation of the regression line describing the relationship between post-mortem interval and RNA quality for skeletal muscle, kidney, liver and heart; presented in Figure 6.3.

	Post-mortem interval to reach threshold minimum RIN	
	Weis *et al*. (138) RIN threshold: **3.95**	Fleige *et al*. (128) RIN threshold: **5**
Muscle	19.8 hours	13.5 hours
Kidney	18.0 hours	11.9 hours
Liver	16.6 hours	10.9 hours
Heart	33.3 hours	25.2 hours

From the perspective of forensic pathology, clearly the major tissue types of diagnostic interest are those such as heart and brain whose dysfunction is most often the cause of death. The outcomes of this research suggest that RNA is best preserved in heart tissue, with an estimated 25.2 to 33.3 hour window during which RNA is of sufficient quality for gene expression analysis; using these published RIN thresholds as a cut-off point (Table 6.4). Clearly, this is an encouraging outcome showing the future potential of gene expression analysis in forensic pathology.

6.3.2 *In vivo* and *ex vivo* RNA degradation behaviour

6.3.2.1 Total RNA quality: Bioanalyzer 2100

The onset and rate of RNA degradation was compared in *in vivo* and *ex vivo* decomposed samples of skeletal muscle, kidney, liver and heart to try to determine whether RNA decay behaviour is appreciably different across the two experimental design strategies. Figures 6.6 and 6.7 present the results of total RNA quality analysis where tissue samples were collected after decomposition under each of these two conditions up to a maximum post-mortem interval of 48 hours.

Figure 6.6A demonstrates that where skeletal muscle was excised from the body prior to decomposition, total RNA fragmentation was much quicker in onset and higher in severity. In samples decomposed *in vivo*, RNA quality fell from mean RIN 7.80 to 6.50 during the first 8 hours post-mortem; whereas in *ex vivo* tissue samples this reduction in RNA quality was much more pronounced, falling to mean RIN 3.45. This difference was deemed to be statistically significant using a 2-sample t-test ($p = 0.001$). This significantly improved total RNA quality in *in vivo* skeletal muscle (mean RIN 3.15) was maintained up to 24 hours post-mortem (2-sample t-test, $p = 0.018$). Unexpectedly, skeletal muscle RIN rose from mean 2.4 to 3.7 upon extension of the post-mortem interval from 24 to 48 hours; the reason for which is not immediately clear. However, these samples were subjected to repeat RIN analysis to eliminate the possibility of any handling error; providing identical results.

For kidney, no significant difference was observed in mean RIN between *in vivo* and *ex vivo* decomposed tissue samples during the first 8 hours post-mortem (2-sample t-test, $p = 0.67$) (Figure 6.6B). In contrast to the trend described in skeletal muscle, at both 24 and 48 hours post-mortem the mean RIN of *ex vivo* decomposed kidney was deemed to be significantly higher than that of *in vivo* kidney (2 sample t-test, $p = 0.000$, 0.024 respectively).

Figure 6.7C demonstrates that the quality of RNA obtained from liver tissue decomposed *in vivo* is consistently higher than that of *ex vivo* liver, at all post-mortem periods examined. This difference was only deemed to be statistically

significant at the 8 hour time point, not at 24 or 48 hours (2-sample t-test, p = 0.048, 0.104 and 0.144 respectively). In liver, the RINs converged at around 2 after 48 hours post-mortem, indicative of extremely poor RNA quality.

Similarly, *in vivo* decomposed heart tissue exhibited significantly improved quality after 8 hours post-mortem relative to *ex vivo* heart (2-sample t-test, p = 0.019) (Figure 6.7D). This difference was not however maintained beyond 8 hours; with no significant difference in RIN detected at the 24 and 48 hour time points (2-sample t-test, p = 0.301 and 0.106 respectively).

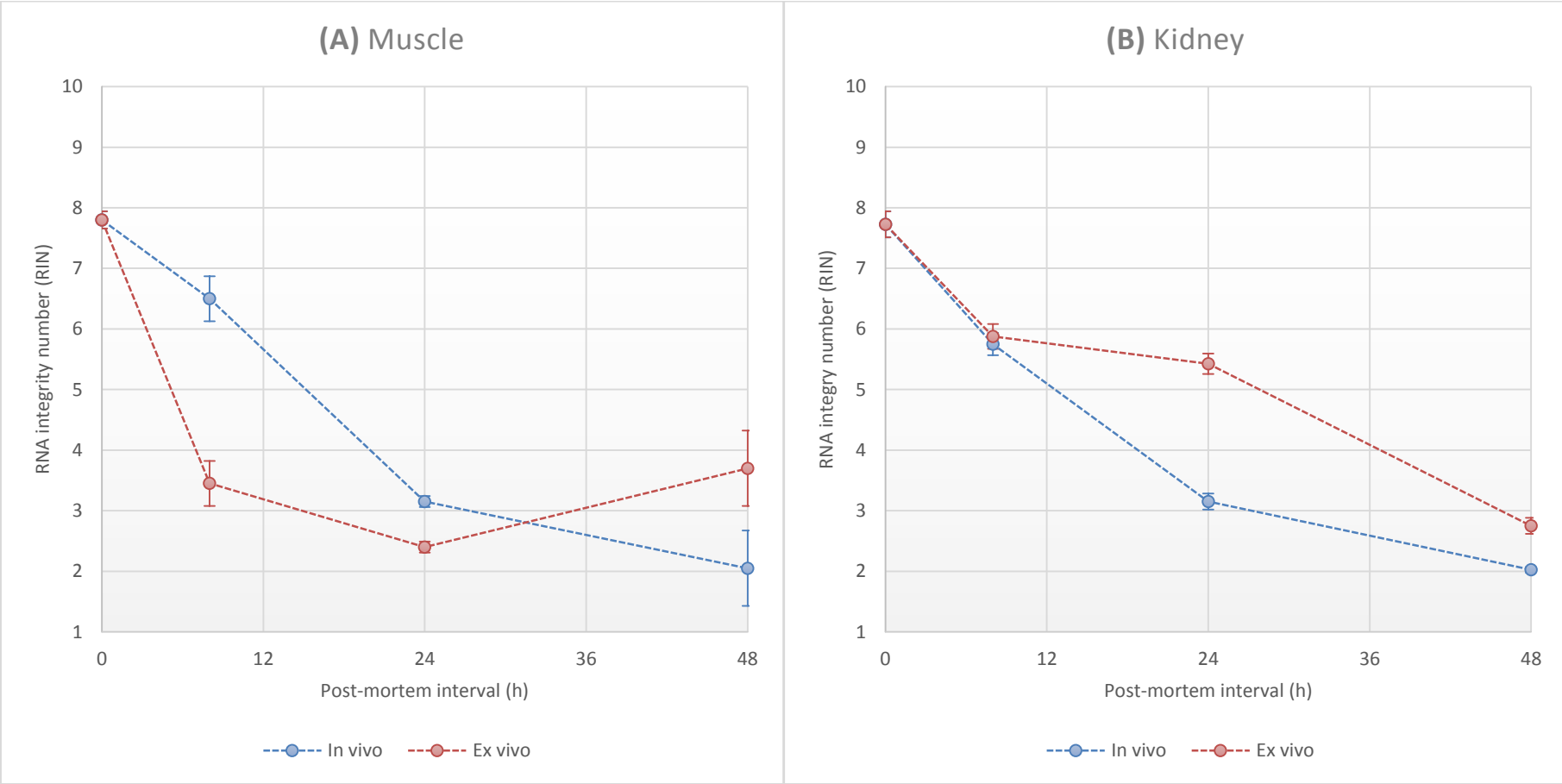

Figure 6.6: **Quality of RNA extracts from (A) skeletal muscle and (B) kidney tissue collected until 48 hours post-mortem, for animals decomposed *in vivo* (blue data points) and *ex vivo* (red data points) at 22 °C.** Points represent RNA quality as quantified by the Bioanalyzer 2100 using the RNA integrity number (RIN) algorithm. Data represents mean ± S.E. for n = 4.

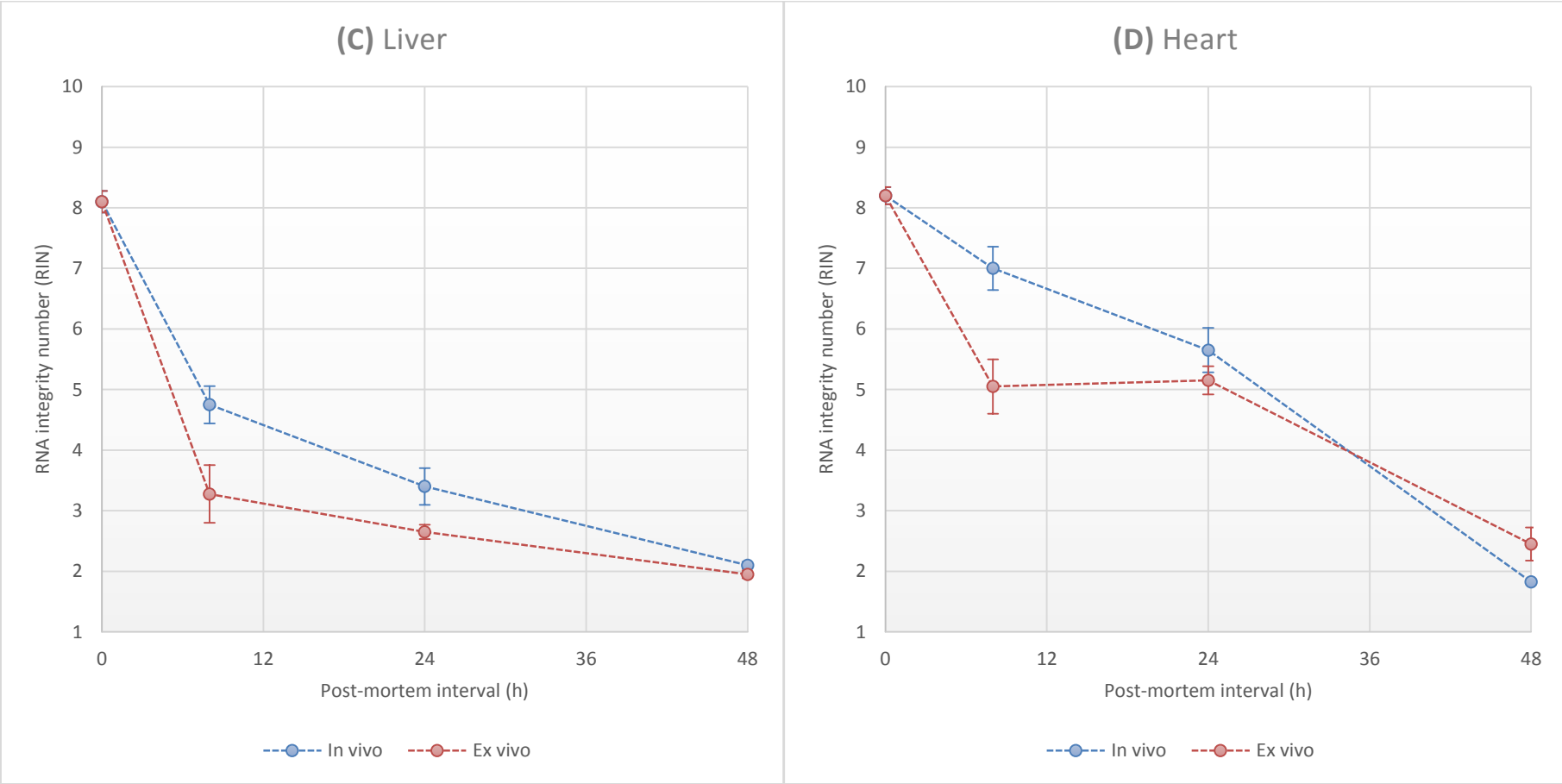

Figure 6.7: **Quality of RNA extracts from (C) liver and (D) heart tissue collected until 48 hours post-mortem, for animals decomposed *in vivo* (blue data points) and *ex vivo* (red data points) at 22 °C.** Points represent RNA quality as quantified by the Bioanalyzer 2100 using the RNA integrity number (RIN) algorithm. Data represents mean ± S.E. for n = 4.

For all four tissue types, it was observed from the raw data that the fragmentation of RNA appeared to be more severe in *in vivo* decomposed tissues at the longest post-mortem interval of 48 hours. This is illustrated in Figure 6.8, which displays the raw electropherogram outputs from the Bioanalyzer 2100. It has been already demonstrated that at the lower end of the RIN spectrum, the algorithm loses the ability to sensitively detect and quantify further RNA fragmentation (Section 5.3.3, Chapter 5). This issue is highlighted in Figure 6.8, where the RNA fragment size distribution for eight tissue samples is presented – all of which returned similar RINs in the range between 1.8 and 2.8. Many of those tissue samples decomposed *in vivo* (top row) exhibit RNA fragments in a smaller size range with the electropherogram shifted to the left; relative to those decomposed *ex vivo* (bottom row).

Overall, this data does not consistently demonstrate that the preservation state of RNA is better when tissue samples were decomposed either *ex vivo* or *in vivo*. In skeletal muscle, liver and heart, the trend in RIN seems to suggest that the onset and severity of RNA is less pronounced in *in vivo* tissues; particularly at the earliest post-mortem intervals. However, any observed improvement in RIN under this experimental design was lost after 48 hours post-mortem, when the RINs tended to converge at the lower end of the spectrum. On the other hand, kidney RNA exhibited an opposing trend; where no significant difference in RIN was observed initially between the *in vivo* and *ex vivo* groups. Upon extension of the post-mortem interval beyond 8 hours it was in fact the *ex vivo* decomposed tissue that exhibited better quality RNA.

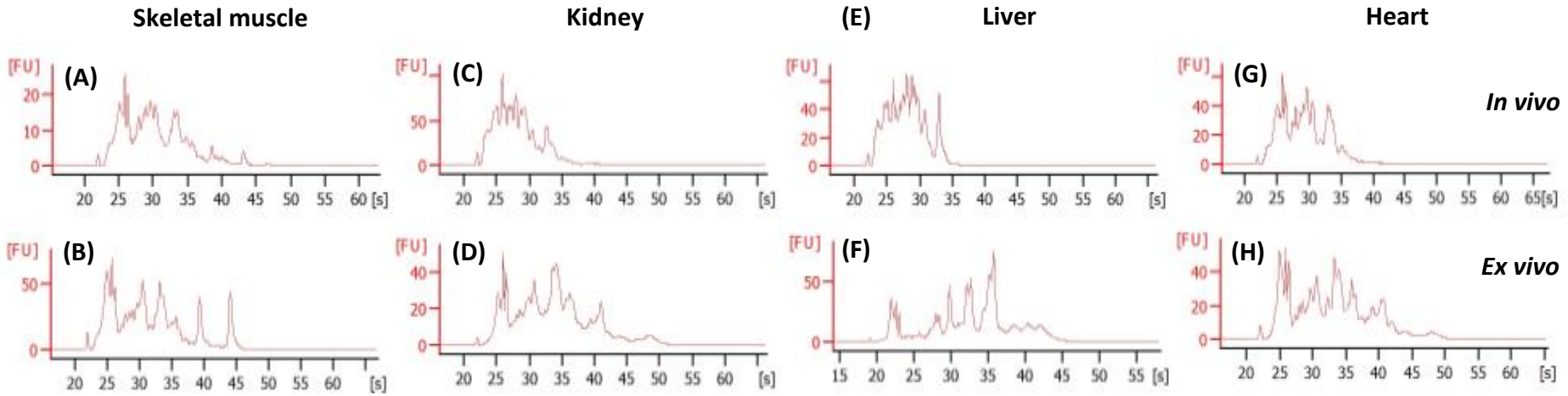

Figure 6.8: **Total RNA quality for tissue samples collected after a 48 hour post-mortem interval: (A) skeletal muscle, *in vivo*, (B) skeletal muscle, *ex vivo*, (C) kidney, *in vivo*, (D) kidney, *ex vivo*, (E) liver, *in vivo*, (F) liver, *ex vivo*, (G) heart, *in vivo* and (H) heart, *ex vivo***. Data presented in the form of the Bioanalyzer 2100 electropherogram output. Data represents one replicate of n = 4 for each condition. All eight tissue samples returned a RIN between 1.8 and 2.8, indicative of extremely poor RNA quality.

6.3.2.2 Degradation of endogenous control gene RNAs: RT-qPCR

The RNA quality data described demonstrates that during the early post-mortem interval, *in vivo* and *ex vivo* decomposed tissues exhibit different degrees of RNA fragmentation. However, it has been shown that the RIN algorithm is poorly sensitive to severe degradation (Section 5.3.3, Chapter 5), and is unable to accurately quantify the high level of fragmentation incurred after extended post-mortem intervals. Such advanced RNA degradation would be expected to cause a reduction in the detectable quantity of 18S rRNA and Gapdh mRNA, measured by RT-qPCR amplification. The expression of both was assessed in *in vivo* and *ex vivo* decomposed skeletal muscle, kidney, liver and heart, to characterise and compare their degradation profiles across the two experimental designs (Figure 6.9, 6.10, 6.11 and 6.12).

Figure 6.9 displays the raw RT-qPCR results upon amplification of 18S rRNA and Gapdh from *in vivo* and *ex vivo* decomposed skeletal muscle. It was found that in *in vivo* decomposed tissue, the mean 18S rRNA C_Q did not rise appreciably over the 48 hour interval examined (one-way ANOVA, p = 0.776) (Figure 6.9A). Only after 48 hours post-mortem was a small but significant increment in mean 18S rRNA C_Q observed in *ex vivo* decomposed skeletal muscle, relative to the control point (one-way ANOVA with Dunnett's Multiple Comparisons with a Control, p = 0.012). At none of the three time points was a significant difference in mean C_Q identified when compared between *in vivo* and *ex vivo* tissues (2 sample T-Test, p = 0.178, 0.566 and 0.163 for 8, 24 and 48 hours respectively). Overall, the RT-qPCR data does not provide any substantive evidence of 18S rRNA degradation at all in skeletal muscle (Figure 6.9A); let alone differential *in/ex vivo* degradation. On the converse, a strong positive correlation was observed between post-mortem interval and Gapdh C_Q in both experimental groups (Pearson's product moment correlation coefficient r = 0.963, p = 0.000; r = 0.906, p = 0.000 for *in vivo* and *ex vivo* respectively) (Figure 6.9B). Despite this evidence of considerable Gapdh mRNA fragmentation, at no point post-mortem did the mean C_Q differ significantly between the two groups (2 sample t-test, p = 0.071, 0.123 and 0.713 for each of 8,

24 and 48 hours). Overall, this data suggests that in skeletal muscle decomposed *in vivo* and *ex vivo*, Gapdh degradation behaviour is similar (Figure 6.9B).

RT-qPCR data for *in vivo* and *ex vivo* decomposed kidney tissue is presented in Figure 6.10. In *ex vivo* decomposed tissue, the mean 18S rRNA C_Q did not rise appreciably over the 48 hour time interval (one-way ANOVA, p = 0.071) (Figure 6.10A). Only after 48 hours post-mortem was a small increase in mean 18S rRNA C_Q observed for *in vivo* decomposed kidney (one-way ANOVA with Fisher's Least Significant Difference test, p = 0.013). No significant difference was observed between mean 18S rRNA C_Q for *in vivo* and *ex vivo* kidney at 8 or 24 hours (2 sample t-test, p = 0.096 and 0.626), but *in vivo* kidney exhibited a significantly higher mean 18S rRNA C_Q of 13.44 than *ex vivo* kidney at 48 hours post-mortem (2 sample t-test, p = 0.022). Similar to skeletal muscle, a strong positive linear correlation was characterised between post-mortem interval and Gapdh C_Q in both experimental groups (Pearson's product moment correlation coefficient, r = 0.974, p = 0.000; r = 0.869, p = 0.000 for *in vivo* and *ex vivo* kidney respectively) (Figure 6.10B). *In vivo* decomposed kidney samples exhibited a significantly higher mean C_Q at all three time points (2 sample t-test, p = 0.023, 0.001 and 0.000 for each of 8, 24 and 48 hours). This provides evidence that Gapdh mRNA degradation is more severe in *in vivo* kidney than it is for those tissue samples decomposed out with the mouse corpse (Figure 6.10B).

Comparable outcomes were observed upon analysis of 18S rRNA and Gapdh mRNA behaviour in post-mortem liver tissue, as illustrated in Figure 6.11. 18S rRNA only displayed overt evidence of degradation in *in vivo* decomposed tissue, after 48 hours post-mortem (one-way ANOVA with Dunnett's Multiple Comparisons with a Control, p = 0.000) (Figure 6.11A). At 8 and 48 hours post-mortem, *in vivo* decomposed liver exhibited a significantly higher mean 18S rRNA C_Q than *ex vivo* liver (2 sample t-test, p = 0.024 and 0.002). A strong positive correlation was observed between Gapdh C_Q and post-mortem interval (Pearson's product moment correlation coefficient, r = 0.966, p = 0.000; r = 0.800, p = 0.000 for each of *in vivo* and *ex vivo* liver) (Figure 6.11B). *In vivo* decomposed liver exhibited a significantly

higher mean Gapdh C_Q than for *ex vivo* decomposed liver, but only at the 48 hour post-mortem interval time point (2 sample t-test, p = 0.029).

Finally, Figure 6.12 presents the RT-qPCR data upon amplification of 18S rRNA and Gapdh mRNA from heart tissue. No detectable degradation of 18S rRNA was observed in heart tissue, in the form of no significant increment in mean C_Q for either of *in vivo* or *ex vivo* decomposed heart tissue (one-way ANOVA, p = 0.989 and 0.377 respectively (Figure 6.12A). For Gapdh, degradation only became apparent after 48 hours post-mortem, characterised by a sharp and statistically significant increase in mean Gapdh C_Q for both *in vivo* and *ex vivo* heart (one-way ANOVA with Dunnett's Multiple Comparisons with a Control, p = 0.000 and 0.012). The decay behaviour of Gapdh was deemed to be consistent between the two experimental designs, with no significant difference in mean C_Q observed for any of the three post-mortem intervals examined (2 sample t-test, p = 0.178, 0.566 and 0.163).

In summary, the RT-qPCR data (Figure 6.9 to 6.12) revealed that in skeletal muscle and heart tissue, removal of tissues from the mouse corpse prior to decomposition had no statistically significant effect on the detected quantity of 18S rRNA and Gapdh mRNA, over the first 48 hours post-mortem. On the contrary, 18S rRNA and Gapdh mRNA exhibited improved long-term preservation in the kidney and liver tissue samples which were decomposed *ex vivo*, in a microcentrifuge tube.

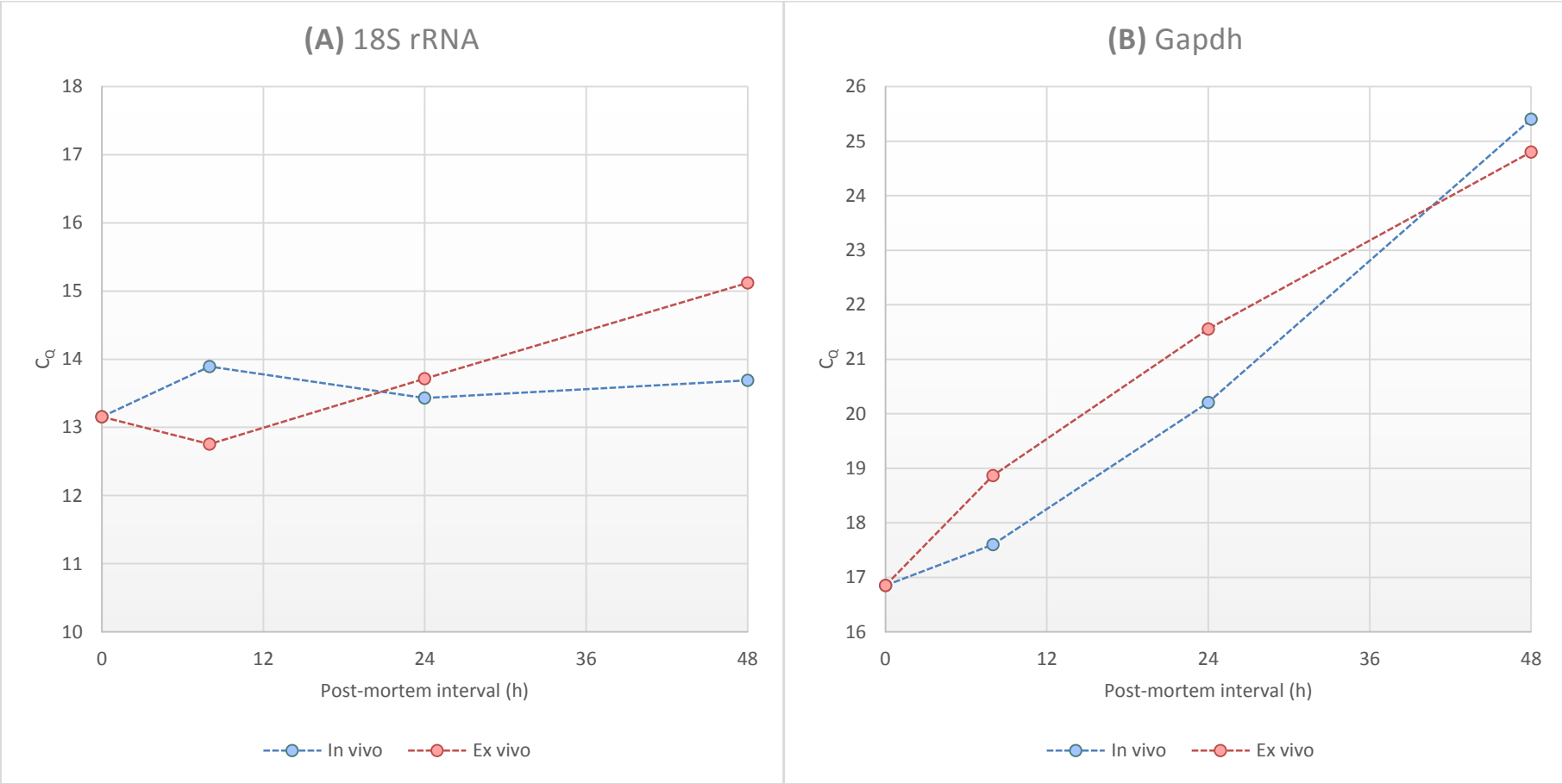

Figure 6.9: **Raw C_Q data for (A) 18S rRNA and (B) Gapdh expression in skeletal muscle collected until 48 hours post-mortem, for animals decomposed *in vivo* (blue data points) and *ex vivo* (red data points) at 22 °C.** Points represent the mean C_Q for n = 4. Error bars have been omitted for clarity.

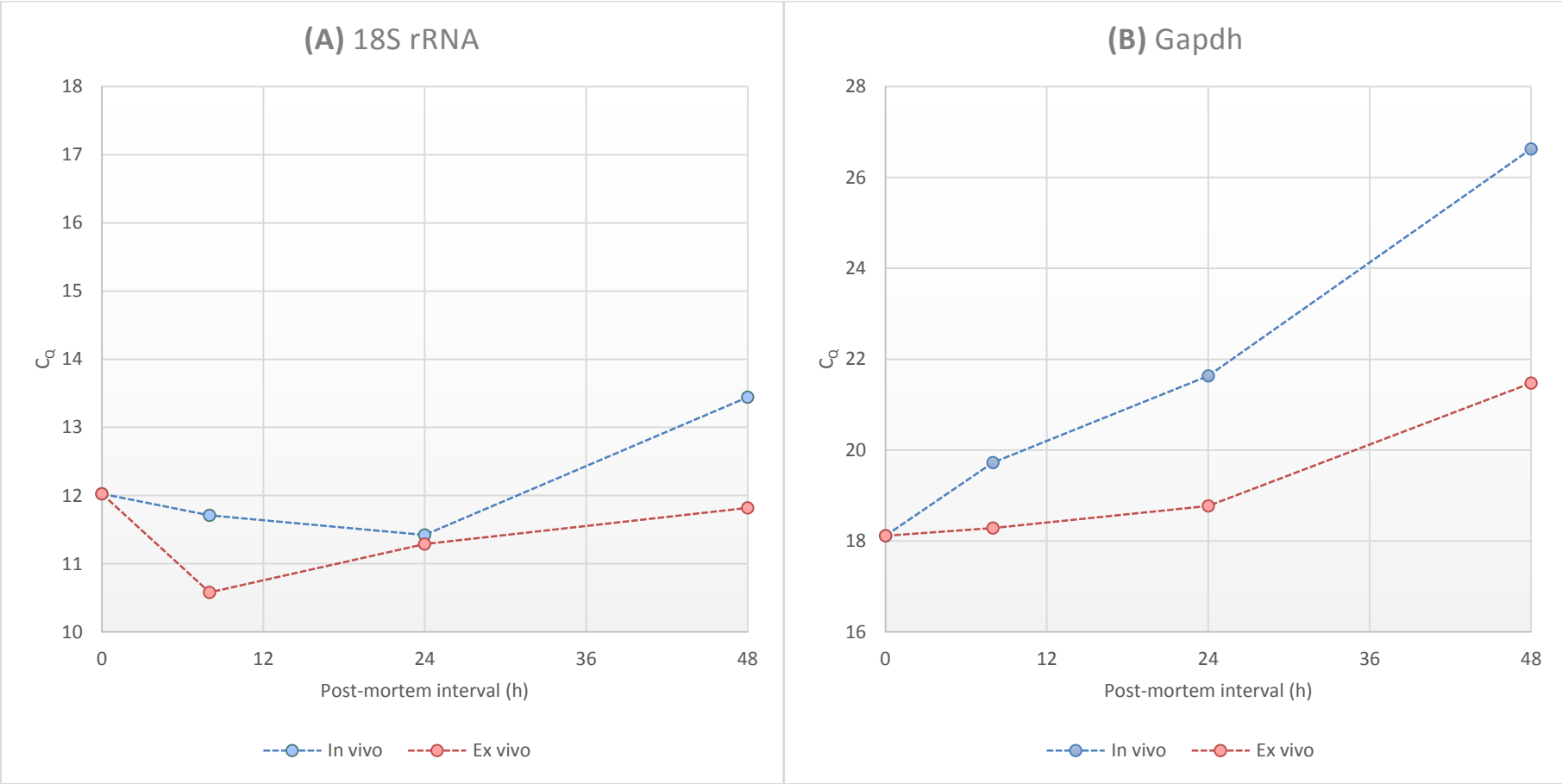

Figure 6.10: **Raw C_Q data for (A) 18S rRNA and (B) Gapdh expression in kidney collected until 48 hours post-mortem, for animals decomposed *in vivo* (blue data points) and *ex vivo* (red data points) at 22 °C.** Points represent the mean C_Q for n = 4. Error bars have been omitted for clarity.

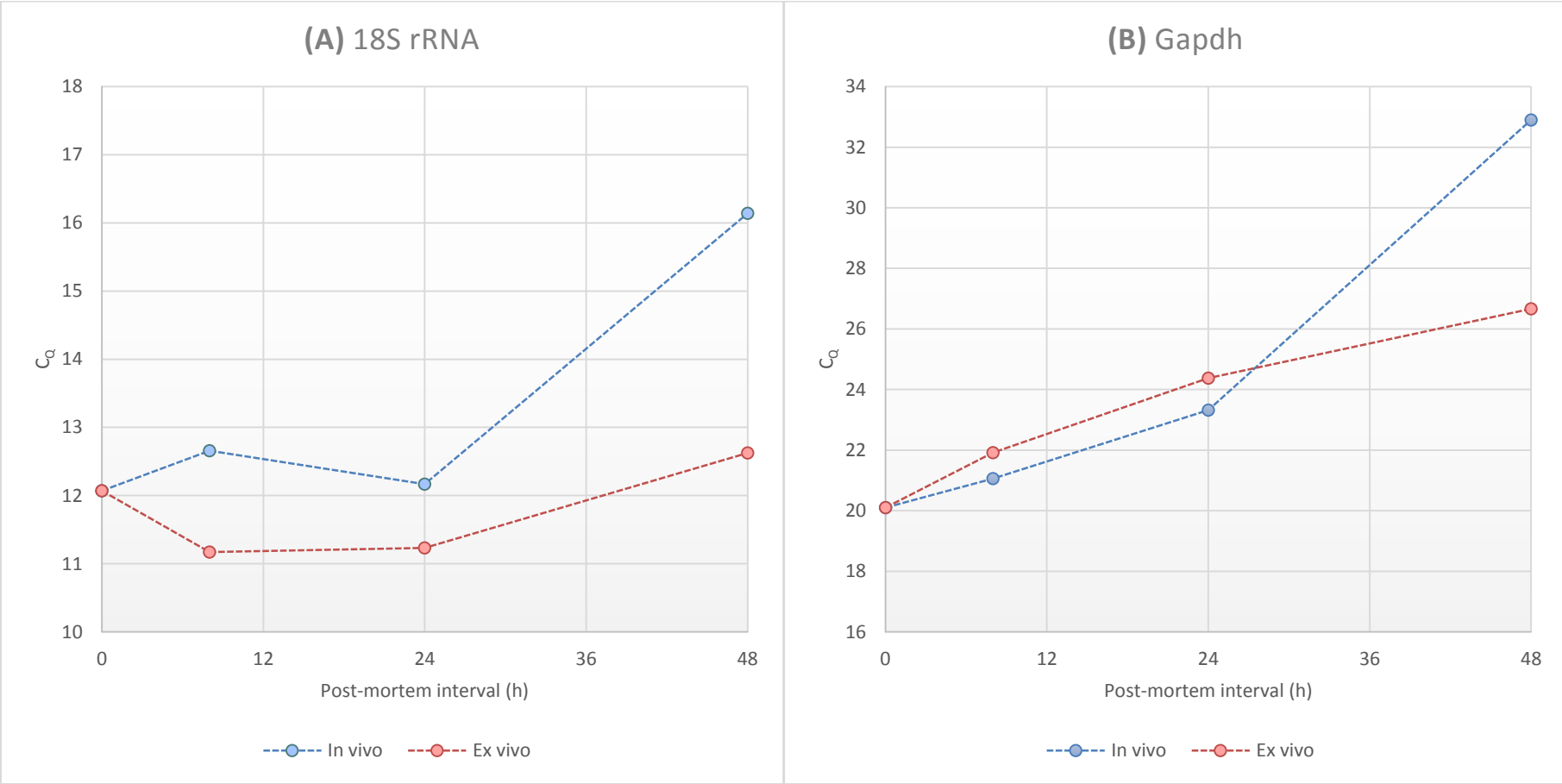

Figure 6.11: **Raw C_Q data for (A) 18S rRNA and (B) Gapdh expression in liver collected until 48 hours post-mortem, for animals decomposed *in vivo* (blue data points) and *ex vivo* (red data points) at 22 °C.** Points represent the mean C_Q for n = 4. Error bars have been omitted for clarity.

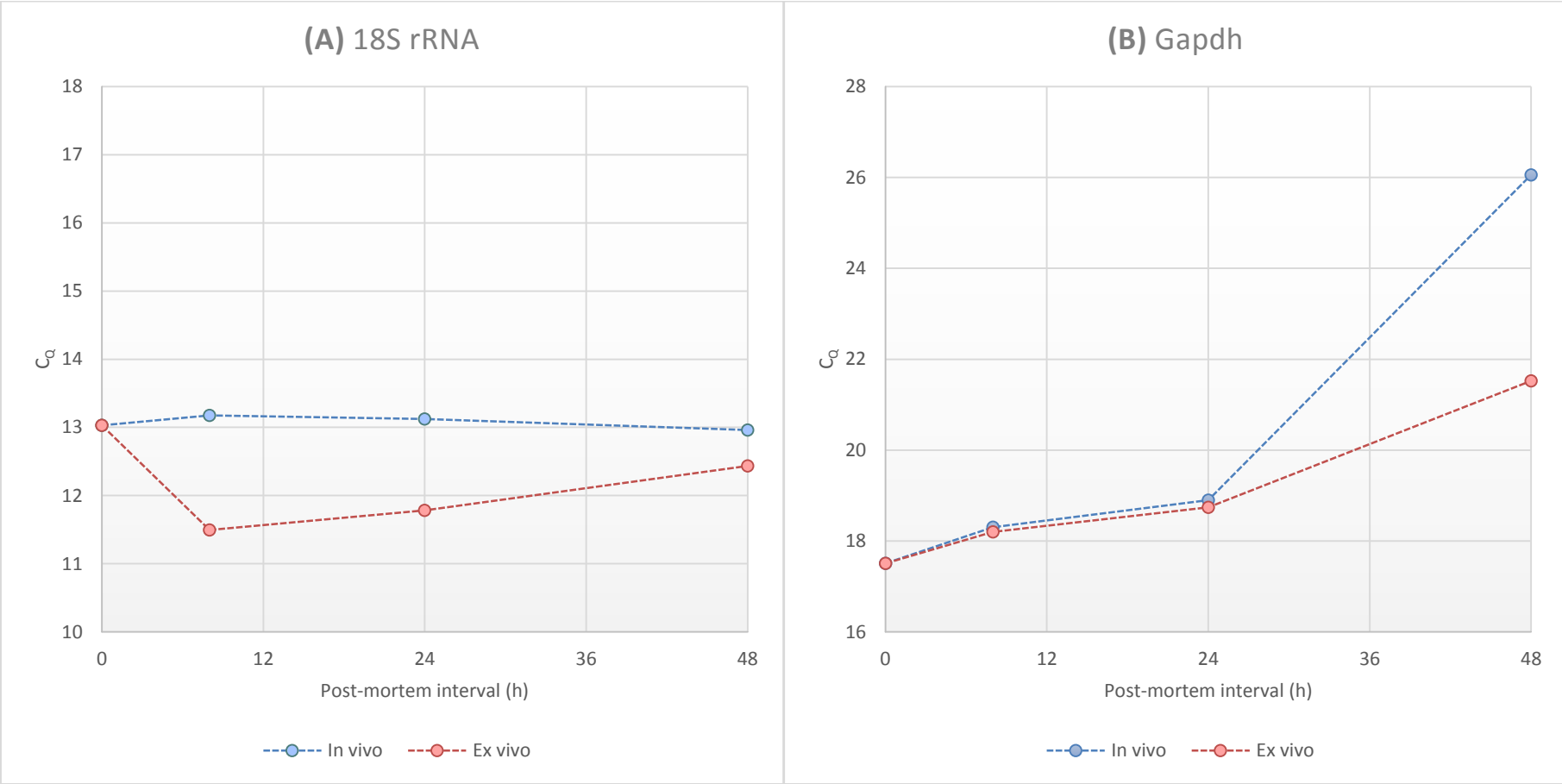

Figure 6.12: **Raw C_Q data for (A) 18S rRNA and (B) Gapdh expression in heart collected until 48 hours post-mortem, for animals decomposed *in vivo* (blue data points) and *ex vivo* (red data points) at 22 °C.** Points represent the mean C_Q for n = 4. Error bars have been omitted for clarity.

6.3.2.3 Discussion: *In vivo* and *ex vivo* RNA decay behaviour

The use of an *ex vivo* decomposition model confers many practical advantages to the study of post-mortem tissue biology; not restricted to the field of molecular genetics. When working with animals, it greatly reduces the number of subjects required for experimentation. It also presents the opportunity to conduct similar 'time wise' studies with human autopsy tissue; where it is not ethically admissible to do this using a cadaver. The use of these *ex vivo* decomposition models is steadily gaining momentum in the forensic literature; as highlighted in Table 6.1 (Section 6.1.1, Chapter 6).

However, very little effort has been expended in validating the use of *ex vivo* decomposition models in the field of forensic molecular genetics. The only study attempting to do so is that of Sampaio-Silva *et al*. (6). Using mouse skeletal muscle of post-mortem interval up to 11 hours as a tissue substrate, Sampaio-Silva *et al*. pertained that removal of tissues from the corpse had no significant effect on their ability to estimate post-mortem interval, using a predictive model based on the detectable quantity of a panel of mRNAs by RT-qPCR. However, in this study the number of tissue samples examined was very limited, no other tissue types than skeletal muscle were considered, and the time span was restricted to only 11 hours post-mortem (6). This chapter has assessed RNA degradation behaviour during the first 48 hours post-mortem across the two experimental conditions: *in vivo* and *ex vivo* decomposition, for each of skeletal muscle, kidney, liver and heart.

It was found that early in the post-mortem period total RNA quality was improved in *in vivo* decomposed skeletal muscle, liver and heart (Figure 6.6, 6.7). The opposite trend was true for kidney; with *ex vivo* kidney exhibiting significantly improved RNA quality (Figure 6.6). However, at 48 hours post-mortem the RINs for both experimental conditions tended to converge at around RIN 2. It has been shown that the RIN is unsuitable for quantification of advanced RNA degradation (Section 5.3.3, Chapter 5), being insensitive to small fluctuations in the fragmentation state of RNA at this extreme end of the RIN spectrum. The raw data output from the Bioanalyzer 2100 suggested that in tissues decomposed *in vivo*, the

size distribution of RNA fragments in *in vivo* decomposed tissues was shorter than that of *ex vivo* tissues, especially for kidney and liver (Figure 6.8).

RT-qPCR was used to quantify the expression of 18S rRNA and Gapdh mRNA. RT-qPCR targets small sequences in the transcript as a whole – 61 nt for 18S rRNA, 107 nt for Gapdh (Tables A1.1 and A1.2, Appendix 1). This means that any detected reduction in the amplifiable quantity of 18S rRNA and Gapdh signifies fragmentation so advanced that even the integrity of these small target sequences has been compromised. On the whole, it was found that in skeletal muscle and heart tissue, no significant difference was found between the detected quantity of 18S rRNA and Gapdh up to 48 hours post-mortem. This supports the findings of Sampaio-Silva *et al*. (6) who demonstrated no difference in RT-qPCR data upon direct comparison of *in vivo*/*ex vivo* decomposed skeletal muscle. Clearly, this is a promising outcome and lends support to the use of this practically advantageous 'test tube simulation' in forensic molecular pathology studies using skeletal muscle and heart as a tissue substrate.

Unfortunately, this outcome did not hold true for kidney and liver. The results obtained here highlight that RNA degradation was earlier in onset and more severe in kidney and liver, relative to skeletal muscle and heart. This was reflected in total RNA quantity, total RNA quality and the measured quantity of 18S rRNA and Gapdh (Figure 6.1, 6.2, 6.4 and 6.5).

In addition, the results indicate that the detectable quantity of Gapdh mRNA was significantly reduced in *in vivo* decomposed kidney. Furthermore, both 18S rRNA and Gapdh mRNA exhibited a significant reduction in *in vivo* decomposed liver. Overall, this suggests that RNA fragmentation is more severe in kidney and liver decomposed within the body; relative to those decomposed in a 'test tube'. When tissues are maintained within the corpse as a whole, it is reasonable to expect that RNA degradation is influenced by enzymatic, chemical and microbial factors from surrounding tissues and organ systems which might enhance RNA degradation. It is possible that because the kidney and liver lie in such close proximity to the gastrointestinal tract within the body, they are susceptible to

attack from microbially derived RNases and other degradative chemicals. As such, segregation of kidney and liver from this source of enzymatic and chemical attack could be the cause of the observed improvement in transcriptome integrity. It is conceivable that because skeletal muscle (of the hind leg) is spatially segregated from the gastrointestinal tract and heart is protected within the pericardial sac (265), they are protected against microbially induced RNA degradation.

6.4 Summary and conclusions

Box 6.1 at the beginning of this chapter presented two research 'questions' which this work endeavoured to answer. To conclude, these questions will be revisited to contextualise the original aims with the data presented in this chapter.

Does RNA degrade at the same rate in skeletal muscle, kidney, liver and heart, or is the decay behaviour tissue specific?

It was found that all of total RNA, 18S rRNA and Gapdh mRNA are best preserved in heart tissue; followed by skeletal muscle, kidney and liver. Using published RIN thresholds the estimated post-mortem interval during which gene expression analysis yields reliable data is significantly extended in heart tissue, to a maximum of 33 hours. This is a promising outcome, as heart is of specific clinical interest with regard to estimating the cause of death in a casework scenario.

Does removal of tissues (skeletal muscle, kidney, liver and heart) from the mouse corpse affect RNA degradation behaviour? Is this 'test tube' simulation an appropriate experimental design for studies in post-mortem gene expression analysis?

Overall, the outcomes of this chapter suggest that decomposing tissue samples in a test tube may not be an appropriate 'simulation' for post-mortem gene expression studies for all tissue types – with total RNA, 18S rRNA and Gapdh mRNA all

exhibiting slightly different decay behaviour between the *in vivo*/*ex vivo* experimental designs. The topic merits further investigation: incorporating a larger number of samples, a more diverse range of tissue types, more RNA targets (including not only endogenous control RNAs) and over a longer post-mortem interval duration.

Chapter 7: Quantification of post-mortem RNA degradation using specialised real time PCR assay design

7.1 Introduction

7.1.1 Research examining the nature of RNA degradation

It is physiologically important that the lifespan of RNA is restricted for the control of gene expression, as discussed in Section 1.2.4, Chapter 1 (14). *In vivo*, RNAs are degraded by enzymes with ribonuclease (RNase) activity. These can be either exoribonucleases, which sequentially remove nucleotides from the free ends of the RNA molecule in either the 3' to 5' direction or 5' to 3' direction; or endoribonucleases, which cleave RNA internally. In living mammalian cells, the primary mechanism of mRNA decay exhibits the following sequence: deadenylation of the 3' end, removal of the 5' m^7G cap and sequential degradation in the 5' to 3' direction (22). Previous chapters have confirmed that RNA degradation does progress with increasing post-mortem interval (Section 5.3, Chapter 5 and Section 6.3.1, Chapter 6). However, the mechanism of RNA degradation in tissues after death has not yet been elucidated. It is hypothesised that this degradation post-mortem will comprise a combination of both enzymatic and chemical factors.

The perceived *in vivo* and *ex vivo* instability of RNA has made it an attractive target in forensic science. Many researchers working in a number of different areas have postulated that quantification of RNA degradation could be used as a measure of 'age' (5, 6, 28, 60, 243, 244). In the case of tissue samples, this 'age' is defined as the post-mortem interval (5, 6). However, the ageing of biological specimens such as blood stains follows an identical premise (28, 60, 243, 244).

So far the outcomes of this thesis, especially those presented in Chapter 5, have not been particularly positive with regard to the idea that quantification of tissue RNA degradation could be used as a measure of the time since death. It has been shown that RNA degradation is strongly influenced by tissue type (Chapter 6)

and the ambient temperature (Chapter 5) during decomposition. This chapter will present the outcomes of two approaches for quantifying RNA degradation; both of which involve specialist qPCR assay design.

7.1.2 Amplification of differently positioned targets on a single RNA

RNA degradation in living cells is known to be biased towards the 5' end. In addition, the use of oligo (dT) priming during reverse transcription (Section 1.4.4, Chapter 1) provides cDNA molecules with the 3' end over-represented relative to the 5' end. The following quote from Swift *et al*. (266) succinctly describes the cDNAs produced following oligo (dT) priming: "*Under ideal conditions, reverse transcription of an RNA with oligo (dT) priming generates a population of cDNAs terminating at the 5' end if the RNA is intact, or at the first cleavage site if the RNA is partially degraded*".

As such, several articles have considered the expression ratio of sequences at the 5' and 3' ends of an RNA molecule as a measure of the degree of fragmentation. Swift *et al*. (266) were the first to suggest this as far back as 2000. By amplifying four target sequences along the length of the 10 kb FASN RNA transcript from chicken endoderm cDNA, they were able to illustrate reduced expression of 5' proximal sequences through degradation. This methodology was subsequently adopted by Bauer *et al*. (5) and applied as an estimate of post-mortem interval (up to 5 days) in human brain and blood samples. They demonstrated that the ratio of expression of 5' to 3' proximal sequences in FASN was linearly correlated with post-mortem interval (Figure 1.6, Section 1.3.2.2.1, Chapter 1). Similarly, Bauer *et al*. (56) applied this principle also for the ageing of blood stains, using instead the target RNAs ACTB and CYP. They were able to illustrate a linear correlation between blood stain age (up to 59 months) and the expression ratio of 5' to 3' proximal sequences in both targets.

Unfortunately, the considerable age of these studies mean that the endpoint PCR and gel band density visualisation techniques are no longer regarded valid for

making such quantitative conclusions. For gene expression studies of this nature, RT-qPCR is now the method of choice.

7.1.3 Amplification of differently sized targets on a single RNA

This alternative approach to quantifying mRNA degradation lies with the assumption that the larger a PCR amplicon, the higher the likelihood that it has undergone degradation. In undegraded RNA, two differently sized amplicons on the same target RNA should be present in equimolar amounts. However, it only takes a single 'break' in a target sequence to render it unamplifiable and thus undetectable. Long PCR amplicons are more susceptible to breakage, meaning that the expression ratio of a short/long target theoretically should change with time.

Sugita *et al*. (129) developed a duplex PCR assay for quantification of ACTB degradation in autolysed human cell lines, using the expression ratio of a short (178 nt) and long (637 nt) target sequence. They illustrated a strong linear correlation between autolysis time and the short/long amplicon ratio; although again the reliability of this outcome is compromised by the non-quantitative nature of the endpoint PCR method used. Similarly, Heinrich *et al*. (82) developed a 5-plex PCR assay to examine the degradation of GAPDH mRNA in human post-mortem tissues, using the expression of five differently sized target sequences between 114 and 866 nucleotides in length. Similar to Sugita *et al*., their endpoint PCR design meant that the study was not able to characterise any specific relationship between post-mortem interval and GAPDH amplification. However, they were able to demonstrate that the longest PCR amplicon (866 nt) 'dropped out' most often, and the shortest (114 nt) amplified in all samples irrespective of post-mortem interval.

Anderson *et al*. (60) successfully applied a quantitative PCR design to the ageing of blood stains. Using 18S rRNA and ACTB as targets, they were able to illustrate a relationship between blood stain age (in days, log transformed) and the relative expression level of 89/301 nt amplicons for ACTB and 171/501 nt amplicons for 18S rRNA; measured in terms of the $2^{-\Delta\Delta CQ}$. However in this study, no qPCR assay quality control data was published to confirm the qPCR efficiency and linearity

of the assays used. Under current qPCR assay design guidelines (267), amplicons greater than 250 nucleotides in length are discouraged as the qPCR efficiency is likely to be compromised.

7.1.4 Experimental design, aims and objectives

This chapter aims to assess the feasibility of both approaches to PCR assay design – alteration of amplicon length and position – on quantifying the degradation of RNA in post-mortem tissues. In addition, it is envisaged that the outcomes of this study may help to identify the nature of post-mortem RNA degradation – i.e. whether it proceeds at 'random' or has a directional (5' to 3', 3' to 5') aspect to it.

As before, mice were used as an animal model for decomposition. Six mice were allowed to decompose intact at either 10 or 22 °C and samples of skeletal muscle collected at six time intervals: 0, 12, 24, 36, 48 and 72 hours. RNA was quantified by UV-visible spectrophotometry and the total RNA quality measured on the Bioanalyzer 2100. The results of RNA quantification and quality analysis on this tissue sample set have been presented in Chapter 5, Sections 5.3.2.1 and 5.3.2.2 and thus will not be reproduced here.

As this work aimed to amplify a number of target sites on a single RNA, a number of features were desirable of the selected RNA:

- It should be relatively long (~2 kb)
- It should possess no processed pseudogenes or other DNA homologs that would cause amplification of DNA contamination
- It should not have a multitude of alternatively spliced transcript variants
- It should have strong intron-exon structure, making for a large selection of primer binding sites

All of these features were assessed using the international 'Gene' database managed by the National Centre for Biotechnology Information (www.ncbi.nlm.nih.gov). Of the six endogenous control RNA targets used in

previous chapters – 18S rRNA, B2m, Actb, Gapdh, Hmbs and Ubc – it was found that many did not fit these criteria. They were selected as RNAs of interest for previous analyses due to their common implementation in clinical and forensic research (204). However, 18S rRNA, Actb and Gapdh suffer from the downfall that their assays are not 100% RNA specific, but can amplify DNA contamination. This occurs because 18S rRNA has no intron-exon structure making for RNA-specific primer binding sites; and Actb and Gapdh both have processed pseudogenes in the murine genome. Additionally, B2m and Ubc have only four and two exons in their structure respectively, reducing the number of available primer binding sites.

As such, a number of new target RNAs were identified for this work. Hmbs was retained as its RNA is 1,553 nucleotides in length with fifteen exons. In addition, Psmc4 (proteasome 26S subunit ATPase 4) and Sdha (succinate dehydrogenase complex subunit A) were selected from the 32 RNAs recommended by *TaqMan*® assay manufacturer Life Technologies as suitable endogenous control RNAs for gene expression studies in mice (268). Psmc4 is 1,436 nucleotides long, with 11 exons; and Sdha 2,859 nucleotides long, with 15 exons.

7.1.4.1 Amplification of differently positioned targets on a single RNA

The nature of RNA degradation in post-mortem tissues has not been thoroughly characterised – whether it proceeds in an enzyme-mediated, sequential fashion (5' to 3' or 3' to 5') or whether RNA is 'broken' at random points along the transcript length due to chemical or enzymatic influences (Section 1.2.4, Chapter 1). By quantifying the expression level of sequences along the length of an RNA, the aim of this chapter is to make some inferences regarding the nature of RNA degradation. In addition, this work permits identification of the sequences most/least affected by degradation in post-mortem tissues; so as to identify the optimum qPCR assay design characteristics for application to partially degraded tissue samples.

Three endogenous control RNAs were selected for examination towards these aims: Hmbs, Psmc4 and Sdha. For each, three TaqMan® qPCR assays were

selected to amplify three sequences interspersed as far apart as possible within the open reading frame, as illustrated in Figure 7.1.

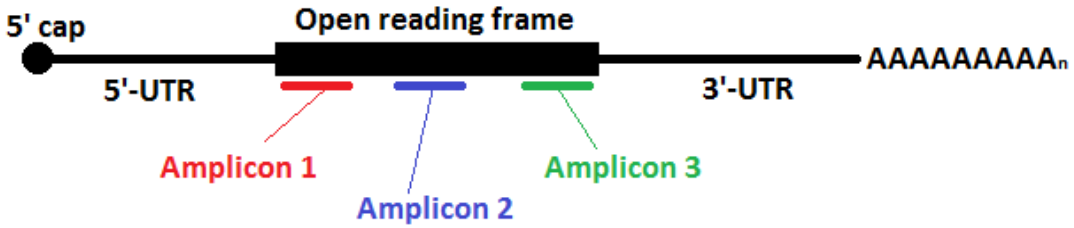

Figure 7.1: **Amplification to assess the directionality of RNA degradation**. Three target sites have been selected within the open reading frame for amplification – a 5' proximal (amplicon 1), central (amplicon 2) and 3' proximal (amplicon 3) target. The ratio of the expression level of these targets to one another may give an indication as to the direction in which RNA degradation proceeds.

Unfortunately, it is not possible to target the extreme 5' and 3' sequences of an RNA by PCR due to the presence of two non-coding untranslated regions (UTRs) which contain similar sequence motifs to other RNAs. The three target sequences were designed to vary in length by less than 10%, so that amplicon length was not a major confounding variable in data analysis. More specific details of the assays themselves are included in the Method, Section 7.2.

These assays were applied to mouse skeletal muscle tissue of post-mortem interval up to 72 hours. Two potential outcomes were envisaged upon RT-qPCR analysis of mouse post-mortem tissue samples: 1) that the expression ratio of amplicons 1, 2 and 3 remains the same over the 72 hour post-mortem interval, implying that the degradation of RNA in tissues is wholly random or mild in severity; or 2) that the expression relationship of amplicons 1, 2 and 3 changes in some form over the time course, implying a degree of directionality and predictability to RNA degradation. If this relative expression relationship was found to change with time, this might provide a novel indicator of RNA quality and ultimately, time since death.

In addition, consideration was made regarding the effect of reverse transcription priming strategy: random vs. oligo (dT) priming. This is already known

to strongly bias the expression of sequences at the 5' and 3' ends in the cDNA product. Random priming gives a more balanced covering of the transcriptome, whereas oligo (dT) priming is biased towards sequences proximal to the 3' poly (A) tail (Section 1.4.4, Chapter 1).

7.1.4.2 Amplification of differently sized targets on a single RNA

Long RNA sequences are more susceptible to breakage. Therefore, quantifying the relative expression of two differently sized sequences on a single RNA could potentially provide a measure of the severity of post-mortem RNA degradation. The aim of this chapter was to assess whether the ratio of a short/long mRNA amplicon on a single RNA molecule would exhibit a predictable relationship with total RNA quality (using the RIN) and ultimately, the post-mortem interval.

One target RNA was selected for examination towards this aim: Psmc4. Two qPCR assays (for use with SYBR® Green amplification) were designed to amplify a long (227 nucleotides) and a short (71 nucleotides) target within the open reading frame of Psmc4, as illustrated in Figure 7.2.

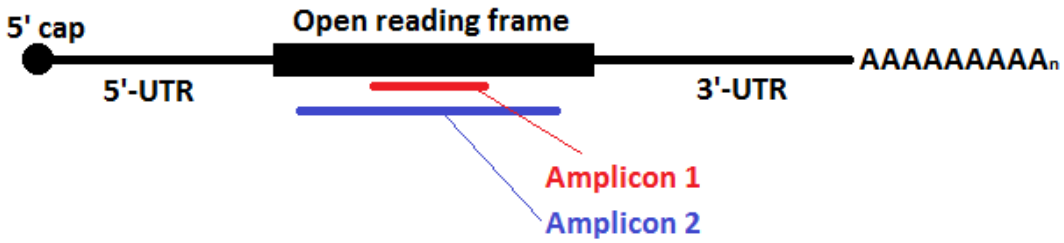

Figure 7.2: **Amplification of differently sized targets to assess the severity of RNA degradation.** Two target sites were selected within the open reading frame – a long (amplicon 1) and a short (amplicon 2) target sequence – and designed to overlap as much as possible. The ratio of expression of these two amplicons may give an indication as to the severity of RNA degradation.

As far as was possible, these two amplicons were designed to overlap at the same position as illustrated in Figure 7.2. These two amplicon lengths represent the recommended extremes for qPCR assays with SYBR® Green (267); with assays over ~250 nucleotides likely to suffer from reduced qPCR efficiency. More specific details on these four assays is included in the Method, Section 7.2.

These two assays were applied to mouse skeletal muscle tissue of post-mortem interval up to 72 hours. It was hypothesised that degradation of tissue RNA during the post-mortem interval would cause more pronounced drop-out of the large qPCR amplicon relative to the small qPCR amplicon, causing a gradual change in their relative expression as quantified using the $2^{-\Delta\Delta CQ}$.

7.1.4.3 Summary: Research objectives

For clarity, Box 7.1 below summarises the questions to be answered through the research presented in Chapter 7.

Box 7.1: Objectives/questions to be answered within Chapter 7

Does RNA degrade 'at **random'** in post-mortem tissues, or does the decay of individuals RNAs retain a **directional** element to it, as is true in live cells – either in the 5' to 3' or 3' to 5' direction?

If RNA degradation does retain a directional element to it, could a duplex qPCR assay targeting two **differently positioned** sequences on a single RNA (5' and 3' proximal) be used as a quantitative measure of post-mortem interval?

Could a duplex qPCR assay targeting two **differently sized** sequences on a single RNA be used as a quantitative measure of post-mortem interval?

7.2 Method

7.2.1 Tissue sample preparation

All steps involving live animals were carried out following ethical guidelines put forth by the Biological Procedures Unit within Strathclyde Institute of Pharmacy and Biomedical Science. Six male, twelve week old C57/BL6J mice were killed by cervical dislocation and their corpses left to decompose intact at 10 °C (n = 3) and 22 °C (n = 3) for a period of three days, as described in Section 5.2.1, Chapter 5. It should be noted that this small sample size was a consequence of the limited resources available for this project, rather than a conscious choice during the experimental design and planning stage. Samples of skeletal muscle were recovered from the hind leg at six time intervals following death: 0, 12, 24, 36, 48 and 72 h. Excised tissue samples were shredded and immediately preserved in RNAlater® to stabilize RNA, as discussed in Section 2.2.2, Chapter 2.

7.2.2 RNA purification, quantification and quality assessment

RNA was purified from skeletal muscle tissue samples using the TRI Reagent® extraction system, using the protocol described in Section 2.2.3.3, Chapter 2. RNA extracts were treated with TURBO DNA-free® to remove residual DNA contamination, as described in Section 2.2.3.4, Chapter 2. RNA was quantified by UV-visible spectrophotometry using the Nanodrop-1000 platform (Section 2.2.4, Chapter 2) and then subjected to quality analysis on the Bioanalyzer 2100 instrument using the protocol described in Section 2.2.5, Chapter 2.

7.2.3 Gene expression analysis by RT-qPCR

RNA (diluted to 100 ng/µL in RNase-free water) was reverse transcribed into cDNA using the High Capacity cDNA Reverse Transcription Kit, as described in Section 2.2.6, Chapter 2. Each RNA sample was reverse transcribed in duplicate: once with random primers, and once with oligo (dT) primers. To prevent qPCR

inhibition due to carry-over of reverse transcriptase and its associated buffers, cDNAs were subsequently amplified at a 1:12 dilution in RNase-free water (Ambion, Life Technologies).

7.2.3.1 Amplification of differently positioned targets on the same RNA

cDNA samples were amplified in duplicate using a panel of nine TaqMan® assays targeting three gene products: Hmbs, Sdha and Psmc4. Details of these assays including the assay ID, the target position on the RNA, the exon boundary across which the amplicon spans and the length of the PCR product are detailed in Tables 7.1, 7.2 and 7.3 for Hmbs, Sdha and Psmc4 respectively. All cDNA samples were amplified in duplicate using the *TaqMan*® qPCR protocol described in Section 2.2.7, Chapter 2. Quality control data for all nine assays can be viewed in Appendix 1, Table A1.3.

Table 7.1: **Selected TaqMan® assays for amplification of the Hmbs transcript in mouse post-mortem tissue**. The Hmbs transcript itself is 1,611 nucleotides long, with 14 exons.

Amplicon	Life Technologies Assay ID	Target position	Target exon boundary	Amplicon length (bases)
5'	Mm00660260_g1	220-301	1-2	82
C	Mm01143545_m1	473-553	6-7	81
3'	Mm01168620_g1	778-858	10-11	81

Table 7.2: **Selected TaqMan® assays for amplification of the Sdha transcript in mouse post-mortem tissue**. The Sdha transcript itself is 2,859 nucleotides long, with 15 exons.

Amplicon	Life Technologies Assay ID	Target position	Target exon boundary	Amplicon length (bases)
5'	Mm01352362_m1	174-240	2-3	67
C	Mm01352368_m1	1098-1170	8-9	73
3'	Mm01352360_m1	1942-2010	14-15	69

Table 7.3: **Selected TaqMan® assays for amplification of the Psmc4 transcript in mouse post-mortem tissue**. The Psmc4 transcript itself is 1,436 nucleotides long, with 11 exons.

Amplicon	Life Technologies Assay ID	Target position	Target exon boundary	Amplicon length (bases)
5'	Mm01176478_m1	104-177	1-2	74
C	Mm00457191_m1	750-827	6-7	78
3'	Mm00821599_g1	1220-1290	10-11	71

As well as presenting the raw C_Q data, the results were analysed by pair-wise comparison using the $2^{-\Delta\Delta CQ}$ formula (described in Section 2.2.7.2, Chapter 2), to compare the relative expression level of the following amplicon pairs:

$2^{-\Delta\Delta CQ}$ (3' – 5') $2^{-\Delta\Delta CQ}$ (3' – C) $2^{-\Delta\Delta CQ}$ (C – 5')

Following the hypothesis made in the introduction that RNA degradation would be more pronounced at the 5' end, this outcome should cause an increase in $2^{-\Delta\Delta CQ}$ for all three of these combinations. Alternatively, should RNA degradation be biased towards the 3' end, this would cause a reduction in $2^{-\Delta\Delta CQ}$ into decimals. 'Random' fragmentation causing loss of all three target sequences in parallel should cause no change in the $2^{-\Delta\Delta CQ}$, remaining approximately 1.

7.2.3.2 Amplification of differently sized targets on the same RNA

PCR primers were designed using the freely available web package Primer BLAST (www.ncbi.nlm.nih.gov/tools/primer-blast/), limiting the search to return amplicons in the size range 70 to 300 bases and those spanning an exon-exon junction. Two target sites were identified for amplification on Psmc4: a long (227 nucleotides) and a short (71 nucleotide) sequence.

The selected primers detailed in Table 7.4 were purchased from Eurofins Genomics (Ebersberg, Germany). For them, quality control data including the results of primer concentration optimisation, dissociation curve analysis, standard curves assessing linearity and qPCR efficiency and controls can be viewed in Section A1.3, Appendix 1. Amplification was performed using the Platinum® SYBR® Green qPCR SuperMix-UDG (Invitrogen, Life Technologies, Paisley, UK). Reactions were set up according to the manufacturer's instructions (267) in a total volume of 12.5 µL: containing 6.25 µL qPCR SuperMix, 0.25 µL forward primer (at the desired concentration), 0.25 µL reverse primer (at the desired concentration), 2.5 µL cDNA template and 3.25 µL RNase-free water. Forward and reverse primer concentrations for each assay are stipulated in Table 7.4, and were determined during assay optimisation as described in Section A1.3, Appendix 1. Amplification was performed on the Stratagene Mx3005P real time PCR instrument using the following thermal cycling parameters: 2 mins at 50 °C to permit uracil-N-glycosylase mediated destruction of DNA carry-over; 10 mins at 95 °C to activate Platinum® *Taq* polymerase; followed by 40 cycles of denaturation at 95 °C for 15 s and

annealing/extension at 60 °C for 1 min. cDNA samples were amplified in duplicate using each of the two qPCR assays.

Table 7.4: **Details of two in-house real time PCR assays for the Psmc4 transcript in mouse post-mortem tissue**. Primer concentrations were determined by assay optimisation, the results of which are documented in Appendix 1. The Psmc4 mRNA is 1,436 nucleotides long, with 11 exons.

Target cDNA	Amplicon length (nt)	Amplicon position	Target exon boundary	Primer sequence	Final primer concentration (nM, F/R)
Psmc4	71	527-597	4-5	F: CATGATGCTCACCTCAGACCA R: GCTTCTGGATGTCCATGCCT	200/300
Psmc4	227	326-552	3-4-5	F: CATCCCCTTGGTCATCGGTC R: GCTTCTGGTCTGAGGTGAGC	300/300

As well as presenting the raw C_Q data for both target sequences, the results have been analysed by pair-wise comparison using the $2^{-\Delta\Delta CQ}$ (short – long) formula (described in Section 2.2.7.2, Chapter 2). Following the hypothesis made in the introduction that the long qPCR amplicon would be more susceptible to degradation, this outcome would cause an increment in the calculated $2^{-\Delta\Delta CQ}$ (short – long). Alternatively, if the two target sequences were found to be equally susceptible to degradation, the fold change in their expression would remain at a $2^{-\Delta\Delta CQ}$ (short – long) of approximately 1.

7.3 Results

7.3.1 Amplification of differently positioned targets on a single RNA

7.3.1.1 Results: Randomly primed cDNA

In this study, three *TaqMan*® assays (with a 3' proximal, 5' proximal and a centrally located amplicon) were applied to each of Hmbs, Sdha and Psmc4 to glean more information about the nature of post-mortem RNA degradation in mouse skeletal muscle. This first data set considers the results with randomly primed cDNA, which should give a balanced representation of the state of the transcriptome. The assays were applied to post-mortem tissue of mice stored at 10 °C during decomposition. This tissue substrate selection was in response to initial RNA quality analysis on the Bioanalyzer 2100. As shown in Figure 5.7 (Section 5.3.2.2, Chapter 5), this tissue sample set provided RNA samples spanning a wide range of measured RNA quality levels; from a maximum mean RIN of 7.8 at the control point, to a minimum mean RIN 2.4 after 72 hours. It was envisaged that this wide range of measured degradation levels would be reflected in the RT-qPCR results.

In this sample set it was found that for all three RNAs, the 5' proximal, 3' proximal and centrally located sequences exhibited very similar decay behaviour – as illustrated in Figure 7.3. The gradual increase in C_Q observed is indicative of a progressive reduction in the quantity of the target sequence. Over the first 24 hours post-mortem, it can be seen that the mean C_Q for all 9 amplified target sequences does not deviate appreciably from the control point. This illustrates that during this time, no detectable reduction in RNA quantity occurred through degradation. The RNA quality (RIN) measurements made on these samples indicated that during the first 24 hours post-mortem, RNA integrity fell from mean RIN 7.80 (< 0.25 hours) to RIN 5.03 (24 hours) (Figure 5.7, Section 5.3.3, Chapter 5). This outcome concurs with the findings of Fleige *et al*. (212) who illustrated that RIN 5 represents a good RNA quality screening threshold for RT-PCR; above which the results of RT-PCR should not be appreciably compromised.

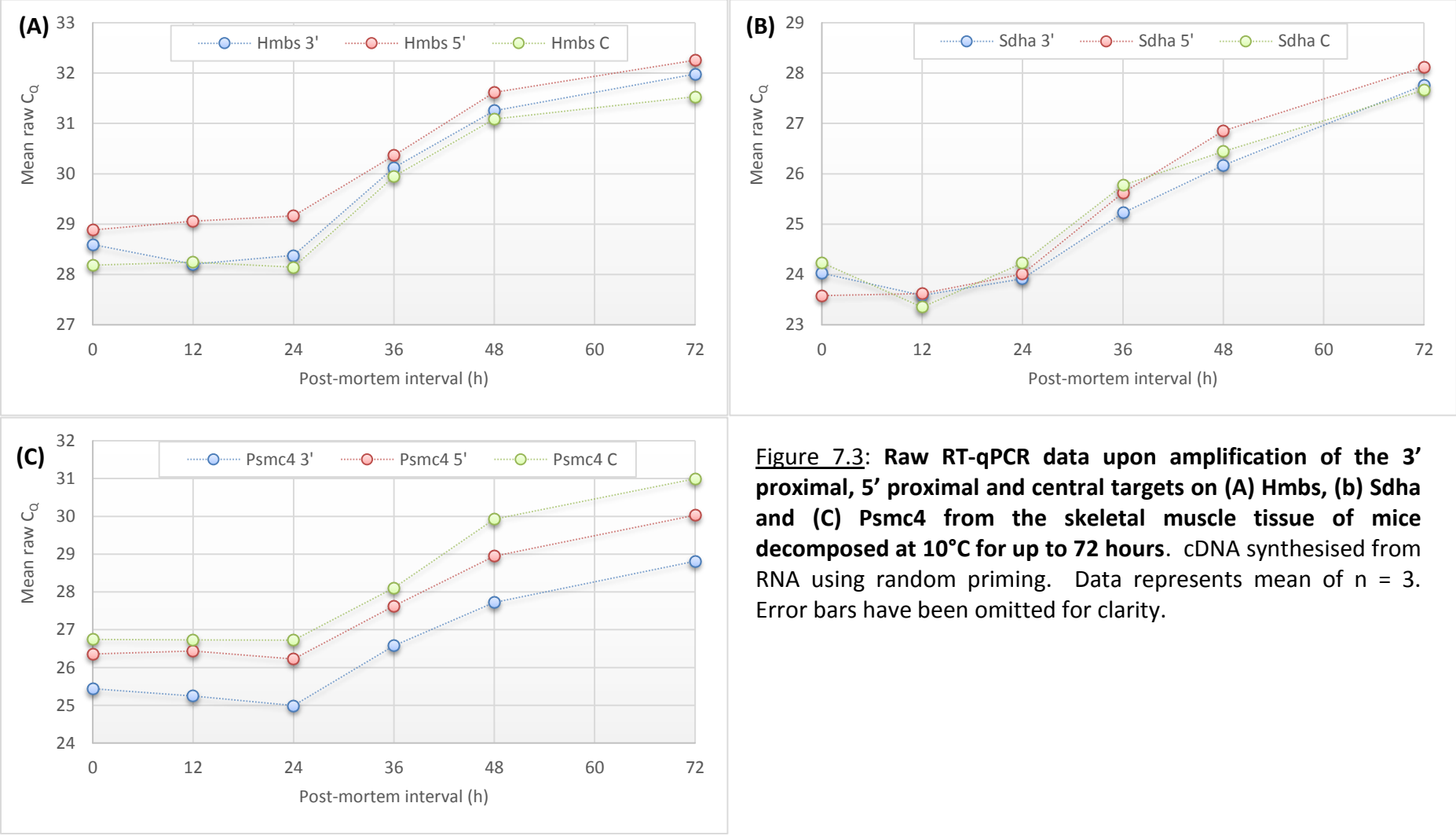

Figure 7.3: **Raw RT-qPCR data upon amplification of the 3' proximal, 5' proximal and central targets on (A) Hmbs, (b) Sdha and (C) Psmc4 from the skeletal muscle tissue of mice decomposed at 10°C for up to 72 hours**. cDNA synthesised from RNA using random priming. Data represents mean of n = 3. Error bars have been omitted for clarity.

For all nine target sequences the increase in C_Q (ΔC_Q) over the 72 hour interval was relatively similar, as demonstrated in Table 7.5. ΔC_Q is shown in Table 7.5 alongside the approximate fold reduction in the quantity of the target sequence. This approximation assumes 100% efficiency of the qPCR, calculating the fold-change as $2^{\Delta CQ}$. Overall, Table 7.5 indicates an approximately 10 to 20 fold reduction in the quantity of Hmbs, Sdha and Psmc4 RNA over a 72 hour post-mortem interval. For Hmbs and Psmc4, no preferential degradation of the 5' proximal target sequence can be observed over this time. However, the slightly higher fold-reduction of the 5' proximal sequence in Sdha might be an indicator of directionality in RNA degradation in the Sdha molecule.

Table 7.5: **Fold reduction in the measured quantity of the 3' proximal, 5' proximal and centrally located target sequences within the Hmbs, Sdha and Psmc4 RNAs.** Data represents the mean of n = 3. cDNA synthesised from RNA using random priming. Mean ΔC_Q calculated from the difference in mean C_Q at the control point and after 72 hours post-mortem. Corresponding reduction in gene expression estimated by $2^{\Delta CQ}$.

	Hmbs 3'	**Hmbs 5'**	**Hmbs C**
Mean ΔC_Q over 72 hours	3.4	3.4	3.4
Corresponding reduction in gene expression	10.6-fold	10.6-fold	10.6-fold
	Sdha 3'	**Sdha 5'**	**Sdha C**
Mean ΔC_Q over 72 hours	3.7	4.5	3.4
Corresponding reduction in gene expression	13-fold	22.6-fold	10.6-fold
	Psmc4 3'	**Psmc4 5'**	**Psmc4 C**
Mean ΔC_Q over 72 hours	3.4	3.7	4.3
Corresponding reduction in gene expression	10.6-fold	13-fold	19.7-fold

To investigate this further, the expression levels (C_Q) of the 5' proximal, 3' proximal and central target sequences were examined by pair-wise comparison to determine whether RNA degradation was biased towards either end of the molecule; the results of which are illustrated in Figure 7.4. Amplicons were paired up for analysis using the $2^{-\Delta\Delta CQ}$ formula as follows: 3' – 5', 3' – C and C – 5'. As such, any bias of degradation towards the 5' end should result in an increase of the $2^{-\Delta\Delta CQ}$; conversely any reduction into decimal values is indicative of 3' targeted degradation.

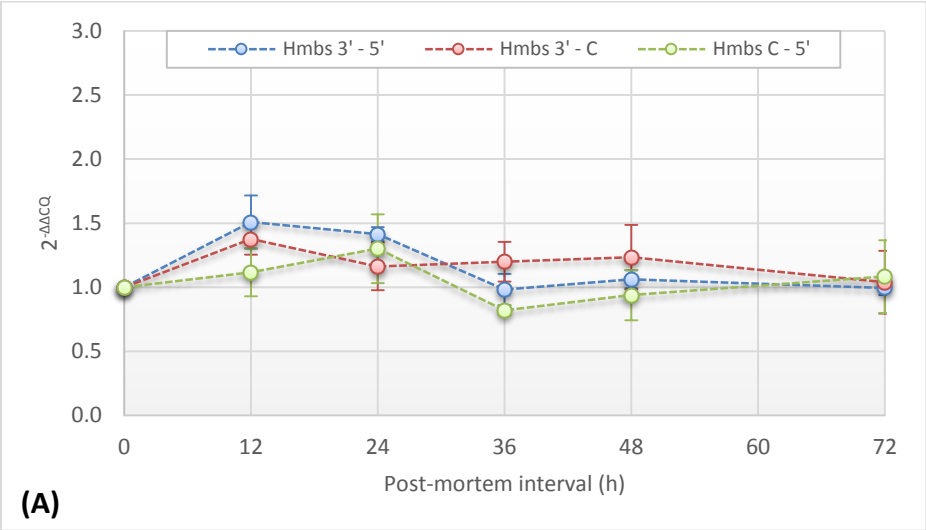

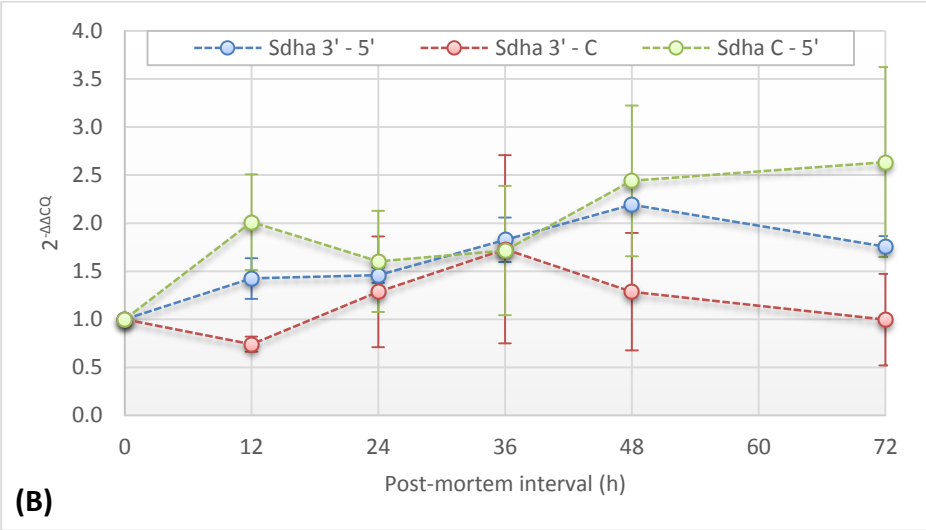

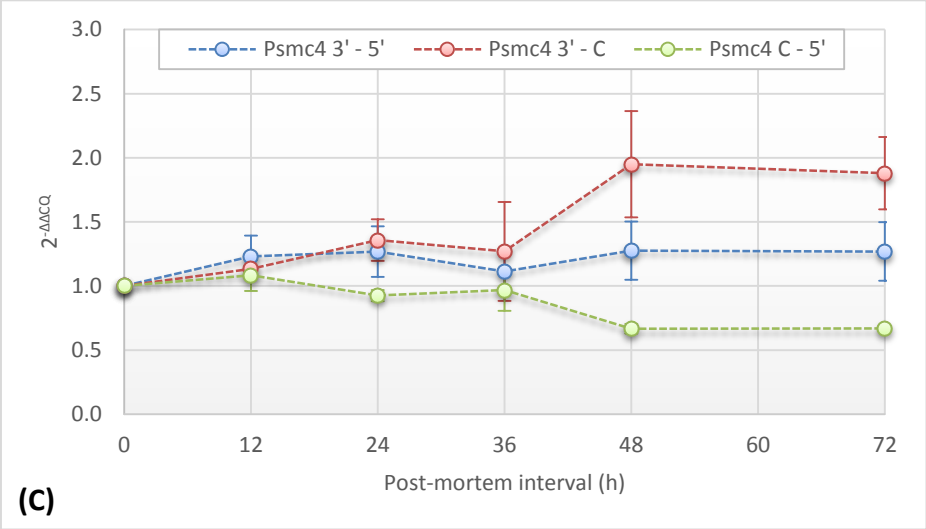

Figure 7.4: **Fold change in expression of the 5' proximal, 3' proximal and centrally located amplicons of (A) Hmbs, (B) Sdha and (C) Psmc4.** Data represents the fold change in gene expression in terms of $2^{-\Delta\Delta CQ}$, for three combinations: 3' – 5', 3' – C and C – 5'. Data points represent the mean of n = 3 ± S.E. cDNA synthesised from RNA using random priming. Note that a $2^{-\Delta\Delta CQ}$ of one indicates no fold change in the relative expression of one target sequence to another.

It can be seen from Figure 7.4 that the magnitude of change in mean $2^{-\Delta\Delta CQ}$ was relatively small. For Hmbs (Figure 7.4A), the maximum increment in mean $2^{-\Delta\Delta CQ}$ for all three target sequence combinations was 1.5. Such a small magnitude of variation in $2^{-\Delta\Delta CQ}$ is not indicative of any biologically significant change; rather being in the margin of error for qPCR raw C_Q measurements.

For Sdha and Psmc4, the results are fairly inconsistent and do not demonstrate any recognisable trend. The $2^{-\Delta\Delta CQ}$ (3' – 5') and (C – 5') pairs both exhibited a small increase over the 72 hours, indicating a slightly reduced quantity of the 5' target sequence relative to the 3' proximal and central sequences (Figure 7.4B). This corresponds with the slightly elevated 22.6-fold reduction in Sdha 5' quantity detailed previously in Table 7.5. The Sdha $2^{-\Delta\Delta CQ}$ (3' – C) remained reasonably consistent over the 72 hour post-mortem interval, indicating no preferential degradation of one target sequence or the other. The $2^{-\Delta\Delta CQ}$ relationship between the expression of the 5' and 3' proximal sequences of Psmc4 didn't deviate visibly from 1 (Figure 7.4C). The slight increment in $2^{-\Delta\Delta CQ}$ (3' – C) and slight reduction in $2^{-\Delta\Delta CQ}$ (C – 5') are both indicative of a small reduction in the measured quantity of the central target RNA sequence. This corresponds with the slightly elevated 19.7-fold reduction in Psmc4 C documented previously in Table 7.5.

However, the magnitude of change in mean $2^{-\Delta\Delta CQ}$ for all pair-wise comparisons for Hmbs, Sdha and Psmc4 is still reasonably small ($0.67 \leq 2^{-\Delta\Delta CQ} \leq 2.64$). Variability between replicate measurements was surprisingly high. This was especially true for Sdha, illustrated by the wide error bars throughout Figure 7.4B. The majority of measured $2^{-\Delta\Delta CQ}$ values are so small as to potentially be in the margin of error for raw C_Q measurements.

This result suggests one of two outcomes. Firstly, it could be that RNA degradation was not severe enough to merit a significant change in the relative expression level of the 3', 5' and centrally located target sequences. However, the Bioanalyzer 2100 electropherogram outputs (Figure 5.8, Section 5.3.3, Chapter 5) for this sample set refute this hypothesis, illustrating strong RNA fragmentation. In addition, as discussed the raw C_Qs themselves suggested an approximately 10 to 20

fold reduction in the measured quantity of RNA by RT-qPCR through degradation. A more plausible explanation for the outcomes observed is that the Hmbs, Sdha and Psmc4 RNAs are being fragmented at 'random' during the 72 hour post-mortem interval, causing a reasonably parallel reduction in the measured quantity of the 3', 5' and centrally located sequences.

To examine whether RNA degradation of increased severity would induce a significant change in the $2^{-\Delta\Delta CQ}$, the 3', 5' and centrally located amplicons of Hmbs were assayed for in the skeletal muscle tissue of mice left to decompose at 22 °C for up to 72 hours. As illustrated in the Bioanalyzer electropherogram outputs in Figure 5.9 (Section 5.3.3, Chapter 5), the RNA had been fragmented in this tissue sample set to a much smaller size distribution.

As before, the decay profile of the 3', 5' and centrally located sequences of Hmbs exhibited a very similar profile, as demonstrated in Figure 7.5. RNA degradation onset immediately within the first 12 hours post-mortem, and the raw C_Q data follows an almost linear profile before plateauing between 48 to 72 hours. The fold-reduction in the measured quantity of Hmbs over the 72 hours is much more pronounced in this sample set – with a mean ΔC_Q of 7.7, 6.5 and 7.1 for each of the 3', 5' and central target sequences corresponding to an approximately 208-fold, 91-fold and 137-fold reduction in their measured quantity over the 72 hour post-mortem interval.

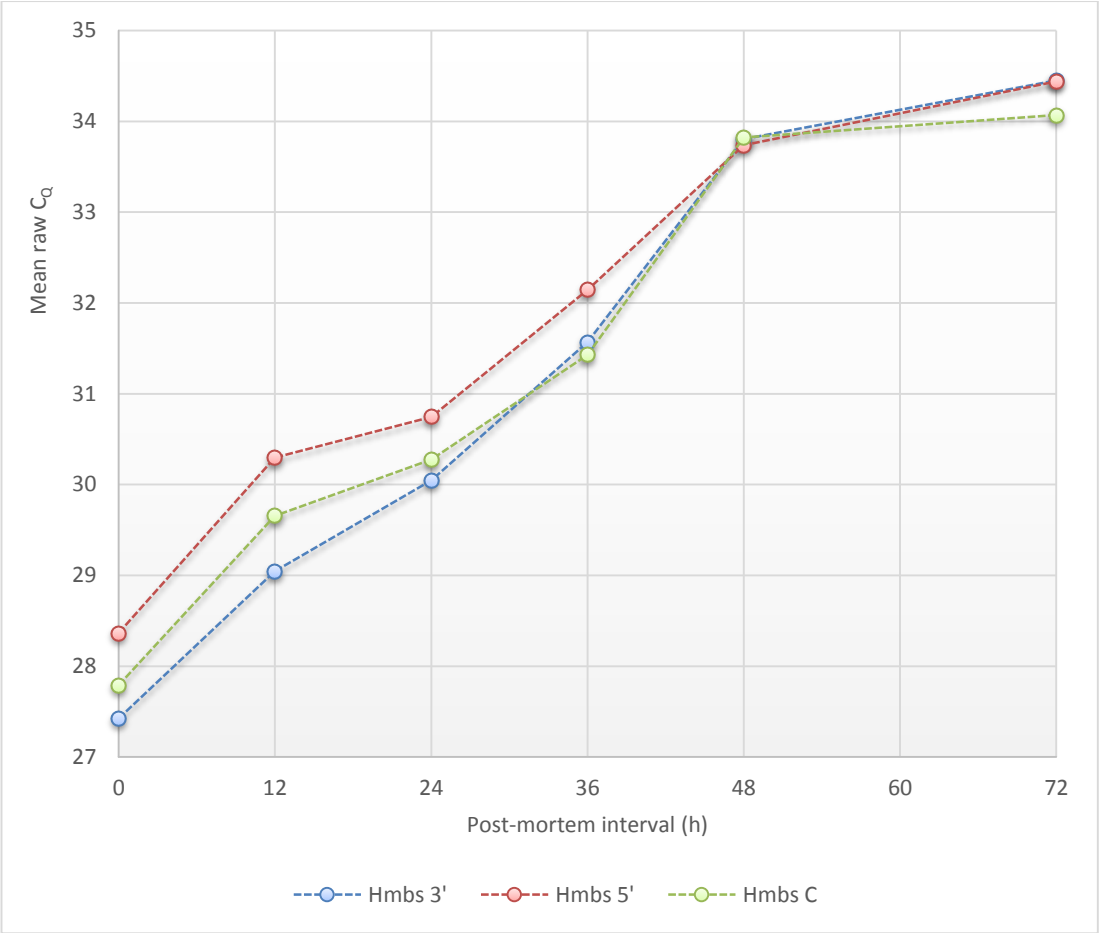

Figure 7.5: **Raw RT-qPCR data upon amplification of the 3' proximal, 5' proximal and central targets on Hmbs from the skeletal muscle of mice decomposed at 22 °C for up to 72 hours**. cDNA synthesised from RNA using random priming. Data represents mean of n = 4. Error bars have been omitted for clarity.

As before, the three amplicons were paired up for analysis using the $2^{-\Delta\Delta CQ}$ formula to try to identify bias in degradation towards either end of the Hmbs molecule; the results of which are illustrated in Figure 7.6.

Even in this sample set which was beset by severe degradation, the magnitude of change in mean $2^{-\Delta\Delta CQ}$ for all three pair-wise comparisons does not deviate appreciably from 1. For all three amplicon pairs, no consistent relationship is apparent between post-mortem interval and $2^{-\Delta\Delta CQ}$. Variability between replicate measurements was strong, illustrated by the wide error bars throughout Figure 7.6. The $2^{-\Delta\Delta CQ}$ (C – 5') remains reasonably consistent at around 1 over the 72 hours post-mortem, indicating no preferential degradation of one target sequence or the

other. Unexpectedly, both $2^{-\Delta\Delta CQ}$ (3' – 5') and (3' – C) ended slightly below 1, indicative of a reduced measured quantity of the 3' proximal target sequence relative to the 5' and central sequences after 72 hours. This corresponds with the slightly elevated 208-fold reduction in the measured quantity of the Hmbs 3' target sequence as estimated from Figure 7.5. However, this small magnitude of change in mean $2^{-\Delta\Delta CQ}$ cannot be confirmed as due to any reproducible physiological degradation; instead lying within the error margin of replicate qPCR measurements.

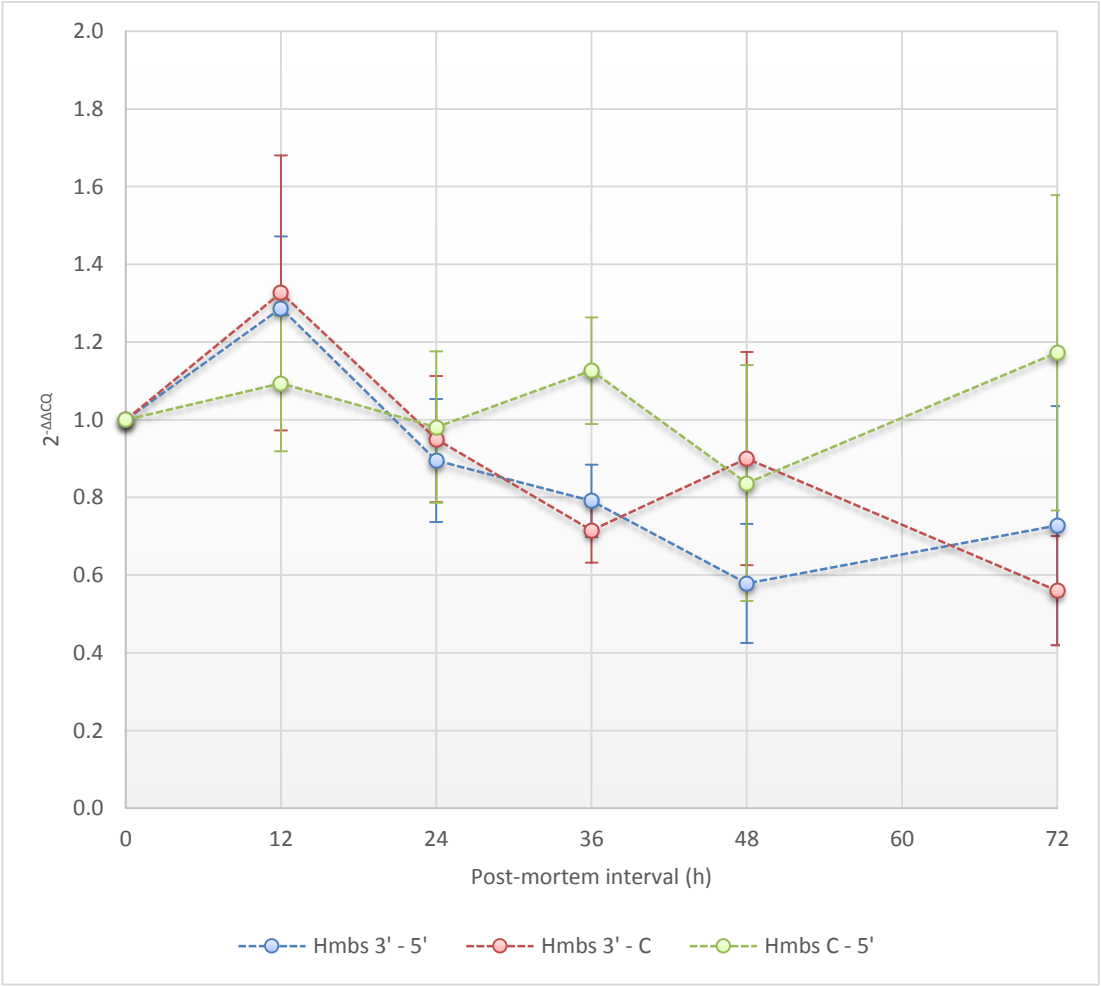

Figure 7.6: **Fold change in expression of the 5' proximal, 3' proximal and centrally located amplicons of Hmbs**. Data represents the fold change in gene expression in terms of $2^{-\Delta\Delta CQ}$, for three combinations: 3' – 5', 3' – C and C – 5'. Data points represent the mean of n = 4 ± S.E. cDNA synthesised from RNA using random priming.

This outcome supports the previous data set, suggesting that post-mortem RNA degradation does not occur in an 'organised', directional fashion but is rather unpredictable. This data is consistent with the hypothesis that Hmbs, Sdha and Psmc4 RNAs are being fragmented at 'random' during the 72 hour post-mortem interval, causing a reasonably parallel reduction in the measured quantity of the 3', 5' and centrally located sequences.

7.3.1.2 Results: Oligo (dT) primed cDNA

The nature of oligo (dT) priming during reverse transcription means that the cDNA products of reverse transcription over-represent the 3' end of all transcripts. All oligo (dT) primed cDNAs contain the poly (A) tail and immediately adjacent 3' proximal sequences, and continued extension towards the 5' end by reverse transcriptase relies on the RNA molecule remaining intact. As such, partial fragmentation of RNAs – regardless of whether this is 'random' or directional in nature – in theory should cause a more pronounced reduction in the measurable quantity of sequences proximal to the 5' end.

Consistent with the previous investigations undertaken, three *TaqMan*® assays (3' proximal, 5' proximal and centrally located) were used to amplify each of Hmbs, Sdha and Psmc4; examining their expression in the skeletal muscle of mice decomposed at 10 °C for up to 72 hours. Figure 7.7 illustrates that the 3' proximal, 5' proximal and centrally located amplicons exhibited a similar degradation pattern. For all three targets, the 3' proximal target sequences consistently exhibited a lower C_Q followed by the centrally located target sequences. The 5' proximal sequences consistently returned a higher C_Q. This is an artefact of the oligo (dT) priming procedure, which causes over-representation of the 3' end of an RNA molecule in the reverse transcribed cDNA subjected to qPCR amplification.

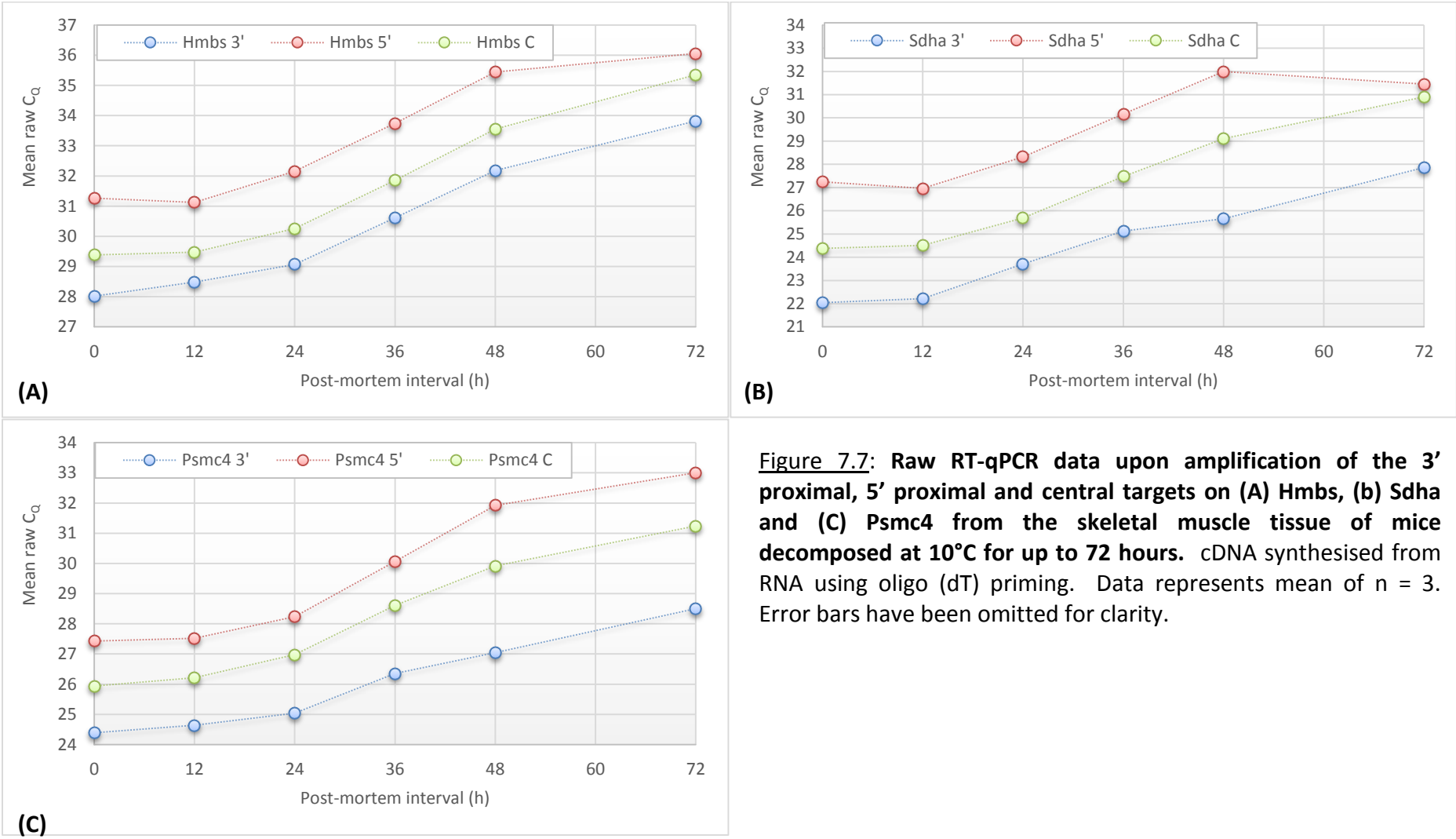

Figure 7.7: **Raw RT-qPCR data upon amplification of the 3' proximal, 5' proximal and central targets on (A) Hmbs, (b) Sdha and (C) Psmc4 from the skeletal muscle tissue of mice decomposed at 10°C for up to 72 hours.** cDNA synthesised from RNA using oligo (dT) priming. Data represents mean of n = 3. Error bars have been omitted for clarity.

For all nine target sequences, the mean increase in C_Q (ΔC_Q) over the full 72 hour post-mortem interval examined is displayed in Table 7.6, alongside the estimated fold reduction in the quantity of each target sequence. In this data set, the measured reduction in RNA expression was found to be much more variable – ranging from a 17.1-fold reduction for the Psmc4 3' proximal sequence to 90.5-fold for the centrally located target sequence on Sdha.

Table 7.6: **Fold reduction in the measured quantity of the 3' proximal, 5' proximal and centrally located target sequences within the Hmbs, Sdha and Psmc4 RNAs.** Data represents the mean of n = 3. cDNA synthesised from RNA using oligo (dT) priming. Mean ΔC_Q calculated from the difference in mean C_Q at the control point and after 72 hours post-mortem. Corresponding reduction in gene expression estimated by $2^{\Delta CQ}$.

	Hmbs 3'	**Hmbs 5'**	**Hmbs C**
Mean ΔC_Q over 72 hours	5.8	4.8	6.0
Corresponding reduction in gene expression	55.7-fold	27.9-fold	64-fold
	Sdha 3'	**Sdha 5'**	**Sdha C**
Mean ΔC_Q over 72 hours	5.8	4.2	6.5
Corresponding reduction in gene expression	55.7-fold	18.4-fold	90.5-fold
	Psmc4 3'	**Psmc4 5'**	**Psmc4 C**
Mean ΔC_Q over 72 hours	4.1	5.6	5.3
Corresponding reduction in gene expression	17.1-fold	48.5-fold	39.4-fold

As before, the expression levels (C_Q) of the 5' proximal, 3' proximal and central target sequences for Hmbs, Sdha and Psmc4 were examined by pair-wise comparison; the results of which are illustrated in Figure 7.8.

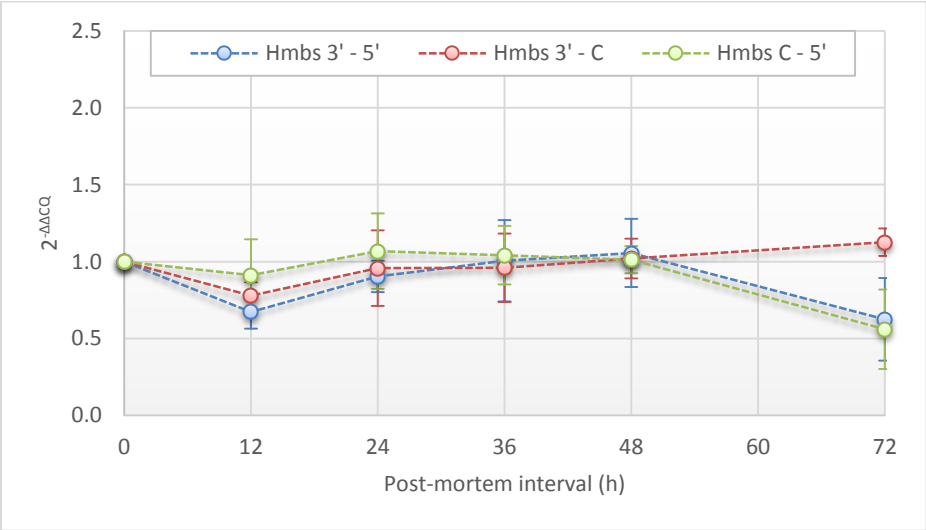

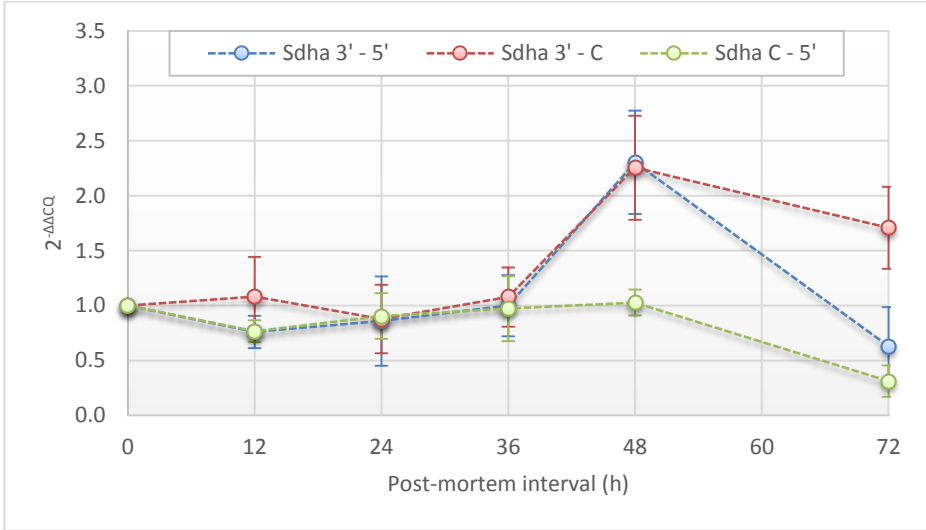

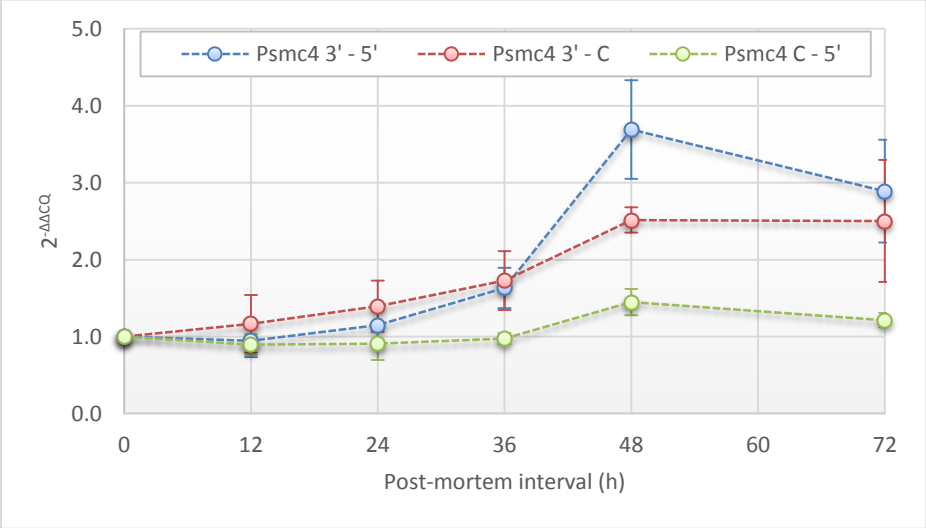

Figure 7.8: **Fold change in expression of the 5' proximal, 3' proximal and centrally located amplicons of (A) Hmbs, (B) Sdha and (C) Psmc4.** Data represents the fold change in gene expression in terms of $2^{-\Delta\Delta CQ}$, for three combinations: 3' – 5', 3' – C and C – 5'. Data points represent the mean of n = 3 ± S.E. cDNA synthesised from RNA using oligo (dT) priming.

It can be observed from Figure 7.8A that for Hmbs the $2^{-\Delta\Delta CQ}$ (3' – 5'), (3' – C) and (C – 5') does not deviate appreciably from 1. This is indicative of a minimal fold change in the expression of the 3' proximal, 5' proximal and centrally located target sequences of this RNA molecule through degradation over the 72 hour post-mortem interval investigated. On the contrary, both Sdha and Psmc4 demonstrated results indicative of improved detection of the 3' proximal RNA sequence (Figure 7.8B and 7.8C). For both, the mean $2^{-\Delta\Delta CQ}$ (3' – 5') and (3' – C) rises sharply between 36 to 48 hours post-mortem. In the case of Sdha, this increase reverses itself upon extension of the post-mortem interval to 72 hours (Figure 7.8B). It is difficult to pinpoint a reason for this change in decay behaviour; however it is consistent with the decay kinetics presented for other endogenous control RNAs in Section 5.3.4, Chapter 5 which suggest that after extended post-mortem periods RNA degradation slows down. Similarly, the $2^{-\Delta\Delta CQ}$ (3' – 5') and (3' – C) for Psmc4 plateaus between 48 to 72 hours but at a higher relative expression level than for Sdha (Figure 7.8C). For both, the $2^{-\Delta\Delta CQ}$ (C – 5') relationship does not increase but remains around or less than 1.

This outcome suggests that the 3' ends of Sdha and Psmc4 remain intact and analysable in oligo (dT) cDNA, but the centrally located and 5' proximal target sequences both suffer due to their increasing distance from the poly (A) tail where reverse transcription priming takes place. For both Sdha and Psmc4, the 3' proximal target sequence lay on the final exon boundary within the open reading frame as illustrated in Tables 7.2 and 7.3 (Section 7.2.3) respectively. This meant that the 3' proximal target sequence was as close to the 3' end and poly (A) tail as was practically possible. On the other hand, it was not possible with the 3' proximal Hmbs target sequence to obtain a suitable qPCR amplicon as close to the end of the molecule; rather, the at the boundary of exons 10 and 11 out of 14 (nucleotide position 778 – 858 of 1,611). This may be a factor explaining the slightly different decay behaviour of Hmbs compared with Sdha and Psmc4, particularly with regard to the 3' proximal target sequence.

It was not possible to conduct a similar analysis on the skeletal muscle of mice decomposed at 22 °C. As determined with the Bioanalyzer 2100 (Figure 5.9,

Section 5.3.3, Chapter 5) the RNAs present in this tissue set were fragmented to a small size distribution. Oligo (dT) priming is known not to be particularly robust against partial degradation of RNA (138), because it relies on maintaining a connection between the target amplicon and the 3' poly (A) tail. Should this connection be lost through fragmentation, reverse transcription of the target sequence into cDNA cannot proceed. Upon application of the three assays against Hmbs to oligo (dT) primed cDNA from this tissue sample set, it was found that the centrally located and particularly the 5' proximal target sequence were mostly lost completely through degradation at longer post-mortem intervals (data not shown). In most instances, the 5' proximal amplicon could not be detected at/beyond 48 hours post-mortem, and in one of the four replicates, fell below the sensitivity of the qPCR assay after only 12 hours post-mortem. This problem was likely exacerbated by the fact that of the three RNAs examined here, Hmbs has the lowest starting basal level of expression, reducing the dynamic range over which the qPCR assays can quantify and track its degradation.

7.3.2 Amplification of differently sized targets on a single RNA

In this study, two assays were applied to Psmc4 to examine the effect of target sequence size on the success of qPCR amplification for partially degraded post-mortem tissue RNA. These two assays targeted a short (71 nucleotide) and long (227 nucleotide) fragment of the Psmc4 transcript, and were engineered to overlap at the same position on the Psmc4 RNA so that target position was not an additional variable in analysis. The assays were applied to RNA extracted from the skeletal muscle of mice left to decompose at 22 °C for up to 72 hours. RNA was reverse transcribed into cDNA using the random priming strategy, to provide a balanced covering of the transcriptome.

The raw data upon qPCR amplification of the short and long target sequences of Psmc4 is illustrated in Figure 7.9. Over the 72 hours, mean raw C_Q is seen to increase for both, indicative of a reduction in the amplifiable quantity of Psmc4 RNA. The measured increase in mean C_Q (ΔC_Q) over the total 72 hours was

slightly higher for the 227 nt amplicon at ΔC_Q 10.00, compared to 8.03 for the 71 nt amplicon. Assuming 100% qPCR efficiency, this gives an approximately 261-fold and 1,024-fold reduction in the expression of the short and long amplicons respectively over the 72 hour period.

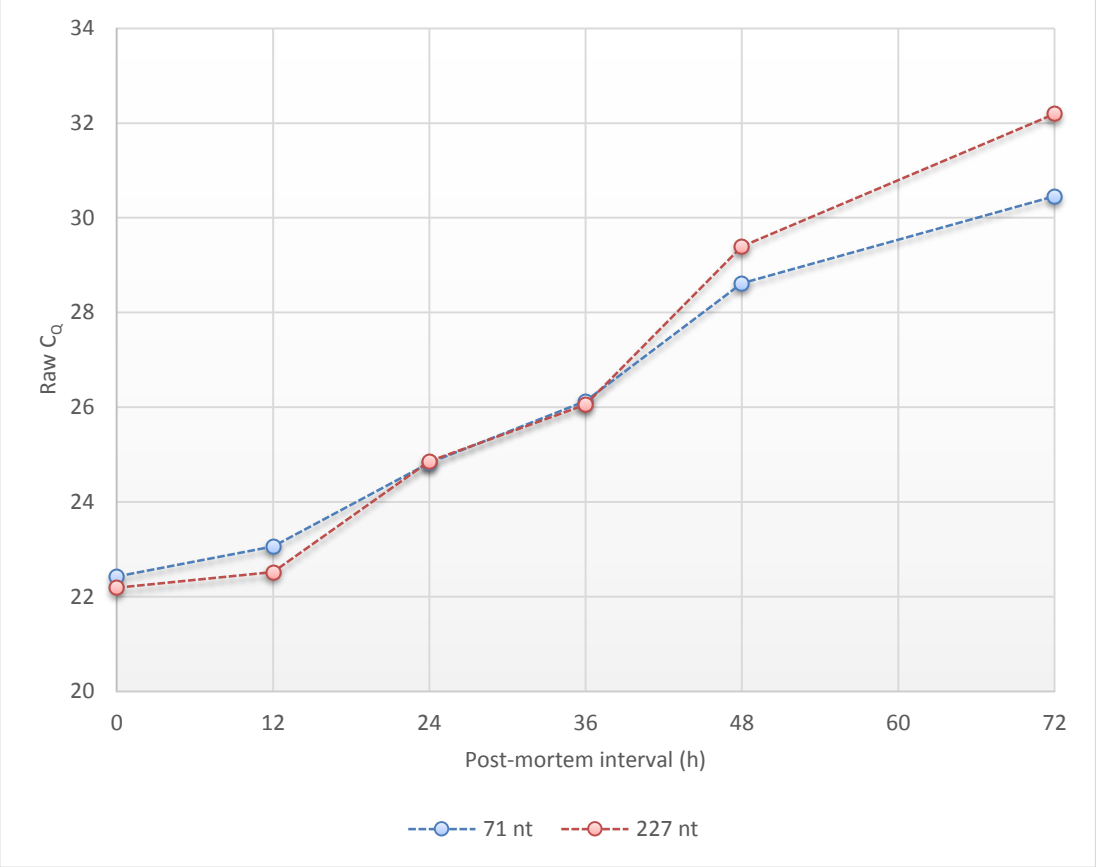

Figure 7.9: **Raw RT-qPCR data upon amplification of the short (71 nucleotide) and long (227 nucleotides) targets on the Psmc4 RNA from the skeletal muscle tissue of mice decomposed at 22 °C for up to 72 hours**. cDNA synthesised from RNA using random priming. Data represents mean of n = 3. Error bars have been omitted for clarity.

Prior to this study, it was hypothesised that RNA degradation over the post-mortem interval would cause more significant reduction in the measured quantity of the long RNA target sequence. This is as a result of its length, which makes it more likely to become 'broken' by post-mortem RNA degradation. The qPCR target sequence only has to be 'broken' once to make it unamplifiable and thus undetectable by RT-qPCR.

The data presented lends support to this proposition. To examine the relative relationship of the short (71 nt) and long (227 nt) amplicons more closely, Figure 7.10 presents the calculated mean $2^{-\Delta\Delta C_Q}$ (short – long). It was found that over the first 36 hours post-mortem, the relative level of these two target sequences deviated very little from 1. This is demonstrated also in Figure 7.9, where the raw C_Q values are tightly packed during this time. After 48 hours, the mean $2^{-\Delta\Delta C_Q}$ (short – long) rises slightly, indicating a 2.21-fold increase in the expression of the 71 nt amplicon of Psmc4 relative to the 227 nt amplicon. This increase stretches to a mean $2^{-\Delta\Delta C_Q}$ of 5.32 after 72 hours post-mortem.

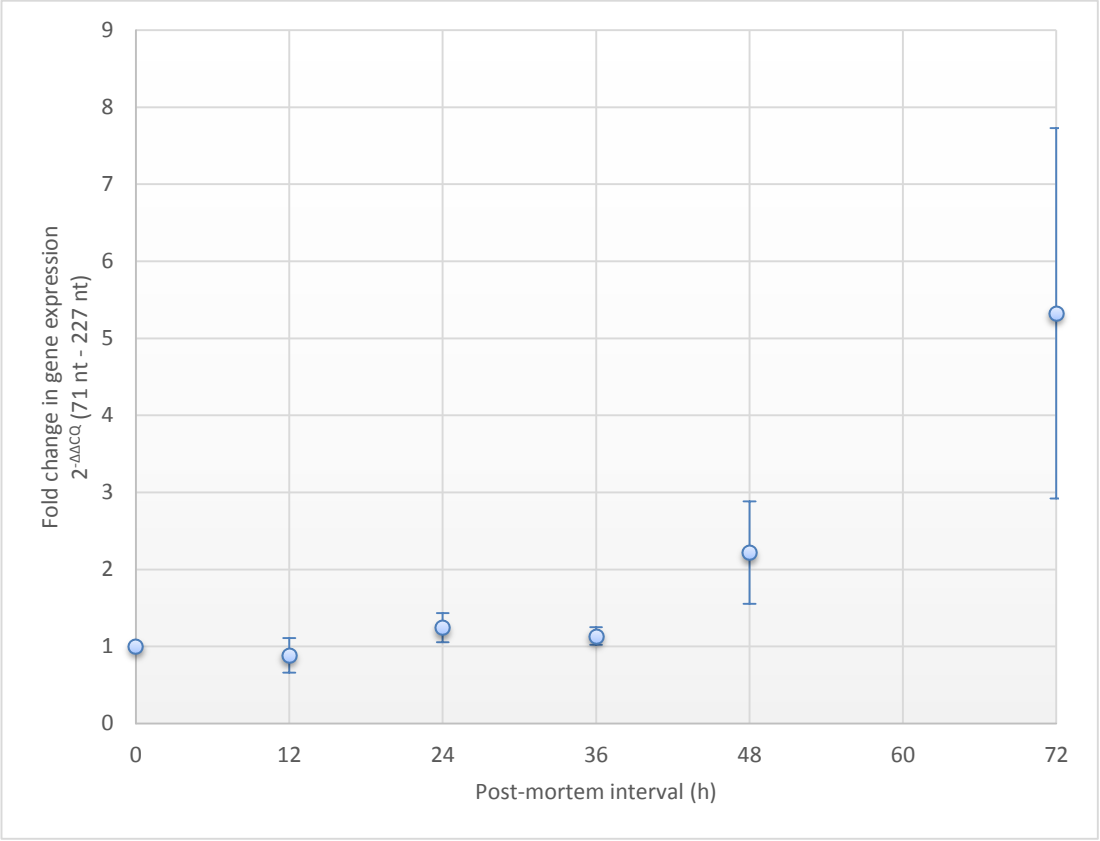

Figure 7.10: **Fold change in expression of the short (71 nucleotides) and long (227 nucleotides) target sequences of Psmc4 in the skeletal muscle of mice decomposed at 22 °C for up to 72 hours**. Data represents the fold change in gene expression in terms of $2^{-\Delta\Delta C_Q}$ (short – long). cDNA synthesised from RNA using random priming. Data points represent the mean of n = 3 ± S.E.

Particularly at the highest post-mortem intervals, the $2^{-\Delta\Delta CQ}$ data was found to be extremely variable between replicates. Figure 7.11 represents the results of linear regression analysis for the $2^{-\Delta\Delta CQ}$ (short – long) data, which was found to fit best with a quadratic profile. At the 48 and 72 hour post-mortem intervals, the difference in $2^{-\Delta\Delta CQ}$ between triplicates was extremely high, causing the wide 95% prediction and confidence intervals. This high level of variability between biological replicates meant that post-mortem interval was deemed to be a poor predictor of $2^{-\Delta\Delta CQ}$, accounting for only 52.9% of its variation (non-adjusted R^2).

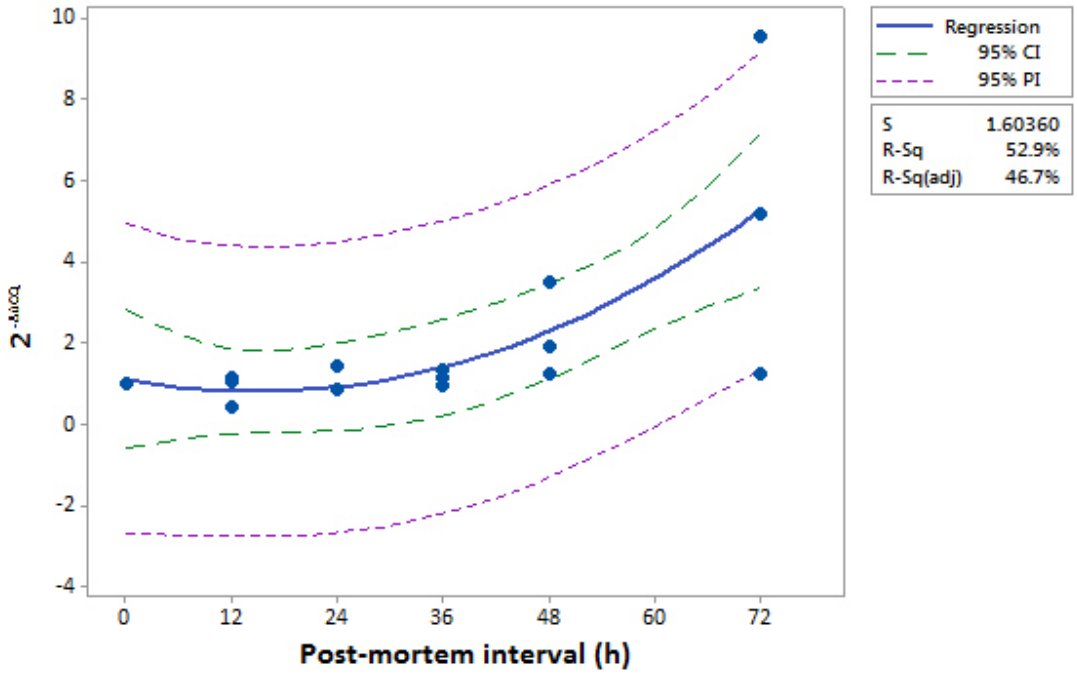

Figure 7.11: **Linear regression analysis of the fold change in expression of the short (71 nucleotides) and long (227 nucleotides) target sequences of Psmc4 in the skeletal muscle of mice decomposed at 22 °C for up to 72 hours**. Data represents the fold change in gene expression in terms of $2^{-\Delta\Delta CQ}$ (short – long). cDNA synthesised from RNA using random priming. Data represents n = 3 per time point. 95% confidence intervals (95% CI) are depicted in green, and 95% prediction intervals (95% PI) in purple.

7.4 Discussion

7.4.1 The nature of post-mortem RNA degradation

Previous chapters have confirmed that after death, RNA is progressively degraded in the tissues of mice (Chapter 5, Chapter 6). However, none of the analyses presented in previous chapters have given any indication as to the nature of this degradation. RNA quality scoring on the Bioanalyzer 2100 gives an indication of the size distribution of RNA fragments, specifically for the highly abundant 28S and 18S rRNAs. In addition, an examination was made of the rate of decay of a number of different RNAs of clinical and/or forensic interest.

The aim of this chapter was to make some inferences regarding the nature of post-mortem RNA degradation, by looking specifically at a small number of RNAs. In live cells, the most common mechanism of degradation is using exoribonucleases which disassemble RNA in the 5' to 3' direction (22). However, the mechanism by which RNA is degraded and lost in post-mortem tissues is unknown. It is proposed here to be a combination of unknown enzymatic and chemical factors. Enzyme efficiency is likely compromised by the suboptimal temperature and pH conditions in cells after death, so it is possible that chemicals produced during autolysis and microbial putrefaction play a major role.

This chapter looked specifically at the degradation of the Hmbs, Sdha and Psmc4 RNAs over a 72 hour post-mortem interval in mouse skeletal muscle. The expression level of sequences near to their 3' end, 5' end and centre were quantified to determine whether degradation was biased towards any particular section of the RNA molecule. Initially, random priming was employed during reverse transcription to give cDNA with a balanced covering of the transcriptome. Two tissue sets were analysed: one giving a wide range of measured RNA qualities (on the Bioanalyzer 2100) from high to low (mice decomposed at 10 °C for up to 72 hours) and one giving a number of extremely poor quality tissue samples (mice decomposed at 22 °C for up to 72 hours).

The outcomes of this work suggest that post-mortem RNA degradation does not occur in an organised fashion as is true of live cells, but is rather unpredictable and variable. The measured quantity of all three of Hmbs, Sdha and Psmc4 was found to reduce significantly with progressing post-mortem interval, indicative of strong degradation. This was irrespective of whether the qPCR assay amplified a sequence proximal to the 3' end, 5' end or in the centre of the RNA molecule. Pair-wise comparison of the relative expression of these three target sequences was performed, looking at three target combinations: $2^{-\Delta\Delta CQ}$ (3' – 5'), $2^{-\Delta\Delta CQ}$ (3' – C) and $2^{-\Delta\Delta CQ}$ (C – 5'). For each combination, no consistent and reproducible relationship was observed. The magnitude of change in their relative expression ($2^{-\Delta\Delta CQ}$) in most instances was very small, often within the margin of error for qPCR replicate measurements. For the $2^{-\Delta\Delta CQ}$ (3' – 5') which was expected to exhibit the most significant fold change in quantity, the $2^{-\Delta\Delta CQ}$ deviated very little from 1 in all of Hmbs, Sdha and Psmc4. Results obtained between biological replicates (different mice) were extremely variable, causing wide margins for error in the mean $2^{-\Delta\Delta CQ}$.

The most likely cause for this trend is that RNA is being degraded indiscriminately either by chemical or enzymatic factors, with no bias as to where the RNA molecule is broken. This has caused an almost parallel reduction in the quantity of the sequences proximal to the 3' and 5' end and in the centre of the molecule. This was true at all levels of the RNA degradation spectrum, from intact to severely degraded samples.

In summary, when random priming has been used during reverse transcription of RNA into cDNA, it seems that the position of the amplicon (3', 5', central) is not a major factor affecting the success of RT-qPCR detection. None of the target sequences examined here consistently and significantly exhibited an improved level of qPCR detection. This is an important assay design consideration when working with post-mortem tissue samples, which are almost certain to contain partially fragmented RNA. The conclusions drawn here suggest that qPCR assays can be designed to amplify any region of an RNA (in poor quality RNA samples) with equivalent success, provided that the amplified cDNA was generated using random priming.

7.4.2 Choice of reverse transcription priming strategy on partially degraded RNA

Random and oligo (dT) priming are the two most commonly implemented strategies used for conversion of RNA into cDNA by reverse transcription (134, 136, 177). Previous work has suggested that of the two, neither provides universally improved cDNA yield. Rather, a study by Stahlberg *et al*. (136) suggested that reverse transcription efficiency can vary between RNA targets, with some exhibiting improved cDNA yield upon random priming and others with oligo (dT) priming. It has been proposed that the oligo (dT) priming strategy is less forgiving of partial degradation of RNA, because of its dependence on the poly (A) tail remaining intact (138).

The results shown in Figure 7.7 indicate that when using oligo (dT) priming, the yield of cDNA produced for all samples was extremely dependent on the position of the qPCR target sequence. As one might expect, the 3' proximal qPCR target – i.e. that closest to the poly (A) tail – was most efficiently reverse transcribed into cDNA. This is highlighted in Figure 7.7 as a substantially lower mean C_Q.

This work has illustrated that the use of random priming during the reverse transcription step is much more suitable than oligo (dT) priming for application to post-mortem tissue samples, which are likely to contain partially fragmented RNAs. As was shown in Tables 7.5 and 7.6, the increase in C_Q (ΔC_Q) over a 72 hour post-mortem interval was much more pronounced when working with cDNA generated by oligo (dT) priming. This increase in mean C_Q is indicative of loss of detectable RNA template through post-mortem degradation. For example, the ΔC_Q (over 72 hours) for the Psmc4 5' proximal target sequence indicated a 13-fold reduction in the quantity of randomly primed Psmc4 cDNA, but oligo (dT) primed Psmc4 cDNA exhibited a 48.5-fold reduction in expression.

Oligo (dT) was also found to perform extremely poorly when used for the reverse transcription of severely fragmented RNA into cDNA. Samples of mouse skeletal muscle decomposed *in vivo* for up to 72 hours at room temperature (22 °C) were assayed for the expression of Hmbs. This was achieved with no issues using

randomly primed cDNA. However, it was not possible to always successfully amplify the 3' proximal, 5' proximal and central amplicons of Hmbs from oligo (dT) cDNA. Often, the quantity of template cDNA fell well below the sensitivity of the assay. This was particularly prevalent for the 5' proximal and centrally located sequences, which could not be amplified from tissue samples with an extended post-mortem interval. For those which could be amplified by qPCR, the amplification curve was so close to the sensitivity of the assay that the reproducibility of replicate measurements was compromised through stochastic amplification. This is known as the 'Monte Carlo' effect, and the scattering of C_Q values is caused by the reduced probability of primer annealing in the early stages of qPCR when the template quantity is very low (134, 247).

What can be deduced from this is that reverse transcription of RNA into cDNA using the random priming strategy is more robust and tolerant of partial RNA degradation, confirming the hypothesis of Stahlberg *et al*. (136). In fact, when using random priming no favourable qPCR target position was identified; with all regions of the RNA molecule equally represented in the cDNA population. As such, these outcomes support the use of reverse transcription using random priming when working with partially decomposed post-mortem tissue samples.

7.4.3 Specialist qPCR primer design for estimation of the post-mortem interval

It has been hypothesised in a number of different research areas that quantification of the degree of RNA degradation could be used as a measure of 'age' (5, 6, 28, 56, 60, 80, 243, 244). In a forensic context, this has been used for the ageing of biological specimens such as blood stains and hair (28, 56, 60, 243, 244). In addition, several researchers have proposed tissue RNA degradation as a potentially quantitative measure of post-mortem interval, as discussed in detail in Section 1.3.2.2.1 , Chapter 1 (4-6, 80).

Up until now, the outcomes of this thesis have not been particularly supportive of the hypothesis that RNA degradation can be used as a quantitative measure of post-mortem interval. It has been shown that the rate of RNA

degradation is strongly variable and unpredictable, and in particular is influenced by tissue type and the environmental conditions. This chapter examined the potential of two assay formats used for estimation of the degree of RNA degradation – amplifying differently located target sequences on a single RNA, and amplifying differently sized target sequences on a single RNA.

7.4.3.1 Amplification of differently positioned targets on a single RNA

Bauer *et al*. were able to demonstrate a linear correlation between the relative expression level of differently positioned target sequences on the FASN transcript and the post-mortem interval (up to 5 days) for human brain and blood samples (5). This was achieved using cDNA generated by oligo (dT) priming, under the premise that degradation would cause preferential loss of the most 5' proximal target sequences. However, this study was conducted prior to the widespread acceptance of real time PCR for gene expression analyses, meaning that their data is not fully quantitative.

This chapter aimed to examine the expression relationship between three differently positioned target sequences on each of Hmbs, Sdha and Psmc4. These three RNA targets were reverse transcribed from post-mortem skeletal muscle tissue RNA (of post-mortem interval up to 72 hours) using oligo (dT) priming. The relationship between the expression of the 3' proximal, 5' proximal and central target sequences on each of Hmbs, Sdha and Psmc4 were compared using the $2^{-\Delta\Delta CQ}$ (3' – 5'), $2^{-\Delta\Delta CQ}$ (3' – C) and $2^{-\Delta\Delta CQ}$ (C – 5') formulae.

It was found that degradation behaviour was variable between each of the three RNAs examined. Hmbs exhibited minimal fold change in the relative expression of the 3' proximal, 5' proximal and centrally located sequences (Figure 7.8A). Sdha and Psmc4 both exhibited a small increase in the $2^{-\Delta\Delta CQ}$ (3' – 5') and $2^{-\Delta\Delta CQ}$ (3' – C), indicative of improved detection of the 3' proximal target sequence (Figure 7.8B and 7.8C). Their relationship remained fairly steady until 36 hours post-mortem interval, after which it took a sharp increase between 36 to 48 hours and plateaued. No substantial change was observed in the $2^{-\Delta\Delta CQ}$ (C – 5') with

increasing post-mortem interval, indicating that both the 5' proximal and centrally located sequences were affected equally by RNA degradation.

This outcome refutes the findings of Bauer *et al*., who used human brain and blood samples of differing post-mortem intervals as a substrate for gene expression analysis (5). The expression relationship between the 3' proximal, 5' proximal and central sequences of Hmbs, Sdha and Psmc4 did not exhibit a linear correlation with post-mortem interval as demonstrated by Bauer *et al*. Unexpectedly, the expression relationship documented was more sigmoidal in shape. This is more in line with the conclusions drawn by Popova *et al*. (269), who pertain that use of 5':3' expression ratios as quality scores during microarray analyses has some quantitative value for moderate RNA degradation, but loses sensitivity and dynamicity in heavily fragmented RNA samples.

Overall, this work indicates that this experimental format may possess some limited merit for quantification of post-mortem interval. However, the non-linear nature of RNA degradation and its high variability between replicates restricts its predictive value.

7.4.3.2 Amplification of differently sized targets on a single RNA

In undegraded RNA, two differently sized target sequences on a single RNA molecule should in theory, be present in equimolar amounts (60). Upon fragmentation of the RNA, it is statistically more likely for the longer target amplicon to be 'broken'. It only takes a single 'break' in the target RNA sequence to render it unamplifiable and thus undetectable by qPCR. As such, it has been shown that the relative expression level of two differently sized RNA target sequences changes over time (60, 129), making for a measure of RNA degradation.

The author is aware of no published works to date that have applied this principle towards estimation of post-mortem interval. This work involved the development of a duplex assay against the Psmc4 RNA transcript, amplifying a short (71 nt) and long (227 nt) target sequence within the RNA. It was hypothesised that

post-mortem RNA fragmentation would cause a more pronounced reduction in the measurable quantity of the long (227 nt) target sequence relative to the short sequence, causing a progressive increase in $2^{-\Delta\Delta CQ}$ over the course of the post-mortem interval.

The data generated confirms this hypothesis, where the mean $2^{-\Delta\Delta CQ}$ (short – long) increased from 1 to 5.32 over the 72 hour post-mortem interval examined (Figure 7.10). This supports the findings of Anderson *et al*. (60) who demonstrated a strong relationship between the expression ratio of a short and long RNA target sequence of each of 18S rRNA and ACTB and blood stain age. However, the expression relationship between the two target sequences was not linear but followed a quadratic profile – with little change apparent during the first 36 hours. In addition, it was found to be extremely variable between replicates, making it poorly predictive of post-mortem interval.

7.5 Summary and conclusions

Box 7.1 at the beginning of this chapter presented three research 'questions' which this work endeavoured to answer. To conclude, these questions will be revisited to contextualise the original aims with the data presented in this chapter.

Does RNA degrade 'at random' in post-mortem tissues, or does the decay of individuals RNAs retain a directional element to it as is true in live cells?

It was found that although significant degradation was apparent from the raw C_Q data, the expression ratio of sequences proximal to the 5' end, 3' end and centre of three mRNAs (Hmbs, Sdha and Psmc4) did not vary significantly over the course of the post-mortem interval. This is suggestive of random fragmentation causing a parallel loss in their measured quantity, rather than the more organised directional degradation.

If RNA degradation does retain a directional element to it, could a duplex qPCR assay targeting two differently positioned sequences on a single RNA be used as a quantitative measure of post-mortem interval?

The magnitude of variation in the expression of the 5' proximal, 3' proximal and centrally located sequences of three mRNAs (Hmbs, Sdha and Psmc4) was extremely small, non-linear and strongly variable between replicates. As such, this suggests that a duplex qPCR assay targeting two differently positioned sequences on a single RNA holds little merit as a measure of post-mortem interval.

Could a duplex qPCR assay targeting two differently sized sequences on a single RNA be used as a quantitative measure of post-mortem interval?

By amplifying a short and long target sequence on a single RNA (Psmc4), it was found that their expression relationship (in terms of the $2^{-\Delta\Delta CQ}$) increased steadily

over the course of the post-mortem interval. Unfortunately, this relationship was not linear and was found to be extremely variable between replicates. This suggests that a duplex qPCR assay targeting two differently sized sequences on a single RNA holds some merit as a measure of post-mortem interval, but not in its current format.

Even under extremely controlled laboratory conditions as has been achieved here, RNA decay behaviour in post-mortem tissues has been demonstrated to be extremely variable and difficult to predict. For researchers who wish to work towards a quantitative assay for estimation of post-mortem interval, a change of tack is likely required. For example, the use of small RNAs such as miRNAs (or tRNAs) might be considered, as these can be amplified with extremely small length qPCR target sequences which have been demonstrated to be more robust against degradation (80). Subjecting samples to gene expression analysis is a costly and time consuming process. As such, unless this method provides overwhelmingly improved accuracy and precision in post-mortem interval estimates over current methodologies (Section 1.3.2.1, Chapter 1) then it is unlikely to prosper in future.

Chapter 8: General discussion, conclusions and recommendations for future work

RNA analysis presents a unique opportunity to answer a wide range of as yet, unanswered questions in forensic science. This thesis has focused on two related research themes – detecting cell-specific RNA expression for identification of biological specimens, and quantifying RNA degradation in post-mortem tissues.

As different cell types are postulated to exhibit their own unique transcriptome, Chapter 3 explored the use of this principle to ascertain whether or not mock casework samples contained traces of menstrual blood, vaginal secretions and skin cell deposits. An analytical protocol was devised and applied to 'blind' biological specimens mimicking casework samples – incorporating a wide range of body fluids and contact traces, both new and degraded. This work validated the reliability and reproducibility of cell-specific RNA detection, contributing to the work of the RNA branch of the EDNAP group (3, 66).

On the whole, the outcomes presented in Chapter 3 support the use of RNA profiling for identification of menstrual blood, vaginal secretions and skin cell deposits. RNA/DNA co-extraction did not appear to compromise the quality of DNA profiles obtained. Surprisingly, it was still possible to successfully characterise RNA markers in stains which had been aged for up to 6 years. This provides evidence of the long-term persistence of RNA in biological specimens, in line with the research aims of the rest of this thesis. Many assays exhibited excellent sensitivity towards their respective body fluid: e.g. 1/64th of a menstrual blood and a vaginal fluid swab could be accurately identified. However, some issues were identified regarding poor sensitivity for a number of RNA markers; particularly the MSX1, LEFTY2 and SFRP4 RNAs in menstrual blood, Lgas RNA for vaginal secretions and the eight skin RNAs. Additionally, a number of RNAs exhibited cross-reactivity to body fluids other than their intended target – particularly the supposed vaginal fluid specific markers Ljen, Lcris, MYOZ1 and MUC4. This highlights the requirement for more work to

identify RNA markers with expression exclusive to their respective body fluid. Alternatively, future work must focus on developing a novel method to quantify total human RNA yield and normalise the input to RT-PCR, to gain an optimum balance of sensitivity and specificity. The use of endogenous control RNAs other than B2M, UBC and UCE should be researched to improve their sensitivity when applied to difficult sample substrates. In addition, the need for future investigations to look closely at the development and validation of interpretation strategies for RNA evidence was also highlighted, particularly with regard to false negatives (30, 71). This 'interpretation' theme was continued throughout the rest of this thesis, with regard to the characterisation of RNA profiles from post-mortem tissues.

As well as exhibiting tissue type specificity, it has been postulated that RNA profiling could in future be used as a diagnostic tool in forensic pathology. However, RNA is a labile molecule and is under constant attack from enzymatic, chemical, microbial and physical factors during the post-mortem interval: defined as the time frame between physiological death until discovery of the body, autopsy and tissue collection (82). This time lag is inevitable, and what happens to RNA during this time is largely unknown. Having already developed and validated a method for the detection of tissue specific RNAs, this research proceeded to broadly analyse the decay behaviour of RNA in post-mortem tissues. The key objective was to determine for how long after death transcriptome analysis provides reliable and informative data regarding gene activity; which is of specific interest in forensic pathology.

Unfortunately, human autopsy samples are extremely heterogeneous with regard to variables such as age, gender, cause of death, health, pharmacological treatments and conditions during the post-mortem interval. Consequently, the use of animal models for preliminary research of this kind has been advocated because of the ease with which these variables can be controlled. This research has used the laboratory mouse as an animal model to study the decay of RNA in skeletal muscle, kidney, liver and heart tissue over the first three days following death.

The analysis of RNA recovered from mouse tissue identified that RNAlater® effectively preserves RNA in skeletal muscle, kidney, liver and heart for up to 8 weeks at -20 °C (Chapter 4). To the author's knowledge, there are no other published works confirming the efficacy of RNAlater® in a time-wise study as was achieved here, and using the sensitive and objective RIN algorithm to quantify RNA fragmentation. As such, these outcomes are valuable to researchers not only in forensic science but also those using RNAlater® in their tissue processing workflow in a clinical and veterinary setting.

Additionally, the effectiveness of two RNA purification strategies at recovering RNA from mouse skeletal muscle, kidney, liver and heart was compared: using the liquid-liquid TRI® Reagent RNA extraction system and RNeasy® silica columns (Chapter 4). Both fresh (0 hours post-mortem interval) and partially decomposed (8 and 24 hours post-mortem interval) tissue samples were examined, to identify any bias in the recovery of RNA of differing degrees of fragmentation. It was found that TRI® Reagent consistently recovered a significantly higher yield of RNA for all four tissue types, and that these RNA extracts exhibited a significantly lower proportion of DNA contamination. This is proposed to stem from the repeated wash steps required with RNeasy®, facilitating the loss of RNA. Overall, RNeasy® provided RNA extracts with a higher measured quality (RIN). This was attributed to the inability of the silica membranes to effectively capture small RNA fragments, causing it to return 'artificially' high RIN values. Accordingly, TRI® Reagent was selected as the extraction methodology of choice for all subsequent investigations.

An interesting further extension of this work would be to consider the effectiveness of these two extraction methodologies when applied for the recovery of RNA from body fluid stains (e.g. blood, semen, saliva, menstrual blood, vaginal secretions) and contact traces. EDNAP has implemented the RNeasy® technology into their recommended RNA analysis workflow (3, 41, 65, 66), but this most likely stems from its reduced reagent toxicity and automatability rather than any results-based benefit. The outcomes of this work demonstrate that TRI® Reagent exhibits

improved RNA recovery, and may in turn enhance the sensitivity of RNA analysis in this alternative setting.

RNA behaviour was examined in the skeletal muscle, kidney, liver and heart tissue of mice decomposed for a range of time intervals up to a maximum of 72 hours (Chapters 5 and 6). At no point over the 72 hour post-mortem interval did the yield of RNA from tissues fall below such a level that it could not be analysed by UV-vis spectrophotometry, on the Bioanalyzer 2100 and by RT-qPCR. In the skeletal muscle of mice stored under room temperature conditions, no decline in total RNA yield was observed over the 72 hour post-mortem interval examined. This surprisingly high level of RNA stability is an encouraging outcome, demonstrating that RNA can still be manipulated in the laboratory for several days after death.

It was found that RNA degradation (as quantified in terms of the RIN) does not proceed in a linear fashion, rather with a 'sigmoid' profile. RNA fragmentation was slow to onset, and RNA quality scores converged at the lower end of the RIN spectrum (around RIN 2) after longer post-mortem intervals. As such, it was concluded that the RIN algorithm is insensitive to severe RNA fragmentation, and may not serve as an effective screening tool prior to downstream analysis for post-mortem tissue RNA. This non-linearity also restricts the informative value of tissue RNA quality (RIN) as a predictor of post-mortem interval.

As expected, it was found that the environmental conditions to which the mouse corpse was exposed had a significant effect on the degradation rate of RNA. Mice were left to decompose at one of three ambient temperatures – 10 °C, 22 °C and 30 °C. The transcriptome was best preserved in those mice stored in cooler conditions – with a significant reduction in RNA quality only detected after 24, 9 and 6 hours at 10, 22 and 30 °C respectively. It was estimated that RNA quality fell below the minimum RIN threshold of 3.95 suggested by Weis *et al*. (138) at 36, 24 and 12 hours upon decomposition at 10, 22 and 30 °C respectively. As such, this work has identified that the time span during which RNA can be reliably analysed is strongly dependent on post-mortem interval factors such as temperature. Further work should consider other post-mortem variables such as humidity or exposure

(e.g. clothing, coverings, burials, submersion in water) and how these affect decomposition as a whole and also the degradation of tissue RNA. In addition, it would be interesting to consider the preservation of RNA under mock mortuary conditions, where the corpse would most likely be stored in a refrigerator at 4 °C; likely to further increase the time span during which tissue RNA quality remains sufficiently high.

Perhaps the most surprising outcome of all has been identifying differential degradation of RNA species over the course of the post-mortem interval (Chapter 5). Even among endogenous control RNAs which were expected to be amongst the most stably expressed RNAs in the transcriptome, significant variability was observed between their decay rates. Of the six RNAs examined 18S rRNA was deemed most stable, most likely as a result of the structural protection conferred upon it by the ribosome (28). B2m and Actb exhibited similar decay profiles, as did Hmbs and Ubc. Gapdh was found to be extremely susceptible to fragmentation. The same rank order of stability was consistent across technical replicates (tissue samples from the same mice), biological replicates (tissue samples from different mice), between tissue types (skeletal muscle, kidney, liver and heart) and across all environmental temperatures considered. This highlights an element of predictability to RNA decay behaviour. Despite this, strong variability in the magnitude of RNA degradation was observed between replicates; limiting its predictive value for post-mortem interval. This strong data variability suggests that in post-mortem tissues, small-scale changes in gene expression most likely cannot be assessed reliably (4). Although differential stability of RNAs post-mortem is not a new phenomenon (87, 93, 233, 234), to the author's knowledge this study represents the first time that it has been demonstrated solely for endogenous control RNAs. This highlights the future requirement that the degradation profile of all RNAs in a diagnostic assay must be thoroughly characterised.

Actb was identified as the most suitable endogenous control RNA for normalisation purposes in mouse skeletal muscle tissue, by both the geNorm and NormFinder softwares. 18S rRNA and Gapdh were deemed poorest, most likely resulting from their 'extremes' of stability. Future work should consider a much

wider range of potential endogenous control RNAs out with the six that this study was restricted to, to identify which (and how many) are best for normalisation of gene expression data pertaining to post-mortem tissues. In addition, it is important that endogenous controls are selected to mirror the anticipated stability level of a diagnostic target RNA, to prevent erroneous attribution of an up- or down-regulation of a gene which is actually an artefact of differential degradation (232).

More work is required to identify a suitable 'cut-off' RIN below which the results of gene expression analysis are likely to be compromised. Two thresholds have been suggested in the literature – a RIN of 3.95 suggested by Weis *et al*. (138) and 5 by Fleige *et al*. (212). However, these two thresholds have not been generated for screening with subsequent RT-qPCR in mind; rather for determining which samples are suitable for microarray and endpoint RT-PCR analysis. Data presented in Chapter 5 highlighted a strong relationship between RIN and the results of RT-qPCR (ΔC_Q), and demonstrated 3.95 to be the more suitable threshold of the two. However, because RT-qPCR uses small target amplicons (in this study ranging from 59 to 107 nt in length) it is much more robust against degradation compared to other technologies. As such, the author advocates that the concept of a 'RIN threshold' for post-mortem tissues should be revisited with this in mind. This would require statistical analysis of a significantly larger number of tissue samples than has been achieved here, representing all areas of the RIN spectrum.

Based on the quantified level of the RNA encoding for the immediate early gene Fos, it has been estimated that mouse skeletal muscle remained transcriptionally active during the first 30 minutes following death. Unfortunately, the detected up-regulation in Fos expression was lost within the first 3 hours, most likely as a result of accelerated Fos mRNA degradation. This mirrors the findings of Ikematsu *et al*. with Fos and other RNA targets (97, 239). This outcome is positive, demonstrating that cells do retain some transcriptional activity during and immediately after the death event. The main focus of future research must be to identify RNAs with up- and down-regulation associated with different causes of death. This would be best achieved using high throughput technologies such as microarrays or RNA sequencing. In addition, assessment should be made of their

degradation profiles during the immediate hours/days following death to determine their long-term diagnostic value.

Most of the research presented throughout this thesis has used an *in vivo* decomposition model, in which tissues (skeletal muscle, kidney, liver and heart) were left to decompose within an intact corpse. However, it is becoming clear that more and more studies are embracing the more practical *ex vivo* decomposition simulation (6). The validity of this approach was explored in Chapter 6, to determine whether RNA decay behaviour is appreciably different across both settings.

It was found that during the first 8 hours post-mortem, the drop in total RNA quality (RIN) was most pronounced in the muscle, liver and heart tissues decomposed *ex vivo*. By 48 hours post-mortem any observed difference between the *in vivo* and *ex vivo* categories was lost, as RNA quality converged at an extremely poor RIN 2. Upon comparison of the RT-qPCR data for 18S rRNA and Gapdh in skeletal muscle and heart, no significant difference in their measured quantity was found between the *in vivo* and *ex vivo* categories. On the converse, the quantity of 18S rRNA and Gapdh mRNA reduced more rapidly in *in vivo* decomposed kidney and liver. It would be interesting in future experimentation to extend the post-mortem interval beyond 48 hours, to determine whether or not a similar effect could be observed in skeletal muscle and heart tissue.

Overall, this data suggested that in the short term, RNA degradation 'kicks in' earliest in tissues removed from the corpse. However, in the longer term, RNA is preserved better in tissues removed from the corpse, segregating them from the influence of other organ systems such as the bacteria-rich gastrointestinal tract. This outcome is concerning and merits further investigation, particularly with regard to the increasing number of studies which attempt to directly compare gene expression data generated under the two experimental designs. As the data suggests an influence of surrounding tissue types on RNA degradation, it would be interesting also to consider how blood loss (e.g. through infliction of a wound) and dehydration affect the redistribution of fluids and migration of bacteria throughout

the corpse, and whether this would affect the rate of tissue and RNA decomposition. In addition, to more thoroughly compare *in vivo* and *ex vivo* decomposition than has been achieved in this pilot study future work should consider a wider range of tissue types and a larger panel of target RNAs, other than solely 18S rRNA and Gapdh mRNA.

Finally, two alternative approaches to RT-qPCR design were considered, both of which aim to elucidate the nature of RNA degradation (i.e. random or directional) and track its progression in post-mortem tissues. Initially, target sequences were amplified proximal to the 3' end, 5' end and centre of the Hmbs, Sdha and Psmc4 mRNAs. It was found that the ratio of their expression did not change significantly in mouse skeletal muscle over a 72 hour post-mortem interval. As a result, this type of RT-qPCR assay design has little or no predictive value for estimation of the degree of RNA degradation and ultimately, the post-mortem interval. From this data, it was concluded that post-mortem RNA degradation most likely proceeds 'at random', causing a parallel reduction in the measured quantity of the 3', 5' and central portions of each RNA target by RT-qPCR. This outcome also suggests that the positioning of a qPCR target on an RNA has no specific ramifications with regard to the success rate of RT-qPCR for partially decomposed tissues; an important consideration in assay design.

The second approach involved amplification of two differently sized target sequences on the Psmc4 mRNA – a 71 and a 227 nucleotide target. Longer target sequences are known to be more susceptible to degradation, a single 'break' preventing qPCR amplification (129). It was found that during the first 36 hours post-mortem, $2^{-\Delta\Delta CQ}$ (short – long) did not deviate appreciably from 1, indicative of no preferential degradation of the 71 or 227 nt Psmc4 sequence. At 48 to 72 hours, the $2^{-\Delta\Delta CQ}$ (short – long) began to rise in line with increasing post-mortem interval.

This outcome suggests that this method of qPCR assay design holds some potential as a method to quantify RNA degradation and in due course, post-mortem interval. However, its predictive value is limited by its insensitivity to mild RNA fragmentation during the early post-mortem interval (≤ 36 hours). The two

amplicons were selected to represent the extremes of length (minimum and maximum) practically analysable by qPCR, and thus it is difficult to envisage that this methodology could be altered to make it more sensitive. Alternative approaches in future might consider the use of small RNAs such as miRNAs, as these can be amplified with extremely small length qPCR target sequences which have been demonstrated to be very robust against degradation (80).

Overall, this thesis has taken a broad look at RNA behaviour in tissues after death. The data presented suggests that the use of RNA degradation as an indicator of post-mortem interval is fraught with difficulties and uncertainties, such as its strong variability between replicates (Chapters 5 and 7) and its apparent dependence on external conditions (Chapter 5) and tissue type (Chapter 6). Several interesting attributes have been identified, such as the preservation of RNA in tissues at low temperatures, the differential decay of endogenous control RNAs, and the dependence of RNA decay behaviour on surrounding tissues/organ systems. The outcomes of this work are applicable not only in forensic pathology, but also in clinical research where post-mortem tissues are used as a substrate to study the molecular basis of disease.

Appendix 1: Quantitative PCR assay quality control data

A1.1 Introduction: Quality control in real time PCR

All of the data presented in this thesis has been analysed using relative quantification methods such as the $2^{-\Delta\Delta CQ}$. Although the use of relative quantification does not directly necessitate the use of a standard curve for calibration purposes, it is essential that a number of features of each PCR assay be characterised for quality control purposes. The term PCR assay refers to a pair of PCR primers and a dye-labelled probe (or just a pair of PCR primers, in the case of a SYBR® Green paired assay), used for quantification of a single cDNA target. Such quality control features include the linearity or the resultant qPCR raw data, qPCR efficiency, reproducibility, sensitivity and results of negative controls.

The linearity and qPCR efficiency of a particular assay can be easily assessed by generation of a standard curve, using a serial dilution of cDNA. Figure A1.1 illustrates an example standard curve for the Sdha assay (utilised in Chapter 7), using a 1:3 dilution series of cDNA in water. Typically, the relationship between the log of cDNA template starting quantity and the raw C_Q should remain linear up to 5 orders of magnitude (162).

When the $\log_{10}$ of the starting RNA concentration and C_Q are plotted, the gradient of the best-fit straight line can be used to estimate the qPCR efficiency, using the following formula:

$$Efficiency = 10^{\left(\frac{-1}{gradient}\right)} \qquad \text{Equation 1}$$

To obtain this as a percentage, it can be converted as follows:

$$\%\, Efficiency = (Efficiency - 1)\, x\, 100 \qquad \text{Equation 2}$$

This efficiency value gives an estimation of the proportion of PCR products that are doubled with every PCR cycle; an efficiency of 100% implying that every target DNA molecule is duplicated during every PCR cycle. Ideally, a top quality qPCR assay

should possess an optimal amplification efficiency of approximately 90-110% (12, 270). The R^2 gives a measure of the linearity of the standard curve, and should be > 0.98.

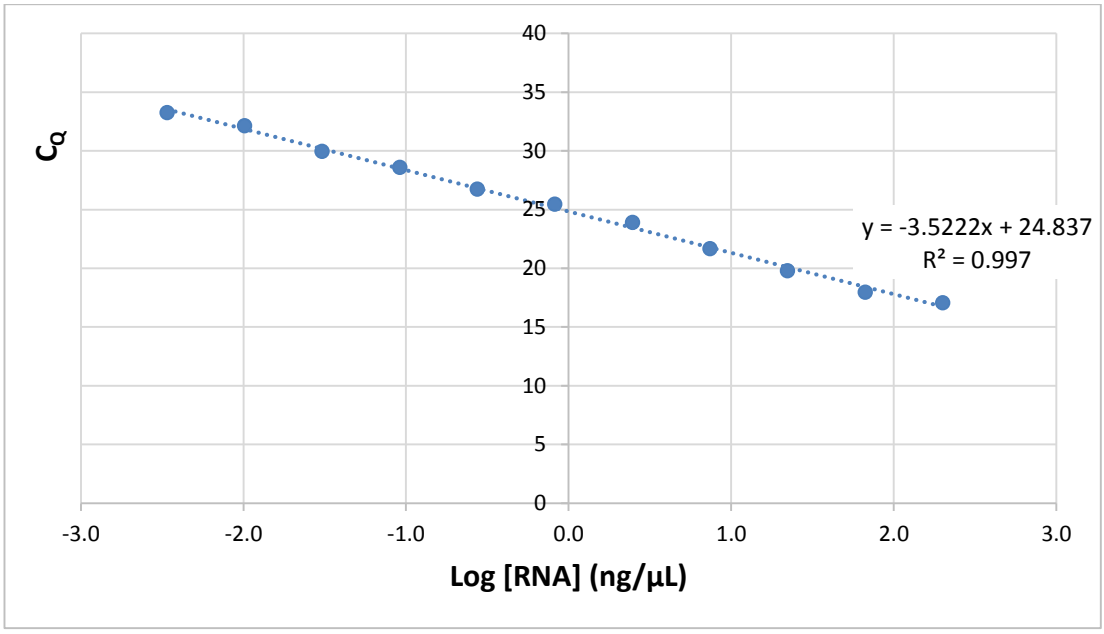

Figure A1.1: **Example standard curve for Sdha TaqMan® assay**. Generated using a 1:3 dilution series of high quality mouse skeletal muscle cDNA ranging in concentration from 200 ng/µL to 0.003 ng/µL of starting RNA.

It is important also to evaluate the reproducibility of the raw C_Qs obtained upon repeated analysis of the same cDNA sample with each qPCR assay. Generally, two types of variation are plotted:

- *Intra-assay variation* – the variability in raw C_Q results obtained upon repeated quantification of a target in a single cDNA sample, within the same qPCR plate and with the same batch of qPCR mastermix
- *Inter-assay variation* – the variability in raw C_Q results obtained upon repeated quantification of a target in a single cDNA sample, across different qPCR plates and with different batches of qPCR mastermix

Finally, the assays are examined using two types of negative control; for both of which they should return a negative result. Firstly, the no template control (NTC) assesses for cDNA contamination by amplification of a blank water sample. The RT- control assesses for amplification of genomic DNA (rather than the desired cDNA), by amplification of an RNA sample subjected to reverse transcription in the absence of reverse transcriptase. Tables A1.2 and A1.3 below illustrate typical NTC and RT- negative controls for each of the assays, but these are completed periodically as standard.

All of the aforementioned quality control parameters should be determined for all qPCR assays prior to their application on experimental samples. Upon publication of the data generated, these quality control parameters should be reported in the resulting manuscript in accordance with the *Minimum Information for Publication of Quantitative Real Time PCR Experiments* (MIQE) guidelines (126), normally within a supplementary table or spreadsheet. The MIQE guidelines provide a huge set of quality control parameters that should be published alongside experimental data for all qPCR experiments.

A1.2 Quality control data: *TaqMan*® PCR assays

The following pages illustrate identity details of all *TaqMan*® assays used in Chapters 5, 6 and 7 of this thesis and their relevant quality control data. All *TaqMan*® assays were purchased from an inventory available through Life Technologies.

Table A1.1: **Details of Life Technologies inventoried *TaqMan*® qPCR assays used throughout Chapters 5, 6 and 7**.

Target RNA	Abbreviation	Protein function	Life Technologies TaqMan® assay ID	Amplicon length (nt)	Assay location	Exon boundary targeted
18S ribosomal RNA	18S rRNA	Essential structural component of the small eukaryotic ribosomal subunit	Mm03928990_g1	61	152-211	N/A
β2-microglobulin	B2m	Component of MHC Class I molecules, involved in the presentation of foreign intracellular antigens to the immune system	Mm00437762_m1	77	111-187	1-2
β-actin	Actb	Cytoskeletal protein which, along with other actin subtypes form microfilaments, involved in maintenance of cell shape and motility	Mm01205647_g1	72	201-271	2-3
Glyceraldehyde-3-phosphate dehydrogenase	Gapdh	Enzyme catalysing the conversion of glyceraldehyde-3-phosphate into glycerate-1,3-bisphosphate during glycolysis	Mm99999915_g1	107	75-181	1-2
Hydroxymethyl-bilane synthase	Hmbs	Enzyme catalysing the tetramerisation of porphobilinogen into hydroxymethylbilane during the haem biosynthetic pathway	Mm00660260_g1 Mm01143545_m1 Mm01168620_g1	82 81 81	220-302 473-554 778-859	1-2 6-7 10-11

Target RNA	Abbreviation	Protein function	Life Technologies TaqMan® assay ID	Amplicon length (nt)	Assay location	Exon boundary targeted
Ubiquitin C	Ubc	Small regulatory protein used to 'tag' proteins for degradation by the proteasome or to alter ther activity of cellular localisation	Mm00446973_m1	80	104-184	1-2
Succinate dehydrogenase complex, subunit A, flavoprotein variant	Sdha	Enzyme catalysing the conversion of succinate to fumarate during the Krebs' cycle	Mm01352362_m1 Mm01352368_m1 Mm01352360_m1	67 73 69	174-241 1098-1171 1942-2011	2-3 8-9 14-15
Proteasome 26S subunit, ATPase 4	Psmc4	ATPase enzyme catalysing the dephosphorylation of ATP to ADP releasing energy Resides within the proteasome, providing energy for protein degradation and amino acid recycling	Mm01176478_m1 Mm00457191_m1 Mm00821599_g1	74 78 71	104-178 750-828 1220-1291	1-2 6-7 10-11
FBJ murine osteosarcoma oncogene	Fos	Immediate early gene pair, rapidly expressed by cells in response to a wide variety of cell stimuli Form the heterodimer AP-1, a key transcription factor	Mm00487425_m1	59	279	1-2
Jun proto-oncogene	Jun		Mm00495062_s1	81	787-867	N/A

Target RNA	Abbreviation	Protein function	Life Technologies TaqMan® assay ID	Amplicon length (nt)	Assay location	Exon boundary targeted
Transforming growth factor beta-1	Tgfb1	Inducible cytokine secreted from many cell types, controls cell growth, proliferation, differentiation and apoptosis	Mm01178820_m1	59	1728-1787	1-2
Caspase 3	Casp3	Member of apoptotic signalling cascade in both the extrinsic and intrinsic apoptosis activation systems	Mm01195084_m1	79	711-789	2-3
Fas receptor	Fas	Cell membrane receptor accepting signals from the Fas ligand	Mm01204974_m1	76	702-777	8-9
Fas associated death domain	Fadd	Adaptor protein involved in extrinsic apoptosis activation system	Mm00438861_m1	98	336-433	1-2
DNA fragmentation factor 40	Dff40	DNase enzyme, induces chromatin condensation and DNA degradation during apoptosis	Mm00438410_m1	67	550-616	3-4
Caspase 6	Casp6	Effector caspase during apoptosis	Mm00438053_m1	90	356-445	4-5
Apoptotic protease activating factor 1	Apaf1	Activator of the intrinsic apoptosis activation system	Mm01223702_m1	62	3261-3322	18-19

Table A1.2: **Summary of *TaqMan*® qPCR assay quality control data for assays used in Chapter 5 and 6.** Intra-assay and inter-assay variation was calculated upon repeat examination of n = 8 replicates.

Target ID	Life Technologies Assay ID	RNA concentration range assayed (ng/µL)	qPCR gradient	% efficiency	R^2	C_Q NTC	C_Q RT-	Inter-assay variation (RSD%)	Intra-assay variation (RSD%)
18S rRNA	Mm03928990_g1	0.001-200	-3.6255	88.72	0.994	36.08	36.98	0.863	0.996
B2m	Mm00437762_m1	0.0069-50	-3.6487	87.96	0.995	No C_Q	No C_Q	0.856	0.739
Actb	Mm01205647_g1	0.069-50	-3.4429	95.18	0.997	No C_Q	No C_Q	0.932	0.750
Gapdh	Mm99999915_g1	0.069-50	-3.2730	102.08	0.996	No C_Q	No C_Q	0.938	1.423
Hmbs	Mm01143545_m1	0.069-50	-3.4964	93.20	0.993	No C_Q	No C_Q	0.764	1.314
Ubc	Mm00446973_m1	0.274-200	-3.4792	93.83	0.990	No C_Q	No C_Q	1.431	0.572
Fos	Mm00487425_m1	0.069-50	-3.5088	92.75	0.997	No C_Q	No C_Q	N.D	N.D
Jun	Mm00495062_s1	N/A	N/A	N/A	N/A	N/A	N/A	N.D	N.D
Tgfb1	Mm01178820_m1	0.069-50	-3.1165	109.35	0.972	No C_Q	No C_Q	N.D	N.D
Casp3	Mm01195084_m1	0.274-200	-3.3160	100.24	0.990	No C_Q	No C_Q	N.D	N.D
Fas	Mm01204974_m1	0.274-200	-3.6244	88.76	0.991	No C_Q	No C_Q	N.D	N.D
Fadd	Mm00438861_m1	0.274-200	-3.4427	95.20	0.993	No C_Q	No C_Q	N.D	N.D
Dff40	Mm00438410_m1	0.274-200	-3.4751	93.98	0.992	No C_Q	No C_Q	N.D	N.D
Casp6	Mm00438053_m1	0.274-200	-3.3313	99.61	0.996	No C_Q	No C_Q	N.D	N.D
Apaf1	Mm01223702_m1	0.274-200	-3.5043	92.91	0.994	No C_Q	No C_Q	N.D	N.D

Table A1.3: **Summary of *TaqMan*® qPCR assay quality control data for assays used in Chapter 7.** Intra-assay and inter-assay variation was calculated upon repeat examination of n = 8 replicates, except where indicated with an asterisk (*) n = 6 was used due to reagent constraints.

Target ID	Life Technologies Assay ID	RNA concentration range assayed (ng/µL)	qPCR gradient	% efficiency	R^2	C_Q NTC	C_Q RT-	Intra-assay variation (%RSD)	Inter-assay variation (%RSD)
Hmbs C	Mm01143545_m1	0.069-50	-3.4964	93.20	0.993	No C_Q	No C_Q	0.764	1.314
Hmbs 3’	Mm01168620_g1	0.091-200	-3.4989	93.11	0.998	No C_Q	No C_Q	0.68	0.15
Hmbs 5’	Mm00660260_g1	0.03-200	-3.5194	92.37	0.996	No C_Q	No C_Q	0.97	0.86
Psmc4 C	Mm00457191_m1	0.03-66.67	-3.6378	88.32	0.996	No C_Q	No C_Q	0.69	0.9*
Psmc4 3’	Mm00821599_g1	0.03-66.67	-3.5726	90.51	0.993	No C_Q	No C_Q	0.67	0.84*
Psmc4 5’	Mm01176478_m1	0.03-200	-3.5873	90.00	0.997	No C_Q	No C_Q	0.68	1.36
Sdha C	Mm01352368_m1	0.03-22.22	-3.5384	91.70	0.998	No C_Q	No C_Q	0.92	1.17
Sdha 3’	Mm01352360_m1	0.01-66.67	-3.6366	88.36	0.996	No C_Q	No C_Q	0.9	1.52
Sdha 5’	Mm01352362_m1	0.003-200	-3.5222	92.27	0.997	No C_Q	No C_Q	1.74	0.19

A1.3 Quality control data: SYBR® Green assays

This section describes work done to optimise the PCR primers designed in Chapter 7, Section 7.2.3.2 for amplification of differently sized targets on a single RNA molecule. These primers were coupled with SYBR® Green technology for development of a real time PCR assay. Subsequent sections describe the outcomes of PCR primer concentration optimisation, dissociation curve analysis and qPCR efficiency and linearity. Both assays were deemed fit for purpose prior to application on post-mortem tissue samples.

A1.3.1 PCR primer optimisation

The first step of qPCR assay optimisation involved determination of the optimum primer concentration at which the qPCR reactions works at its highest efficiency. The optimum primer concentration is defined as the combination at which the C_Q of a single sample is lowest. Figures A1.2 and A1.3 display the results of primer matrix optimisation for the Psmc4 short amplicon (71 nucleotides) and Psmc4 long amplicon (227 nucleotides) respectively. Initially, 100 nM, 200 nM and 300 nM combinations of the forward and reverse primers (detailed in Table 7.4, Section 7.2.3.2, Chapter 7) were examined for each assay. The results of the first primer matrix optimisations suggested that 200 and 300 nM were most likely to provide the best results; as such, primer optimisation was limited only to their combinations to conserve reagents. It was concluded that PCR amplification was at its optimum efficiency with a 200/300 and 300/300 nm forward/reverse primer concentration for each of the short (71 nucleotides) and long (227 nucleotides) target sequences of Psmc4.

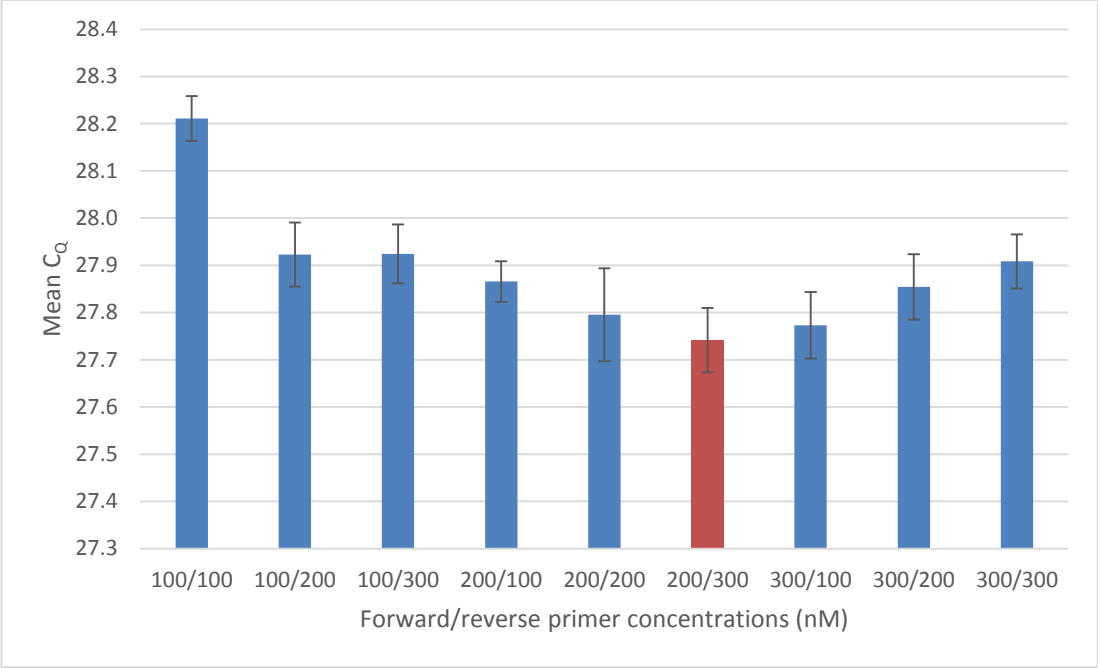

Figure A1.2: **Results upon real time PCR optimisation of primer concentration for the short Psmc4 amplicon (71 nucleotides).** 200/300 nM primer concentration combination provided the lowest C_Q of 27.74, as demonstrated in red. Data represents mean ± S.E. for n = 7.

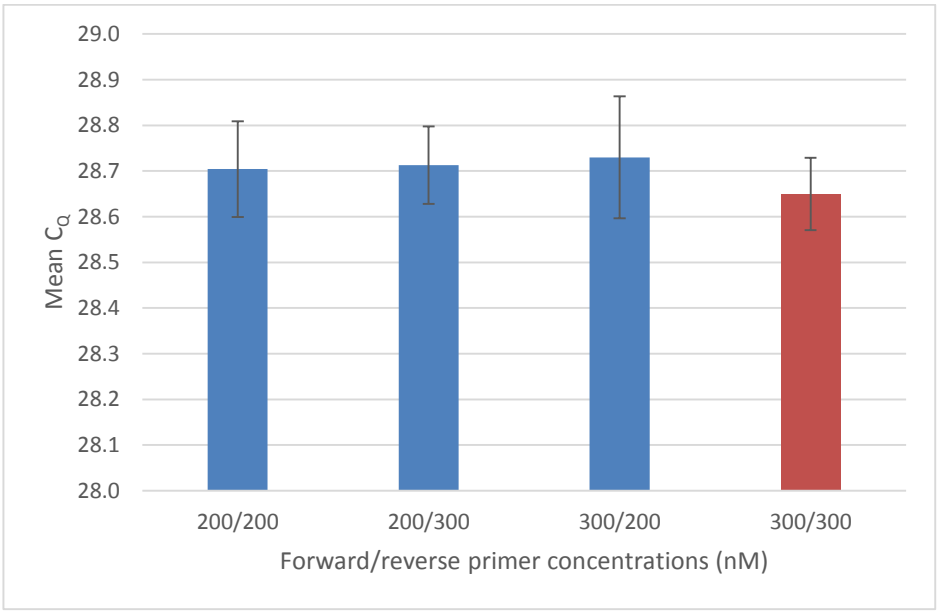

Figure A1.3: **Results upon real time PCR optimisation of primer concentration for the long Psmc4 amplicon (227 nucleotides).** 300/300 nM primer concentration combination provided the lowest C_Q of 28.65, as demonstrated in red. Data represents mean ± S.E. for n = 7.

A1.3.2 PCR amplification specificity

It is imperative that a qPCR assay only amplifies a single sequence of cDNA, and that no non-specific amplification occurs. Non-specific amplification can occur when the primers anneal to a similar sequence of cDNA other than the intended target. Amplification specificity can be assessed using a dissociation curve. To form a dissociation curve, the double stranded DNA PCR product is slowly heated from 55 to 94 °C and the fluorescence continually measured. The temperature at which this dsDNA melts into single stranded form is defined by its length and GC content, but is highly specific to the sequence. Upon melting, the fluorescence of SYBR® Green dye drops dramatically, as it is no longer able to intercalate with dsDNA. This change in fluorescence is illustrated in Figure A1.4.

As a result, a good quality assay should provide a dissociation curve with a single, well revolved peak. Figure A1.4 illustrates a single dissociation curve for one of the two Psmc4 assays (short target, 71 nucleotides). Both dissociation curves indicated that no non-specific amplification occurred with their respective assays.

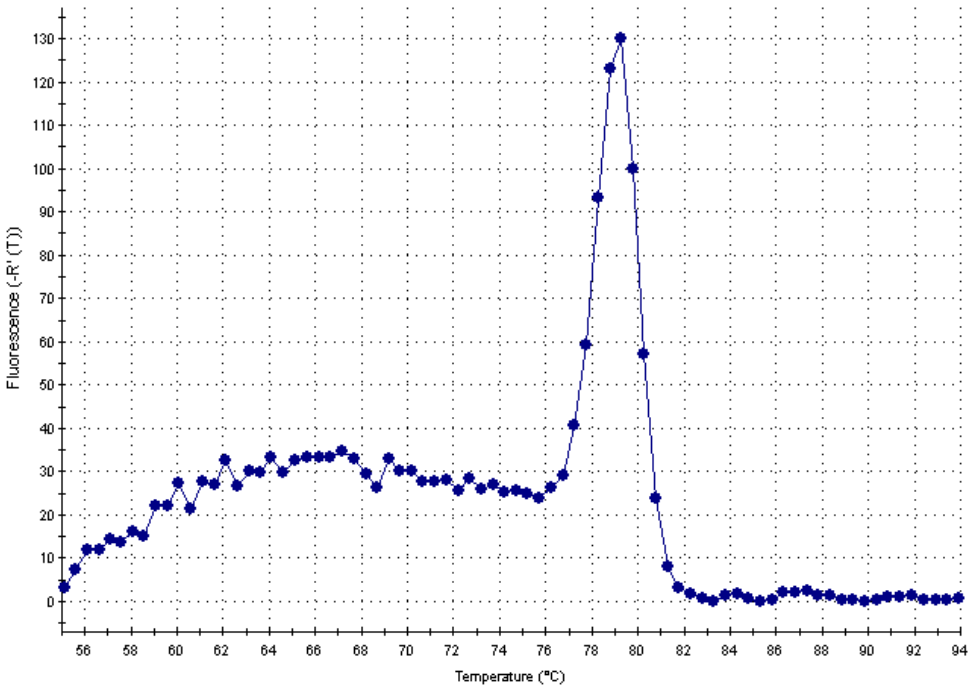

Figure A1.4: **Dissociation curve for the Psmc4 short (71 nucleotides) PCR product**. Melt curve analysis performed between 55 and 94 °C.

A1.3.3 Standard curves and PCR efficiency

The final step of qPCR assay development involved testing of the qPCR efficiency with the use of a dilution series of cDNA. The standard curve for the short (71 nucleotides) amplicon of Psmc4 is included for illustrative purposes in Figure A1.5. Raw C_Q values are plotted for a 1:3 dilution series of mouse skeletal muscle cDNA, prepared in house.

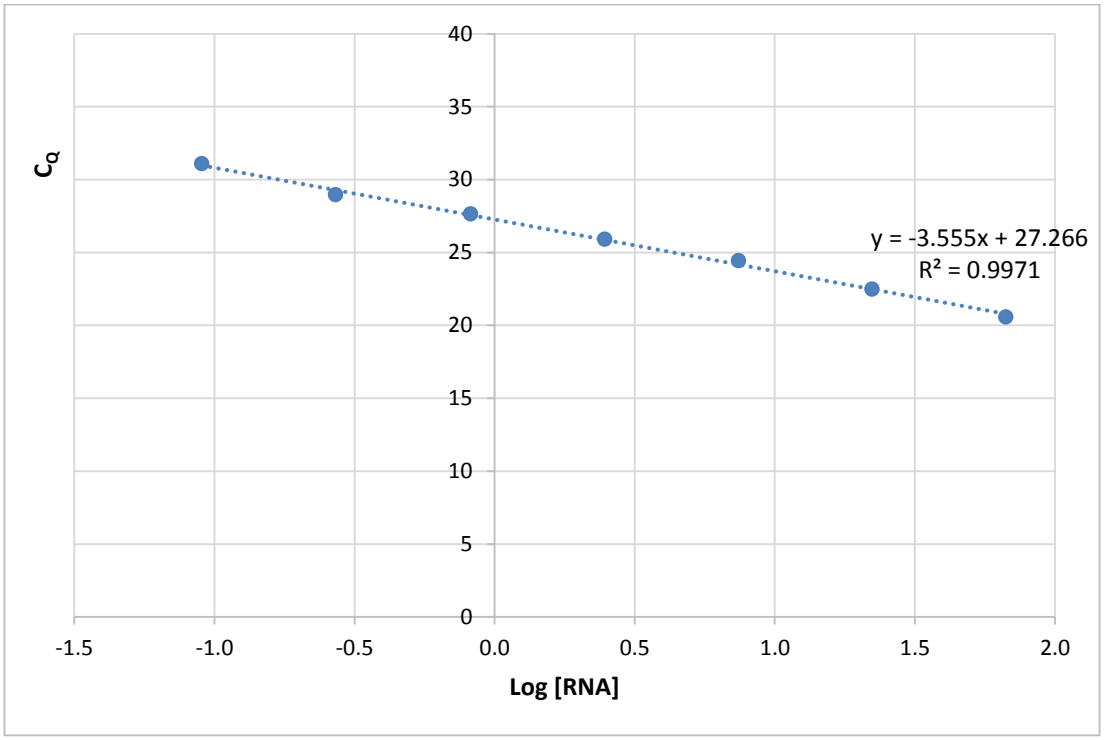

Figure A1.5: **Standard curve illustrated for the Psmc4, short amplicon.** Data points illustrate the mean C_Q (n = 2) over a 1:3 dilution series of cDNA, with an approximate RNA input concentration range of 0.09 to 66.67 ng/µL. The gradient of -3.555 approximates to a qPCR efficiency of 91.11%.

Both SYBR® Green qPCR assays exhibited a sufficient qPCR efficiency and linearity (R^2) to merit their application to post-mortem tissue samples – illustrated in Table A1.4. Unfortunately it was not possible to characterise intra-assay variation, inter-assay variation; due to financial constraints restricting the purchase of further reagents.

Table A1.4: **Quality control data for both SYBR® Green assays used in Chapter 7.**

Target	Input [RNA] range (ng/µL)	qPCR gradient	% Efficiency	R^2	NTC C_Q	RT- C_Q
Psmc4, short amplicon	0.09-66.67	-3.5550	91.11	0.997	No C_Q	No C_Q
Psmc4, long amplicon	0.09-66.67	-3.6719	87.21	0.998	No C_Q	No C_Q

Appendix 2: Electropherogram outputs after RNA analysis of forensic specimens for identification of tissue origin

Chapter 3 details the results obtained after analysing a wide range of mock casework samples for RNAs specific to semen, menstrual blood, vaginal secretions and skin cell deposits. This appendix provides a number of representative electropherograms to illustrate the typical raw data output following these analyses.

Figure A2.1: **Electropherogram of six menstrual blood specific RNA markers and three endogenous control RNAs amplified from ¼ of a menstrual blood swab ('stain 3')**. The nine markers are divided into three PCR multiplexes – the matrix metalloproteinase 3-plex (MMP11, MMP7, MMP10), the menstrual blood 3-plex (MSX1, LEFTY2, SFRP4) and an endogenous control RNA 3-plex (B2M, UBC and UCE).

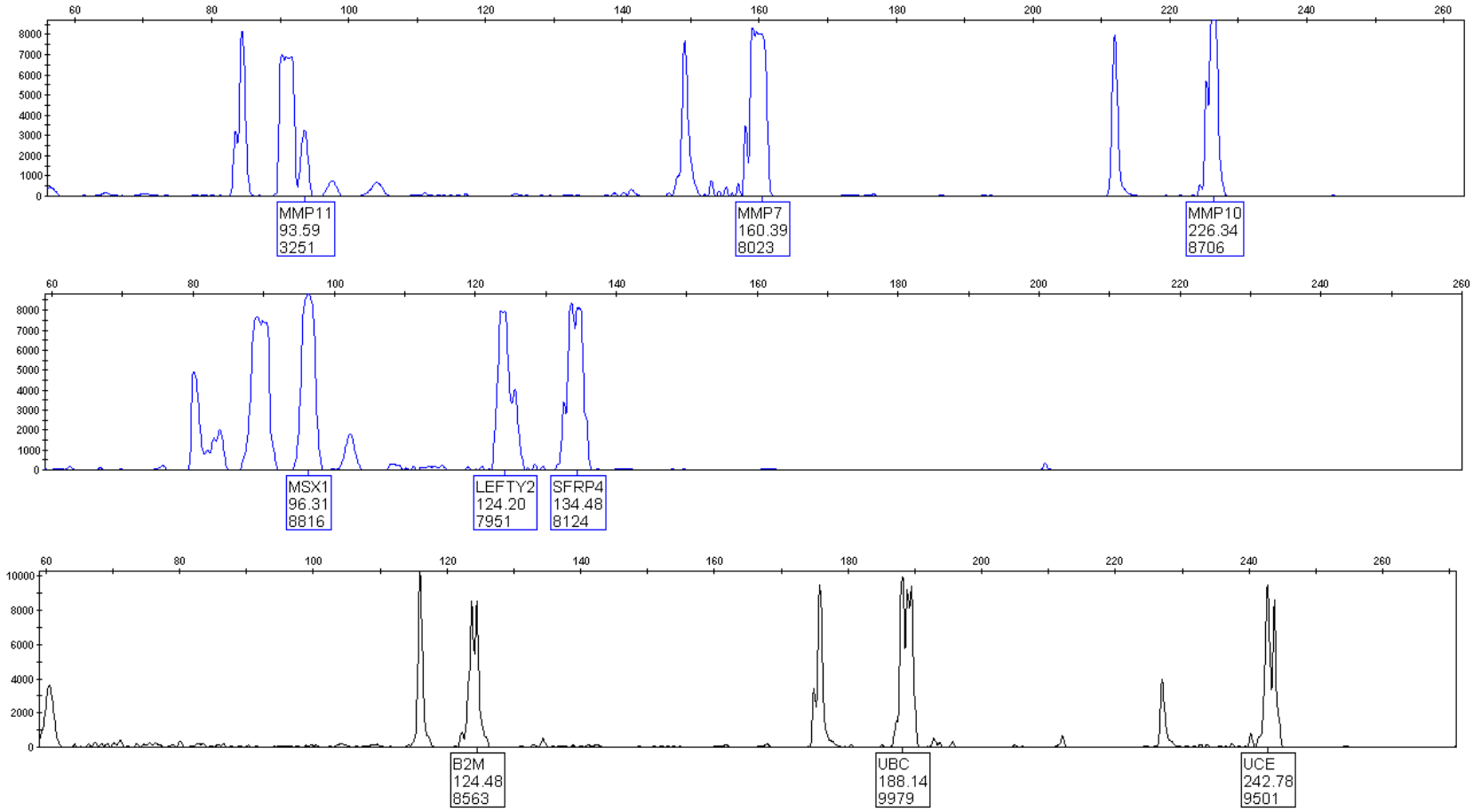

Figure A2.2: **Electropherogram of seven vaginal fluid markers amplified from 1/16th of a vaginal swab**. The seven markers are divided into three PCR multiplexes – the vaginal 3-plex (MYOZ1, CYP2B7P1 and MUC4), Lacto 3-plex (Ljen, Lcris and Lgas) and HBD1 singleplex.

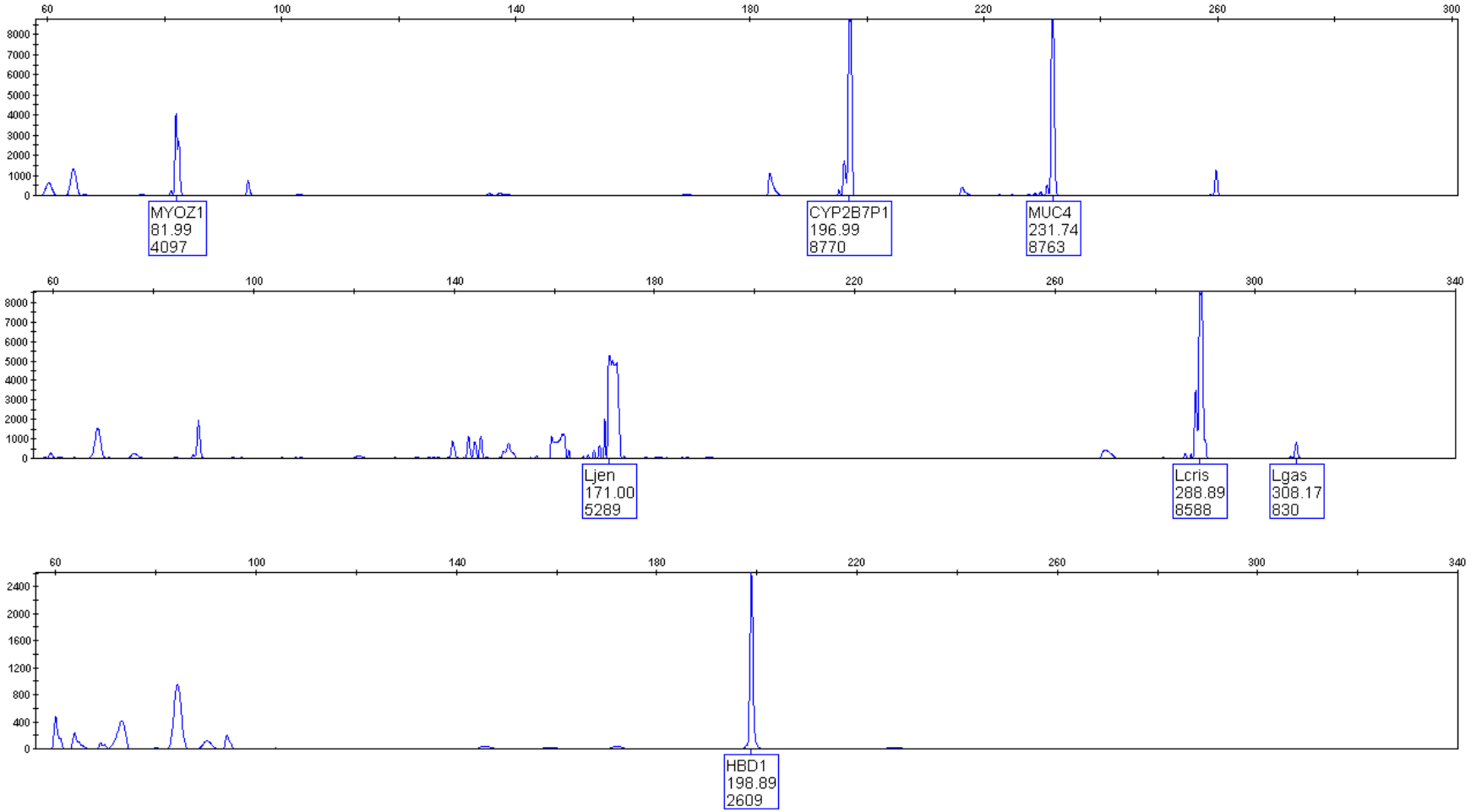

Figure A2.3: **Electropherogram of eight skin markers and three endogenous control RNA markers amplified from 200 ng skin RNA**. The eleven markers are divided into three PCR multiplexes – the skin 1 5-plex (LCE1C, IL1F7, LCE1D, LCE2D and CCL27), the skin 2 3-plex (LOR, CDSN and the missing KRT9) and the HKG 3-plex (B2M, UBC and UCE).

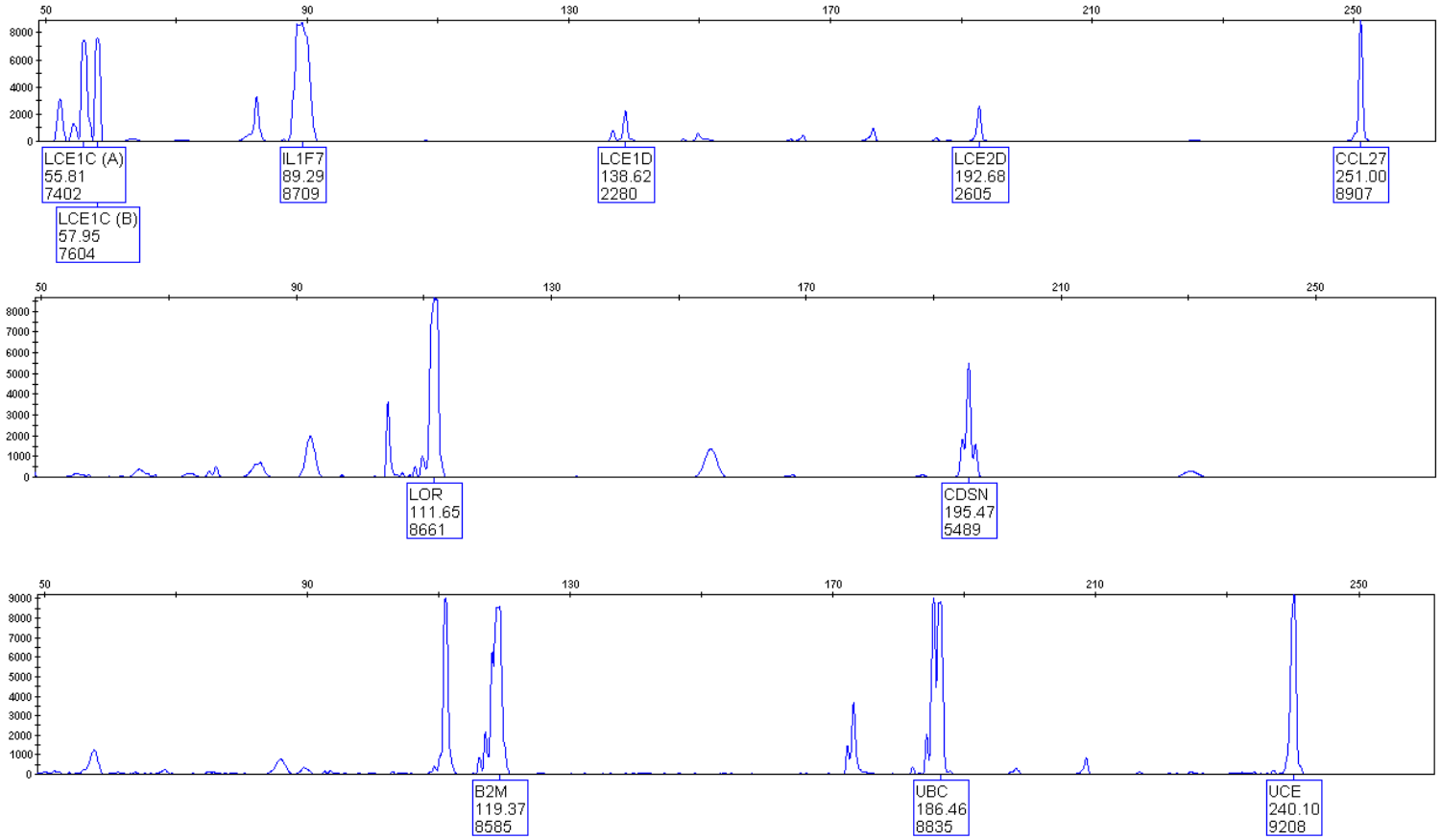

Appendix 3: Assessment of RNA degradation in post-mortem tissues: Raw data

Table A3.1: **$2^{-\Delta\Delta CQ}$ data illustrating the post-mortem fold change in gene expression for all pair-wise comparisons of 18S rRNA, B2m, Actb, Gapdh, Hmbs and Ubc**. Results represent mean of n = 3 skeletal muscle tissue samples for each of 10, 22 and 30°C. 'ND' signifies that this post-mortem interval time point was not examined.

		Mean $2^{-\Delta\Delta CQ}$		
RNA pairing	**Post-mortem interval (h)**	**10 °C**	**22 °C**	**30 °C**
18S rRNA – B2m	0.25	1.000	1.000	1.000
	3	ND	1.460	1.065
	6	ND	0.916	3.757
	9	ND	1.062	ND
	12	4.472	1.450	4.965
	24	4.762	0.989	15.829
	36	4.871	2.235	33.096
	48	2.677	1.692	ND
	72	3.090	1.149	ND
18S rRNA – Actb	0.25	1.000	1.000	1.000
	3	ND	1.245	1.290
	6	ND	0.645	4.016
	9	ND	0.588	ND
	12	3.356	1.651	7.329
	24	3.792	1.336	18.380
	36	5.060	2.721	20.452
	48	3.157	2.679	ND
	72	3.272	1.705	ND

18S rRNA – Gapdh	0.25	1.000	1.000	1.000
	3	ND	1.031	1.152
	6	ND	1.423	5.556
	9	ND	1.375	ND
	12	2.371	2.901	67.442
	24	4.264	9.431	543.425
	36	9.710	81.899	238.205
	48	8.509	141.013	ND
	72	37.337	95.376	ND
B2m – Actb	0.25	1.000	1.000	1.000
	3	ND	1.071	1.038
	6	ND	0.887	1.254
	9	ND	0.638	ND
	12	0.748	1.219	1.673
	24	0.962	1.433	1.284
	36	1.162	1.227	1.132
	48	1.429	1.596	ND
	72	1.176	1.396	ND
B2m – Gapdh	0.25	1.000	1.000	1.000
	3	ND	0.873	1.252
	6	ND	1.807	1.574
	9	ND	1.434	ND
	12	0.639	1.961	14.344
	24	1.228	9.044	34.883
	36	2.228	33.430	13.450
	48	4.875	86.479	ND
	72	15.866	88.136	ND
Actb – Gapdh	0.25	1.000	1.000	1.000
	3	ND	0.818	1.288
	6	ND	2.194	1.311
	9	ND	2.308	ND
	12	0.838	2.019	9.136
	24	1.195	6.998	31.641
	36	1.794	27.012	15.183
	48	3.182	54.239	ND
	72	12.061	73.524	ND

18S rRNA – Hmbs	0.25	1.000	1.000	1.000
	3	ND	0.997	0.958
	6	ND	0.555	2.313
	9	ND	0.765	ND
	12	1.960	1.585	16.440
	24	3.669	5.176	59.474
	36	8.650	20.889	51.822
	48	5.741	40.806	ND
	72	8.982	12.083	ND
B2m – Hmbs	0.25	1.000	1.000	1.000
	3	ND	0.917	0.977
	6	ND	0.905	1.019
	9	ND	0.819	ND
	12	0.515	1.147	3.801
	24	0.886	5.325	3.839
	36	1.906	9.974	2.667
	48	3.232	24.111	ND
	72	3.405	9.655	ND
Actb - Hmbs	0.25	1.000	1.000	1.000
	3	ND	0.832	1.005
	6	ND	1.062	0.838
	9	ND	1.312	ND
	12	0.669	1.088	2.275
	24	0.911	3.916	4.013
	36	1.706	7.971	3.408
	48	2.056	14.200	ND
	72	2.948	6.166	ND
Hmbs – Gapdh	0.25	1.000	1.000	1.000
	3	ND	1.007	1.384
	6	ND	2.397	1.899
	9	ND	1.789	ND
	12	1.224	1.847	3.788
	24	1.631	1.705	9.001
	36	1.095	3.602	4.997
	48	1.712	4.231	ND
	72	4.358	18.101	ND

18S rRNA – Ubc	0.25	1.000	1.000	1.000
	3	ND	0.962	1.242
	6	ND	0.827	3.660
	9	ND	0.972	ND
	12	2.485	1.678	35.714
	24	2.540	5.092	151.747
	36	7.866	14.562	119.180
	48	4.765	31.802	ND
	72	22.400	23.981	ND
B2m – Ubc	0.25	1.000	1.000	1.000
	3	ND	0.775	1.089
	6	ND	1.152	1.254
	9	ND	1.001	ND
	12	0.626	1.260	7.086
	24	0.675	5.533	8.962
	36	1.692	7.183	5.571
	48	2.642	21.308	ND
	72	9.218	23.806	ND
Actb – Ubc	0.25	1.000	1.000	1.000
	3	ND	0.744	1.079
	6	ND	1.390	1.030
	9	ND	1.648	ND
	12	0.813	1.156	4.442
	24	0.678	3.940	10.636
	36	1.427	5.818	7.487
	48	1.727	14.715	ND
	72	7.120	21.576	ND
Ubc – Gapdh	0.25	1.000	1.000	1.000
	3	ND	1.083	1.238
	6	ND	1.662	1.312
	9	ND	1.475	ND
	12	1.015	1.964	1.936
	24	1.753	1.727	4.098
	36	1.262	5.202	2.225
	48	1.749	6.547	ND
	72	1.612	4.316	ND

Hmbs – Ubc	0.25	1.000	1.000	1.000
	3	ND	0.914	1.153
	6	ND	1.407	1.385
	9	ND	1.234	ND
	12	1.243	1.058	1.907
	24	0.866	1.035	2.364
	36	0.855	0.768	2.279
	48	0.909	1.314	ND
	72	2.584	5.769	ND

References

1. Bauer, M. (2007). RNA in forensic science. *Forensic Sci Int: Genet* **1**(1): 69-74.
2. Bauer, M., Patzelt, D. (2002). Evaluation of mRNA markers for the identification of menstrual blood. *J Forensic Sci* **47**(6): 1278-82.
3. Haas, C., Hanson, E., Anjos, M.J., Ballantyne, K.N., Banemann, R., Bhoelai, B., Borges, E., Carvalho, M., Courts, C., De Cock, G., Drobnic, K., Dötsch, M., Fleming, R., Franchi, C., Gomes, I., Hadzic, G., Harbison, S.A., Harteveld, J., Hjort, B., Hollard, C., Hoff-Olsen, P., Hüls, C., Keyser, C., Maroňas, O., McCallum, N. *et al*. (2014). RNA/DNA co-analysis from human menstrual blood and vaginal secretion stains: Results of a fourth and fifth collaborative EDNAP exercise. *Forensic Sci Int: Genet* **8**(1): 203-12.
4. Vennemann, M., Koppelkamm, A. (2010). mRNA profiling in forensic genetics I: Possibilities and limitations. *Forensic Sci Int* **203**(1): 71-5.
5. Bauer, M., Gramlich, I., Polzin, S., Patzelt, D. (2003). Quantification of mRNA degradation as possible indicator of postmortem interval—a pilot study. *Legal Med* **5**(4): 220-7.
6. Sampaio-Silva, F., Magalhães, T., Carvalho, F., Dinis-Oliveira, R.J., Silvestre, R. (2013). Profiling of RNA degradation for estimation of post-morterm (mortem) interval. *PLoS ONE* **8**(2): e56507.
7. Elliott, D., Ladomery, M. (2011). *Molecular Biology of RNA*. 1st ed. New York: Oxford University Press.
8. Haas, C., Klesser, B., Maake, C., Bär, W., Kratzer, A. (2009). mRNA profiling for body fluid identification by reverse transcription endpoint PCR and realtime PCR. *Forensic Sci Int: Genet* **3**(2): 80-8.
9. Tan, S.C., Yiap, B.C. (2009). DNA, RNA, and protein extraction: the past and the present. *BioMed Res Int* **2009:** 1-10.
10. Köhler, A. (2007). Exporting RNA from the nucleus to the cytoplasm. *Nat Rev Mol Cell Biol* **8**(10): 761-73.

11. Meyer, S., Temme, C., Wahle, E. (2004). Messenger RNA turnover in eukaryotes: pathways and enzymes. *Crit Reviews in Biochem and Mol Biol* **39**(4): 197-216.
12. Vennemann, M., Koppelkamm, A. (2010). Postmortem mRNA profiling II: Practical considerations. *Forensic Sci Int* **203**(1-3): 76-82.
13. Yang, E., van Nimwegen, E., Zavolan, M., Rajewsky, N., Schroeder, M., Magnasco, M., Darnell, J.E. (2003). Decay rates of human mRNAs: correlation with functional characteristics and sequence attributes. *Genome Res* **13**(8): 1863-72.
14. Wang, Y., Liu, C.L., Storey, J.D., Tibshirani, R.J., Herschlag, D., Brown, P.O. (2002). Precision and functional specificity in mRNA decay. *Proc Nat Acad Sci* **99**(9): 5860-5.
15. Mitchell, P., Tollervey, D. (2000). mRNA stability in eukaryotes. *Current Op Genet Develop* **10**(2): 193-8.
16. Chen, C., You, Y., Shyu, A. (1992). Two cellular proteins bind specifically to a purine-rich sequence necessary for the destabilization function of a c-fos protein-coding region determinant of mRNA instability. *Mol Cell Biol* **12**(12): 5748-57.
17. Ross, J. (1996). Control of messenger RNA stability in higher eukaryotes. *Trends Genet* **12**(5): 171-5.
18. Gingerich, T.J., Feige, J.J., LaMarre, J. (2004). AU-rich elements and the control of gene expression through regulated mRNA stability. *Animal Health Res Rev* **5**: 49-64.
19. Shim, J., Karin, M. (2002). The control of mRNA stability in response to extracellular stimuli. *Mol Cell* **14**(3): 323-31.
20. Houseley, J., Tollervey, D. (2009). The many pathways of RNA degradation. *Cell* **136**(4): 763-76.
21. Tourrière, H., Chebli, K., Tazi, J. (2002). mRNA degradation machines in eukaryotic cells. *Biochimie* **84**(8): 821-37.
22. Parker, R., Song, H. (2004). The enzymes and control of eukaryotic mRNA turnover. *Nat Struct Mol Biol* **11**(2): 121-7.

23. Parker, R., Sheth, U. (2007). P bodies and the control of mRNA translation and degradation. *Mol Cell Rev* **25**(5): 635-46.

24. Guhaniyogi, J., Brewer, G. (2001). Regulation of mRNA stability in mammalian cells. *Gene* **265**(1): 11-23.

25. van Hoof, A., Parker, R. (2002). Messenger RNA degradation: beginning at the end. *Curr Biology* **12**(8): R285-R7.

26. Juusola, J., Ballantyne, J. (2003). Messenger RNA profiling: a prototype method to supplant conventional methods for body fluid identification. *Forensic Sci Int* **135**(2): 85-96.

27. Haas, C., Hanson, E., Kratzer, A., Bär, W., Ballantyne, J. (2011). Selection of highly specific and sensitive mRNA biomarkers for the identification of blood. *Forensic Sci Int: Genet* **5**(5): 449-58.

28. Anderson, S., Howard, B., Hobbs, G.R., Bishop, C.P. (2005). A method for determining the age of a bloodstain. *Forensic Sci Int* **148**(1): 37-45.

29. Fleming, R.I., Harbison, S.A. (2010). The development of a mRNA multiplex RT-PCR assay for the definitive identification of body fluids. *Forensic Sci Int: Genet* **4**(4): 244-56.

30. Bauer, M., Patzelt, D. (2008). Identification of menstrual blood by real time RT-PCR: technical improvements and the practical value of negative test results. *Forensic Sci Int* **174**(1): 55-9.

31. Zubakov, D., Hanekamp, E., Kokshoorn, M., Van IJcken, W., Kayser, M. (2008). Stable RNA markers for identification of blood and saliva stains revealed from whole genome expression analysis of time-wise degraded samples. *Int J Legal Med* **122**(2): 135-42.

32. Virkler, K., Lednev, I.K. (2009). Analysis of body fluids for forensic purposes: from laboratory testing to non-destructive rapid confirmatory identification at a crime scene. *Forensic Sci Int* **188**(1): 1-17.

33. Roeder, A.D., Haas, C. (2013). mRNA profiling using a minimum of five mRNA markers per body fluid and a novel scoring method for body fluid identification. *Int J Legal Med* **127**(4): 707-21.

34. Barni, F., Lewis, S.W., Berti, A., Miskelly, G.M., Lago, G. (2007). Forensic application of the luminol reaction as a presumptive test for latent blood detection. *Talanta* **72**(3): 896-913.

35. Virkler, K., Lednev, I.K. (2008). Raman spectroscopy offers great potential for the nondestructive confirmatory identification of body fluids. *Forensic Sci Int* **181**(1): e1-e5.

36. Vandenberg, N., Oorschot, R.A.H. (2006). The use of Polilight® in the detection of seminal fluid, saliva, and bloodstains and comparison with conventional chemical-based screening tests. *J Forensic Sci* **51**(2): 361-70.

37. Kashyap, V.K. (1989). A simple immunosorbent assay for detection of human blood. *J Immunoassay* **10**(4): 315-24.

38. Hochmeister, M.N., Budowle, B., Rudin, O., Gehrig, C., Borer, U., Thali, M., Dirnhofer, R. (1999). Evaluation of prostate-specific antigen (PSA) membrane test assays for the forensic identification of seminal fluid. *J Forensic Sci* **44**(1): 1057-60.

39. Pang, B., Cheung, B.K.K. (2008). Applicability of two commercially available kits for forensic identification of saliva stains. *J Forensic Sci* **53**(5): 1117-22.

40. Haas, C., Hanson, E., Morling, N., Ballantyne, J. (2011). Collaborative EDNAP exercises on messenger RNA/DNA co-analysis for body fluid identification (blood, saliva, semen) and STR profiling. *Forensic Sci Int: Genet Suppl Series* **3**(1): e5-e6.

41. Haas, C., Hanson, E., Bär, W., Banemann, R., Bento, A., Berti, A., Borges, E., Bouakaze, C., Carracedo, A., Carvalho, M. (2011). mRNA profiling for the identification of blood - Results of a collaborative EDNAP exercise. *Forensic Sci Int: Genet* **5**(1): 21-6.

42. Setzer, M., Juusola, J., Ballantyne, J. (2008). Recovery and stability of RNA in vaginal swabs and blood, semen, and saliva stains. *J Forensic Sci* **53**(2): 296-305.

43. Fleming, R.I., Harbison, S.A. (2010). The use of bacteria for the identification of vaginal secretions. *Forensic Sci Int: Genet* **4**(5): 311-5.

44. Nussbaumer, C., Gharehbaghi-Schnell, E., Korschineck, I. (2006). Messenger RNA profiling: a novel method for body fluid identification by real-time PCR. *Forensic Sci Int* **157**(2): 181-6.

45. Bauer, M., Kraus, A., Patzelt, D. (1999). Detection of epithelial cells in dried blood stains by reverse transcriptase-polymerase chain reaction. *J Forensic Sci* **44**: 1232-6.

46. Fang, R., Manohar, C.F., Shulse, C., Brevnov, M., Wong, A., Petrauskene, O., Brzoska, P., Furtado, M., (2006). Real-time PCR assays for the detection of tissue and body fluid specific mRNAs. Int Congress Series **1288**: 685-7.

47. Haas, C., Klesser, B., Kratzer, A., Bär, W. (2008). mRNA profiling for body fluid identification. *Forensic Sci Int: Genet Suppl Series* **1**(1): 37-8.

48. Bauer, M., Patzelt, D. (2003). Protamine mRNA as molecular marker for spermatozoa in semen stains. *Int J Legal Med* **117**(3): 175-9.

49. Goh, S.-H., Josleyn, M., Lee, Y.T., Danner, R.L., Gherman, R.B., Cam, M.C., Miller, J.L. (2007). The human reticulocyte transcriptome. *Physiol Genomics*. **30**(2): 172-8.

50. Lindenbergh, A., de Pagter, M., Ramdayal, G., Visser, M., Zubakov, D., Kayser, M., Sijen, T. (2012). A multiplex mRNA-profiling system for the forensic identification of body fluids and contact traces. *Forensic Sci Int: Genet* **6**(5): 565-77.

51. Lindenbergh, A., van den Berge, M., Oostra, R.J., Cleypool, C., Bruggink, A., Kloosterman, A., Sijen, T. (2013). Development of a mRNA profiling multiplex for the inference of organ tissues. *Int J Legal Med* **127**(5): 891-900.

52. Hanson, E., Haas, C., Jucker, R., Ballantyne, J. (2011). Identification of skin in touch/contact forensic samples by messenger RNA profiling. *Forensic Sci Int: Genet Suppl Series* **3**(1): e305-6.

53. Visser, M., Zubakov, D., Ballantyne, K.N., Kayser, M. (2011). mRNA-based skin identification for forensic applications. *Int J Legal Med* **125**(2): 253-63.

54. Jakubowska, J., Maciejewska, A., Pawłowski, R., Bielawski, K.P. (2012). mRNA profiling for vaginal fluid and menstrual blood identification. *Forensic Sci Int: Genet* **7**(2): 272-8.

55. Haas, C., Muheim, C., Kratzer, A., Bar, W., Maake, C. (2009). mRNA profiling for the identification of sperm and seminal plasma. *Forensic Sci Int: Genet Suppl Series* **2**(1): 534-5.

56. Bauer, M., Polzin, S., Patzelt, D. (2003). Quantification of RNA degradation by semi-quantitative duplex and competitive RT-PCR: a possible indicator of the age of bloodstains? *Forensic Sci Int* **138**(1): 94-103.

57. Ferri, G., Bini, C., Ceccardi, S., Pelotti, S. (2004). Successful identification of two years old menstrual bloodstain by using MMP-11 shorter amplicons. *J Forensic Sci* **49**(6): 1387.

58. Kohlmeier, F., Schneider, P.M. (2012). Successful mRNA profiling of 23 years old blood stains. *Forensic Sci Int: Genet* **6**(2): 274-6.

59. Zubakov, D., Kokshoorn, M., Kloosterman, A., Kayser, M. (2009). New markers for old stains: stable mRNA markers for blood and saliva identification from up to 16-year-old stains. *Int J Legal Med* **123**(1): 71-4.

60. Anderson, S.E., Hobbs, G.R., Bishop, C.P. (2011). Multivariate analysis for estimating the age of a bloodstain. *J Forensic Sci* **56**(1): 186-93.

61. Meer, D., Uchimoto, M.L., Williams, G. (2013). Simultaneous analysis of micro-RNA and DNA for determining the body fluid origin of DNA profiles. *J Forensic Sci* **58**(4): 967-71.

62. Wang, Z., Zhang, J., Luo, H., Ye, Y., Yan, J., Hou, Y. (2013). Screening and confirmation of microRNA markers for forensic body fluid identification. *Forensic Sci Int: Genet* **7**(1): 116-23.

63. Hanson, E.K., Lubenow, H., Ballantyne, J. (2009). Identification of forensically relevant body fluids using a panel of differentially expressed microRNAs. *Anal Biochem* **387**(2): 303-14.

64. Akutsu, T., Motani, H., Watanabe, K., Iwase, H., Sakurada, K. (2012). Detection of bacterial 16S ribosomal RNA genes for forensic identification of vaginal fluid. *Legal Med* **14**(3): 160-2.

65. Haas, C., Hanson, E., Anjos, M., Banemann, R., Berti, A., Borges, E., Bouakaze, C., Carracedo, A., Carvalho, M., Castella, V. (2011). RNA/DNA co-analysis from blood stains - Results of a second collaborative EDNAP exercise. *Forensic Sci Int Genet* **6**(1): 70-80.

66. Haas, C., Hanson, E., Anjos, M.J., Banemann, R., Berti, A., Borges, E., Carracedo, A., Carvalho, M., Courts, C., De Cock, G., Dotsch, M., Flynn, S., Gomes, I., Hollard, C., Hjort, B., Hoff-Olsen, P., Hribikova, K., Lindenbergh, A., Ludes, B., Maronas, O., McCallum, N.A., Moore, D., Morling, N., Niederstatter, H., Noel, F., Parson, W., Popielarz, C., Rapone, C., Roeder, A.D., Ruiz, Y., Sauer, E., Schneider, P.M., Sijen, T., Syndercombe Court, D., Sviezena, B., Turanska, M., Vidaki, A., Zatkalikova, L., Ballantyne, J. (2012). RNA/DNA co-analysis from human saliva and semen stains–Results of a third collaborative EDNAP exercise. *Forensic Sci Int: Genet* **7**(2): 230-9.

67. Juusola, J., Ballantyne, J. (2007). mRNA profiling for body fluid identification by multiplex quantitative RT-PCR. *J Forensic Sci* **52**(6): 1252-62.

68. Hanson, E.K., Ballantyne, J. (2013). Highly specific mRNA biomarkers for the identification of vaginal secretions in sexual assault investigations. *Sci Justice* **53**(1): 14-22.

69. Sakurada, K., Akutsu, T., Watanabe, K., Fujinami, Y., Yoshino, M. (2011). Expression of statherin mRNA and protein in nasal and vaginal secretions. *Legal Med* **13**(6): 309-13.

70. Richard, M.L., Harper, K.A., Craig, R.L., Onorato, A.J., Robertson, J.M., Donfack, J. (2012). Evaluation of mRNA marker specificity for the identification of five human body fluids by capillary electrophoresis. *Forensic Sci Int: Genet*. **6**(4): 452-60.

71. Lindenbergh, A., Maaskant, P., Sijen, T. (2012). Implementation of RNA profiling in forensic casework. *Forensic Sci Int: Genet* **7**(1): 159-66.

72. Heinrich, M., Lutz-Bonengel, S., Matt, K., Schmidt, U. (2007). Real-time PCR detection of five different ‘‘endogenous control gene’’ transcripts in forensic autopsy material. *Forensic Sci Int: Genet* **1**(2): 163-9.

73. Phang, T.W., Shi, C., Chia, J., Ong, C. (1994). Amplification of cDNA via RT-PCR using RNA extracted from postmortem tissues. *J Forensic Sci* **39**(5): 1275.

74. Grissom, S.F., Lobenhofer, E.K., Tucker, C.J. (2005). A qualitative assessment of direct-labeled cDNA products prior to microarray analysis. *BMC Genomics* **6**(1): 36.

75. Muggenthaler, H., Sinicina, I., Hubig, M., Mall, G. (2011). Database of post-mortem rectal cooling cases under strictly controlled conditions: a useful tool in death time estimation. *Int J Legal Med* **126**(1): 79-87.

76. Hayashi, T., Ishida, Y., Kimura, A., Takayasu, T., Eisenmenger, W., Kondo, T. (2004). Forensic application of VEGF expression to skin wound age determination. *Int J Legal Med* **118**(6): 320-5.

77. Madea, B., Saukko, P., Oliva, A., Musshoff, F. (2010). Molecular pathology in forensic medicine: Introduction. *Forensic Sci Int*. **203**(1) :3-14.

78. Zhu, G., Chang, Y., Zuo, J., Dong, X., Zhang, M., Hu, G., Fang, F. (2001). Fudenine, a C-terminal truncated rat homologue of mouse prominin, is blood glucose-regulated and can up-regulate the expression of GAPDH. *Biochem Biophys Res Commun* **281**(4): 951-6.

79. Huggett, J., Dheda, K., Bustin, S., Zumla, A. (2005). Real-time RT-PCR normalisation; strategies and considerations. *Genes Immun* **6**(4): 279-84.

80. Li, W.C., Ma, K.J., Lv, Y.H., Zhang, P., Pan, H., Zhang, H., Wang, H.J., Ma, D., Chen, L. (2014). Post-mortem interval determination using 18S rRNA and microRNA. *Sci Justice* **54**(4): 307-10.

81. Koppelkamm, A., Vennemann, B., Lutz-Bonengel, S., Fracasso, T., Vennemann, M. (2011). RNA integrity in post-mortem samples: influencing parameters and implications on RT-qPCR assays. *Int J Legal Med* **125**(4): 573-80.

82. Heinrich, M., Matt, K., Lutz-Bonengel, S., Schmidt, U. (2007). Successful RNA extraction from various human postmortem tissues. *Int J Legal Med* **121**(2): 136-42.

83. Preece, P., Cairns, N.J. (2003). Quantifying mRNA in postmortem human brain: influence of gender, age at death, postmortem interval, brain pH, agonal state and inter-lobe mRNA variance. *Mol Brain Res* **118**(1): 60-71.

84. Miller, C.L., Diglisic, S., Leister, F., Webster, M., Yolken, R.H. (2004). Evaluating RNA status for RT-PCR in extracts of postmortem human brain tissue. *BioTechniques* **36**(4): 628-33.

85. Bahar, B., Monahan, F., Moloney, A., Schmidt, O., MacHugh, D., Sweeney, T. (2007). Long-term stability of RNA in post-mortem bovine skeletal muscle, liver and subcutaneous adipose tissues. *BMC Mol Biol* **8**(1): 108-20.

86. Marchuk, L., Sciore, P., Reno, C., Frank, C., Hart, D. (1998). Postmortem stability of total RNA isolated from rabbit ligament, tendon and cartilage. *Biochim Biophys Acta* **1379**(2): 171-7.

87. Kuliwaba, J.S., Fazzalari, N.L., Findlay, D.M. (2005). Stability of RNA isolated from human trabecular bone at post-mortem and surgery. *Biochim Biophys Acta* **1740**(1): 1-11.

88. Zhao, D., Ishikawa, T., Quan, L., Michiue, T., Zhu, B.L., Maeda, H. (2009). Postmortem quantitative mRNA analyses of death investigation in forensic pathology: An overview and prospects. *Legal Med* **11**: S43-S5.

89. Wang, Q., Ishikawa, T., Michiue, T., Zhu, B.L., Guan, D.W., Maeda, H. (2012). Intrapulmonary aquaporin-5 expression as a possible biomarker for discriminating smothering and choking from sudden cardiac death: A pilot study. *Forensic Sci Int* **220**(1): 154-7.

90. Zhu, B.L., Tanaka, S., Ishikawa, T., Zhao, D., Li, D.R., Michiue, T., Quan, L., Maeda, H. (2008). Forensic pathological investigation of myocardial hypoxia-inducible factor-1 [alpha], erythropoietin and vascular endothelial growth factor in cardiac death. *Legal Med* **10**(1): 11-9.

91. Zhao, D., Ishikawa, T., Quan, L., Michiue, T., Yoshida, C., Komatu, A., Chen, J.H., Wang, Q., Zhu, B.L., Maeda, H. (2009). Postmortem mRNA quantification for investigation of infantile death: A comparison with adult cases. *Legal Med* **11**(1): S286-S9.

92. Zhao, D., Zhu, B.L., Ishikawa, T., Li, D.R., Michiue, T., Maeda, H. (2006). Quantitative RT-PCR assays of hypoxia-inducible factor-1a, erythropoietin and vascular endothelial growth factor mRNA transcripts in the kidneys with regard to the cause of death in medicolegal autopsy. *Legal Med*. **8**(1): 258-63.

93. Zhao, D., Zhu, B.L., Ishikawa, T., Quan, L., Li, D.R., Maeda, H. (2006). Real-time RT-PCR quantitative assays and postmortem degradation profiles of erythropoietin, vascular endothelial growth factor and hypoxia-inducible

factor 1 alpha mRNA transcripts in forensic autopsy materials. *Legal Med* **8**(2): 132-6.

94. Zhao, D., Ishikawa, T., Quan, L., Li, D.R., Michiue, T., Yoshida, C., Komatu, A., Chen, J.H., Zhu, B.L., Maeda, H. (2008). Tissue-specific differences in mRNA quantification of glucose transporter 1 and vascular endothelial growth factor with special regard to death investigations of fatal injuries. *Forensic Sci Int* **177**(2): 176-83.

95. Chen, J.H., Michiue, T., Ishikawa, T., Maeda, H. (2012). Difference in molecular pathology of natriuretic peptides in the myocardium between acute asphyxial and cardiac deaths. *Legal Med* **14**(4): 177-82.

96. Ishida, K., Zhu, B.L., Maeda, H. (2002). A quantitative RT-PCR assay of surfactant-associated protein A1 and A2 mRNA transcripts as a diagnostic tool for acute asphyxial death. *Legal Med* **4**(1): 7-12.

97. Ikematsu, K., Tsuda, R., Nakasono, I. (2006). Gene response of mouse skin to pressure injury in the neck region. *Legal Med* **8**(2): 128-31.

98. Takahashi, S. (2008). Expression levels of mRNAs for catecholamine biosynthetic enzymes as markers of acute response to contusion stress during the early postmortem period. *Tohoku J Exp Med* **216**(3): 239-48.

99. Sun, J., Wang, Y., Zhang, L., Gao, C., Zhang, L., Guo, Z. (2010). Time-dependent expression of skeletal muscle troponin I mRNA in the contused skeletal muscle of rats: a possible marker for wound age estimation. *Int J Legal Med* **124**(1): 27-33.

100. Matsuo, A., Ikematsu, K., Nakasono, I. (2009). C-fos, fos-B, c-jun and dusp-1 expression in the mouse heart after single and repeated methamphetamine administration. *Legal Med* **11**(6): 285-90.

101. Becker, J., Schmidt, P., Musshoff, F., Fitzenreiter, M., Madea, B. (2004). MOR1 receptor mRNA expression in human brains of drug-related fatalities—a real-time PCR quantification. *Forensic Sci Int* **140**(1): 13-20.

102. Liu, J., Lewohl, J.M., Dodd, P.R., Randall, P.K., Harris, R.A., Mayfield, R.D. (2004). Gene expression profiling of individual cases reveals consistent transcriptional changes in alcoholic human brain. *J Neurochem* **90**(5): 1050-8.

103. Grellner, W., Madea, B. (2007). Demands on scientific studies: vitality of wounds and wound age estimation. *Forensic Sci Int* **165**(2): 150-4.

104. Sato, Y., Ohshima, T. (2000). The expression of mRNA of proinflammatory cytokines during skin wound healing in mice: a preliminary study for forensic wound age estimation (II). *Int J Legal Med* **113**(3): 140-5.

105. Bryan, D., Walker, K.B., Ferguson, M., Thorpe, R. (2005). Cytokine gene expression in a murine wound healing model. *Cytokine* **31**(6): 429-38.

106. Takamiya, M., Saigusa, K., Nakayashiki, N., Aoki, Y. (2003). Studies on mRNA expression of basic fibroblast growth factor in wound healing for wound age determination. *Int J Legal Med* **117**(1): 46-50.

107. Werner, S., Peters, K.G., Longaker, M.T., Fuller-Pace, F., Banda, M.J., Williams, L.T. (1992). Large induction of keratinocyte growth factor expression in the dermis during wound healing. *Proc Nad Acad Sci* **89**(15): 6896-900.

108. Fahey III, T.J., Sherry, B., Tracey, K.J., van Deventer, S., Jones II, W.G., Minei, J.P., Morgello, S., Shires, G.T., Cerami, A. (1990). Cytokine production in a model of wound healing: the appearance of MIP-1, MIP-2, cachectin/TNF and IL-I. *Cytokine* **2**(2): 92-9.

109. Takamiya, M., Saigusa, K., Kumagai, R., Nakayashiki, N., Aoki, Y. (2005). Studies on mRNA expression of tissue-type plasminogen activator in bruises for wound age estimation. *Int J Legal Med* **119**(1): 16-21.

110. Phillips, K., McCallum, N., Welch, L. (2012). A comparison of methods for forensic DNA extraction: Chelex-100 and the QIAGEN DNA Investigator Kit (manual and automated). *Forensic Sci Int: Genet*. **6**(2): 282-5.

111. Haas, C., Hanson, E., Anjos, M.J., Banemann, R., Berti, A., Borges, E., Carracedo, A., Carvalho, M., Courts, C., De Cock, G., Dötsch, M., Flynn, S., Gomes, I., Hollard, C., Hjort, B., Hoff-Olsen, P., Hribiková, K., Lindenbergh, A., Ludes, B., Maroňas, O., McCallum, N., *et al*. (2013). RNA/DNA co-analysis from human saliva and semen stains–Results of a third collaborative EDNAP exercise. *Forensic Sci Int: Genet* **7**(2): 230-9.

112. Boom, R.C.J.A., Sol, C.J., Salimans, M.M., Jansen, C.L., Wertheim-van Dillen, P.M., Van der Noordaa, J.P.M.E. (1990). Rapid and simple method for purification of nucleic acids. *J Clin Microbiol* **28**(3): 495-503.

113. Marko, M.A., Chipperfield, R., Birnboim, H.C. (1982). A procedure for the large-scale isolation of highly purified plasmid DNA using alkaline extraction and binding to glass powder. *Anal Biochem* **121**(2): 382-7.

114. Farrell, R.E. (2010). *RNA Methodologies: A Laboratory Guide for Isolation and Characterisation*. 4th ed. London: Elsevier Inc.

115. Chomczynski, P., Sacchi, N. (1987). Single-step method of RNA isolation by acid guanidinium thiocyanate-phenol-chloroform extraction. *Anal Biochem* **162**(1): 156-9.

116. Chomczynski, P., Sacchi, N. (2006). The single-step method of RNA isolation by acid guanidinium thiocyanate–phenol–chloroform extraction: twenty-something years on. *Nat Protoc* **1**(2): 581-5.

117. Fan, H., Gulley, M.L. DNA extraction from fresh or frozen tissues. Molecular Pathology Protocols: Springer; 2001. p. 5-10.

118. Gayral, P., Weinert, L., Chiari, Y., Tsagkogeorga, G., Ballenghien, M., Galtier, N. (2011). Next-generation sequencing of transcriptomes: a guide to RNA isolation in nonmodel animals. *Mol Ecol Resour* **11**(4): 650-61.

119. Cavaluzzi, M.J., Borer, P.N. (2004). Revised UV extinction coefficients for nucleoside-5'-monophosphates and unpaired DNA and RNA. *Nucleic Acid Res* **32**(1): e13.

120. Gallagher, S.R. (1997). Quantitation of DNA and RNA with absorption and fluorescence spectroscopy. Current Protocols in Immunology. New Jersey: John Wiley and Sons.

121. Saunders, G.C., Parkes, H.C. (1999). Analytical Molecular Biology: Quality and Validation. Teddington: LGC.

122. Ambion, Life Technologies. TURBO DNA-free™ Kit: TURBO™ DNase Treatment and Removal Reagents [online] [October 2012; May 2014]. Available at: http://tools.lifetechnologies.com/content/sfs/manuals/cms_055740.pdf.

123. Kallansrud, G., Ward, B. (1996). A comparison of measured and calculated single-and double-stranded oligodeoxynucleotide extinction coefficients. *Anal Biochem* **236**(1): 134-8.

124. Tataurov, A.V., You, Y., Owczarzy, R. (2008). Predicting ultraviolet spectrum of single stranded and double stranded deoxyribonucleic acids. *Biophys Chem* **133**(1): 66-70.

125. Teare, J.M., Islam, R., Flanagan, R., Gallagher, S.R., Davies, M.G., Grabau, C. (1997). Measurement of nucleic acid concentrations using the DyNA Quant and the GeneQuant. *BioTechniques* **22**(6): 1170-4.

126. Bustin, S.A., Benes, V., Garson, J.A., Hellemans, J., Huggett, J., Kubista, M., Mueller, R., Nolan, T., Pfaffl, M.W., Shipley, G.L. (2009). The MIQE guidelines: minimum information for publication of quantitative real-time PCR experiments. *Clin Chem* **55**(4): 611-22.

127. Fontanesi, L., Colombo, M., Beretti, F., Russo, V. (2008). Evaluation of post mortem stability of porcine skeletal muscle RNA. *Meat Sci* **80**(4): 1345-51.

128. Fleige, S., Pfaffl, M.W. (2006). RNA integrity and the effect on the real-time qRT-PCR performance. *Mol Aspect Med* **27**(2): 126-39.

129. Sugita, M., Haney, J.L., Gemmill, R.M., Franklin, W.A. (2001). One-step duplex reverse transcription-polymerase chain reaction for quantitative assessment of RNA degradation. *Anal Biochem* **295**(1): 113.

130. Thermo Fisher Scientific. Nanodrop-1000 Spectrophotometer V3.7 Users Manual [online] [July 2008, June 2014]. Available at: http://nanodrop.com/Library/nd-1000-v3.7-users-manual-8.5x11.pdf.

131. Schroeder, A., Mueller, O., Stocker, S., Salowsky, R., Leiber, M., Gassmann, M., Lightfoot, S., Menzel, W., Granzow, M., Ragg, T. (2006). The RIN: an RNA integrity number for assigning integrity values to RNA measurements. *BMC Mol Biol* **7**(1): 3-17.

132. Agilent Technologies. Agilent RNA 6000 Pico Kit Guide [online] [November 2010, May 2014]. Available at: http://www.chem.agilent.com/library/usermanuals/Public/G2938-90046_RNA600Pico_KG_EN.pdf.

133. Effenhauser, C.S., Paulus, A., Manz, A., Widmer, H.M. (1994). High-speed separation of antisense oligonucleotides on a micromachined capillary electrophoresis device. *Anal Chem* **66**(18): 2949-53.

134. Bustin, S.A., Nolan, T. (2004). Pitfalls of quantitative real-time reverse-transcription polymerase chain reaction. *J Biomol Techniques* **15**(3): 155-66.

135. Atz, M., Walsh, D., Cartagena, P., Li, J., Evans, S., Choudary, P., Overman, K., Stein, R., Tomita, H., Potkin, S. (2007). Methodological considerations for gene expression profiling of human brain. *J Neurosci Methods* **163**(2): 295-309.

136. Ståhlberg, A., Håkansson, J., Xian, X., Semb, H., Kubista, M. (2004). Properties of the reverse transcription reaction in mRNA quantification. *Cin Chem* **50**(3): 509-15.

137. Ståhlberg, A., Kubista, M., Pfaffl, M.W. (2004). Comparison of reverse transcriptases in gene expression analysis. *Clin Chem* **50**(9): 1678-80.

138. Weis, S., Llenos, I.C., Dulay, J.R., Elashoff, M., Martinez-Murillo, F., Miller, C.L. (2007). Quality control for microarray analysis of human brain samples: the impact of postmortem factors, RNA characteristics, and histopathology. *J Neurosci Methods* **165**(2): 198-209.

139. Curry, J., McHale, C., Smith, M.T. (2002). Low efficiency of the Moloney murine leukemia virus reverse transcriptase during reverse transcription of rare t (8; 21) fusion gene transcripts. *BioTechniques* **32**(4): 768.

140. Saiki, R.K., Scharf, S.J., Faloona, F., Mullis, K.B., Horn, G.T., Erlich, H.A., Arnheim, N. (1985). Enzymatic amplification of beta-globin genomic sequences and restriction site analysis for diagnosis of sickle cell anemia. *Science* **230**(4732): 1350-4.

141. Mullis, K.B., Faloona, F.A. (1987). Specific synthesis of DNA in vitro via a polymerase-catalyzed chain reaction. *Methods Enzymol* **155**: 335.

142. Saiki, R.K., Gelfand, D.H., Stoffel, S., Scharf, S.J., Higuchi, R., Horn, G.T., Mullis, K.B., Erlich, H.A. (1988). Primer-directed enzymatic amplification of DNA with a thermostable DNA polymerase. *Science* **239**(4839): 487-91.

143. Butler, J.M. (2012). Advanced Topics in Forensic DNA Typing: Methodology. London: Elsevier Inc.

144. Bustin, S.A. (2002). Quantification of mRNA using real-time reverse transcription PCR (RT-PCR): trends and problems. *J Mol Endocrinol* **29**(1): 23-39.

145. Orlando, C., Pinzani, P., Pazzagli, M. (2005). Developments in quantitative PCR. *Clin Chem Lab Med* **36**(5): 255-69.

146. Zipper, H., Brunner, H., Bernhagen, J., Vitzthum, F. (2004). Investigations on DNA intercalation and surface binding by SYBR Green I, its structure determination and methodological implications. *Nucleic Acid Res* **32**(12): e103-e113.

147. Ishiguro, T., Saitoh, J., Yawata, H., Yamagishi, H., Iwasaki, S., Mitoma, Y. (1995). Homogeneous quantitative assay of hepatitis C virus RNA by polymerase chain reaction in the presence of a fluorescent intercalator. *Anal Biochem* **229**(2): 207-13.

148. Lie, Y.S., Petropoulos, C.J. (1998). Advances in quantitative PCR technology: 5' nuclease assays. *Curr Opin Biotechnol* **9**(1): 43-8.

149. Livak, K.J., Flood, S.J., Marmaro, J., Giusti, W., Deetz, K. (1995). Oligonucleotides with fluorescent dyes at opposite ends provide a quenched probe system useful for detecting PCR product and nucleic acid hybridization. *Genome Res* **4**(6): 357-62.

150. Holland, P.M., Abramson, R.D., Watson, R., Gelfand, D.H. (1991). Detection of specific polymerase chain reaction product by utilizing the 5'----3'exonuclease activity of Thermus aquaticus DNA polymerase. *Proc Nat Acad Sci* **88**(16): 7276-80.

151. Lee, L.G., Connell, C.R., Bloch, W. (1993). Allelic discrimination by nick-translation PCR with fluorgenic probes. *Nucleic Acid Res* **21**(16): 3761-6.

152. Heid, C.A., Stevens, J., Livak, K.J., Williams, P.M. (1996). Real time quantitative PCR. *Genome Res*. **6**(10):986-94.

153. Gibson, U., Heid, C.A., Williams, P.M. (1996). A novel method for real time quantitative RT-PCR. *Genome Res* **6**(10): 995-1001.

154. Preece, P., Virley, D.J., Costandi, M., Coombes, R., Moss, S.J., Mudge, A.W., Jazin, E., Cairns, N.J. (2003). An optimistic view for quantifying mRNA in post-mortem human brain. *Mol Brain Res* **116**(1): 7-16.

155. Life Technologies. TaqMan Universal PCR Master Mix: Protocol, [online], [July 2010; August 2013]. Available at: http://tools.invitrogen.com/content/sfs/manuals/cms_042996.pdf.

156. Pfaffl, M.W. (2001). A new mathematical model for relative quantification in real-time RT–PCR. *Nucleic Acid Res* **29**(9): e45-e51.

157. Čikoš, Š., Bukovská, A., Koppel, J. (2007). Relative quantification of mRNA: comparison of methods currently used for real-time PCR data analysis. *BMC Mol Biol* **8**(1): 113.

158. Ririe, K.M., Rasmussen, R.P., Wittwer, C.T. (1997). Product differentiation by analysis of DNA melting curves during the polymerase chain reaction. *Anal Biochem* **245**(2): 154-60.

159. Bustin, S.A. (2000). Absolute quantification of mRNA using real-time reverse transcription polymerase chain reaction assays. *J Mol Endocrinol* **25**(2): 169-93.

160. Koppelkamm, A., Vennemann, B., Fracasso, T., Lutz-Bonengel, S., Schmidt, U., Heinrich, M. (2010). Validation of adequate endogenous reference genes for the normalisation of qPCR gene expression data in human post mortem tissue. *Int J Legal Med* **124**(5): 371-80.

161. Livak, K.J., Schmittgen, T.D. (2001). Analysis of relative gene expression data using real-time quantitative PCR and the 2-[Delta][Delta] CT method. *Methods* **25**(4): 402-8.

162. Muller, P.Y., Janovjak, H., Miserez, A.R., Dobbie, Z. (2002). Short technical report processing of gene expression data generated by quantitative Real-Time RT-PCR. *BioTechniques* **32**(6): 1372-9.

163. Zhong, H., Simons, J.W. (1999). Direct comparison of GAPDH, β-actin, cyclophilin, and 28S rRNA as internal standards for quantifying RNA levels under hypoxia. *Biochem Biophys Res Commun* **259**(3): 523-6.

164. Chang, T.J., Juan, C.C., Yin, P.H., Chi, C.W., Tsay, H.J. (1998). Up-regulation of beta-actin, cyclophilin and GAPDH in N1S1 rat hepatoma. *Oncol Rep* **5**(2): 469-540.

165. Deindl, E., Boengler, K., van Royen, N., Schaper, W. (2002). Differential expression of GAPDH and β-actin in growing collateral arteries. *Mol Cell Biochem* **236**(1): 139-46.

166. Selvey, S., Thompson, E.W., Matthaei, K., Lea, R.A., Irving, M.G., Griffiths, L.R. (2001). β-Actin - an unsuitable internal control for RT-PCR. *Mol Cell Probes* **15**(5): 307-11.

167. Qiagen. AllPrep DNA/RNA Mini Handbook [Online] [January 2014, November 2005]. Available at: http://www.qiagen.com/gb/resources/resourcedetail?id=bbd50261-3b80-4657-ad58-6a5a97b88821&lang=en.

168. Qiagen. RNeasy® Mini Kit Handbook [online] [June 2012; May 2014]. Available at: http://www.qiagen.com/resources/resourcedetail?id=14e7cf6e-521a-4cf7-8cbc-bf9f6fa33e24&lang=en.

169. Arcturus Bioscience Inc., Life Technologies. PicoPure® RNA Isolation Kit [Online] [January 2004, September 2014]. Available at: https://www.lifetechnologies.com/order/catalog/product/KIT0204?ICID=search-product.

170. Invitrogen, Life Technologies. SuperScript® III First Strand Synthesis System for RT-PCR [Online] [January 2013; June 2014]. Available at: http://tools.lifetechnologies.com/content/sfs/manuals/superscriptIIIfirststrand_pps.pdf.

171. Qiagen. Multiplex PCR Handbook [Online] [August 2014, October 2010]. Available at: http://www.qiagen.com/gb/resources/resourcedetail?id=a541a49c-cd06-40ca-b1d2-563d0324ad6c&lang=en.

172. Qiagen. Investigator® Quantiplex Handbook [Online] [October 2012; November 2011]. Available at: http://www.qiagen.com/resources/resourcedetail?id=6378fac5-aa2f-4140-9518-c0712ca317ae&lang=en.

173. Qiagen. Investigator® Decaplex SE Handbook [Online] [October 2010; November 2011]. No longer available online.

174. Animals (Scientific Procedures) Act 1986. Schedule 1: Appropriate Methods of Humane Killing, Section F4. [Online] [Accessed September 2014]. Available at: http://www.legislation.gov.uk/ukpga/1986/14/schedule/1.

175. Qiagen. RNeasy® Fibrous Tissue Handbook [online] [October 2010; May 2014]. Available at: http://www.qiagen.com/resources/resourcedetail?id=8039840d-4815-4375-8933-bc09247e47c0&lang=en.

176. Sigma Aldrich Ltd. TRI Reagent® Protocol [online] [May 2014]. Available at: http://www.sigmaaldrich.com/technical-documents/protocols/biology/tri-reagent.html.

177. Applied Biosystems, Life Technologies. High Capacity cDNA Reverse Transcription Kits: Protocol [online] [June 2010; May 2014]. Available at: http://tools.lifetechnologies.com/content/sfs/manuals/cms_042557.pdf.

178. Vandesompele, J., De Preter, K., Pattyn, F., Poppe, B., Van Roy, N., De Paepe, A., Speleman, F. (2002). Accurate normalization of real-time quantitative RT-PCR data by geometric averaging of multiple internal control genes. *Genome Biol* **3**(7): 1-12.

179. Andersen, C.L., Jensen, J.L., Ørntoft, T.F. (2004). Normalization of real-time quantitative reverse transcription-PCR data: a model-based variance estimation approach to identify genes suited for normalization, applied to bladder and colon cancer data sets. *Cancer Res* **64**(15): 5245-50.

180. Fleming, R.I., Bowden, A.L., Hermiz, W., Buckleton, J.S., Harbison, S. (2010). The definitive identification of body fluids using mRNA. *Sci Justice* **50**(1): 46.

181. Hanson, E., Haas, C., Jucker, R., Ballantyne, J. (2012). Specific and sensitive mRNA biomarkers for the identification of skin in 'touch DNA' evidence. *Forensic Sci Int: Genet* **6**(5): 548-58.

182. Juusola, J., Ballantyne, J. (2005). Multiplex mRNA profiling for the identification of body fluids. *Forensic Sci Int* **152**(1): 1-12.

183. Sakurada, K., Ikegaya, H., Fukushima, H., Akutsu, T., Watanabe, K., Yoshino, M. (2009). Evaluation of mRNA-based approach for identification of saliva and semen. *Legal Med* **11**(3): 125-8.

184. Scientific Working Group on DNA Analysis Methods (SWGDAM). Validation Guidelines for DNA Analysis Methods [Online] [July 2014, December 2012]. Available at: http://swgdam.org/SWGDAM_Validation_Guidelines_APPROVED_Dec_2012.pdf.

185. Idris, N., Carraway, K.L. (1999). Sialomucin complex (Muc4) expression in the rat female reproductive tract. *Biol Reprod* **61**(6): 1431-8.

186. Dicks, L.M., Silvester, M., Lawson, P.A., Collins, M.D. (2000). Lactobacillus fornicalis sp. nov., isolated from the posterior fornix of the human vagina. *Int J Syst Evol Microbiol* **50**(3): 1253-8.

187. Erhart, W., Alkasi, Ö., Brunke, G., Wegener, F., Maass, N., Arnold, N., Arlt, A., Meinhold-Heerlein, I. (2011). Induction of human β-defensins and psoriasin in vulvovaginal human papillomavirus–associated lesions. *J Infect Dis* **204**(3): 391-9.

188. Nallasamy, S., Li, Q., Bagchi, M.K., Bagchi, I.C. (2012). Msx homeobox genes critically regulate embryo implantation by controlling paracrine signaling between uterine stroma and epithelium. *PLoS Genet* **8**(2): 1-13.

189. Kothapalli, R., Buyuksal, I., Wu, S.Q., Chegini, N., Tabibzadeh, S. (1997). Detection of ebaf, a novel human gene of the transforming growth factor beta superfamily association of gene expression with endometrial bleeding. *J Clin Invest* **99**(10): 2342.

190. Carmon, K.S., Loose, D.S. (2008). Secreted frizzled-related protein 4 regulates two Wnt7a signaling pathways and inhibits proliferation in endometrial cancer cells. *Mol Cancer Res* **6**(6): 1017-28.

191. Dinarello, C.A., Bufler, P., (2013). Interleukin-37. *Semin Immunol* **1**(1): 1.

192. Vermeij, W.P., Alia, A., Backendorf, C. (2011). ROS quenching potential of the epidermal cornified cell envelope. *J Invest Dermatol* **131**(7): 1435-41.

193. Goteri, G., Rupoli, S., Campanati, A., Costagliola, A., Sabato, S., Stramazzotti, D., Picardi, P., Canafoglia, L., Pulini, S., Ganzetti, G. (2009). Lesional skin chemokine CTACK/CCL27 expression in mycosis fungoides and disease control by IFN-α and PUVA therapy. *Am J Transl Res* **1**(2): 203.

194. Kalinin, A., Marekov, L.N., Steinert, P. (2001). Assembly of the epidermal cornified cell envelope. *J Cell Sci* **114**(17): 3069-70.

195. Kobayashi, S., Tanaka, T., Matsuyoshi, N., Imamura, S. (1996). Keratin 9 point mutation in the pedigree of epidermolytic hereditary palmoplantar keratoderma perturbs keratin intermediate filament network formation. *FEBS Lett* **386**(2): 149-55.

196. Oji, V., Eckl, K.M., Aufenvenne, K., Nätebus, M., Tarinski, T., Ackermann, K., Seller, N., Metze, D., Nürnberg, G., Fölster-Holst, R. (2010). Loss of corneodesmosin leads to severe skin barrier defect, pruritus, and atopy: unraveling the peeling skin disease. *Am J Human Genet* **87**(2): 274-81.

197. Baker, D.J., Grimes, E.A., Hopwood, A.J. (2011). D-dimer assays for the identification of menstrual blood. *Forensic Sci Int* **212**(1): 210-4.

198. Bauer, M., Patzelt, D. (2003). A method for simultaneous RNA and DNA isolation from dried blood and semen stains. *Forensic Sci Int* **136**(1): 76-8.

199. Randall, B. (1988). Glycogenated squamous epithelial cells as a marker of foreign body penetration in sexual assault. *J Forensic Sci* **33**(2): 511-4.

200. Van Oorschot, R.A.H., Jones, M.K. (1997). DNA fingerprints from fingerprints. *Nature* **387**(6635): 767.

201. Aditya, S., Sharma, A., Bhattacharyya, C., Chaudhuri, K. (2011). Generating STR profiles from Touch DNA. *J Forensic Leg Med* **18**(7): 295.

202. Ambion, Life Technologies. Working with RNA, the Basics: Avoiding, Detecting and Inhibiting RNase [Online] [2012, August 2014]. Available at: http://www.lifetechnologies.com/content/dam/LifeTech/migration/files/dna-rna-purification-analysis/pdfs.par.91610.file.dat/co24813%20-%20rna%20basics1-final-high.pdf.

203. Applied Biosystems, Life Technologies. RNase Zap® Solution: RNase Decontamination Solution [Online] [August 2014, September 2008]. Available at: http://tools.lifetechnologies.com/content/sfs/manuals/cms_056889.pdf.

204. Perez-Novo, C.A., Claeys, C., Speleman, G., Van Cauwanberge, P., Bachert, C., Vandesompele, J. (2005). Impact of RNA quality on reference gene expression stability. *BioTechniques* **39**(1): 52-6.

205. Ambion, Life Technologies. RNAlater® Tissue Collection: RNA Stabilization Solution Handbook [online] [March 2011; May 2014]. Available at: http://tools.lifetechnologies.com/content/sfs/manuals/7020MF.pdf.

206. Seear, P.J., Sweeney, G. (2008). Stability of RNA isolated from post-mortem tissues of Atlantic salmon (Salmo salar L.). *Fish Physiol Biochem* **34**(1): 19-24.

207. Wu, Y., Llewellyn, D.J., Dennis, E.S. (2002). A quick and easy method for isolating good-quality RNA from cotton (Gossypium hirsutum L.) tissues. *Plant Mol Biol Report* **20**(3): 213-8.

208. Kurakawa, T., Kubota, H., Tsuji, H., Matsuda, K., Asahara, T., Takahashi, T., Ramamurthy, T., Hamabata, T., Takahashi, E., Miyoshi, S. (2012). Development of a sensitive rRNA-targeted reverse transcription-quantitative polymerase chain reaction for detection of Vibrio cholerae/mimicus, V. parahaemolyticus/alginolyticus and Campylobacter jejuni/coli. *Microbiol Immunol* **56**(1): 10-20.

209. Moore, R.A., Tuanyok, A., Woods, D.E. (2008). Survival of Burkholderia pseudomallei in water. *BMC Res Notes* **1**(1): 11.

210. PrimerDigital Ltd. Preparation of DNA and RNA Preservation Medium [online] [2014; June 2014]. Available at: http://primerdigital.com/nasafe.html.

211. Sheehan, D. (2009). Physical Biochemistry: Principles and Applications. 2nd ed. Chichester: John Wiley and Sons Ltd.

212. Fleige, S., Walf, V., Huch, S., Prgomet, C., Sehm, J., Pfaffl, M.W. (2006). Comparison of relative mRNA quantification models and the impact of RNA integrity in quantitative real-time RT-PCR. *Biotechnol Lett* **28**(19): 1601-13.

213. Chowdary, D., Lathrop, J., Skelton, J., Curtin, K., Briggs, T., Zhang, Y., Yu, J., Wang, Y., Mazumder, A. (2006). Prognostic gene expression signatures can be measured in tissues collected in RNAlater preservative. *J Med Diagn* **8**(1): 31-9.

214. Roos-van Groningen, M.C., Eikmans, M., Baelde, H.J., de Heer, E., Bruijn, J.A. (2004). Improvement of extraction and processing of RNA from renal biopsies. *Kidney Int* **65**(1): 97-105.

215. Bachoon, D.S., Chen, F., Hodson, R.E. (2001). RNA recovery and detection of mRNA by RT-PCR from preserved prokaryotic samples. *FEMS Microbiol Lett* **201**(2): 127-32.

216. Grotzer, M.A., Patti, R., Geoerger, B., Eggert, A., Chou, T.T., Phillips, P.C. (2000). Biological stability of RNA isolated from RNAlater-treated brain tumor and neuroblastoma xenografts. *Med Pediatr Oncol* **34**(6): 438-42.

217. Mutter, G.L., Zahrieh, D., Liu, C.L., Neuberg, D., Finkelstein, D., Baker, H.E., Warrington, J.A. (2004). Comparison of frozen and RNALater solid tissue storage methods for use in RNA expression microarrays. *BMC Genomics* **5**(1): 88.

218. Micke, P., Ohshima, M., Tahmasebpoor, S., Ren, Z.P., Östman, A., Pontén, F., Botling, J. (2006). Biobanking of fresh frozen tissue: RNA is stable in nonfixed surgical specimens. *Lab Invest* **86**(2): 202-11.

219. Deng, M.Y., Wang, H.J., Ward, G.B., Beckham, T.R., McKenna, T.S. (2005). Comparison of six RNA extraction methods for the detection of classical swine fever virus by real-time and conventional reverse transcription–PCR. *J Vet Diagn Invest* **17**(6): 574-8.

220. Wang, W.X., Wilfred, B.R., Baldwin, D.A., Isett, R.B., Ren, N., Stromberg, A., Nelson, P.T. (2008). Focus on RNA isolation: obtaining RNA for microRNA (miRNA) expression profiling analyses of neural tissue. *Biochim Biophys Acta* **1779**(11): 749-57.

221. Bohmann, K., Hennig, G., Rogel, U., Poremba, C., Mueller, B.M., Fritz, P., Stoerkel, S., Schaefer, K.L. (2009). RNA extraction from archival formalin-fixed paraffin-embedded tissue: a comparison of manual, semiautomated, and fully automated purification methods. *Clin Chem*. **55**(9): 1719-27.

222. Santiago-Vázquez, L.Z., Ranzer, L.K., Kerr, R.G. (2006). Comparison of two total RNA extraction protocols using the marine gorgonian coral *Pseudopterogorgia elisabethae* and its symbiont *Symbiodinium spp. Elec J Biotech* **9**(5):1-10.

223. Xiang, X., Qiu, D., Hegele, R.D., Tan, W.C. (2001). Comparison of different methods of total RNA extraction for viral detection in sputum. *J Virol Methods* **94**(1): 129-35.

224. Carlsson, B., Jernas, M., Lindell, K., Carlsson, L.M.S. (2000). Total RNA and array-based expression monitoring. *Nat Biotechnol* **18**(6):579.

225. Haimov-Kochman, R., Fisher, S.J., Winn, V.D. (2006). Modification of the standard Trizol-based technique improves the integrity of RNA isolated from RNase-rich placental tissue. *Clin Chem* **52**(1): 159-60.

226. Eldh, M., Lötvall, J., Malmhäll, C., Ekström, K. (2012). Importance of RNA isolation methods for analysis of exosomal RNA: evaluation of different methods. *Mol Immunol* **50**(4): 278-86.

227. Bahn, S., Augood, S., Ryan, M., Standaert, D., Starkey, M., Emson, P. (2001). Gene expression profiling in the post-mortem human brain--no cause for dismay. *J Chem Neuroanat* **22**(1): 79-94.

228. Trotter, S.A., Brill, I., Louis, B., Bennett, J.P. (2002). Stability of gene expression in postmortem brain revealed by cDNA gene array analysis. *Brain Res* **942**(1): 120-3.

229. Barton, A., Pearson, R., Najlerahim, A., Harrison, P. (1993). Pre- and postmortem influences on brain RNA. *J Neurochem* **61**(1): 1-11.

230. Barrachina, M., Castano, E., Ferrer, I. (2006). TaqMan PCR assay in the control of RNA normalization in human post-mortem brain tissue. *Neurochem Int* **49**(3): 276-84.

231. Lee, J., Hever, A., Willhite, D., Zlotnik, A., Hevezi, P. (2005). Effects of RNA degradation on gene expression analysis of human postmortem tissues. *FASEB J* **19**(10): 1356.

232. Bond, B.C., Virley, D.J., Cairns, N.J., Hunter, A.J., Moore, G.B.T., Moss, S.J., Mudge, A.W., Walsh, F.S., Jazin, E., Preece, P. (2002). The quantification of gene expression in an animal model of brain ischaemia using TaqMan™ real-time RT-PCR. *Mol Brain Res* **106**(1): 101-16.

233. Inoue, H., Kimura, A., Tuji, T. (2002). Degradation profile of mRNA in a dead rat body: basic semi-quantification study. *Forensic Sci Int* **130**(2): 127-32.

234. Pardue, S., Zimmerman, A.L., Morrison-Bogorad, M. (1994). Selective postmortem degradation of inducible heat shock protein 70 (hsp70) mRNAs in rat brain. *Cell Mol Neurobiol* **14**(4): 341-57.

235. Saukko, P.J., Knight, B. (2004). Knight's Forensic Pathology. London: CRC Press.

236. Fontanesi, L., Galimberti, G., Calo, D.G., Colombo, M., Astolfi, A., Formica, S., Russo, V. (2011). Microarray gene expression analysis of porcine skeletal muscle sampled at several post mortem time points. *Meat Sci* **88**(4): 604-9.

237. Chandra, D.B., Agarwal, T.N., Bihari, V. (1979). Estimation of the time of death by papillary behaviour at different temperatures. *Indian J Ophthalmol* **27**(4): 208.

238. Maeda, H., Zhu, B., Ishikawa, T., Michiue, T. (2010). Forensic molecular pathology of violent deaths. *Forensic Sci Int* **203**(1): 83-92.

239. Ikematsu, K., Takahashi, H., Kondo, T., Tsuda, R., Nakasono, I. (2008). Temporal expression of immediate early gene mRNA during the supravital reaction in mouse brain and lung after mechanical asphyxiation. *Forensic Sci Int* **179**(2): 152-6.

240. Sanoudou, D., Kang, P.B., Haslett, J.N., Han, M., Kunkel, L.M., Beggs, A.H. (2004). Transcriptional profile of postmortem skeletal muscle. *Physiol Genomics* **16**(2): 222-8.

241. Vass, A.A. (2001). Beyond the grave - understanding human decomposition. *Microbiol Today* **28**: 190-3.

242. Fitzpatrick, R., Casey, O.M., Morris, D., Smith, T., Powell, R., Sreenan, J.M. (2002). Postmortem stability of RNA isolated from bovine reproductive tissues. *Biochim Biophys Acta* **1574**(1): 10-4.

243. Alrowaithi, M.A., McCallum, N.A., Watson, N.D. (2014). A method for determining the age of a bloodstain. *Forensic Sci Int* **234**: e30.

244. Hampson, C., Louhelainen, J., McColl, S. (2011). An RNA expression method for aging forensic hair samples. *J Forensic Sci* **56**(2): 359-65.

245. Zhang, J., Byrne, C.D. (1999). Differential priming of RNA templates during cDNA synthesis markedly affects both accuracy and reproducibility of quantitative competitive reverse-transcriptase PCR. *Biochem J*. **337**(2): 231.

246. MultiD Analyses AB. GenEx: Users Guide, Version 1.0 [Online] [January 2012, June 2014]. Available at: http://www.gene-quantification.de/genex-user-guide.pdf.

247. Karrer, E.E., Lincoln, J.E., Hogenhout, S., Bennett, A.B., Bostock, R.M., Martineau, B., Lucas, W.J., Gilchrist, D.G., Alexander, D. (1995). In situ isolation of mRNA from individual plant cells: creation of cell-specific cDNA libraries. *Proc Nat Acad Sci* **92**(9): 3814-8.

248. Gorzelniak, K., Janke, J., Engeli, S., Sharma, A.M. (2001). Validation of endogenous controls for gene expression studies in human adipocytes and preadipocytes. *Horm Metab Res* **33**(10): 625-7.

249. Nyström, K., Biller, M., Grahn, A., Lindh, M., Larson, G., Olofsson, S. (2004). Real time PCR for monitoring regulation of host gene expression in herpes simplex virus type 1-infected human diploid cells. *J Virol Methods* **118**(2): 83-94.

250. Bémeur, C., Ste-Marie, L., Desjardins, P., Hazell, A.S., Vachon, L., Butterworth, R., Montgomery, J. (2004). Decreased β-actin mRNA expression in hyperglycemic focal cerebral ischemia in the rat. *Neurosci Lett* **357**(3): 211-4.

251. Janovick-Guretzky, N.A., Dann, H.M., Carlson, D.B., Murphy, M.R., Loor, J.J., Drackley, J.K. (2007). Housekeeping gene expression in bovine liver is affected by physiological state, feed intake, and dietary treatment. *J Dairy Sci* **90**(5): 2246-52.

252. Jemiolo, B., Trappe, S. (2004). Single muscle fiber gene expression in human skeletal muscle: validation of internal control with exercise. *Biochem Biophys Res Commun* **320**(3): 1043-50.

253. Glare, E.M., Divjak, M., Bailey, M.J., Walters, E.H. (2002). β-Actin and GAPDH housekeeping gene expression in asthmatic airways is variable and not suitable for normalising mRNA levels. *Thorax* **57**(9): 765-70.

254. Gutala, R.V., Reddy, P.H. (2004). The use of real-time PCR analysis in a gene expression study of Alzheimer's disease post-mortem brains. *J Neurosci Methods* **132**(1): 101-7.

255. Iascone, M.R., Vittorini, S., Collavoli, A., Cupelli, A., Kraft, G., Biagini, A., Clerico, A. (1999). A rapid procedure for the quantitation of natriuretic peptide RNAs by competitive RT-PCR in congenital heart defects. *J Endocrinol Invest* **22**(11): 835-42.

256. Sagynaliev, E., Steinert, R., Nestler, G., Lippert, H., Knoch, M., Reymond, M.A. (2005). Web-based data warehouse on gene expression in human colorectal cancer. *Proteomics* **5**(12): 3066-78.

257. Popow, A., Nowak, D., Malicka-Blaszkiewicz, M. (2006). Actin cytoskeleton and beta-actin expression in correlation with higher invasiveness of selected hepatoma morris 5123 cells. *J Physiol Pharmacol* **57**(1): 111-23.

258. Itani, M., Yamamoto, Y., Doi, Y., Miyaishi, S. (2011). Quantitative analysis of DNA degradation in the dead body. *Acta Med Okayama* **65**(5): 299-306.

259. Riggsby, W.S., Sirotkin, K. (1988). The autodegradation of deoxyribonucleic acid (DNA) in human rib bone and its relationship to the time interval since death. *J Forensic Sci* **33**(1): 144-53.

260. Yasojima, K., McGeer, E.G., McGeer, P.L. (2001). High stability of mRNAs postmortem and protocols for their assessment by RT-PCR. *Brain Res Protoc* **8**(3): 212-8.

261. Vass, A.A., Barshick, S.A., Sega, G., Caton, J., Skeen, J.T., Love, J.C., Synstelien, J.A. (2002). Decompostion chemistry of human remains: a new methodology for determining the postmortem interval. *J Forensic Sci* **47**(3): 542-53.

262. Antonov, J., Goldstein, D.R., Oberli, A., Baltzer, A., Pirotta, M., Fleischmann, A., Altermatt, H.J., Jaggi, R. (2005). Reliable gene expression measurements from degraded RNA by quantitative real-time PCR depend on short amplicons and a proper normalization. *Lab Invest* **85**(8): 1040-50.

263. Shyu, A.B., Belasco, J.G., Greenberg, M.E. (1991). Two distinct destabilizing elements in the c-fos message trigger deadenylation as a first step in rapid mRNA decay. *Gene Develop* **5**(2): 221-31.

264. Catts, V.S., Catts, S.V., Fernandez, H.R., Taylor, J.M., Coulson, E.J., Lutze-Mann, L.H. (2005). A microarray study of post-mortem mRNA degradation in mouse brain tissue. *Mol Brain Res* **138**(2): 164-77.

265. Tortora, G.J., Derrickson, B.H. (2009). Principles of Human Anatomy and Physiology. Hoboken: John Wiley and Sons Inc.

266. Swift, G.H., Peyton, M., MacDonald, R. (2000). Assessment of RNA quality by semi-quantitative RT-PCR of multiple regions of a long ubiquitous mRNA. *BioTechniques* **28**(3): 524-31.

267. Invitrogen, Life Technologies. Platinum® SYBR® Green qPCR SuperMix-UDG [Online] [June 2010, September 2014]. Available at:

http://tools.lifetechnologies.com/content/sfs/manuals/platinum_qpcr_sybr_man.pdf.

268. Applied Biosystems, Life Technologies. TaqMan® array mouse endogenous control plate (96-well) [Online] [September 2014]. Available at: https://www.lifetechnologies.com/order/catalog/product/4426701?ICID=search-product.

269. Popova, T., Mennerich, D., Weith, A., Quast, K. (2008). Effect of RNA quality on transcript intensity levels in microarray analysis of human post-mortem brain tissues. *BMC Genomics* **9**(1): 91.

270. Bustin, S.A. (2004). A to Z of Quantitative PCR. 1st ed. La Jolla, CA: International University Lane.